МІНІСТЕРСТВО ОСВІТИ І НАУКИ УКРАЇНИ
ІВАНО-ФРАНКІВСЬКИЙ НАЦІОНАЛЬНИЙ
ТЕХНІЧНИЙ УНІВЕРСИТЕТ НАФТИ І ГАЗУ

ЕКОЛОГІЧНА БЕЗПЕКА ТА ЗБАЛАНСОВАНЕ РЕСУРСОКОРИСТУВАННЯ

Науково-технічний журнал

Том 17, № 1
2026

ІВАНО-ФРАНКІВСЬК
2026

ISSN (print) 2415-3184
ISSN (online) 2522-9508
УДК 502/504; 574

Засновник:
Івано-Франківський національний технічний університет нафти і газу (ІФНТУНГ)

Рік заснування: 2010

Періодичність випуску: двічі на рік

Ідентифікатор медіа: R30-01429
(Рішення Національної ради України з питань телебачення і радіомовлення
№ 1154, протокол № 24 від 26 жовтня 2023 року)

Журнал включено до категорії «Б» Переліку наукових фахових видань України
Спеціальності: Е2 Екологія;
Е4 Науки про Землю
(Наказ Міністерства освіти і науки України № 928 від 11 червня 2026 року)

Кластер: Науки про Землю та навколишнє середовище

Журнал представлено в таких міжнародних наукометричних базах даних, репозитаріях та пошукових системах:
EBSCO, ERIH PLUS, Crossref, Національна бібліотека України імені В.І. Вернадського, Фахові видання України, Google Академія, Polska Bibliografia Naukowa, UCSB Library, Dimensions, University of Hull Library, University of Oslo Library, Open Ukrainian Citation Index (OUCI), OpenAlex, Sherpa Romeo, Bielefeld Academic Search Engine (BASE), J-Gate, WorldCat, DOAJ, Litmaps, Scopus

Адреса редакції:
Івано-Франківський національний технічний університет нафти і газу
76019, вул. Карпатська, 15, м. Івано-Франківськ, Україна
E-mail: mail@esbur.com.ua
https://esbur.com.ua/uk

MINISTRY OF EDUCATION AND SCIENCE OF UKRAINE
IVANO-FRANKIVSK NATIONAL
TECHNICAL UNIVERSITY OF OIL AND GAS

ECOLOGICAL SAFETY AND BALANCED USE OF RESOURCES

Scientific and Technical Journal

Vol. 17, No. 1
2026

IVANO-FRANKIVSK
2026

ISSN (print) 2415-3184
ISSN (online) 2522-9508
UDC 502/504; 574

Founder:
Ivano-Frankivsk National Technical University of Oil and Gas (IFNTUOG)

Year of foundation: 2010

Frequency: semi-annual

Media identifier: R30-01429
(Decision of the National Council of Television and Radio Broadcasting of Ukraine
No. 1154, Minutes No. 24 of October 26, 2023)

The journal is listed in the List of Scientific Professional Publications of Ukraine (category "B")
Specialties: 0521 Environmental sciences;
0522 Natural environments and wildlife; 0532 Earth sciences
(Order of the Ministry of Education and Science of Ukraine No. 928 of June 11, 2026)

Cluster: Earth and environmental sciences

The journal is presented in the following international scientometric databases, repositories and scientific systems:
EBSCO, ERIH PLUS, Crossref, Vernadsky National Library of Ukraine,
Professional Publications of Ukraine, Google Scholar, Polska Bibliografia Naukowa,
UCSB Library, Dimensions, University of Hull Library, University of Oslo Library,
Open Ukrainian Citation Index (OUCI), OpenAlex, Sherpa Romeo,
Bielefeld Academic Search Engine (BASE), J-Gate, WorldCat, DOAJ, Litmaps, Scopus

Editors office address:
Ivano-Frankivsk National Technical University of Oil and Gas
76019, 15 Karpatska Str., Ivano-Frankivsk, Ukraine
E-mail: mail@esbur.com.ua
https://esbur.com.ua/en

Редакційна колегія

Editorial Board

Зміст

Contents

Vol. 17, No. 1
2026

Ecological Safety and Balanced Use of Resources

ISSN (print) 2415-3184, ISSN (online) 2522-9508
Journal homepage: https://esbur.com.ua/en

Received: 15.10.2025. Revised: 14.05.2026. Accepted: 12.06.2026. Published: 30.06.2026.

UDC 502/504:556.5:[543.2/.3/.4+631.4]

DOI: 10.63341/esbur/1.2026.09

Petroleum hydrocarbons in soil and water matrices: Testing a new rapid extraction procedure and FTIR spectroscopy for integrated risk assessment in micro- and low-order catchments

Mykhailo Mykytsei*

Postgraduate Student, Leading Chemist
Ivano-Frankivsk National Technical University of Oil and Gas
76019, 15 Karpatska Str., Ivano-Frankivsk, Ukraine
Laboratory for Water and Soil Monitoring of the Western Region, Dniester Basin Water Resources
76014, 23a Ukrainskoi Peremohy Str., Ivano-Frankivsk, Ukraine
https://orcid.org/0000-0003-2613-7729

Yaroslav Adamenko

Doctor of Technical Sciences, Professor
Ivano-Frankivsk National Technical University of Oil and Gas
76019, 15 Karpatska Str., Ivano-Frankivsk, Ukraine
https://orcid.org/0000-0001-5665-7958

Viktoriia Navrotska

Master, Chemist
Ivano-Frankivsk National Technical University of Oil and Gas
76019, 15 Karpatska Str., Ivano-Frankivsk, Ukraine
Laboratory for Water and Soil Monitoring of the Western Region, Dniester Basin Water Resources
76014, 23a Ukrainskoi Peremohy Str., Ivano-Frankivsk, Ukraine
https://orcid.org/0009-0002-5408-7554

Abstract. The aim of the study was to develop a fast and effective approach that would enable subsequent integrated risk assessment in micro- and low-order catchments. The procedure involved an alternative sampling strategy, a rapid one-step cyclohexane extraction, extract purification through florisil, concentration, and analysis using an Agilent Cary 630 FTIR spectrometer equipped with a TumblIR 100 sampling module, with possible adaptation to 1,000 µm or other commercially available systems to achieve lower detection limits. Validation results showed that for soil matrices (wet soil, bottom sediments) the method provides good internal consistency with a relative standard deviation of approximately 11% (n = 10) and a systematic bias of approximately -11.5%, with recovery of 88.5%. The expanded measurement uncertainty is ±24% for soil and ±31.9% for water, which corresponds to typical levels for these environmental matrices. For water matrices (surface and drainage waters, soil washings, percolates) recovery exceeds 94%, systematic bias is small, and precision is at an acceptable level. Model experiments evaluating the effects of the sampling strategy revealed significant systematic shifts: -47% for soil percolate, -43.5% for soil (w = 45%), and -40.3% for water-saturated soil, indicating heterogeneous TPH distribution in samples prior to extraction. Assessment using green analytical chemistry indices via AGREE and AGREEprep tools demonstrated the advantages of the developed procedure over conventional standard methods: the overall AGREE index for the developed method is 0.61 (compared to 0.20-0.33 for the gravimetric method, infrared (IR) method according to the MVI, and ASTM D7678-17. It was established that, within Ivano-Frankivsk,

Suggested Citation: Mykytsei, M., Adamenko, Ya., & Navrotska, V. (2026). Petroleum hydrocarbons in soil and water matrices: Testing a new rapid extraction procedure and FTIR spectroscopy for integrated risk assessment in micro- and low-order catchments. *Ecological Safety and Balanced Use of Resources*, 17(1), 9-29. doi: 10.63341/esbur/1.2026.09.

*Corresponding author (*mmtecoif@gmail.com*)

concentrations in road dust and roadside soils ranged from 1.6-2.8×10^3 mg/kg and locally reached 4.7-6.5×10^5 mg/kg, posing high risks associated with stormwater runoff and pollutant discharge into storm drains, eventually entering the Bystrytsia Solotvynska River

Keywords: sample preparation; method validation; measurement uncertainty; matrix effects; watershed contamination

Introduction

Petroleum hydrocarbons are among the most widespread and environmentally hazardous pollutants in urban and industrial ecosystems. They readily accumulate in soils and surface deposits, are capable of migrating via surface runoff into water bodies, and form persistent contamination hotspots. This issue is of particular relevance for small catchments, where even local pollution sources can rapidly lead to the degradation of the entire hydroecosystem. Under contemporary conditions, there is an increasing need for rapid, reliable, and cost-effective methods for assessing this type of contamination to ensure effective environmental monitoring and risk management.

Petroleum hydrocarbons are incorporated into the environment of urbanised and industrial areas through accumulation on solid surfaces and in soils, as reported by O. Trysniuk *et al.* (2020), as well as in the near-surface geological environment, as noted by E. Kuzmenko *et al.* (2025) They represented one of the main groups of anthropogenic environmental pollutants and are common constituents of street dust and road debris as forms of solid dispersed deposits in urban and industrial areas. Their input into the environment is driven by various sources of anthropogenic pressure, including the operation of petrol filling stations, which is accompanied by emissions of volatile organic compounds and potential leaks of petroleum products into soil and aquatic environments, according to M. Troshyn *et al.* (2025). Additionally, B. Herasymenko (2024) emphasised that accidental leaks from oil and gas pipelines have been identified as a significant source of hydrocarbon input into the soil cover, leading to persistent changes in its physicochemical and biological properties. Military conditions further intensify the scale of petroleum soil contamination, forming new hotspots of ecosystem degradation, as noted by H. Hrytsuliak *et al.* (2025), which necessitates further restoration measures. Under the influence of atmospheric precipitation, they were mobilised by surface runoff and infiltration flows, transported through artificial and natural drainage systems, as well as within soil and rock strata, and, under favourable hydrological and hydrogeological conditions, are dispersed into water bodies or, by forming local or transitory hydrocarbon contamination plumes, create risks for ecosystems of micro- and low-order catchments as a whole. In addition, military strikes by russia and acts of sabotage caused the destruction of numerous facilities for the storage and transportation of petroleum products throughout Ukraine, which was accompanied by fires and large-scale spills. Unlike fires, which are recognised as an important source of formation and mobilisation of polycyclic aromatic hydrocarbons (PAHs) that enter the environment through the combustion of organic matter and are subsequently redistributed between the atmospheric, soil, and aquatic compartments, as shown in the review by I. Campos & N. Abrantes (2021), petroleum product spills lead to long-term contamination of the land surface, with a high risk of infiltration into the aeration zone and the formation of persistent degradation zones within the geological environment, as reported by R. Havryliuk *et al.* (2024).

Determination of the total petroleum hydrocarbons (TPH) content in soils and sediments is a key element of environmental contamination assessment and the planning of remediation measures. However, despite the global significance of petroleum contamination of the upper soil and geological environment, existing analytical methods often remain labour-intensive and resource-consuming. As noted by B. Abdykarimov *et al.* (2025), the development of rapid, accurate, and efficient analytical approaches still represents a significant scientific and practical challenge. Despite the high applied significance of the petroleum contamination problem in Ukraine and the urgent challenges associated with the impact of war on the environment, researchers continue to face a number of difficulties in determining petroleum hydrocarbons in various environmental matrices during applied studies. Outdated analytical equipment, the complexity and labour intensity of extraction procedures, as well as potential health hazards for operators limit the possibilities for conducting rapid and reliable measurements. Institutional and laboratory-analytical support of many institutions remains insufficient, which often leads to results with limited accuracy, low reproducibility, and questionable reliability, according to Resolution of the Cabinet of Ministers of Ukraine No. 610-r (2023). The combination of these factors emphasises the need to develop and implement modern, safer, and more effective methods for controlling petroleum product contamination.

These circumstances emphasise the relevance of developing and implementing analytically reliable and environmentally safe procedures for sampling and determining petroleum hydrocarbons in various environmental matrices, which is a necessary prerequisite for proper diagnosis of environmental conditions, environmental risk assessment, pollution monitoring, and substantiation of environmental protection measures. Accordingly, the aim of the study was to develop and experimentally validate a rapid analytical method for the determination of petroleum hydrocarbons in soils and waters of small catchments using an extraction approach combined with FTIR spectroscopy. The scientific novelty of the study lies in the development and experimental confirmation of the effectiveness of a new rapid

extraction and FTIR spectroscopy procedure adapted to contemporary scientific and practical challenges, which can be effectively and promptly applied for integrated environmental risk assessment in micro- and low-order catchments.

Literature Review

For the quantitative assessment of petroleum hydrocarbon content in water and the environment, their concentration is regulated as the TPH indicator in accordance with EU legislation. TPH represent a generalised term that encompasses several hundred chemical compounds derived from crude oil and composed of carbon and hydrogen atoms, including benzene, toluene, xylenes, hexanes, naphthalene, fluorene, jet fuel, mineral oils, and related substances, as noted by A. Simion *et al.* (2022). In Ukraine, standard methods are used to determine TPH (most often under the term "petroleum products"). For water and soils, classical, normatively established approaches oriented toward reproducibility and compatibility with the state control system remain the most widespread. For aqueous matrices, methods based on extraction with organic solvents followed by gravimetric determination (MVI No. 081/12-0645-09, 2010), IR analysis (MVI No. 081/12-0877-13, 2014), or gas chromatographic analysis (DSTU ISO/TR 11046-2001, 2002; DSTU ISO 9377-2:2015, 2016) are commonly applied. In soils and bottom sediments, Soxhlet or liquid-solid extraction is typically followed by gravimetric analysis (MVI No. 081/12-0116-03, 2004; MVI No. 081/12-0725-10, 2011), IR analysis (DSTU ISO/TR 11046-2001, 2001; MVI No. 081/12-0637-09, 2009), or gas chromatography (DSTU ISO 16703:2007, 2007).

Among the existing methods for measuring petroleum product content, the fluorimetric method using the FLUORAT analyser is very often applied in Ukraine; it is based on extraction of petroleum products from the sample with hexane, optional purification of the extract, and allows determination of the mass concentration of petroleum products in water in the range of 0.005-50 mg/L. Gas chromatography (GC-FID, less often GC-MS) is mainly used in reference and research laboratories for detailed analysis of fractional composition, whereas more "green" approaches (SPME, direct IR probing, express methods) are still implemented on a limited scale and are mostly applied within scientific developments and pilot studies rather than routine state monitoring. This may be due to the still limited availability of modern analytical equipment.

In the reviews by A. Adeniji *et al.* (2017) and Z. Yue *et al.* (2021), the strengths and weaknesses of traditional methods for determining TPH in environmental samples are summarised, with some being more suitable for field screening and others for laboratory analysis. Infrared spectroscopy (EPA 418.1), gravimetry (EPA 1664A), gas chromatography with FID and MSD (EPA 8015, 8270, 625), UV spectrophotometry, immunoassays (EPA 4030, 4035), as well as Raman and fluorescence spectroscopy are discussed; preparation of liquid samples is usually performed by liquid-liquid (LLE) or solid-phase (SPE) extraction, whereas solid matrices are mainly extracted by Soxhlet. The authors emphasise that IR spectroscopy is gradually replacing other approaches due to the need to eliminate halogenated solvents classified as ozone-depleting and underline the key role of sampling strategy. At the same time, TPH analytical procedures differ substantially in terms of the range of fractions determined and specificity: methods with different extraction efficiencies may yield different TPH concentrations for the same sample, and the use of different calibration standards and extractive solvents complicates result comparability, making a detailed understanding of the applied methodology critically important for correct data interpretation.

A. Imam *et al.* (2019) emphasised the key role of chemical analysis and the importance of using chromatography, spectroscopy, and various sample pretreatment methods for effective monitoring and evaluation of bioremediation experiments. The review by B. Abdykarimov *et al.* (2025) showed that Soxhlet extraction, despite its low environmental friendliness, remains a widespread method for determining TPH due to its high extraction efficiency, whereas more environmentally friendly methods, such as gas chromatography-mass spectrometry with solid-phase microextraction and direct IR probing, reduce solvent use and minimise sample preparation. This review highlighted the need to balance analytical efficiency and environmental sustainability and demonstrates pathways for improving the greenness of methods in forensic and environmental monitoring. J. Płotka-Wasylka *et al.* (2021) also noted that analytical chemistry is increasingly oriented toward the principles of green analytical chemistry (GAC), especially in sample preparation, with the aim of developing environmentally safe and more sustainable analytical procedures. Critical evaluation of such methods should consider validation criteria, practical and financial aspects alongside GAC principles, as reported by S. Hammad *et al.* (2025).

L. Wang *et al.* (2020) noted that in traditional contaminated-site assessment, soil sampling and transportation of samples from sites are excessively expensive and labour-intensive, whereas the use of portable and accessible field equipment provides a rapid and cost-effective solution to complement complex laboratory analyses. According to the researchers, portable Fourier transform infrared (FTIR) spectroscopy offers advantages such as immediate results, ease of use, and non-destructive measurements, enabling rapid on-site characterisation. Information obtained from IR spectroscopy has the potential to provide baseline data for environmental modelling. For example, when an oil spill or leak occurs on land, multiphase trapping and pH distribution in porous soil media depend on the hydraulic and physical properties of the soil as well as its hydration. The obtained data on these properties and measured TPH concentrations can be applied in mathematical models to assess potential risks of surface- and groundwater contamination downstream through migration and transport from contaminated sites.

Although under field conditions portable instrumental methods provide rapid results and better spatial coverage, which can meet the need for locating site hot spots P. Rostron *et al.* (2014), and this is generally a trend in the application of in situ methods for characterisation of TPH-contaminated sites L. Wang *et al.* (2021), field measurements using methods that provide near-laboratory-quality data for rapid quantitative, definitive, and defensible sampling remain challenging. A. Fuente-Ballesteros *et al.* (2025) associate current directions for improving environmental efficiency with miniaturisation of analytical systems, reduction of solvent use, and implementation of field measurements. An increasing number of researchers report on this. New analytical procedures should comply with GAC principles, which is achieved both by modification of traditional methods and by the development of specialised sustainable methodologies. At the same time, it is often emphasised that classical laboratory approaches, even after optimisation, are frequently poorly suited for operational environmental monitoring, particularly under conditions of accidental releases or acute toxic impacts, which necessitates the use of fast-acting, compact, resource-efficient, and, where possible, portable analytical solutions.

In conclusion, it should be considered that analytical and monitoring systems are not a neutral reflection of the environment but the result of conscious construction of system boundaries of interest A. Knight *et al.* (2019). The choice of analytical methods determines which processes and risks become visible and which remain outside attention. Increasing the green index of analytical procedures in this study should be regarded as a conscious rethinking of system boundaries: from "ideal accuracy" to "sufficient environmental relevance" and from "universality" to "contextual adequacy". This enables adaptation, simplification, and improvement of various analytical procedures to the specificity of the environment and research objectives while simultaneously enhancing their environmental efficiency. Overall, a conceptually sound and environmentally justified solution-though requiring appropriate scientific validation-is the application of such a rethinking concept to diagnostic and monitoring tasks, where the system of interest with defined boundaries can be the landscape-hydrological continuum. Micro- and low-order catchments were selected as the focus of the study in the context of improving diagnostic and monitoring procedures for contamination, since such systems are considered the most sensitive to local anthropogenic impacts, as noted by J. Richardson (2019), and reflect the features of the hydrological continuum within the landscape. In addition, the scale of low-order catchments enables the effective application of models for identifying local pollution sources and accounting for fine-scale landscape features, which is important for the development of local water resource conservation measures, according to M. Mykytsei *et al.* (2024).

Thus, the analysis of current approaches for the determination of petroleum hydrocarbons in environmental media demonstrates a wide range of analytical methods that differ significantly in sensitivity, selectivity, labour intensity, and environmental sustainability. Despite substantial advances in instrumental techniques, conventional approaches such as extraction-gravimetric and spectroscopic methods still form the basis of regulatory monitoring, while modern rapid and field-based techniques remain limited in practical implementation. A key issue is the lack of standardisation of results due to differences in extraction procedures, calibration strategies, and analytical standards. Current trends in analytical chemistry are increasingly focused on improving the environmental performance of methods, reducing solvent consumption, and shifting part of measurements to field conditions using portable instruments, particularly FTIR spectroscopy. In this context, the development of rapid, reproducible, and environmentally safe methodologies adapted to the local conditions of small catchments becomes especially important, as they can provide both sufficient analytical reliability and practical applicability for environmental monitoring purposes.

Materials and Methods

Description of the research area

Demonstration experimental studies to test the methodological procedures were conducted between March and May 2025 within three micro-catchments identified as contamination hot spots (Fig. 1).

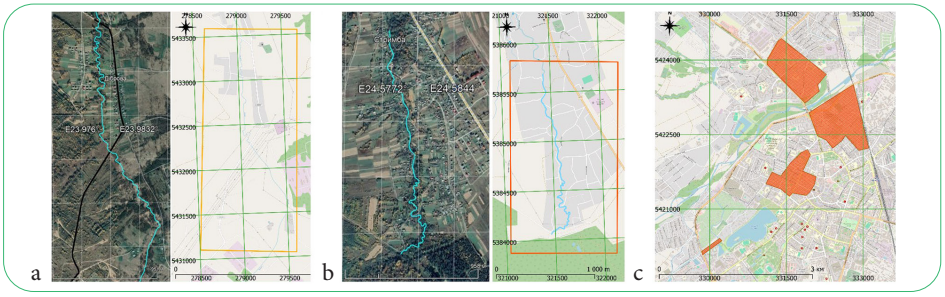

Figure 1. Study sites (micro-catchments) identified as "hot spots" with potential TPH contamination, selected to demonstrate the applicability of the proposed analytical procedure

Note: a – study site (micro-catchment of the Lushchava River (zone of oil extraction influence)); b – catchment of the mountain Strymba River within the area of an accidental oil spill (30.09.2023); c – urbanised micro-catchment within the catchment of the Bystrytsia Solotvynska River (Ivano-Frankivsk)

Source: created by the authors

Figure 1a – the technogenically loaded catchment area of the Lushchava River within the zone of influence of the activities of NGVU "Dolynanaftogaz". This area represents a part of the catchment of the small Lushchava River within the settlements of Dibrova, Yavoriv, and Solukiv, Dolyna District, located in the zone of oil extraction and known for multiple environmentally hazardous emergency incidents (2017-2018). The watercourse, with a length of 15 km, originates in shrub-covered wetland areas 6 km south of the town of Dolyna and flows in a north-eastern direction. The channel is weakly sinuous, unbranched, with an average flow velocity of 0.2 m/s. The soil cover of the basin area consists of light loamy podzolic soils, locally alternating with alkaline podzolised soils. In its upper reaches, the river channel is hydraulically connected with anthropogenic elements of the flow drainage network, such as roadside ditches, gullies, and open drainage channels, which may act as primary water pathways and reservoirs for the transfer of petroleum hydrocarbons;

Figure 1b – the catchment area of the small mountain river Strymba, within a site known for an accidental rupture of an oil pipeline with a diameter of 150 mm on 30 September 2023, which resulted in an oil spill along the watercourse and a large-scale fire. According to data from the Dniester Basin Water Resources Administration, after the accident the concentration of petroleum products in the Strymba River exceeded hygienic standards for drinking and domestic water use by 10.6 times, and for fishery water bodies by 64 times. Subsequent consequences remained unknown and uninvestigated. The emergency situation demonstrated high environmental risks associated with the operation of oil pipelines in regions with a developed hydrographic network, as well as the necessity of implementing effective monitoring and response measures for such emergency situations. The micro-catchment area is predominantly covered by forest vegetation;

Figure 1c – the part of the Bystrytsia Solotvynska River catchment transformed by urbanisation, within the territory of the urban and suburban zones of the city of Ivano-Frankivsk. The micro-catchment covered the functioning system of an open-flow network of channels and small ditches used for runoff regulation, as well as the main open directed channel of an ancient small watercourse that crosses the western (in the past also the north-western) part of the city – the Stebnytska mlynivka (Mykytsei *et al*., 2024). In addition, through the system of stormwater sewer collectors of this territory, part of the storm and snowmelt wastewater of the settlement is discharged into the Bystrytsia Solotvynska River without treatment (collector outlets are located along V. Stefanyk Embankment Street).

In addition, through the system of stormwater sewer collectors of this territory, part of the storm and snowmelt wastewater of the settlement is discharged into the Bystrytsia Solotvynska River without treatment (collector outlets are located along V. Stefanyk Embankment Street). The main attribute of this micro-catchment is defined as surface sealing and artificial routing of stormwater runoff from the city territory as pathways for interception and transport of pollutants to the point of discharge into the main watercourse. For all territories during March and April 2025, weather conditions in Ivano-Frankivsk were dynamic and diverse, which is typical for the transitional period from winter to spring. March began with moderately cool weather: daytime temperatures ranged from +3°C to +16°C, while nighttime temperatures ranged from -5°C to +7°C. In the middle of the month, gradual warming was observed, with daytime temperatures up to +16°C and nighttime temperatures around +7°C. April was characterised by a significant increase in temperature: during the first ten days, daytime temperatures ranged from +3…+9°C, and nighttime temperatures from -3 to +5°C. In the second half of the month, temperatures increased to +15…+21°C during the day and +6…+9°C at night.

In March and April 2025, moderate precipitation was observed, typical for the spring period in the region. In March, the average precipitation amounted to approximately 55-66 mm, distributed over 11-13 days with precipitation. This indicates moderate humidity, with a predominance of rain and wet snow, especially at the beginning of the month. In April, precipitation slightly increased, reaching an average of 60-79 mm, with more frequent short-term rains and possible thunderstorms. Rapid and abrupt fluctuations in weather conditions against the background of changing climatic factors may significantly enhance the desorption of petroleum products that previously entered the environment from surface soil layers, road surfaces, and street dirt in urban systems, as well as under conditions of increased pollutant accumulation resulting from industrial activities or local emergency situations. Taken together, this often leads to intensive wash-off of petroleum products in stormwater runoff and an increased risk of secondary delayed or long-term persistent pollution of water bodies.

Experimental base, equipment, and tools

The basis for experimental tests and innovative developments within the framework of the memorandum of cooperation between the Ivano-Frankivsk National Technical University of Oil and Gas and the Dniester Basin Water Resources Administration was the Water Monitoring Laboratory of the Western Region. In 2023, within the framework of humanitarian and technical support to Ukraine, this laboratory in Ivano-Frankivsk received a modern Cary 630 FTIR infrared spectrometer (Agilent Technologies, USA), provided by the German Federal Agency for Technical Assistance. This instrument is generally intended for operational infrared analysis and provides the possibility of express determination of organic pollutants in water and soil matrices with minimal sample volume requirements. It was equipped with a TumblIR sampling module with a fixed path length in the 100 μm analysis mode.

Additional analytical equipment included a conductometer pH meter (HORIBA, Japan), electronic laboratory scales with an accuracy of ±0.0001 g, and electronic labo-

ratory scales with an accuracy of ±0.1 g. Auxiliary equipment included piston dispensers with adjustable dosing volume in the range of 0.5-5 ml and in the range of 100-1,000 µl, and a drying oven. Extraction flasks were carefully cleaned, rinsed with distilled water, dried at 130°C, labelled, weighed, and packed for field sampling. Medical syringes with a nominal volume of 5 ml equipped with an irrigation tip (for liquid sampling) and 2 ml syringes with a cut connector for sampling individual solid material samples were used for sampling. Cyclohexane was used as the extraction solvent, replacing any carbon tetrachloride, freon, or fluorinated solvents. Cyclohexane is a less toxic and more environmentally safe solvent compared to traditional solvents such as freon-113, carbon tetrachloride, or toluene. An additional advantage is that its absorption spectrum in the IR region minimally interferes with the detection of characteristic petroleum hydrocarbon bands during FTIR analysis, making it particularly suitable for express methods. An analytical standard of tetradecane from Sigma-Aldrich was used for instrument calibration.

Instrument calibration

A series of freshly prepared solutions from a certified standard sample of tetradecane and high-purity cyclohexane, with nominal concentrations of 0.5, 4, 6, 8, 25, 100 mg/ml, were measured under the same instrumental conditions in 5 repetitions. The instrument setup parameters for spectral data collection are presented in Table 1.

The collected spectral data in the MicroLab PC software were used in the process of creating a calibration model according to the Simple Beer's Law algorithm, which was implemented in the MicroLab Quant environment (Fig. 2).

Table 1. Instrument settings parameters of the Agilent Cary 630 FTIR infrared spectrometer for collecting spectral data of standard solutions of nominal concentrations

Parameters	Set parameter value
Spectral range (cm^{-1})	1,400-1,300
Background scan	32
Sample Scans	32
Resolution (cm^{-1})	4
Zero filling factor	4
Phase correction	Merz method of phase correction
Apodisation	Gappa-Genzel smoothing (apodisation) function
Sampling Technology	Transmission Cell: TumblIR_100 µm

Source: created by the authors

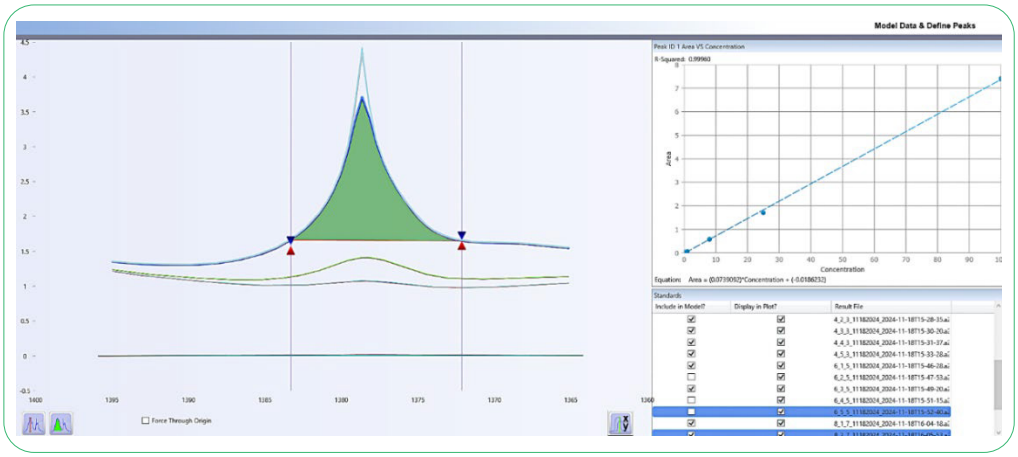

Figure 2. Calibration model for determining the mass concentration of TPH using Simple Beer's Law, implemented in the MicroLab Quant

Source: created by the authors

In the created quantitative model project, the nominal concentration values for each standard were entered, after which the Simple Beer's Law method was selected from the list of algorithms. This method is based on a direct linear relationship between optical absorbance and analyte concentration according to the Beer-Lambert law equation ($A = \varepsilon bc$). The spectral feature used as the analytical signal for the model was the peak area, which was set interactively in the spectral display window using the baseline and peak boundary positioning tools. The software automatically constructed the calibration line in the form of the equation $y = mx + b$, where y is the signal intensity, x is the concentration, m is the slope, and b is the intercept.

To assess the accuracy and reliability of the model, the Model Evaluation tools were applied, which included cross-validation (with stepwise exclusion of each standard

from the model) and verification on an independent sample set, for which concentration values were entered manually and predicted values were calculated automatically. During the evaluation, the model was assessed by key statistical indicators – the coefficient of determination (R^2), the overall standard error, and a plot comparing predicted and actual values. The coefficient of determination of the constructed calibration curve was 0.9996, indicating a very high approximation and acceptability of the model. After the modelling was completed and the parameter conformity was confirmed, the model was saved as a project file (.mpq), which included the defined component with all calibration parameters for further quantitative analysis in MicroLab PC.

Validation study

The intra-laboratory validation study was conducted in accordance with the requirements of the ISO/IEC 17025:2017 (2017) standard "General requirements for the competence of testing and calibration laboratories", which establishes the fundamental criteria for ensuring the quality and reliability of laboratory measurements. The assessment of analytical uncertainty was carried out in accordance with the conceptual principles set out in the Guide to the Expression of Uncertainty in Measurement (GUM), published by the International Organization for Standardisation (ISO) in 1993, as well as in the adapted version of the American standard (US GUM) adopted by the American National Standards Institute (ANSI/NCSL Z540-2-1997, 1997). The practical implementation of uncertainty assessment was based on the algorithm of the Standard Operating Procedure (2003) of the Quality Assurance and Laboratory Accreditation Department of the Navy, which describes in detail the methodology for using a QC-based Nested Approach with the application of a Microsoft Excel spreadsheet for automated evaluation. The use of this approach allows effective distribution of uncertainty sources, their quantitative evaluation, calculation of expanded uncertainty with the possibility of correction for bias, as well as visual analysis through histogram plotting to identify significant components. This approach complies with the recommendations of ISO/IEC 17025:2017 (2017) and can be adapted using other methods that meet these requirements.

Field sampling procedure

The sampling volume and the type of equipment used were adapted according to the objectives of the analytical method. The instrument capabilities and the expected concentration range were taken into account, while the main emphasis was placed on achieving the environmentally required minimum to meet the procedure's objective, with a deliberate refusal of formal universality in order to potentially improve the green index. Operational sampling was carried out using carefully cleaned used glass vials from small-volume (20 cm^3) paraphase extraction for GC-MS, with hermetic caps and Teflon septa. A small amount of solid sample matrix (1.5-2 cm^3 of soil or road dust) or approximately 10 ml of natural water was introduced by mechanical syringe sampling. This ensured rapid sampling while minimising the risk of cross-contamination. Acidification of the samples immediately after delivery to the laboratory to pH < 2 was carried out by adding 20-30 µl of formic acid instead of the known practices of acidification with hazardous HCl and H_2SO_4, which did not affect the quality of the results.

Extraction and concentration procedure

Extraction of samples with a fixed single volume of cyclohexane was carried out directly in the sampling vials by mechanical shaking. All vials of one analytical series (up to 50 units) were placed in a rigid transport container with internal partitions that provided stable fixation of the vials and prevented their mutual movement. Mechanical shaking was performed manually by intensive movements of the container for 5 minutes, ensuring equal duration and intensity of mechanical action for all samples. After extraction, 10 ml of deionised water with pH ≈5.6 ± 0.2 was added to the extraction vials containing soil samples to transfer the extract from the solid sample to the solution surface and ensure its further accurate sampling. From each vial, the entire possible volume of extract was taken, avoiding the inclusion of the aqueous layer, after which it was passed through a small layer of Florisil into cleaned chromatographic vials. At the first stage, TPH concentrations in the extract were determined before further concentration, using the separately filtered extract residue. If the measurement result was below the instrument's limit of detection, the extract preparation was continued. For this, 2 ml of the purified extract of the same sample was evaporated in a drying chamber equipped with an exhaust system and a fan at a temperature of 35-40°C. The dry residue was resuspended in a small volume of solvent (50 µl) using a piston dispenser with a disposable tip, repeatedly initiating the jet within the vial environment to achieve complete dissolution and uniform mixing. After that, 40 µl was quickly introduced into the instrument to avoid losses associated with evaporation.

Results and Discussion

Method validation and comparative evaluation of analytical procedures

The methodology for assessing analytical measurement uncertainty using an Excel-based QC nested approach (Nested Approach) (Fig. 3) was applied to determine the contributions of various factors to the overall uncertainty of test results (Fig. 4a; Fig. 4b) obtained using this method, as well as to evaluate systematic procedural error.

Calibration standard of tetradecane in cyclohexane with a nominal concentration of 8 mg/mL, and the calibration verification standard with a nominal concentration of 5 mg/mL were analysed in 10 parallel replicates in order to account for internal instrumental measurement effects and the effects of preparing the standard spike.

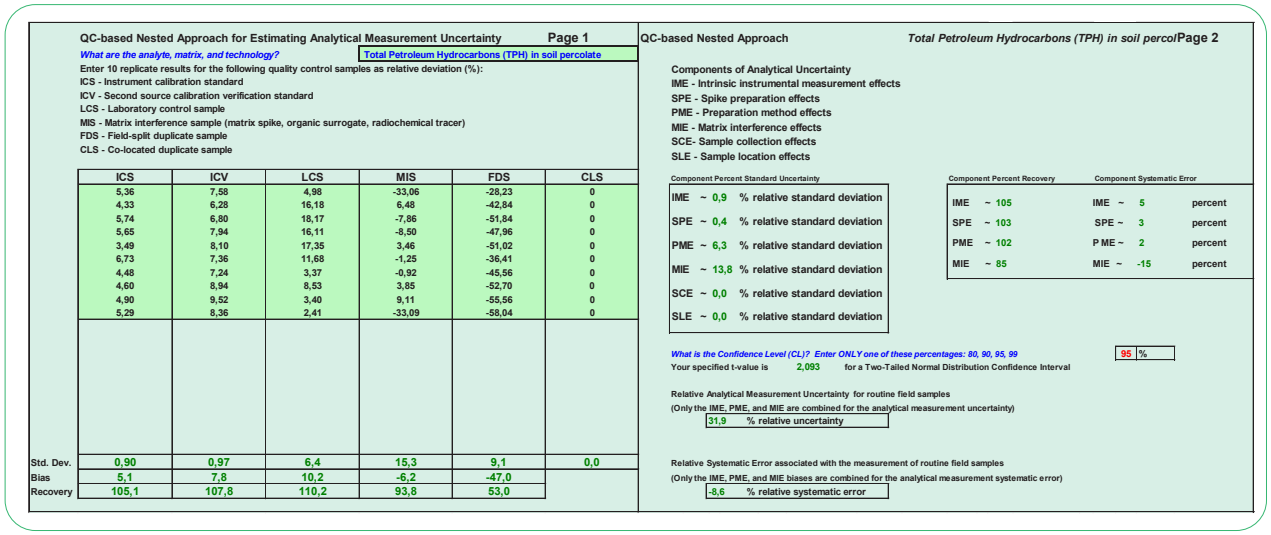

Figure 3. Example of implementing the methodology for assessing analytical measurement uncertainty in Excel using a QC-based nested approach (Nested Approach)
Source: created by the authors based on W. Ingersoll (2003)

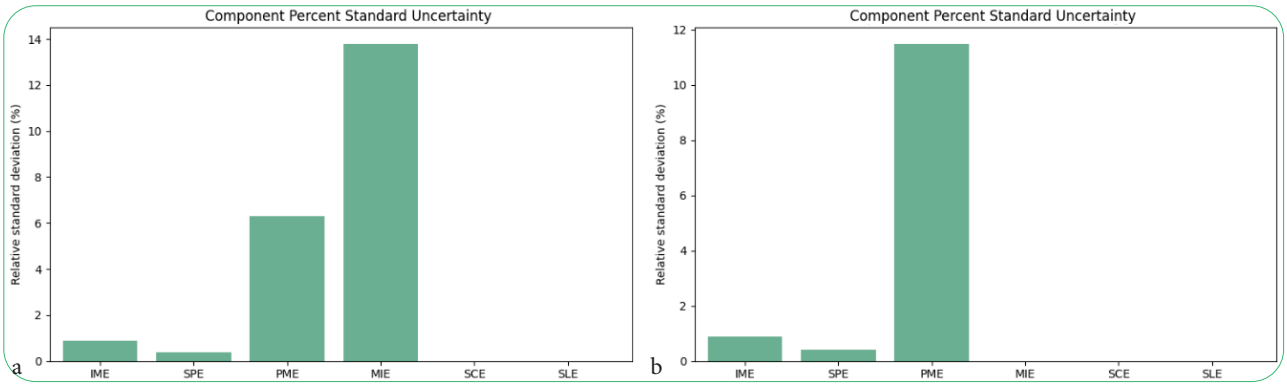

Figure 4. Contribution of individual stages of the analytical procedure to the relative expanded standard uncertainty (U, %) for k = 2 (p = 0.95) in determining TPH in water (a) and in soil (b)
Source: created by the authors

To determine the contribution of the sample preparation procedure, model samples were prepared in 10 replicates (Table 2) and analysed to reproduce the extraction process from liquid and solid matrices. Instead of a water matrix, 10 ml of deionised water were placed into clean 20 ml glass flasks. To model extraction from a solid matrix, 1.5 g of clean calcined sand were pre-weighed into the flasks and moistened with 0.45 ml of deionised water. A volume of 50 µl of tetradecane solution in cyclohexane with a concentration of 250 mg/mL was added to each flask to reach the nominal concentration in the extract of 5 mg/mL. After the standard was added, the flasks were shaken vigorously. Acidification to pH < 2 was performed by adding 20-30 µl of formic acid. For extraction, 2.5 ml of pure cyclohexane was added to each sample, and intensive mechanical shaking was carried out for 5-7 minutes.

Table 2. Results of laboratory measurements for the main components of analytical variation

No.	Standard solutions			Laboratory samples				Matrix samples			
				Deionised water		Calcined sand		Soil percolate		Soil	
	Tetradecane 8 mg/mL	CCS 5 mg/mL	Grude oil 8 mg/mL	nominal concentration of tetradecane in the extract 5 mg/mL							
				C_i, mg/mL	C_{ex}, mg/mL	C_i, mg/mL	C_{ex}, mg/mL	C_i, mg/mL	C_{ex}, mg/mL	C_i, mg/mL	C_{ex}, mg/mL
1	8.429	5.379	7.789	44.616	5.249	51.745	6.088	28.449	3.347	36.915	4.343
2	8.346	5.314	7.861	49.376	5.809	49.824	5.862	45.252	5.324	40.706	4.789
3	8.459	5.34	7.75	50.223	5.909	37.86	4.454	39.161	4.607	39.736	4.675
4	8.452	5.397	7.939	49.348	5.806	46.956	5.524	38.889	4.575	42.688	5.022

Table 2. Continued

No.	Standard solutions			Laboratory samples				Matrix samples			
				Deionised water		Calcined sand		Soil percolate		Soil	
				nominal concentration of tetradecane in the extract 5 mg/mL							
	Tetradecane 8 mg/mL	CCS 5 mg/mL	Grude oil 8 mg/mL	C_i, mg/mL	C_{ex}, mg/mL	C_i, mg/mL	C_{ex}, mg/mL	C_i, mg/mL	C_{ex}, mg/mL	C_i, mg/mL	C_{ex}, mg/mL
5	8.279	5.405	7.578	49.873	5.867	49.425	5.815	43.97	5.173	31.477	3.703
6	8.538	5.368	7.627	47.466	5.584	43.371	5.102	41.968	4.937	35.173	4.138
7	8.358	5.362	8.118	43.934	5.169	50.206	5.907	42.109	4.954	41.468	4.879
8	8.368	5.447	7.94	46.126	5.427	50.847	5.982	44.135	5.192	30.699	3.612
9	8.392	5.476	8.119	43.943	5.170	55.385	6.516	46.372	5.456	36.84	4.334
10	8.423	5.418	8.254	43.524	5.120	50.5	5.941	28.436	3.345	40.601	4.777

Note: CCS – calibration verification standard; Ci – concentration measured by the instrument; Cex – concentration recalculated to the initial volume of the extractant
Source: created by the authors

In the soil sample preparation models, an additional 10 ml of deionised water was added along the walls of the flask to bring the organic layer (extract) to the surface. After phase separation, the maximum possible volume of extract was withdrawn from each flask, avoiding the aqueous layer, and 2 ml was passed through a small layer of florisil (0.2 g) into clean flasks. Concentration of the extracts was performed in a drying chamber equipped with an exhaust system and a fan at a temperature of 35-40°C. To determine matrix effects, 10 parallel samples of real soil samples and fresh soil percolate samples, previously spiked with tetradecane to a nominal extract concentration of 5 mg/mL, were processed. For this purpose, 10 ml of fresh soil wash with a mass concentration of suspended solids of 230 mg/dm^3 was added to 20 ml flasks. For the soil matrix, 2 g of dry homogenised topsoil were weighed into flasks and moistened by adding 0.45 ml of deionised water. After spiking with the standard solution, all the above-described steps of the procedure were repeated before analysis.

To determine the systematic bias caused by the sampling procedure for liquid matrices and by the mixing (homogenisation) process of the composite sample of solid matrices obtained from different sampling points within the study area, and to enable correct recalculation of the measured concentration to the actual average content within the test site, a separate series of experiments was conducted (Table 3). For soil samples, two clean containers were weighed twice with 0.5 kg of previously dried, stone-free soil. Two grams of crude oil dissolved in cyclohexane were added to one portion, thoroughly mixed to achieve maximum homogenisation, moistened to 25% with deionised water, mixed again, and left for 24 hours. The second uncontaminated portion was moistened to 25% moisture and kept under the same conditions, after which both portions were mixed thoroughly. Ten replicate samples (~2 cm^3) were collected by mechanical pressing using a cut-off syringe and placed into pre-weighed extraction flasks. For the aqueous matrix, a soil filtrate (percolate) was prepared by passing distilled water through a layer of uncontaminated soil (10-15 cm). To 1,000 ml of the filtrate, 0.5 g of crude oil was added, followed by vigorous mixing. Composite samples were formed in 10 parallel extraction vials (10 ml each) using a syringe irrigation tip, so that each sample consisted of separate aliquots of the filtrate collected during sample mixing. The samples were reweighed on an analytical balance in closed vials. Subsequent sample preparation and analysis were performed as described above.

Table 3. Results of laboratory measurements of variations caused by the sampling procedure

No.	Soil percolate (nominal concentration of crude oil 500 mg/L)			Soil, w = 25% (nominal concentration of crude oil 1,000 mg/kg d.w.)			Soil, w = 45% (nominal concentration of crude oil 1,000 mg/kg d.w.)		
	V (mL)	C_i, mg/mL	C_s, mg/L	m(dry), g	C_i, mg/mL	C_s, mg/L	m(dry), g	C_i, mg/mL	C_s, mg/L
1	11.2278	13.699	358.852	2.4239	4.539	550.760	1.1550	1.876	477.718
2	11.5503	11.223	285.783	3.2837	5.77	516.809	0.8464	2.064	717.229
3	11.8595	9.71	240.810	2.7162	4.937	534.592	1.0931	2.144	576.867
4	11.262	9.963	260.193	2.7546	5.075	541.874	0.8113	2.115	766.739
5	10.6591	8.876	244.916	4.2302	6.841	475.639	1.1353	2.306	597.430
6	10.7534	11.624	317.930	2.8856	5.625	573.344	0.9282	1.851	586.502
7	11.2683	10.428	272.185	2.4910	7.241	854.969	1.1329	2.208	573.235
8	11.2284	9.028	236.480	2.5034	4.802	564.168	1.1080	2.029	538.608
9	12.011	9.075	222.223	3.5561	6.178	510.966	1.0189	2.216	639.656
10	11.3103	8.068	209.804	3.3017	5.893	524.960	0.9731	1.654	499.939

Note: V – volume of the composite sample; Ci – concentration measured by the instrument; Cs – concentration recalculated to the initial volume/mass of the sample; m(dry) – mass of the dry soil sample
Source: created by the authors

In addition, to verify the intensity of the crude oil signal in comparison with the calibration standard, a solution of crude oil in cyclohexane (5 mg/mL) was analysed in 10 replicates. The solution was prepared in a Class A volumetric flask (10 ml) by accurately weighing 50 mg of crude oil. All validation results were tested for normality of distribution using the Shapiro-Wilk test. The test statistic (W) values for all data sets exceeded the critical value of 0.781 (at a significance level of 0.01 and a sample size of n = 10), confirming normal distribution. Instrumental and matrix-specific characteristics were established (Table 4), demonstrating both the analytical suitability of the method and the influence of complex effects prior to the extraction stage in practical application. However, all results and their interpretation should primarily be considered in the context of the method's intended purpose, hardware configuration, and application concept. The instrumental limits of detection (LOD_{inst} = 0.15 mg/mL) and quantification (LOQ_{inst} = 0.5 mg/mL) for the configuration with the TumblIR 100 μm sampling module of the Agilent Cary 630 FTIR correspond to the expected parameters for rapid analysis while maintaining a classical instrumental-laboratory approach.

Table 4. Summary of operational characteristics of the analytical procedure

Type of sample (environmental matrix)	Operating characteristics of the analytical procedure								
	LOD_{inst}	LOQ_{inst} (MRL)	S_r, %	Bias, %	R, %	SE, %	U (k = 2.0)	SCE	
								Bias, %	R, %
Soil at natural moisture, w = 25% (n = 10)	0.15 mg/mL	0.5 mg/mL	11.07	-11.5	88.5	-13.7	±24.0	-43.5	56.5
Overwatered soil, w = 45% (n = 10)								-40.3	59.7
Surface water, drainage water, soil leachates, percolate (n = 10)			16.26	-6.2	93.8	-8.6	±31.9	-47.0	53.0

Note: LOD_{inst} – instrument limit of detection; LOQ_{inst} – instrument limit of quantification (for Transmission Cell: TumblIR_100 μm); MRL – minimum laboratory reporting level (the concentration level for which the analytical procedure performance criteria have been verified); S_r – relative standard deviation of repeatability; SE – relative systematic error (bias); U – procedural relative expanded uncertainty (p = 0.95); SCE – sample collection effects (field-homogenised composite sample)
Source: created by the authors

However, this sensitivity can be easily increased by changing the optical path length to 1,000 μm through replacing the sampling module, as provided by P. Scardina *et al.* (2014) in the FTIR method based on ASTM D7678 (2022) using DialPath 1,000 μm. For wet soils and bottom sediments, the analysis demonstrates good internal consistency (RSD ≈11%, n = 10) and a small systematic bias (bias -11.5%), indicating sufficient precision for quantitative determination of petroleum hydrocarbons in complex matrices with natural moisture content. Compared to chromatographic GC-FID methods, which showed poorer repeatability and reproducibility when working with dried soils (Sr 6.3%, SR 9.9%), as reported by M. Şenilă *et al.* (2015), the proposed approach demonstrates comparable performance without multistage extraction or sample drying. Similar relative standard deviation values (3.8-12.5%) were also reported for ultrasound-assisted centrifugal extraction with IR detection by H. Qin & H. Huang (2021). Despite some underestimation of the results (bias), the obtained values remain within the range typical of laboratory methods for petroleum hydrocarbon determination in soils with natural moisture content, according to M. Şenilă *et al.* (2015) and H. Qin & H. Huang (2021).

The obtained results indicate a high efficiency of the proposed approach for the extraction of petroleum hydrocarbons from soil matrices. In particular, the recovery of petroleum hydrocarbons during mechanical extraction reached 88.5%, which is comparable to or higher than the values reported in recent studies for the extraction of PAHs and petroleum hydrocarbons. Thus, H. Guo *et al.* (2025) demonstrated that mechanical shaking using dichloromethane provided an average recovery of polycyclic aromatic hydrocarbons of approximately 85%, whereas conventional Soxhlet extraction without sample pretreatment achieved only about 53% recovery. After solvent pretreatment of the samples, the efficiency of Soxhlet extraction increased to approximately 94%, while mechanical shaking exceeded 100% recovery for certain compounds, which the authors attributed to matrix heterogeneity and the sorption behaviour of analytes on fine-dispersed particles. The study also emphasised that mechanical shaking ensures efficient contact between the solvent and particles of wet fine-grained matrices, thereby promoting enhanced desorption of petroleum hydrocarbons. The recovery value of 88.5% obtained in the present study confirms the effectiveness of the applied approach and is consistent with current findings regarding the performance of mechanical extraction methods for the determination of petroleum hydrocarbons in complex natural matrices. At the same time, the obtained expanded measurement uncertainty values for soils (±24%) and water samples (±31.9%) correspond to typical ranges reported for environmental analyses of naturally heterogeneous objects and do not exceed the levels described in methodological guidelines and contemporary analytical studies for similar matrices.

For aqueous matrices, the analytical characteristics of the procedure remain stable: recovery is higher than in soils, close to 94%, systematic deviation is small, and precision is at a borderline but acceptable level. The increased total uncertainty and significant SCE in this case reflect real processes of losses and redistribution of petroleum hydrocarbons in the aquatic environment before analysis. In the

proposed method, cyclohexane extraction (which does not contain methyl groups and therefore does not cause interference in the 1,380 cm^{-1} region), combined with extract purification through florisil and operation at high concentrations (LOQ 0.5 mg/mL) ensured the absence of significant instrumental matrix effects. However, for application at low concentrations (especially when using 1,000 μm DialPath) additional research on potential influence is required, considering that review data on the use of FTIR spectroscopy for qualitative and quantitative analysis of organic components and TPH in soils often indicate that soil matrix spectra are largely determined by their mineral and organic composition, which requires corrections and mathematical data processing to interpret organic contaminant signals against the matrix background.

Model experiments to evaluate the contributions of Sample Collection Effects (SCE) were conducted separately for water matrices (soil percolate) and soil matrices (derno-podzolic soil) and showed significant bias: -47% (for soil percolate), -43.5% for soil (w = 45%) and -40.3% for overwatered soil (w = 45%). Recoveries at 50-60% indicate substantial heterogeneity of TPH concentration in the overall sample volume even after mixing, i.e., already before the extraction stage, which occurs due to complex interphase interactions, sorption processes, sample heterogeneity, and transformations during sampling and homogenisation. The obtained results for SCE generally confirm the importance of ensuring a sufficient number of analytical replicates and sample size if the research strategy involves assessing the average level of contamination within the study area.

In addition, a comparative assessment of several well-known analytical procedures for TPH determination in water and soil was performed using the AGREE and AGREEprep tools F. Pena-Pereira *et al.* (2020) (Table 5). Evaluation was performed using 12 AGREE criteria for the overall method and 10 AGREEprep criteria for the sample preparation stage, according to the workflow protocol. The obtained values of the integral AGREE index (Fig. 5) for the classical well-known normative methods were predictably very low: 0.20 for the gravimetric method, 0.26 for the infrared spectrophotometry method according to MVI, and 0.33 for the ASTM D7678-17 (2022) standard.

Table 5. List of TPH determination methods evaluated using AGREE/AGREEprep

No.	Name and code of the analytical procedure
I	MVI № 081/12-0645-09 (2010). WASTEWATER, SURFACE, GROUNDWATER. Method for measuring the mass concentration of petroleum products using the gravimetric method
II	MVI № 081/12-0877-13 (2014). WASTEWATER, SURFACE, GROUNDWATER. Method for measuring the mass concentration of petroleum products using infrared spectrophotometry
III	ASTM D7678 – 17 (2022). Standard test method for determination of total oil and grease (TOG) and TPH in water and wastewater by solvent extraction using mid-infrared laser spectroscopy
IV, V	Developed author's procedure for TPH analysis based on Cary 630 FTIR, Agilent Technologies. (IV – calculation of the procedural index for TPH analysis in water; V – the same in soils and bottom sediments)

Source: created by the authors

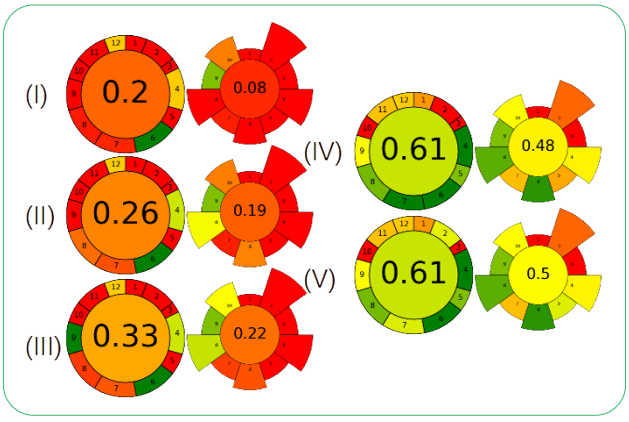

Figure 5. Results of the calculation of green indices for several well-known procedures for TPH analysis using the GREEnness analytical calculator, and the additional AGREEprep tool

Note: numbering corresponds to Table 5

Source: created by the authors based on F. Pena-Pereira *et al.* (2020)

Such values are associated with large sample volumes, multi-stage sample preparation (5-6 operations), the use of toxic organic solvents, aggressive precursor acids, and increased energy consumption. For the developed procedure, the AGREE index value was 0.61 for both water and soil matrices. This is due to smaller sample volumes, a reduced number of sample preparation stages, the transition to automation of certain operations, and a significant reduction in extractant consumption. The separate assessment of the sample preparation stage using AGREEprep showed index values in the range of 0.08-0.22 for the normative methods and 0.48-0.50 for the developed procedure. It should be noted that the assessments for the developed procedures were obtained for the configuration with a 100 μm optical path, which requires an extractant evaporation stage. When using an attachment with a larger optical path (1,000 μm), the sample preparation procedure can be shortened by eliminating this stage, which will increase the index value and corresponds to the conclusions of B. Abdykarimov *et al.* (2025). The obtained results reflect relative differences between procedures according to the criteria of GAC within the applied assessment methodology. Thus, although the method cannot be classified as fully GAC due to the use of cyclohexane as an extractant, the AGREE/AGREEprep assessment demonstrates its noticeably better procedural safety and environmental friendliness compared to classical laboratory methods.

Field study results and analysis of TPH contamination in urban, suburban, and industrial zones

Sampling from the three demonstration territories (Fig. 6) was carried out using disposable piston medical syringes, from which the connector tip was previously removed to enable the collection of solid samples by mechanical pressing. Samples were placed in clean, pre-weighed amber glass vials for headspace extraction (20 ml) with screw caps and PTFE septa. For sampling liquid matrices, medical syringes with an attached irrigation tip were used, which was immersed under the water surface. During the collection of composite water samples, equal aliquots were transferred into a vial to a total volume of approximately 10 ml.

Figure 6. Sampling of soil and water in potential TPH contamination hot spots

Note: a – study area (micro-watershed of the Lushchava River within the oil production impact zone); b – watershed of the mountainous Strymba River within the area of the oil spill accident (30.09.2023); c – urbanised micro-watershed within the Bystrytsia Solotvynska River basin (suburbs of Ivano-Frankivsk)

Source: created by the authors

To assess the average level of TPH contamination for each selected area within the urban and suburban zones of Ivano-Frankivsk, composite samples were formed from road soil and street dust samples. All samples were delivered to the laboratory (Fig. 7) for analysis. For composite samples, after mixing the entire volume, the analytical aliquot was taken in three replicates from each container, corresponding to a separate averaging area.

Figure 7. Method validation tests and analysis of field samples based on the Water Monitoring Laboratory of the Western Region of the Dniester Basin Water Resources Management, Ivano-Frankivsk

Source: created by the authors

The results of the analysis indicate that the analytical procedure is capable of correctly handling matrices of different origin – from perennial flowing waters to temporary storm runoff collected directly from puddles and watercourses along roads. In the water of the Lushchava River downstream of the potential anthropogenic impact zone, the TPH content was below the detection limit ($<LOD_{inst} = 0.15$ mg/mL) (Table 6), whereas the soil sample from the shoreline exhibited a TPH mass concentration of 211.14 mg/kg (moderate/

low contamination), indicating contact of the riverbank with oil film patches moving on the water surface and being trapped in the coastal soils downstream from the extraction area.

Table 6. Results of field sample testing of soil and water for TPH within the Lushchava River catchment area (in the operational zone of the "Dolynanaftogaz" Oil and Gas Production Department)

No.	Sample type	Sample name	Mass concentration	% of mass	U[3], % (k = 2; p = 0.95)
1	Water samples	Lushchava River (downstream of oil production influence zone)	< LOD_{inst}[1]	-	±31.9
2		Roadside and verge water flows during rainfall	3.77 mg/dm³	< LOQ_{inst}[2]	
3		Puddles and ruts filled with rainwater within 10-15 m of operating pump jack No. 1	257.93 mg/dm³	0.026	
4		Puddles and ruts filled with rainwater within 3-5 m of operating pump jack No. 1	7.35 mg/dm³	< LOQ_{inst}	
5		Shoreline of swampy water bodies adjacent to a paved road	< LOD_{inst}	-	
6		Bottom of a natural ditch along a paved road	727.00 mg/dm³	0.073	
7	Soil samples	Left bank of the Lushchava River (exposed eroded terraces, riverbank line)	211.14 mg/kg	0.021	±24.0
8		Within 10-12 m of a decommissioned well	189.97 mg/kg	0.019	
9		Within 10-12 m of operating pump jack No. 1	35,853.90 mg/kg	3.585	
10		Within 2-3 m of operating pump jack No. 1	167.92 mg/kg	0.017	
11		Within 10-12 m of operating pump jack No. 2	338.40 mg/kg	0.034	
12		Within 2-3 m of operating pump jack No. 2	16,186.58 mg/kg	1.619	
13		Inactive unpaved (field) road overgrown with reeds	25.41 mg/kg	< LOQ_{inst}	
14		Within 10-15 m of an operating well	37,265.37 mg/kg	3.727	
15		Lesya Ukrainka Street, roadside verge	691.28 mg/kg	0.07	

Note: [1] – LOD_{inst} = 0.15 mg/mL; [2] – LOQ_{inst} = 0.5 mg/mL (according to Table 3); [3] – expanded procedural uncertainty (according to Table 3)

Source: created by the authors

In samples of surface stormwater collected on roads and roadside areas, significantly higher concentrations were recorded (3.77 mg/dm³ in water streams during rainfall; 257.93 mg/dm³ in puddles and ruts within a radius of 10-15 m from the operating oil pumping unit No. 1; 7.35 mg/dm³ in puddles and ruts within a radius of 3-5 m from the operating oil pumping unit No. 1). The highest values were obtained for water from a natural ditch along a paved road (727.00 mg/dm³), confirming the role of linear elements of the drainage network as effective pathways for accumulation and transport of petroleum hydrocarbons. The obtained distribution of concentrations in water samples reflects high spatial variability caused by surface runoff formation conditions, the nature of underlying surfaces, and the influence of weather factors during the spring period. Dynamic temperature regimes and moderate precipitation contribute to the mobilisation of petroleum hydrocarbons from surface soil layers, road pavement, and anthropogenic elements, resulting in their short-term but intense input into water bodies. In this context, the obtained results demonstrate that the developed procedure provides quantitative determination of TPH in water matrices under conditions of pulse loads and abrupt concentration changes.

These observations are consistent with international data on spatial heterogeneity and migration of TPH in the environment. For example, Y. Wu *et al.* (2024) indicated that TPH concentrations in soils and water largely depend on local hydrogeological conditions, with TPH often accumulating in surface soil layers and showing limited vertical migration to groundwater due to adsorption and diffusion, which confirms the high spatial variability of contamination similar to that observed in this study. Similarly, W. Sim *et al.* (2024) showed that in industrially polluted regions, concentrations of petroleum-derived components in surface waters and bottom sediments significantly exceeded natural background levels, while the distribution patterns of TPH depended on the intensity of anthropogenic runoff and seasonal precipitation fluctuations, reinforcing the role of surface runoff as a pathway for pollutant transport.

Analysis of soil samples revealed a wide range of TPH concentrations, from 189.97 mg/kg to 37,265.37 mg/kg. In percentage terms, this corresponds to 0.019-3.73% of the sample mass. The highest TPH values were recorded in areas influenced by active oil pumping units and wells, reflecting the localised input and accumulation of petroleum components in near-surface horizons. At the same time, within the catchment area of the Lushchava River under the influence of the "Dolyanaftogaz" oil and gas production department (NGVU "Dolynanaftogaz"), significant variability in values was recorded even at comparable distances from potential sources (e.g., 189.97-35,853.90 mg/kg within a radius of 10-12 m), indicating a complex influence of microrelief, surface runoff directions, and previous anthropogenic events on the spatial distribution of pollutants. Maximum concentrations do not always

correspond to the minimum distance to the source, which emphasises the heterogeneity of contamination and the limitations of using spatial criteria alone for interpreting field measurement results. The obtained data are considered as a demonstration of the analytical capabilities of the method when working with heterogeneous soil matrices, rather than a basis for final assessment of the environmental status of the area.

Results of the analysis of water samples from the Strymba River indicate a clearly expressed longitudinal gradient of TPH concentrations downstream (Table 7, Fig. 8). The highest values were recorded in water near the accident epicentre: 18.85 mg/dm^3 in the shoreline zone with mechanically disturbed bottom sediment and visible oil films. At distances of 100-700 m downstream, concentrations decreased to 12.17 and 2.65 mg/dm^3, respectively, reflecting dilution, sedimentation, and redistribution processes of petroleum hydrocarbons in the channel system. From distances of 1.5-2 km downstream, petroleum hydrocarbon concentrations in water samples were minimal or not detected (<LOD_{inst}), indicating the limited range of their stable presence in the water phase under the given hydrodynamic regime.

Analysis of soils and bottom sediments revealed a much more complex and heterogeneous spatial distribution of petroleum hydrocarbons. In disturbed bottom sediment near the accident epicentre (319.79 mg/kg) and on eroded bank protrusions, significant differences in concentrations were recorded: 60.22 mg/kg on the right protrusion and 4,826.92 mg/kg on the left, indicating an asymmetric nature of deposition and accumulation of petroleum products. Much higher values in soils on the left bank protrusion compared to the right may be due to local flow features, channel morphology, and directions of petroleum fraction movement at the time of the accident discharge. Bottom sediments are characterised by a mosaic distribution of TPH concentrations along the flow, as noted by U. Umueni *et al.* (2025). Elevated values were found both in close proximity to the pollution source (2,063.75 mg/kg at 100 m downstream) and at certain locations more than 1 km downstream (1,476.60 mg/kg at 1.5 km and 873.23 mg/kg at 2 km). Such a distribution indicates a significant role of mechanical transport of fine silt-clay fractions, repeated resuspension of bottom sediments and their local redeposition, which is consistent with the conclusions of U. Umueni *et al.* (2025).

Table 7. Results of field sample testing of soil and water for TPH within the area of the pipeline rupture accident on 30.09.2023 on the Strymba River

No.	Sample type	Sample name	Mass concentration	% of mass	U, % (k = 2; p = 0.95)
1	Water samples	Near the accident epicentre (≈20 m), riverbank zone, disturbed bottom sediment of the Strymba River (oil films visible on the water surface)	18.85 mg/dm^3	0.002	±31.9
2		100 m downstream, water from the mechanically disturbed bottom sediment zone, depth 7-10 cm	12.17 mg/dm^3	< LOQ_{inst}	
3		700 m downstream, water from the mechanically disturbed bottom sediment zone, depth 7-10 cm	2.65 mg/dm^3	< LOQ_{inst}	
4		1.5 km downstream, water from the mechanically disturbed bottom sediment zone, depth 7-10 cm	< LOD_{inst}	-	
5		2 km downstream, water from the mechanically disturbed bottom sediment zone, depth 7-10 cm	< LOD_{inst}	-	
6	Soil samples	Near the accident epicentre (≈ 20 m), disturbed bottom sediment (oil films visible on the water surface)	319.79 mg/kg	0.032	±24.0
7		Right eroded riverbank protrusion, ≈20 m from the accident epicentre	60.22 mg/kg	0.006	
8		Left eroded riverbank protrusion, ≈20 m from the accident epicentre	4,826.92 mg/kg	0.483	
9	Bottom sediments (fine-dispersed fluvial bottom sediments of silt-clay composition)	100 m downstream, bottom sediment, depth 7-10 cm	2,063.75 mg/kg	0.206	±24.0
10		200 m downstream, bottom sediment, depth 7-10 cm	523.50 mg/kg	0.052	
11		300 m downstream, bottom sediment, depth 7-10 cm	< LOD_{inst}	-	
12		600 m downstream, bottom sediment, depth 7-10 cm	< LOD_{inst}	-	
13		850 m downstream, bottom sediment, depth 7-10 cm	540.23 mg/kg	0.054	
14		1 km downstream, bottom sediment, depth 7-10 cm	< LOD_{inst}	-	
15		1.3 km downstream, bottom sediment, depth 7-10 cm	157.98 mg/kg	0.016	
16		1.5 km downstream, bottom sediment, depth 7-10 cm	1,476.60 mg/kg	0.148	
17		2 km downstream, bottom sediment, depth 7-10 cm	873.23 mg/kg	0.087	

Source: created by the authors

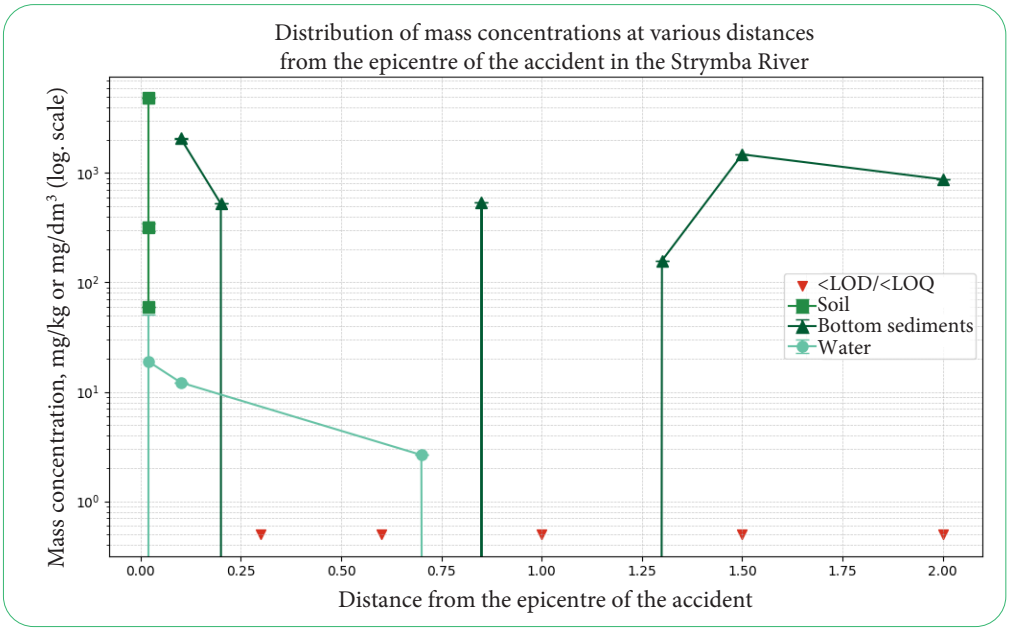

Figure 8. Integrated longitudinal concentration profile of TPH based on the analysis of different types of environmental matrices: water, soil, and bottom sediments

Source: created by the authors

The absence of a uniform decrease in concentrations with distance from the accident epicentre highlights the complexity of petroleum hydrocarbon migration processes in fluvial systems. Thus, the obtained results demonstrate that the aqueous phase responds to the accidental input of petroleum hydrocarbons mainly in a short-term and spatially limited manner, whereas shoreline soils and bottom sediments act as more inert components capable of accumulating contaminants and forming extended zones. In this context, the applied analytical procedure demonstrated stable performance for different types of environmental matrices formed both in the zone of direct accident impact and at considerable distances from the source.

Soil and street dust samples (roadside/curb mud) within the urban and suburban zones of Ivano-Frankivsk city (the urbanised part of the Bystrytsia Solotvynska micro-catchment) showed significantly higher concentrations of TPH (Table 8) compared to samples from the mountain basin of the Strymba River. In most samples, mean mass concentrations ranged within 1.6-2.8×10³ mg/kg, indicating a persistent impact of road operation, technical leaks, and accumulation of petroleum product fractions in dust and soil deposits along transportation routes M. Bayramoğlu Karşi (2025), and stormwater collectors, where these contaminations pose particular risks to aquatic ecosystems, as reported by E. Amurri *et al.* (2025) and D. Frau *et al.* (2026).

Table 8. Results of field sample tests of soil and street dust (roadside dust) for TPH within the city of Ivano-Frankivsk

No.	Sample type	Sample name	Mass concentration	% of mass	No.	U, % (k = 2; p = 0.95)
1	Soil / road dust (composite sample, combined)	Drahomyrchany village, open drainage along H9 road and Nadrichna Street: roadside soils, road dust and particulate matter, bed soils and embankment soils of roadside drainage ditches along an 850 m section	1,437.27 mg/kg	2,068.98 mg/kg	0.207	±24.0
			3,451.50 mg/kg			
			1,318.17 mg/kg			
2		Ivano-Frankivsk city, Khimikiv Street – Celevycha Street: roadside soils, dust and debris accumulations in the curb zone near stormwater inlets along a 1.5 km section	2,306.07 mg/kg	1,945.03 mg/kg	0.195	
			1,863.05 mg/kg			
			1,665.98 mg/kg			
3		Ivano-Frankivsk city, Nadrichna Street – Promyslova Street – Makohona Street – O. Kobylianska Street: roadside soils, dust and debris accumulations in the curb zone near stormwater inlets along a 1.8 km section	2,837.90 mg/kg	2,419.30 mg/kg	0.242	
			1,908.92 mg/kg			
			2,511.08 mg/kg			

Table 8. Continued

No.	Sample type	Sample name	Mass concentration	% of mass	No.	U, % (k = 2; p = 0.95)
4	Soil / road dust (composite sample, combined)	Ivano-Frankivsk city, P. Orlyk Street – Belvederska Street – Pivnichnyi Boulevard – Korolya Danyla Street: roadside soils, dust and debris accumulations in the curb zone near stormwater inlets along a 2 km section	2,655.02 mg/kg 2,455.18 mg/kg 3,276.09 mg/kg	2,795.43 mg/kg	0.280	±24.0
5		Krykhivtsi village, Priozerna Street, near the water intake structures of the city lake on the mlynivka Stebnytska River: roadside soils, dust and debris accumulations along the channel edges in puddle formation zones	573,037.18 mg/kg 650,435.55 mg/kg 179,126.25 mg/kg	4,67532.99 mg/kg	46.753	
6	Water samples	Krykhivtsi village, Priozerna Street, near the water intake structures of the city lake on the mlynivka Stebnytska River: puddles at the edge of the water distribution structure	433.82 mg/dm³		0.043	±31.9

Source: created by the authors

The highest values were recorded in roadside deposits along the sections of Nadrychna St. – Promyslova St. – Makohona St. – O. Kobylianska St. (point 3) and P. Orlyk St. – Belvederska St. – Northern Boulevard – King Danylo St. (point 4), which is consistent with traffic intensity. A distinct case is the sample from Krykhivtsi village, where mass concentrations reached 4.7-6.5×10^5 mg/kg (mean 4.7×10^5 mg/kg), which is an order of magnitude higher than at other sampling points. Such elevated values in direct contact with the water intake structures of the city lake on the mlynivka Stebnytska river channel are a consequence of vehicular traffic along a road constructed with environmental violations along the protective riparian strip. The presence of puddles with fuel films and the accumulation of dust/debris with high petroleum hydrocarbon content in the riparian zones create high local threats and risks to the urban aquatic ecosystem. Rainwater puddles at this location also contained a very high measurable amount of petroleum hydrocarbons (433.82 mg/dm^3), confirming the potential for pollutant migration from surface accumulations into water bodies under conditions of standing water and limited self-purification in the urban hydrological network.

Therefore, the results of field investigations within the urban microcatchment of the Bystrytsia Solotvynska river confirm that the main mechanisms of petroleum hydrocarbon transport and accumulation are surface sealing, artificial runoff routing, accumulation of dust and debris in curb zones, and the untreated discharge of stormwater into the water body. Thus, for each of the three studied territories, a pronounced spatial-typological heterogeneity of TPH distribution was observed, manifested as local zones of elevated concentrations in close proximity to potential pollution sources (oil and gas infrastructure, accidental spills, urban runoff) and varying degrees of pollutant migration through aquatic and terrestrial media.

It should be noted that at the scale of microcatchments and small-order catchments, the effects of pulse loadings formed during precipitation, snowmelt, or accidental events are also significant and more traceable. The identification, quantitative assessment, and control of the first flush (FF) are considered critically important in urban stormwater management Z. Gao *et al.* (2023). This well-known "first flush" concept describes how pollutants accumulated on soil surfaces, road pavements, drainage channels, and other anthropogenic landscape elements can be rapidly mobilised and transported into the watercourse as a short-term but highly concentrated runoff M. Maniquiz-Redillas *et al.* (2022). Such a mechanism is typical and may have critical consequences for small catchments, where the ratio of catchment area to pollutant source area is small and hydrological processes are highly dependent on local conditions (precipitation intensity, surface condition, imperviousness, presence of drainage channels). Consequently, risks may arise not from average background pollution levels in water, but from short-term concentration peaks that have substantial ecological impacts, especially when such peaks recur or coincide with additional stressors (low flow, high temperatures, reduced dissolved oxygen).

The results of field investigations conducted across three distinct types of environments-an oil-production micro-catchment (Lushava), an accident-affected mountainous stream (Strymba), and an urban basin (Ivano-Frankivsk, Bystrytsia Solotvynska River) – indicate a common fundamental mechanism governing the spatiotemporal dynamics of TPH. In all cases, the observed behaviour is consistent with the FF concept and the pulse-driven nature of hydrological contaminant mobilisation. As demonstrated in recent studies by Z. Gao *et al.* (2023), the first flush effect is characteristic of small- and medium-sized catchments, where short-term peak discharges during rainfall or snowmelt events lead to the rapid wash-off of surface-accumulated pollutants. Moreover, M. Maniquiz-Redillas *et al.* (2022) emphasise that the key controlling factor is not the mean contamination level but rather short-term peak concentrations generated by intensive wash-off from anthropogenic and natural surfaces.

This behaviour is most pronounced in the urban environment of Ivano-Frankivsk. Elevated TPH concentrations in roadside soils and in accumulated road dust and debris (approximately 1.6-2.8×10^3 mg/kg at most sampling points

and up to 4.7×10^5 mg/kg at local hotspots) indicate a substantial surface reservoir of contaminants. Under conditions of a high proportion of impervious surfaces, a well-developed system of curbs and stormwater inlets, and engineered surface runoff pathways, an environment is formed that strongly facilitates the first flush mechanism. Measured TPH concentrations in rainwater puddles (433.82 mg/dm^3) and roadside drainage channels confirm that the initial phase of precipitation rapidly mobilises accumulated petroleum fractions, generating short-term but highly elevated peak loads to the drainage network. Thus, urban conditions combine both substantial contaminant accumulation and highly efficient pulse-driven transport into the aquatic system, which is consistent with the classical manifestation of FF as the dominant process in urban runoff.

A similar mechanism is observed in the Lushava catchment, although with a different spatial organisation of processes. Despite relatively low concentrations in the water phase (up to 727 mg/dm^3 in drainage elements), soils in the vicinity of anthropogenic impact sources exhibit very high TPH levels (up to 37,265 mg/kg). This indicates the formation of local contamination depots that do not continuously interact with the aquatic phase and are activated only under specific hydro-meteorological conditions. In this context, the first flush effect manifests as an episodic mobilisation mechanism, whereby precipitation or surface runoff events trigger the short-term release of petroleum hydrocarbons from soil reservoirs into watercourses. A characteristic feature is the pronounced variability of concentrations in the water phase, including values below detection limits, confirming the pulsed nature of contaminant inputs. In the case of an accidental oil pipeline rupture above the Strymba River channel, a spatially extended variant of the first flush effect is observed. At the impact zone, a sharp peak in water concentration is recorded (18.85 mg/dm^3), followed by a rapid downstream decrease. At the same time, a highly heterogeneous and mosaic pattern of TPH accumulation develops in bottom sediments and soils, including secondary maxima located more than 1 km downstream (873-1,476 mg/kg).

A key process is that a portion of petroleum hydrocarbons, after initial deposition, is not removed from the system but becomes buried within bottom sediments through mechanical coverage by sediment layers. These buried fractions remain potentially mobile and can be re-released into the water column during hydrodynamic disturbances of the riverbed, such as floods, intense rainfall events, erosional processes, or mechanical disruption of sediments (e.g., by riparian root systems). This leads to a phenomenon of secondary pulsed remobilisation, which can be interpreted as a "buried first flush" (buried FF), i.e., a reactivation of contaminant release from sedimentary reservoirs. In this context, the first flush process in mountainous streams acquires a multi-phase character, comprising an initial hydrological impulse in the water phase and a delayed but reactivated sediment-associated impulse linked to periodic remobilisation of contaminated bottom deposits. Overall, the results demonstrate that the first flush is a universal mechanism governing TPH mobilisation across different catchment types. However, its manifestation strongly depends on landscape structure, contaminant source characteristics, and hydrological regime. In all cases, risk is governed not by mean concentrations but by the magnitude and recurrence of pulse loadings, which is consistent with modern interpretations of the FF concept.

In this context, the developed and tested analytical procedure for quantitative determination of TPH provides a consistent quantitative basis across different matrices (various water matrices, soil, bottom sediments, road dust/debris), which is a necessary condition for the correct construction of risk matrices and pollutant transport scenarios and for integrated risk assessment. These assessments involve analysis of several components: (I) characterisation of sources and their potential activity, (II) evaluation of transport pathways (surface runoff, drainage networks, groundwater flow, transport to bottom sediments), (III) quantitative evaluation of concentrations in different matrices reflecting both current pollution and accumulation, and (IV) determination of the frequency and intensity of pulse events generating peak loads. Such approaches allow the construction of risk matrices that reflect not only mean pollution levels but also the probability of hazardous pulse states. Consequently, integrated risk assessment in microcatchments can be used to identify priority monitoring zones, develop emergency response scenarios, evaluate the effectiveness of measures to limit pollutant transport, and support management decisions aimed at minimising short-term peak impacts and long-term pollution accumulation.

Conclusions

Although FTIR methods are widely used for the determination of petroleum and hydrophobic organic contaminants in environmental matrices due to their speed and relative simplicity, they are generally considered to have inherent limitations in selectivity and sensitivity compared to other analytical techniques, such as gas chromatography coupled with mass spectrometric detection (GC-MS) or GC-FID methods for TPH in water/soil. At the same time, studies evaluating the optimisation and validation of FTIR methods using similar approaches (e.g., the use of alternative solvents or other conceptual modifications) demonstrate that the FTIR analytical approach can, conversely, be significantly faster and more efficient for diagnostic and monitoring purposes, owing to the capabilities of modern FTIR spectrometer designs, which allow sample preparation to be modified and adapted more effectively.

Field testing of environmental samples in selected areas showed that the proposed method enables rapid and reliable quantification of TPH mass concentrations in various matrices (water, soil, sediments, road dust/deposits) with acceptable procedural uncertainty, as confirmed by validation. The obtained quantitative data demonstrated a wide range of contamination levels depending on the type of matrix and proximity to anthropogenic sources. In soils,

TPH concentrations varied from 189.97 to 37,265.37 mg/kg, with local maxima exceeding 16,000-35,000 mg/kg in areas influenced by oil extraction infrastructure. In urban roadside deposits, mean concentrations were typically within 1.6-2.8×10^3 mg/kg, while extreme values reached 4.7-6.5×10^5 mg/kg in zones of direct technogenic impact. In water samples, concentrations ranged from below the detection limit (<0.15 mg/dm^3) in river water to 3.77-727.0 mg/dm^3 in surface runoff and drainage elements, indicating strong pulse-driven variability of contamination. The described sampling procedure is aligned with the analytical method and is focused on assessing primary pollutant transport pathways (rills, drainage channels) and extends the "first flush" concept for further application of the obtained data in spatial contamination dispersion models and environmental risk assessment. This approach is an important step in studying contaminant migration, as these hydrocarbons may be the most mobile under flowing water conditions and thus contribute to the further spread of pollution in ecosystems. The procedure facilitates adaptation of sampling to the needs of rapid environmental assessment of urban and industrial areas within the framework of comprehensive and integrated environmental analysis and risk assessment in low-order catchments.

Further research should be directed toward applying the validated analytical procedure for quantitative determination of petroleum hydrocarbons within integrated risk assessments of micro-catchments, involving modelling of hydrological regimes and transport processes (surface runoff, drainage networks, sediments), as well as quantitative consideration of both impulsive and chronic cyclical loadings. Such an approach allows obtaining quantitative parameters necessary for constructing risk matrices and scenarios, assessing the resilience of aquatic ecosystems, and making management decisions to minimise both short-term peak impacts and long-term accumulation of petroleum pollutants.

Acknowledgements

We express our sincere gratitude to the Head of the Water Monitoring Laboratory of the Western Region of the Dniester Basin Water Resources Management, Mr. M. Zasidko, for providing the laboratory base for conducting research work within the framework of the Memorandum of Cooperation and the joint implementation of innovative scientific studies.

Funding

This research received no external funding.

Conflict of Interest

None.

References

[1] Abdykarimov, B., Alimzhanova, M., López-Serna, R., & Syrgabek, Y. (2025). Green analytical procedure index assessment for total petroleum hydrocarbons determination methods in soil and sediments. A review. *Trends in Environmental Analytical Chemistry*, 46, article number e00262. doi: 10.1016/j.teac.2025.e00262.

[2] Adeniji, A.O., Okoh, O.O., & Okoh, A.I. (2017). Analytical methods for the determination of total petroleum hydrocarbons distribution in water and sediments of aquatic systems: A review. *Journal of Chemistry*, 2017(1), article number 5178937. doi: 10.1155/2017/5178937.

[3] Amurri, E., Molnar, I., & Magill, C.R. (2025). Origins and fate of polycyclic aromatic hydrocarbons (PAHs) in sustainable drainage systems (SuDS) in a Scottish urban area: Implications for groundwater systems. *Journal of Contaminant Hydrology*, 276, article number 104767. doi: 10.1016/j.jconhyd.2025.104767.

[4] ANSI/NCSL Z540-2-1997. (1997). *U.S. Guide to the expression of uncertainty in measurement*. Retrieved from https://ncsli.org/page/z5402.

[5] ASTM D7678-17. (2022). *Standard test method for determination of total oil and grease (TOG) and total petroleum hydrocarbons (TPH) in water and wastewater by solvent extraction using mid-infrared laser spectroscopy*. Retrieved from https://store.astm.org/d7678-17.html.

[6] Bayramoğlu Karşi, M.B. (2025). Investigation of oil and grease in surface soils of gas station, automobile repair workshop, urban, recreational area, and rural sites using FT-IR. *Accreditation and Quality Assurance*, 30, 153-165. doi: 10.1007/s00769-024-01624-8.

[7] Campos, I., & Abrantes, N. (2021). Forest fires as drivers of contamination of polycyclic aromatic hydrocarbons to the terrestrial and aquatic ecosystems. *Current Opinion in Environmental Science & Health*, 24, article number 00293. doi: 10.1016/j.coesh.2021.100293.

[8] DSTU ISO 16703:2007. (2007). *Soil quality. Determination of hydrocarbon content in the range C10 to C40 by gas chromatography*. Retrieved from https://online.budstandart.com/ua/catalog/doc-page.html?id_doc=53560.

[9] DSTU ISO 9377-2:2015. (2015). *Water quality. Determination of petroleum hydrocarbons in water. Part 2. Method using solvent extraction and gas chromatography*. Retrieved from https://online.budstandart.com/ua/catalog/doc-page.html?id_doc=73832.

[10] DSTU ISO/TR 11046:2001. (2001). *Soil quality. Determination of mineral oil content. Method by infrared spectrometry and gas chromatography*. Retrieved from https://online.budstandart.com/ua/catalog/doc-page?id_doc=48499.

[11] Frau, D., Gutierrez, M.F., & López, E. (2026). The role of precipitation events in the water quality of a buffer urban ecosystem. *Environmental Monitoring and Assessment*, 198, article number 54. doi: 10.1007/s10661-025-14911-9.

[12] Fuente-Ballesteros, A., Ares, A.M., & Bernal, J. (2025). Paving the way towards green contaminant analysis: Strategies and considerations for sustainable analytical chemistry. *Green Analytical Chemistry*, 12, article number 100221. doi: 10.1016/j.greeac.2025.100221.
[13] Gao, Z., Zhang, Q., Li, J., Wang, Y., Dzakpasu, M., & Wang, X.C. (2023). First flush stormwater pollution in urban catchments: A review of its characterization and quantification towards optimization of control measures. *Journal of Environmental Management*, 340, article number 117976. doi: 10.1016/j.jenvman.2023.117976.
[14] Guo, H., Samadi, N., Firoozbakht, M., Kuznetsova, A., & Siddique, T. (2025). Pre-treatment with extraction solvent yields higher recovery: Method optimisation for efficient determination of polycyclic aromatic hydrocarbons in organic-rich fine-textured wastes. *Journal of Environmental Quality*, 54(5), 1033-1044. doi: 10.1002/jeq2.70033.
[15] Hammad, S.F., Hamid, M.A.A., Adly, L., & Elagamy, S.H. (2025). Comprehensive review of greenness, whiteness, and blueness assessments of analytical methods. *Green Analytical Chemistry*, 12, article number 100209. doi: 10.1016/j.greeac.2025.100209.
[16] Havryliuk, R., Shpak, O., Lohvynenko, O., & Zapolskiy, I. (2024). Methodical aspects of the assessment of the state of subsur face contamination with petroleum products caused by the military aggression of the Russian Federation against Ukraine. *Bulletin of V.N. Karazin Kharkiv National University, Series "Geology. Geography. Ecology"*, 61, 23-38. doi: 10.26565/2410-7360-2024-61-02.
[17] Herasymenko, B. (2024). Contamination of soil cover with hydrocarbons in case of emergency leaks from oil and gas pipelines: Analysis of the problematic state. *Modern Engineering and Innovative Technologies*, 1(34-01), 181-190. doi: 10.30890/2567-5273.2024-34-00-025.
[18] Hrytsuliak, H., Kotsiubynskyi, A., Zarytskyi, V., Solomchak, D., Lynnyk, D., Kalyn, T., & Bohdan, H. (2025). Restoration of oil-contaminated soils by cultivating plants for phytoremediation. In *Systems, decision and control in energy* (pp. 617-625). Cham: Springer Nature Switzerland. doi: 10.1007/978-3-031-90466-0_26.
[19] Imam, A., Suman, S.K., Ghosh, D., & Kanaujia, P.K. (2019). Analytical approaches used in monitoring the bioremediation of hydrocarbons in petroleum-contaminated soil and sludge. *TrAC Trends in Analytical Chemistry*, 118, 50-64. doi: 10.1016/j.trac.2019.05.023.
[20] Ingersoll, W. (2003). *QC-base uncertainty SOP*. The USA: US Navy Naval Sea Systems Command Laboratory Quality and Accreditation Office.
[21] ISO/IEC 17025:2017. (2017). *General requirements for the competence of testing and calibration laboratories*. Retrieved from https://www.iso.org/standard/66912.html.
[22] Knight, A.T., *et al.* (2019). Improving conservation practice with principles and tools from systems thinking and evaluation. *Sustainability Science*, 14(6), 1531-1548. doi: 10.1007/s11625-019-00676-x.
[23] Kuzmenko, E., Bahriy, S., Shtohryn, M., & Dzioba, U. (2025). Determination of sources of groundwater pollution by petroleum products (on the example of the Solotvyno area in the Carpathian region). *Bulletin of Taras Shevchenko National University of Kyiv. Geology*, 3(86), 40-47. doi: 10.17721/1728-2713.86.06.
[24] Maniquiz-Redillas, M., Robles, M.E., Cruz, G., Reyes, N.J., & Kim, L.H. (2022). First flush stormwater runoff in urban catchments: A bibliometric and comprehensive review. *Hydrology*, 9(4), article number 63. doi: 10.3390/hydrology9040063.
[25] MVI No 081/12-0645-09. (2010). *Wastewater, surface, groundwater. Method for measuring the mass concentration of petroleum products using the gravimetric method*. Retrieved from https://zakon.isu.net.ua/sites/default/files/normdocs/mbb_081_12-0645-09.pdf.
[26] MVI No. 081/12-0116-03. (2004). *Soils. Method for measuring the mass fraction of petroleum products by the gravimetric method*. Retrieved from https://online.budstandart.com/ua/catalog/doc-page?id_doc=76437.
[27] MVI No. 081/12-0725-10. (2011). *Soils. Method for measuring the mass fraction of petroleum products (non-polar hydrocarbons) by the gravimetric method*. Retrieved from https://surl.li/gdntcq.
[28] MVI No. 081/12-0877-13. (2014). *Wastewater, surface, groundwater. Method for measuring the mass concentration of petroleum products using infrared spectrophotometry*. Retrieved from https://zakon.isu.net.ua/sites/default/files/normdocs/0877-13.pdf.
[29] Mykytsei, M., Kundelska, T., Yatsyshyn, T., & Hrytsuliak, H. (2024). Research on the level of "urban stream syndrome" in small streams of urbanised areas using the example of the Mlynivka River (Ivano-Frankivsk City). In *Systems, decision and control in energy* (pp. 613-627). Cham: Springer Nature Switzerland. doi: 10.1007/978-3-031-67091-6_29.
[30] Mykytsey, M.T. (2024). Conceptual basis for the search and eco-diagnostics of risk zones in watersheds. *Man and Environment. Issues of Neoecology*, 42, 51-69. doi: 10.26565/1992-4224-2024-42-04.
[31] Pena-Pereira, F., Wojnowski, W., & Tobiszewski, M. (2020). AGREE-analytical GREEnness metric approach and software. *Analytical Chemistry*, 92(14), 10076-10082. doi: 10.1021/acs.analchem.0c01887.
[32] Płotka-Wasylka, J., & Wojnowski, W. (2021). Complementary green analytical procedure index (ComplexGAPI) and software. *Green Chemistry*, 23(21), 8657-8665. doi: 10.1039/d1gc02318g.

[33] Qin, H., & Huang, H. (2021). A method for determining the content of petroleum hydrocarbons in soil. *International Journal of Scientific Research and Management*, 9(3), 40-55. doi: 10.18535/ijsrm/v9i3.c01.
[34] Resolution of the Cabinet of Ministers of Ukraine No. 610-r "On Approval of the Concept of the State Target Environmental Monitoring Program". (2023, July). Retrieved from https://zakon.rada.gov.ua/laws/show/610-2023-%D1%80#Text.
[35] Richardson, J.S. (2019). Biological diversity in headwater streams. *Water*, 11(2), article number 366. doi: 10.3390/w11020366.
[36] Rostron, P.D., Heathcote, J.A., & Ramsey, M.H. (2014). Comparison between *in situ* and *ex situ* gamma measurements on land areas within a decommissioning nuclear site: A case study at Dounreay. *Journal of Radiological Protection*, 34, 495-508. doi: 10.1088/0952-4746/34/3/495.
[37] Scardina, P., Copeta, G., & Teragni, P. (2014). *Analysis of oil in water using the Agilent Cary 630 FTIR: Solutions for your analytical business*. Italy: Agilent Technologies.
[38] Şenilă, M., Levei, E., Şenilă, L.R., Cadar, O., Roman, M., & Miclean, M. (2015). Analytical capability and validation of a method for total petroleum hydrocarbon determination in soil using GC-FID. *Studia Universitatis Babes-Bolyai. Chemia*, 60(2), 137-146.
[39] Sim, W., Ekpe, O.D., Lee, E.H., Arafath, S.Y., Lee, M., Kim, K.H., & Oh, J.E. (2024). Distribution and ecological risk assessment of priority water pollutants in surface river sediments with emphasis on industrially affected areas. *Chemosphere*, 352, article number 141275. doi: 10.1016/j.chemosphere.2024.141275.
[40] Simion, A.F., Găman, A.N., & Lăutaru, V.A. (2022). Analysis of total content of petroleum products in water by using FTIR spectroscopy. *MATEC Web of Conferences*, 373, article number 00063. doi: 10.1051/matecconf/202237300063.
[41] Troshyn, M., Kyslytsia, L., & Pushkash, O. (2025). The impact of gas stations (GS) on the environment. In *VIII international scientific and practical conference "Education and science of today: Intersectoral issues and development of sciences"* (pp. 343-348). Cambridge: ΛΌΓΟΣ. doi: 10.36074/logos-09.05.2025.072.
[42] Trysniuk, V.M., Okharyev, V.O., Trysniuk, T.V., & Holovan, Yu.M. (2020). Environmental monitoring system for soil contamination by petroleum products. *Environmental Safety and Natural Resources*, 34(2), 22-29. doi: 10.32347/2411-4049.2020.2.22-29.
[43] Umueni, U.E., Etukudo, N.J., Okoye, P.I., Okpoji, A.U., Eze, V.C., Aningo, G.N., Ekwere, I.O., & Garuba, M.H. (2025). Geochemical and ecological risk assessment of petroleum hydrocarbons in sediments of the Forcados River, Delta State. *Asian Journal of Geographical Research*, 8(4), 287-298. doi: 10.9734/ajgr/2025/v8i4337.
[44] Wang, H., Rajesh, L., Ganesh, K., Lopes, A.R., Hoelen, T.P., & Lowry, G.V. (2026). Comparison of robot-deployable sensing methods for autonomous in-field screening of total petroleum hydrocarbons. *Journal of Hazardous Materials*, 503, article number 141208. doi: 10.1016/j.jhazmat.2026.141208.
[45] Wang, L., Cheng, Y., Lamb, D., & Naidu, R. (2020). The application of rapid handheld FTIR petroleum hydrocarbon-contaminant measurement with transport models for site assessment: A case study. *Geoderma*, 361, article number 114017. doi: 10.1016/j.geoderma.2019.114017.
[46] Wang, L., Cheng, Y., Naidu, R., & Bowman, M. (2021). The key factors for the fate and transport of petroleum hydrocarbons in soil with related *in/ex situ* measurement methods: An overview. *Frontiers in Environmental Science*, 9, article number 756404. doi: 10.3389/fenvs.2021.756404.
[47] Wu, Y., Yu, J., Huang, Z., Jiang, Y., Zeng, Z., Han, L., Deng, S., & Yu, J. (2024). Migration of total petroleum hydrocarbon and heavy metal contaminants in the soil-groundwater interface of a petrochemical site using machine learning: Impacts of convection and diffusion. *RSC Advances*, 14(44), 32304-32313. doi: 10.1039/d4ra06060a.
[48] Yue, Z., Shi, Q., Ai, J., Peng, S., Miao, X., & Wang, Z. (2021). Review of analytical methods for petroleum hydrocarbons in water and sediments of aquatic systems. *IOP Conference Series: Earth and Environmental Science*, 621, article number 012011. doi: 10.1088/1755-1315/621/1/012011.

Нафтові вуглеводні в ґрунтових та водних матрицях: випробування нової процедури експрес-екстракції та FTIR-спектроскопії для інтегрованої оцінки ризиків на мікро- та низькопорядкових водозборах

Михайло Микицей
Аспірант, провідний хімік
Івано-Франківський національний технічний університет нафти і газу
76019, вул. Карпатська, 15, м. Івано-Франківськ, Україна
Лабораторія моніторингу вод і ґрунтів Західного регіону Дністровського БУВР
76014, вул. Української Перемоги, 23а, м. Івано-Франківськ, Україна
https://orcid.org/0000-0003-2613-7729
Ярослав Адаменко
Доктор технічних наук, професор
Івано-Франківський національний технічний університет нафти і газу
76019, вул. Карпатська, 15, м. Івано-Франківськ, Україна
https://orcid.org/0000-0001-5665-7958
Вікторія Навроцька
Магістр, хімік
Івано-Франківський національний технічний університет нафти і газу
76019, вул. Карпатська, 15, м. Івано-Франківськ, Україна
Лабораторія моніторингу вод і ґрунтів Західного регіону Дністровського БУВР
76014, вул. Української Перемоги, 23а, м. Івано-Франківськ, Україна
https://orcid.org/0009-0002-5408-7554

Анотація. Метою дослідження було розробити швидкий і ефективний підхід, чим забезпечити можливість подальшої інтегрованої оцінки ризиків у мікро- та низькопорядкових водозборах. Процедура передбачала альтернативний підхід до відбору зразків, швидку одноетапну екстракцію циклогексаном, очищення екстракту через флорисил, концентрування та аналіз на FTIR-спектрометрі Agilent Cary 630 із пробовідбірним модулем TumblIR 100 з можливою адаптацією під 1 000 мкм, або інші комерційно доступні системи, для досягнення нижчих концентрацій. Результати валідаційних випробувань показали, що для ґрунтових матриць (вологий ґрунт, донні осади) метод забезпечує добру внутрішню узгодженість відносний стандартний відхил ≈11 % (n = 10) та систематичне зміщення ≈-11,5 %, при відновленні 88,5 %. Розширена невизначеність вимірювань становить ±24 % для ґрунту та ±31,9 % для води, що відповідає типовим рівням для цих екологічних матриць. Для водних матриць (поверхневі та дренажні води, ґрунтові змиви, перколяти) відновлення перевищує 94 %, систематичне зміщення є невеликим, а прецизійність знаходиться на прийнятному рівні. При цьому модельні експерименти для оцінки ефектів стратегії відбору зразків показали значні систематичні зсуви: -47 % для ґрунтового перколяту, -43,5 % для ґрунту (w = 45 %) та -40,3 % для перезволоженого ґрунту, що свідчить про неоднорідність розподілу ТРН у пробах до етапу екстракції. Оцінка за індексами зеленої аналітичної хімії з використанням інструментів AGREE та AGREEprep показала переваги розробленої методики над класичними нормативними процедурами: інтегральний індекс AGREE для розробленого методу становить 0,61 (у порівнянні з 0,20-0,33 для гравіметричного методу, ІЧ-методики за МВВ та ASTM D7678-17. Було встановлено, що в межах Івано-Франківська концентрації в складі дорожнього пилу та придорожніх ґрунтах становили 1,6-2,8×10^3 мг/кг, а локально – до 4,7-6,5×10^5 мг/кг, що обумовлює високі ризики, пов'язані з імпульсним навантаженням під час опадів, змивом забруднювачів у дощові колектори з подальшим потраплянням у річку Бистрицю Солотвинську

Ключові слова: пробопідготовка; валідація методу; невизначеність вимірювань; матричні ефекти; забруднення водозборів

Vol. 17, No. 1
2026

Ecological Safety and Balanced Use of Resources

ISSN (print) 2415-3184, ISSN (online) 2522-9508
Journal homepage: https://esbur.com.ua/en

Received: 08.12.2025. Revised: 29.04.2026. Accepted: 12.06.2026. Published: 30.06.2026.

UDC 550.42:504.5:631.48

DOI: 10.63341/esbur/1.2026.30

Multi-index geochemical assessment of urban soil contamination under technogenic pressure

Olga Mislyuk
PhD in Chemical Sciences, Associate Professor
Cherkasy State Technological University
18006, 460 Shevchenko Blvd., Cherkasy, Ukraine
https://orcid.org/0000-0003-0401-9836

Oksana Yehorova*
PhD in Technical Sciences, Associate Professor
Cherkasy State Technological University
18006, 460 Shevchenko Blvd., Cherkasy, Ukraine
https://orcid.org/0000-0002-7801-5582

Olena Khomenko
PhD in Chemical Sciences, Associate Professor
Cherkasy State Technological University
18006, 460 Shevchenko Blvd., Cherkasy, Ukraine
https://orcid.org/0000-0001-9329-0577

Oleksandr Loboda
Doctor of Chemical Sciences, Associate Professor,
Cherkasy State Technological University
18006, 460 Shevchenko Blvd., Cherkasy, Ukraine
https://orcid.org/0000-0001-5524-3251

Abstract. Soil contamination with heavy metals is becoming an increasingly serious problem worldwide. For this reason, a comprehensive quantitative assessment of the quality status of urban soils under technogenic pressure is important for understanding contamination patterns and potential ecological risks. The aim of this study was to conduct a spatiotemporal analysis of heavy metal contents and assess their impact on the urban soils of Cherkasy, as well as to identify sources of contamination for informed management decisions. Risk assessment was carried out using a multi-index geochemical approach, employing single-factor indices (geoaccumulation index Igeo, pollution index PI, ecological risk index Er) and composite indices (pollution load index PLI, Nemerow index, and potential ecological risk index RI). Statistical correlation analysis was used to identify probable sources of contamination. The analysis revealed significant spatial variations in metal concentrations. The coefficient of variation (CV) for Mn, Zn, Pb, Cu, and Cd was high (51% < CV ≤ 100%) across different sites, indicating strong spatial heterogeneity. In contrast, Ni showed moderate variation (21% < CV ≤ 50%), suggesting a natural-anthropogenic origin in the soil. A strong correlation between Pb and Cu indicated shared sources of pollution, likely from thermal power plants, paint and electrical manufacturing enterprises, and motor transport. High correlation coefficients between Ni and Mn suggest a mixed influence of geogenic (soil erosion) and anthropogenic sources (machinery and chemical industry enterprises, thermal power plants, and motor transport). A significant potential ecological risk for soil ecosystems was identified for Cd contamination in the study area. The multi-index approach to assessing heavy metal contamination across different

Suggested Citation: Mislyuk, O., Yehorova, O., Khomenko, O., & Loboda, O. (2025). Multi-index geochemical assessment of urban soil contamination under technogenic pressure. *Ecological Safety and Balanced Use of Resources*, 17(1), 30-48. doi: 10.63341/esbur/1.2026.30.

*Corresponding author (*ok.yehorova@chdtu.edu.ua*)

urban locations showed that the most critical situations occurred in the southeastern and eastern industrial hubs. In residential-industrial areas, urban soils predominantly exhibited low to moderate contamination levels. Cadmium (Cd) was identified as the main potentially ecologically hazardous metal. The results of this study can serve as a basis for the development and implementation of targeted risk management strategies

Keywords: heavy metals; urban soils; correlations; spatial variability; ecological risk; anthropogenic impact

Introduction

Rapid urban growth and industrial development are closely linked to the accumulation of heavy metals in urban soils. These pollutants pose serious risks to urban ecosystems and are a growing concern at local, regional, and global scales. As cities expand and population density increases, along with intensified industrial and infrastructural activity, more potentially toxic elements are introduced into the environment and gradually build up in surface soils over time. Because these substances are persistent and do not break down naturally, they can enter food chains and ultimately threaten ecosystem balance and human health. For this reason, monitoring and assessing heavy metal contamination in urban soils has become an essential part of sustainable urban environmental management and the protection of public health.

L.S. Mustapha *et al.* (2025) noted that soil contamination by heavy metals constituted a serious contemporary environmental issue, driven by their resistance to biodegradation, toxicity, and their capacity for geoaccumulation and bioaccumulation. Q. Yang *et al.* (2018) observed that the content and variability of heavy metal concentrations in soils were largely determined by the parent material and the geological background of a given area. However, intensive anthropogenic activity significantly altered these patterns. Soil formed the foundation of terrestrial ecosystems and served as the primary sink for most environmental pollutants. As noted by L. He *et al.* (2023), heavy metals typically originated from various sources, including industrial activities, fossil fuel combustion, transportation, and waste disposal. They could enter soils from both local and distant emission sources and might therefore be deposited *in situ* or, when adsorbed onto dust particles, transported over considerable distances by air currents. Once released into the atmosphere, metals contaminated urban landscapes through dry or wet deposition. Following atmospheric deposition into soils, metals exhibited significantly greater mobility than those already present in the soil matrix, due to their higher reactivity. Although the concentration of atmospheric metals was relatively low, their hazard could exceed that of metals already present in soils. Y. Zhou *et al.* (2022) emphasised that urban landscapes in industrial zones and roadside areas were most heavily affected due to multiple sources of industrial emissions and intense traffic flows. The degree of contamination increased with proximity to the emission source. The accumulation of heavy metals led to soil degradation, disrupted the functioning of soil ecosystems, and posed a threat to human health. A significant presence of heavy metals in urban soils was considered an indicator of urban environmental quality, and the assessment of topsoil contamination in populated areas represented one of the key environmental challenges facing modern cities. It was therefore essential to identify potential sources of pollution, assess the risk of heavy metal contamination in soils, and propose effective remediation strategies.

The most promising approach for identifying areas of elevated environmental hazard is the comprehensive assessment of potential ecological risk. This approach makes it possible to determine acceptable levels of anthropogenic pressure in order to maintain the balance of the natural environment and ensure the regeneration of its key components, as well as to support informed decision-making aimed at minimising anthropogenic impacts. A key element in the comprehensive quantitative assessment of the ecological state of soil, as a fundamental component of technogenically impacted ecosystems contaminated by heavy metals, is the use of pollution indices (indicators). J.B. Kowalska *et al.* (2018) compared the similarities and differences among 18 indices proposed by various researchers for assessing the levels and risks of soil contamination by heavy metals. Each coefficient or index provides information on the individual levels of contamination by each analysed heavy metal; the overall extent of pollution; the sources of heavy metals; the potential ecological risk; areas with the highest potential risk of heavy metal accumulation; and the capacity of the surface soil horizon to accumulate heavy metals.

An important role in the determination of certain pollution indices is played by the establishment of an appropriate geochemical background, which should be based on soil- and site-specific criteria, as well as on the purpose and scale of the heavy metal impact assessment. The selection of an appropriate index is crucial for correctly interpreting contamination levels, identifying the origin of heavy metals, and evaluating potential ecological risks. In this context, both land-use types (agricultural, forest, and urban areas) and the purpose of calculating pollution indices should be taken into account. Moreover, a multi-index approach can be highly valuable for predicting the future resilience of ecosystems. S.L.C. Ferreira *et al.* (2022) noted that the application of a single index often fails to provide a comprehensive representation of soil contamination levels and the associated ecological risks, which may lead to biased assessment results and negatively affect the scientific validity of environmental quality management. Studies by Z. Yu *et al.* (2021) and M. Jin *et al.* (2025) emphasised that, in order to improve the reliability of soil contamination assessments, it is advisable to employ a set of indices, as multi-indicator approaches allow for a more comprehensive and objective characterisation of heavy metal

pollution levels and the associated ecological risks. By quantitatively investigating and identifying the hazards arising from environmental contamination, it becomes possible to predict the likelihood and significance of potential disturbances to ecosystem integrity and public health, as well as to establish the priority and urgency of measures aimed at managing the negative impacts of technogenic factors.

The study by Y. Kuang *et al.* (2024) analysed the characteristics of heavy metal contamination in soils of the city of Chenzhou and assessed the associated risks to human health. To interpret the monitoring results, the following indices were employed: the enrichment factor, geoaccumulation index (I_{geo}), integrated pollution index, potential ecological risk index (*RI*), and health risk assessment models. The findings indicated that the accumulation of excessive amounts of heavy metals in soil matrices could lead to adverse consequences for both local ecosystems and human health. Statistical analysis further demonstrated that intensive industrial activity had a direct impact on the degree of soil contamination. The authors proposed incorporating ecological risk indicators into comprehensive monitoring programmes of urban ecosystems, as these indicators reflected environmental hazards to human health arising from the migration of hazardous metal compounds in urban soils. The analytical report by O.O. Reznikova *et al.* (2020) emphasised that the effective functioning of a national system for assessing risks and threats is a key element of strategic planning and ensuring national resilience, as demonstrated by the experience of many developed countries worldwide. The application of modern methods and technologies for assessing potential risks in Ukraine would enhance the reliability of environmental monitoring results and provide a robust evidence base for further analysis. Taking into account the specific features of the country's administrative-territorial structure and drawing on international experience, the authors argued that multi-level systems for risk and threat assessment are the most effective, whereby analysis is conducted at national, regional, and/or local levels.

Although considerable attention has been paid to heavy metal contamination of soils in Ukraine, there remains a lack of systematic reviews addressing the spatiotemporal distribution of heavy metals in soils and the associated ecological risks, particularly with consideration of different types of geochemical pollution indices at both regional and national scales. For these reasons, the present study is important for understanding the patterns of contamination and potential ecological risks, identifying sources of pollution, and supporting informed environmental management decisions. The aim of this study was to assess the level of heavy metal contamination in the urban soils of the city of Cherkasy in order to provide a scientific basis for urban environmental quality management measures. To achieve this aim, the following objectives were established: to investigate the spatio-temporal patterns of heavy metal distribution in the urban soils of Cherkasy; to evaluate the ecological condition of the city's soil cover using a multi-index approach based on the application of both single-factor and integrated indices, taking into account regional characteristics; to identify the probable sources of heavy metal inputs into urban soils through the application of statistical and correlation analyses.

Materials and Methods

Within the framework of this study, the city of Cherkasy was selected as a model object for assessing the potential ecological risks of heavy metal contamination in urban landscapes. The city is subject to significant aerotechnogenic pressure, which leads to the chemical degradation of urban soils. A considerable impact on the environmental state of the city is exerted by the thermal power sector, chemical and machine-building industries, as well as road transport (Mislyuk *et al.*, 2023). Meteorological conditions also play an important role. The city is located within a zone of environmental risk related to air quality deterioration (Fig. 1), owing to climatic conditions that are unfavourable for the dispersion of atmospheric pollutants. The potential genetic resilience of the natural environment is predominantly low, and the capacity of natural systems to withstand external technogenic pressures is insufficient (Yehorova *et al.*, 2025).

Each study site was geolocated using GPS coordinates, which made it possible to develop a geospatial database linked to the precise locations of the sampling sites (Fig. 2).

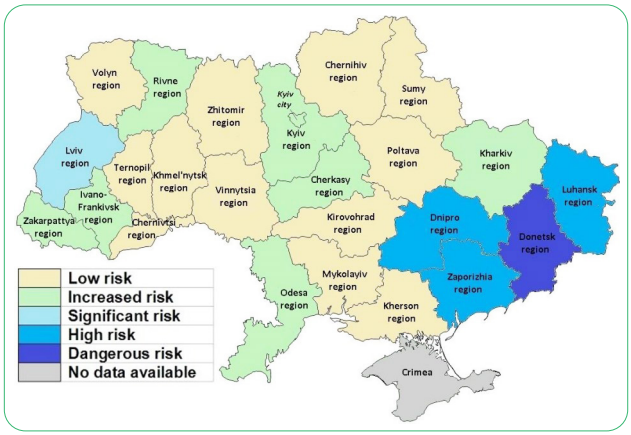

Figure 1. Ecological risk of air quality deterioration across the regions of Ukraine, taking into account the degree of chemical hazard

Source: O.V. Rybalova *et al.*, (2022)

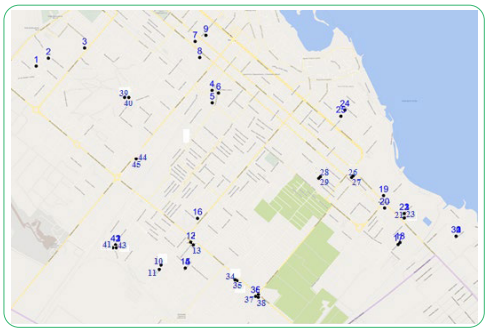

Figure 1. Location of the monitoring sites

Source: compiled by the author

To assess the degree of soil degradation caused by heavy metal contamination, a systematic approach was applied, incorporating bibliosemantic, comparative-analytical, and statistical methods. Statistical data analysis was performed using Microsoft Office Excel software. Correlation analysis was employed to identify potential sources of contamination. A set of geochemical indices and guidelines, in accordance with US EPA standards, was used to evaluate contamination levels and associated ecological risks. Potential ecological risks were assessed using both single-factor indices (I_{geoi}, pollution index *PI* and ecological risk index(*Er*)) and integrated indices (*PLI*, $PI_{Nemerow}$ and *RI*).

Single-factor indices. I_{geo_i} was calculated using the following formula:

$$I_{geo_i} = log_2\left(\frac{C_i}{GB_i}\right), \quad (1)$$

where C_i – the concentration of the metal in the soil; GB_i – its geochemical background value.

Considering the geographical context of the study area, background concentrations of heavy metals in soils of the Forest-Steppe zone of Ukraine were used, specifically for typical low-humus chernozems (genetic horizon HE). Based on the values of the index, contamination levels were classified into seven distinct classes (Table 1).

The *PI* was calculated using the following formula:

$$PI = \frac{C_i}{GB_i}. \quad (2)$$

Contamination was classified according to the scale presented in Table 2.

Table 1. Soil quality according to I_{geo} values

Class	Values of I_{geo}	Soil quality
0	$I \leq 0$	unpolluted
1	0-1	unpolluted to moderately polluted
2	1-2	moderately polluted
3	2-3	moderately to highly polluted
4	3-4	highly polluted
5	4-5	highly to extremely high polluted
6	5-6	extremely high polluted

Source: J.B. Kowalska *et al.* (2018)

Table 2. Contamination classes of single *PI*

Class	Value of *PI*	Soil pollution
1	$PI < 1$	absent
2	$1 < PI < 2$	low
3	$2 < PI < 3$	moderate
4	$3 < PI < 5$	strong
5	$PI > 5$	very strong

Source: J.B. Kowalska *et al.* (2018)

The ecological risk index of the *i*-th metal (Er_i) was evaluated using the following equation:

$$Er_i = TR_i \cdot PI, \quad (3)$$

where *PI* – the calculated pollution index for the individual metal; TR_i – its toxic-response factor (Hakanson & Charlesworth, 1980).

Multi-factor indices. To assess the overall extent of contamination, the Pollution Load Index (*PLI*) was determined as the geometric mean of the pollution indices (*PI*) of individual heavy metals, using the following formula:

$$PLI = \sqrt[n]{PI_1 \cdot PI_2 \cdot PI_3 \cdot \ldots \cdot PI_n}, \quad (4)$$

where *n* – the number of analysed heavy metals; *PI* – the calculated values of the pollution index for each individual metal.

To assess soil contamination levels using the *PLI*, the scale proposed by Papadimou *et al.* (2023) was applied. *PLI* is classified into six classes: Class I: $PLI < 0$, no pollution; Class II: $0 < PLI < 1$, low degree of pollution; Class III: $1 < PLI < 2$, moderate degree of pollution; Class IV: $2 < PLI < 4$, high degree of pollution; Class V: $4 < PLI < 8$, very high degree of pollution; and Class VI: $8 < PLI < 16$, extremely high degree of pollution. $PI_{Nemerow}$, which evaluates the overall contamination level by multiple metals, taking into account both the average and maximum values of single-metal pollution indices, and was calculated using the following formula:

$$PI_{Nemerow} = \sqrt{\frac{\left(\frac{1}{n}\sum_{i-1}^{n} PI\right)^2 + PI_{max}^2}{n}}, \quad (5)$$

where *PI* – the calculated pollution index for each individual metal; PI_{max} is the maximum pollution index value among all heavy metals; *n* – is the number of heavy metals.

Soil quality was assessed according to the scale presented in Table 3.

Table 3. $PI_{Nemerow}$ soil pollution classes

$PI_{Nemerow}$	≤ 0.7	0.7-1	1-2	2-3	≥ 3
Quality of soil	Clean	Warning limit	Slight pollution	Moderate pollution	Heavy pollution

Source: J.B. Kowalska *et al.* (2018)

The potential ecological risk to the soil environment and ecosystems was determined as the sum of the individual risks from each studied metal (*Er*), using the following formula:

$$RI = \sum_{i-1}^{n} Er_i, \quad (6)$$

where Er_i – is the ecological risk index of the *i*-th metal.

Risk assessment was conducted according to the scale presented in Table 4.

This approach enabled the identification of contamination levels and the assessment of the overall ecological threat associated with metal accumulation in soils, thereby providing a basis for comparing environmental conditions across the investigated urban ecosystems.

Table 4. Classification of the potential ecological risk index and integrated potential ecological risk index

Er_i	Pollution Degree	*RI*	Hazards Level
<40	Slight	<150	Slight
40-80	Moderate	150~300	Moderate
80-160	Strong	300~600	Strong
160-320	Very strong	≥600	Very strong
≥320	Extremely strong		

Source: H. Cheng *et al.* (2019)

Results and Discussion

The city of Cherkasy is located in the Forest-Steppe zone. Based on geomorphological and orohydrographic characteristics, the city's landscapes are predominantly formed by loess and loess-like loams, as well as sand-derived loams. The soil cover is heterogeneous, characterised by a light mechanical composition and the presence of anthropogenic inclusions (e.g., construction debris) and allochthonous materials. Soils are contaminated with xenobiotics, including heavy metals (Yehorova *et al.*, 2025). A significant impact on urban soils is exerted by aerotechnogenic pollution, which ranks as the leading source of technogenic contaminants in urban landscapes in terms of environmental influence. The primary pollutants in the city are enterprises from the energy and chemical industries (Regional Report, 2025). In 2024, the largest emissions were recorded from the Cherkasy Thermal Power Plant (PraT "Cherkaske Khimvolokno" VP "Cherkaska TPP"), totalling over 29,637 tons, which is 647.845 tons more than in 2023, due to increased coal consumption. Concentrations and the overall level of technogenic load, the city of Cherkasy ranks among the most environmentally burdened settlements in the region. Based on the Comprehensive Air Pollution Index (API), calculated from monthly average concentrations of sulfur dioxide, ammonia, formaldehyde, nitrogen dioxide, and carbon monoxide, the air pollution level in Cherkasy is classified as elevated (5-7) and high (7-14) (Fig. 3).

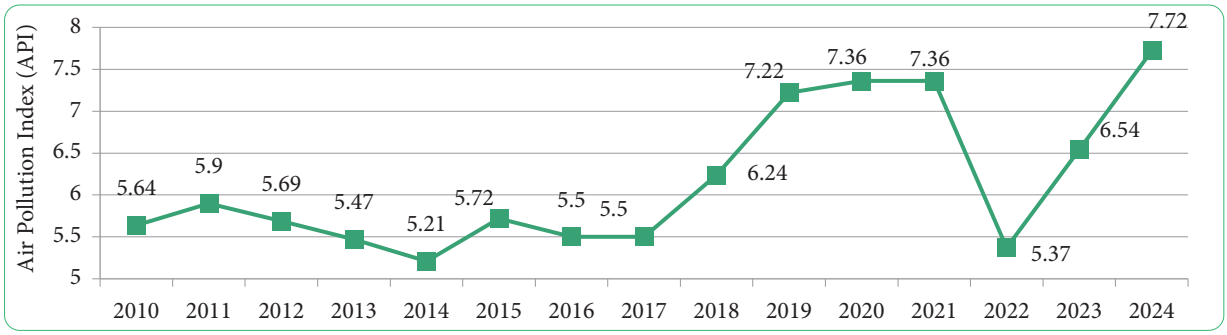

Figure 3. Dynamics of the comprehensive air PI in Cherkasy from 2010 to 2024

Source: compiled by the authors

Meteorological conditions play a significant role in shaping air quality. The city is located in climatic conditions unfavourable for the dispersion of pollutants, within a zone of high atmospheric pollution potential. The inherent genetic stability of the natural environment is mostly low, and the self-purifying capacity of nature is insufficient to counteract external technogenic loads. Despite the decline in industrial activity, air pollution levels for individual pollutants remain high. One of the main reasons for this is the atmosphere's limited self-cleaning capacity. Long-term observations indicate that processes promoting the accumulation of harmful pollutants, rather than their dispersion, predominate

in the city (atmospheric meteorological potential $K_m > 1$) (Yehorova *et al.*, 2025). Heavy metals present in emissions from industrial facilities and mobile sources (Fig. 4) contaminate urban landscapes through dry or wet deposition.

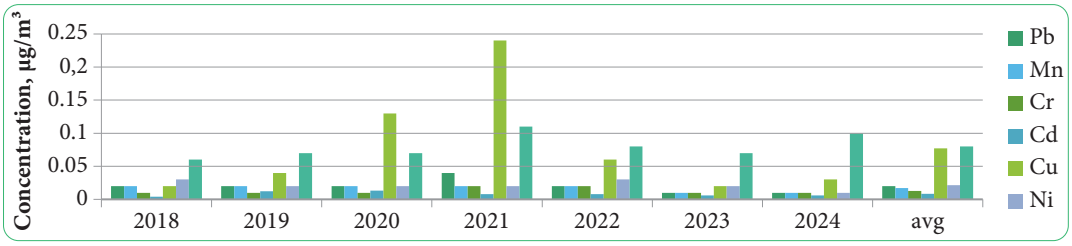

Figure 4. Heavy metal concentrations in the atmospheric air of Cherkasy, µg/m³
Source: compiled by the authors

As a result of intensive technogenesis within urban areas, stable geochemical anomalies are formed in urban soils (Yehorova *et al.*, 2025), accompanied by the disruption of natural soil self-purification mechanisms, alterations in the physicochemical properties of the environment, and an increase in the mobility of pollutants. Such transformations of urbanised geosystems intensify ecotoxicological pressure and contribute to the accumulation of heavy metals in the near-surface atmospheric layer, soils, and biota. Once released into the environment, these elements can persist for extended periods in various ecosystem components, moving through surface runoff, infiltration into groundwater, or wind-driven dust transport. This mobility of pollutants facilitates their wide dispersion beyond emission sources and increases environmental and public health risks, even at considerable distances (He *et al.*, 2023). Soil samples were analysed for heavy metal content by specialists of the Central Laboratory of the Ukrainian Hydrometeorological Center using the method of atomic emission spectrometry. Descriptive statistics of heavy metal concentrations at the reference points are presented in Table 5.

Correlation relationships between different metal pollutants were found to be quite pronounced in some cases (Fig. 5).

Table 5. Results of soil monitoring in Cherkasy in 2016 and 2021

Sampling Site No.	Pb, mg/kg		Zn, mg/kg		Cu, mg/kg		Ni, mg/kg		Mn, mg/kg		Cd, mg/kg	
	2016	2021	2016	2021	2016	2021	2016	2021	2016	2021	2016	2021
1	20	8	51	37	11	5	13	11	179	237	0.50	0.50
2	70	11	259	85	54	32	42	16	419	311	1.75	0.75
3	13	7	47	32	13	6	19	9	302	250	0.75	0.75
4	15	8	50	40	9	8	19	12	207	170	0.50	0.50
5	94	7	319	45	37	4	28	11	324	241	1.25	0.75
6	21	12	58	48	14	10	19	13	330	303	1.00	0.25
7	22	13	43	43	10	11	16	15	274	267	1.00	0.25
8	66	18	244	43	26	12	18	10	307	179	1.00	1.00
9	38	11	95	47	20	10	23	12	386	175	1.00	0.50
10	45	16	62	158	17	21	20	20	246	430	1.25	1.00
11	40	12	88	49	21	11	20	17	319	311	0.50	0.50
12	23	23	87	207	18	76	14	14	218	457	1.00	0.75
13	40	8	191	31	20	7	20	16	341	399	0.50	0.25
14	29	30	70	215	17	42	19	37	414	2,406	0.75	0.75
15	49	41	71	260	17	73	11	50	313	2,402	1.00	1.00
16	213	25	296	199	104	53	16	42	207	2,389	1.25	1.25
17	38	510	318	311	87	132	20	25	279	580	1.00	1.00
18	126	22	251	129	25	10	20	15	319	465	2.00	0.25
19	65	11	274	145	50	11	18	16	330	325	1.00	0.75
20	30	23	214	129	31	14	15	20	408	892	0.50	1.25
21	40	9	184	96	23	11	19	20	358	250	0.25	0.25
22	49	8	169	100	28	10	23	24	369	245	0.50	0.50
23	28	11	48	158	9	14	13	20	190	232	0.00	0.00
24	40	9	244	29	18	5	17	12	195	175	0.50	0.50
25	32	30	69	49	25	15	23	11	274	241	0.50	0.25
26	77	7	251	39	24	4	16	6	173	87	0.00	0.00
27	155	7	206	41	28	5	23	7	319	91	0.25	0.00
28	40	27	176	207	34	14	25	19	330	364	0.25	0.25

Table 5. Continued

Sampling Site No.	Pb, mg/kg		Zn, mg/kg		Cu, mg/kg		Ni, mg/kg		Mn, mg/kg		Cd, mg/kg	
	2016	2021	2016	2021	2016	2021	2016	2021	2016	2021	2016	2021
29	111	9	273	88	23	22	23	15	475	338	0.75	0.75
30	21	19	91	50	16	28	23	16	285	281	0.00	0.75
31	38	11	311	29	20	11	23	20	307	259	0.75	0.25
32	23	8	65	39	13	10	14	20	123	267	0.25	0.50
33	41	14	99	44	19	23	23	21	285	311	0.00	0.50
34	45	14	236	47	25	13	28	16	1,181	241	0.75	0.25
35	31	8	191	39	18	13	15	18	274	303	0.25	0.50
36	56	12	199	45	20	15	24	15	498	320	0.25	0.50
37	83	9	221	39	31	14	23	15	307	232	0.50	0.25
38	56	15	214	43	19	19	16	15	319	272	0.00	0.25
39	67	9	229	40	26	8	18	13	1,408	201	0.50	0.25
40	68	6	206	29	45	4	11	10	257	188	0.00	0.00
41	44	5	73	43	21	7	21	7	263	245	0.00	0.00
42	27	26	68	49	17	17	15	12	285	285	0.25	0.25
43	40	9	86	39	21	8	18	16	363	254	0.25	0.50
44	29	9	69	207	23	24	22	20	212	355	0.50	0.50
45	33	8	68	174	18	27	11	17	291	289	0.25	0.25
mini	13	5	43	29	9	4	11	6	123	87	0	0
max	213	510	319	311	104	132	42	50	1,408	2,406	2	1.25
medium	52	25	159	89	26	20	19	17	344	434	0.6	0,5
SD	38.2	74.4	91.0	73.4	18.1	23.4	5.5	8.4	222.6	546.6	0.5	0.3
CV, %	70	300	60	80	70	120	30	50	60	130	80	70
Background site	11		52		20		26		735		0.13	

Source: compiled by the authors

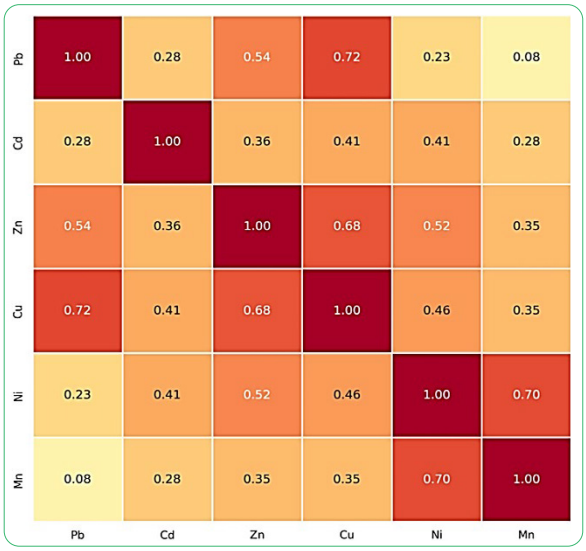

Figure 5. Correlation matrix of heavy metals in the soils of Cherkasy
Source: compiled by the authors

Strong correlations (correlation coefficient $r > 0.7$) were observed between Pb and Cu ($r = 0.72$) and between Ni and Mn ($r = 0.70$), indicating that the sources of these elements may be similar. Moderate correlations ($0.50 < r < 0.69$) were found for Cu and Zn ($r = 0.68$), Pb and Zn ($r = 0.54$), and Ni and Zn ($r = 0.52$). Mn exhibited weak correlations ($r < 0.4$) with all metals except Ni, suggesting that the patterns of Mn input and accumulation may differ from those of the other metals. Using soil monitoring data on heavy metal concentrations, the I_{geo} was calculated to evaluate the extent of anthropogenic influence on heavy metal levels, taking into account possible natural fluctuations in background concentrations (Table 6). Geoaccumulation indices varied significantly across time and space (Figs. 6 and 7). In 2016,

based on Pb content, only 3% of the studied soils were classified as uncontaminated ($I_{geo} \leq 0$), 25% ranged from uncontaminated to moderately contaminated ($0 < I_{geo} \leq 1$), 48% were moderately contaminated ($1 < I_{geo} \leq 2$), 22% ranged from moderately to strongly contaminated ($2 < I_{geo} \leq 3$), and 2% were strongly contaminated ($3 < I_{geo} \leq 4$).

Table 6. Calculated values of the Igeo for Soil Contamination in the City of Cherkasy

Sampling Site No.	I_{geo}											
	Pb		Zn		Cu		Ni		Mn		Cd	
	2016	2021	2016	2021	2016	2021	2016	2021	2016	2021	2016	2021
1	0.3	-1.0	-0.6	-1.1	-1.4	-2.6	-1.6	-1.8	-2.6	-2.2	1.4	1.4
2	2.1	-0.6	1.7	0.1	0.8	0.1	0.1	-1.3	-1.4	-1.8	3.2	1.9
3	-0.3	-1.2	-0.7	-1.3	-1.2	-2.3	-1.0	-2.1	-1.9	-2.1	1.9	1.9
4	-0.1	-1.0	-0.6	-1.0	-1.7	-1.9	-1.0	-1.7	-2.4	-2.7	1.4	1.4
5	2.5	-1.2	2.0	-0.8	0.3	-2.9	-0.5	-1.8	-1.8	-2.2	2.7	1.9
6	0.3	-0.5	-0.4	-0.7	-1.1	-1.6	-1.0	-1.6	-1.7	-1.9	2.4	0.4
7	0.4	-0.3	-0.9	-0.9	-1.6	-1.4	-1.3	-1.4	-2.0	-2.0	2.4	0.4
8	2.0	0.1	1.6	-0.9	-0.2	-1.3	-1.1	-2.0	-1.8	-2.6	2.4	2.4
9	1.2	-0.6	0.3	-0.7	-0.6	-1.6	-0.8	-1.7	-1.5	-2.7	2.4	1.4
10	1.4	0.0	-0.3	1.0	-0.8	-0.5	-1.0	-1.0	-2.2	-1.4	2.7	2.4
11	1.3	-0.5	0.2	-0.7	-0.5	-1.4	-1.0	-1.2	-1.8	-1.8	1.4	1.4
12	0.5	0.5	0.2	1.4	-0.7	1.3	-1.5	-1.5	-2.3	-1.3	2.4	1.9
13	1.3	-1.0	1.3	-1.3	-0.6	-2.1	-1.0	-1.3	-1.7	-1.5	1.4	0.4
14	0.8	0.9	-0.2	1.5	-0.8	0.5	-1.0	-0.1	-1.4	1.1	1.9	1.9
15	1.6	1.3	-0.1	1.7	-0.8	1.3	-1.8	0.4	-1.8	1.1	2.4	2.4
16	3.7	0.6	1.9	1.4	1.8	0.8	-1.3	0.1	-2.4	1.1	2.7	2.7
17	1.2	4.9	2.0	2.0	1.5	2.1	-1.0	-0.6	-2.0	-0.9	2.4	2.4
18	2.9	0.4	1.7	0.7	-0.3	-1.6	-1.0	-1.4	-1.8	-1.2	3.4	0.4
19	2.0	-0.6	1.8	0.9	0.7	-1.4	-1.1	-1.3	-1.7	-1.8	2.4	1.9
20	0.9	0.5	1.5	0.7	0.0	-1.1	-1.4	-1.0	-1.4	-0.3	1.4	2.7
21	1.3	-0.9	1.2	0.3	-0.4	-1.4	-1.0	-1.0	-1.6	-2.1	0.4	0.4
22	1.6	-1.0	1.1	0.4	-0.1	-1.6	-0.8	-0.7	-1.6	-2.2	1.4	1.4
23	0.8	-0.6	-0.7	1.0	-1.7	-1.1	-1.6	-1.0	-2.5	-2.2	0.0	0.0
24	1.3	-0.9	1.6	-1.4	-0.7	-2.6	-1.2	-1.7	-2.5	-2.7	1.4	1.4
25	1.0	0.9	-0.2	-0.7	-0.3	-1.0	-0.8	-1.8	-2.0	-2.2	1.4	0.4
26	2.2	-1.2	1.7	-1.0	-0.3	-2.9	-1.3	-2.7	-2.7	-3.7	0.0	0.0
27	3.2	-1.2	1.4	-0.9	-0.1	-2.6	-0.8	-2.5	-1.8	-3.6	0.4	0.0
28	1.3	0.7	1.2	1.4	0.2	-1.1	-0.6	-1.0	-1.7	-1.6	0.4	0.4
29	2.8	-0.9	1.8	0.2	-0.4	-0.4	-0.8	-1.4	-1.2	-1.7	1.9	1.9
30	0.3	0.2	0.2	-0.6	-0.9	-0.1	-0.8	-1.3	-2.0	-2.0	0.0	1.9
31	1.2	-0.6	2.0	-1.4	-0.6	-1.4	-0.8	-1.0	-1.8	-2.1	1.9	0.4
32	0.5	-1.0	-0.3	-1.0	-1.2	-1.6	-1.5	-1.0	-3.2	-2.0	0.4	1.4
33	1.3	-0.2	0.3	-0.8	-0.7	-0.4	-0.8	-0.9	-2.0	-1.8	0.0	1.4
34	1.4	-0.2	1.6	-0.7	-0.3	-1.2	-0.5	-1.3	0.1	-2.2	1.9	0.4
35	0.9	-1.0	1.3	-1.0	-0.7	-1.2	-1.4	-1.1	-2.0	-1.9	0.4	1.4
36	1.8	-0.5	1.4	-0.8	-0.6	-1.0	-0.7	-1.4	-1.1	-1.8	0.4	1.4
37	2.3	-0.9	1.5	-1.0	0.0	-1.1	-0.8	-1.4	-1.8	-2.2	1.4	0.4
38	1.8	-0.1	1.5	-0.9	-0.7	-0.7	-1.3	-1.4	-1.8	-2.0	0.0	0.4
39	2.0	-0.9	1.6	-1.0	-0.2	-1.9	-1.1	-1.6	0.4	-2.5	1.4	0.4
40	2.0	-1.5	1.4	-1.4	0.6	-2.9	-1.8	-2.0	-2.1	-2.6	0.0	0.0
41	1.4	-1.7	-0.1	-0.9	-0.5	-2.1	-0.9	-2.5	-2.1	-2.2	0.0	0.0
42	0.7	0.7	-0.2	-0.7	-0.8	-0.8	-1.4	-1.7	-2.0	-2.0	0.4	0.4
43	1.3	-0.9	0.1	-1.0	-0.5	-1.9	-1.1	-1.3	-1.6	-2.1	0.4	1.4
44	0.8	-0.9	-0.2	1.4	-0.4	-0.3	-0.8	-1.0	-2.4	-1.6	1.4	1.4
45	1.0	-1.0	-0.2	1.2	-0.7	-0.2	-1.8	-1.2	-1.9	-1.9	0.4	0.4
min	-0.3	-1.7	-0.9	-1.4	-1.7	-2.9	-1.8	-2.7	-3.2	-3.7	0.0	0.0
max	3.7	4.9	2.0	2.0	1.8	2.1	0.1	0.4	0.4	1.1	3.4	2.7
mean	1.4	-0.3	0.7	-0.2	-0.4	-1.1	-1.1	-1.3	-1.8	-1.8	1.4	1.1

Source: compiled by the authors

Figure 6. Geoaccumulation indices (I_{geo}) of heavy metals in the soils of Cherkasy city in 2016
Source: compiled by the authors

By 2021, 69% of the soils were uncontaminated, 24% were uncontaminated to moderately contaminated, 3% were moderately contaminated, and 3% were strongly contaminated.

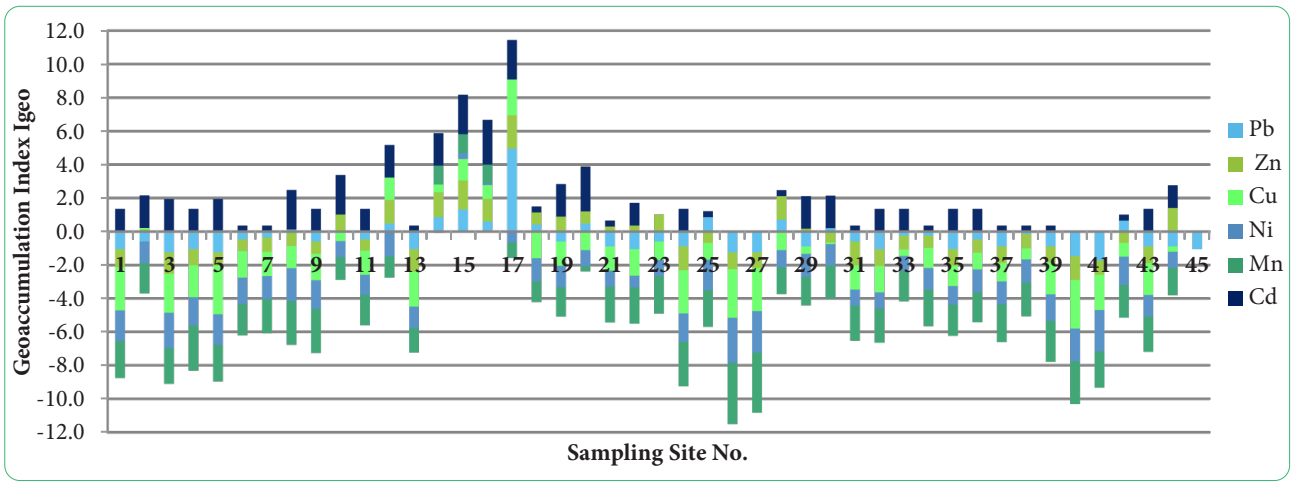

Figure 7. Geoaccumulation indices (I_{geo}) of heavy metals in the soils of Cherkasy city in 2021
Source: compiled by the authors

In 2016, the I_{geo} values for Zn indicated soil contamination levels as follows: 33% of sampling points were uncontaminated, 13% were uncontaminated to moderately contaminated, 47% were moderately contaminated, and 7% were moderately to strongly contaminated. By 2021, the soil condition had improved significantly: 62% of the studied soils were uncontaminated, 16% were uncontaminated to moderately contaminated, 18% were moderately contaminated, and 2% were moderately to strongly contaminated. In 2016, the I_{geo} values for Cu indicated that 84% of the studied soils were uncontaminated, 11% were uncontaminated to moderately contaminated, and 5% were moderately contaminated. By 2021, 86% of soils were uncontaminated, 7% were uncontaminated to moderately contaminated, 5% were moderately contaminated, and 2% were moderately to strongly contaminated. For Ni, the I_{geo} values in 2016 and 2021 showed that 98% and 96% of soils, respectively, were uncontaminated, while 2% and 4% were uncontaminated to moderately contaminated. Regarding Mn, in 2016 and 2021, 96% and 93% of soils were uncontaminated, and 4% and 7% were uncontaminated to moderately contaminated, respectively. For Cd, the I_{geo} values in 2016 and 2021 indicated that only 16% and 12% of soils were uncontaminated, 20% and 32% were uncontaminated to moderately contaminated, 36% and 45% were moderately contaminated, and 24% and 11% were moderately to strongly contaminated. In 2016, 4% of soils were strongly contaminated with Cd. Overall, the I_{geo} indicates that Pb and Cd exhibit significantly higher levels of contamination, whereas the other metals generally show only minor pollution. The results of the assessment of soil contamination hazards associated with heavy metals, conducted using both single-metal *PI* and integrated multi-element pollution indices (*PLI* and $PI_{Nemerow}$), are presented in Table 7.

Table 7. Individual metal *PI* and integrated pollution indices accounting for the multi-element nature of contamination (*PLI* and $PI_{Nemerow}$)

Sampling Site No.	PI												PLI		$PI_{Nemerow}$	
	Pb		Zn		Cu		Ni		Mn		Cd					
	2016	2021	2016	2021	2016	2021	2016	2021	2016	2021	2016	2021	2016	2021	2016	2021
1	1.8	0.7	1.0	0.7	0.6	0.3	0.5	0.4	0.2	0.3	3.8	3.8	0.9	0.6	2	2
2	6.4	1.0	5.0	1.6	2.7	1.6	1.6	0.6	0.6	0.4	13.5	5.8	3.2	1.3	6	2
3	1.2	0.6	0.9	0.6	0.7	0.3	0.7	0.3	0.4	0.3	5.8	5.8	1.0	0.7	2	2
4	1.4	0.7	1.0	0.8	0.5	0.4	0.7	0.5	0.3	0.2	3.8	3.8	0.9	0.7	2	2
5	8.5	0.6	6.1	0.9	1.9	0.2	1.1	0.4	0.4	0.3	9.6	5.8	2.8	0.7	4	2
6	1.9	1.1	1.1	0.9	0.7	0.5	0.7	0.5	0.4	0.4	7.7	1.9	1.2	0.8	3	1
7	2.0	1.2	0.8	0.8	0.5	0.6	0.6	0.6	0.4	0.4	7.7	1.9	1.1	0.8	3	1
8	6.0	1.6	4.7	0.8	1.3	0.6	0.7	0.4	0.4	0.2	7.7	7.7	2.1	0.9	3	3
9	3.5	1.0	1.8	0.9	1.0	0.5	0.9	0.5	0.5	0.2	7.7	3.8	1.7	0.8	3	2
10	4.1	1.5	1.2	3.0	0.9	1.1	0.8	0.8	0.3	0.6	9.6	7.7	1.5	1.6	4	3
11	3.6	1.1	1.7	0.9	1.1	0.6	0.8	0.7	0.4	0.4	3.8	3.8	1.4	0.9	2	2
12	2.1	2.1	1.7	4.0	0.9	3.8	0.5	0.5	0.3	0.6	7.7	5.8	1.3	2.0	3	3
13	3.6	0.7	3.7	0.6	1.0	0.4	0.8	0.6	0.5	0.5	3.8	1.9	1.6	0.7	2	1
14	2.6	2.7	1.3	4.1	0.9	2.1	0.7	1.4	0.6	3.3	5.8	5.8	1.4	2.9	2	3
15	4.5	3.7	1.4	5.0	0.9	3.7	0.4	1.9	0.4	3.3	7.7	7.7	1.4	3.9	3	4
16	19.4	2.3	5.7	3.8	5.2	2.7	0.6	1.6	0.3	3.3	9.6	9.6	3.1	3.2	8	4
17	3.5	46.4	6.1	6.0	4.4	6.6	0.8	1.0	0.4	0.8	7.7	7.7	2.4	4.7	4	19
18	11.5	2.0	4.8	2.5	1.3	0.5	0.8	0.6	0.4	0.6	15.4	1.9	2.7	1.1	7	1
19	5.9	1.0	5.3	2.8	2.5	0.6	0.7	0.6	0.4	0.4	7.7	5.8	2.4	1.2	3	2
20	2.7	2.1	4.1	2.5	1.6	0.7	0.6	0.8	0.6	1.2	3.8	9.6	1.7	1.8	2	4
21	3.6	0.8	3.5	1.8	1.2	0.6	0.7	0.8	0.5	0.3	1.9	1.9	1.5	0.9	2	1
22	4.5	0.7	3.3	1.9	1.4	0.5	0.9	0.9	0.5	0.3	3.8	3.8	1.8	1.0	2	2
23	2.5	1.0	0.9	3.0	0.5	0.7	0.5	0.8	0.3	0.3	0.0	0.0	0.7	0.9	1	1
24	3.6	0.8	4.7	0.6	0.9	0.3	0.7	0.5	0.3	0.2	3.8	3.8	1.5	0.6	2	2
25	2.9	2.7	1.3	0.9	1.3	0.8	0.9	0.4	0.4	0.3	3.8	1.9	1.4	0.9	2	1
26	7.0	0.6	4.8	0.8	1.2	0.2	0.6	0.2	0.2	0.1	0.0	0.0	1.4	0.3	3	0
27	14.1	0.6	4.0	0.8	1.4	0.3	0.9	0.3	0.4	0.1	1.9	0.0	2.0	0.3	6	0
28	3.6	2.5	3.4	4.0	1.7	0.7	1.0	0.7	0.4	0.5	1.9	1.9	1.6	1.3	2	2
29	10.1	0.8	5.3	1.7	1.2	1.1	0.9	0.6	0.6	0.5	5.8	5.8	2.4	1.2	4	2
30	1.9	1.7	1.8	1.0	0.8	1.4	0.9	0.6	0.4	0.4	0.0	5.8	1.0	1.2	1	2
31	3.5	1.0	6.0	0.6	1.0	0.6	0.9	0.8	0.4	0.4	5.8	1.9	1.9	0.7	3	1
32	2.1	0.7	1.3	0.8	0.7	0.5	0.5	0.8	0.2	0.4	1.9	3.8	0.8	0.8	1	2
33	3.7	1.3	1.9	0.8	1.0	1.2	0.9	0.8	0.4	0.4	0.0	3.8	1.2	1.1	2	2
34	4.1	1.3	4.5	0.9	1.3	0.7	1.1	0.6	1.6	0.3	5.8	1.9	2.5	0.8	3	1
35	2.8	0.7	3.7	0.8	0.9	0.7	0.6	0.7	0.4	0.4	1.9	3.8	1.3	0.9	2	2
36	5.1	1.1	3.8	0.9	1.0	0.8	0.9	0.6	0.7	0.4	1.9	3.8	1.7	0.9	2	2
37	7.5	0.8	4.3	0.8	1.6	0.7	0.9	0.6	0.4	0.3	3.8	1.9	2.0	0.7	3	1
38	5.1	1.4	4.1	0.8	1.0	1.0	0.6	0.6	0.4	0.4	0.0	1.9	1.4	0.9	2	1
39	6.1	0.8	4.4	0.8	1.3	0.4	0.7	0.5	1.9	0.3	3.8	1.9	2.4	0.6	3	1
40	6.2	0.5	4.0	0.6	2.3	0.2	0.4	0.4	0.3	0.3	0.0	0.0	1.5	0.4	3	0
41	4.0	0.5	1.4	0.8	1.1	0.4	0.8	0.3	0.4	0.3	0.0	0.0	1.1	0.4	2	0
42	2.5	2.4	1.3	0.9	0.9	0.9	0.6	0.5	0.4	0.4	1.9	1.9	1.0	0.9	1	1
43	3.6	0.8	1.7	0.8	1.1	0.4	0.7	0.6	0.5	0.3	1.9	3.8	1.3	0.8	2	2
44	2.6	0.8	1.3	4.0	1.2	1.2	0.8	0.8	0.3	0.5	3.8	3.8	1.2	1.3	2	2
45	3.0	0.7	1.3	3.3	0.9	1.4	0.4	0.7	0.4	0.4	1.9	1.9	1.0	1.1	1	1
min	1.2	0.5	0.8	0.6	0.5	0.2	0.4	0.2	0.2	0.1	0	0	0.7	0.3	1	0
max	19.4	46.4	6.1	6.0	5.2	6.6	1.6	1.9	1.9	3.3	15.4	9.6	3.2	4.7	9	6
mean	4.7	2.3	3.0	1.7	1.3	1.0	0.7	0.7	0.5	0.6	4.6	3.8	1.6	1.2	2	1

Source: compiled by the authors

Soil pollution indices also varied significantly over time and space for different metals and sampling sites (Figures 8 and 9). Based on the average *PI* values, the metals were ranked as follows: Pb (4.7) > Cd (4.6) > Zn (3.0) > Cu (1.3) > Ni (0.7) > Mn (0.5) in 2016, and Cd (3.8) > Pb (2.3) > Zn (1.7) > Cu (1.0) > Ni (0.7) > Mn (0.6) in 2021.

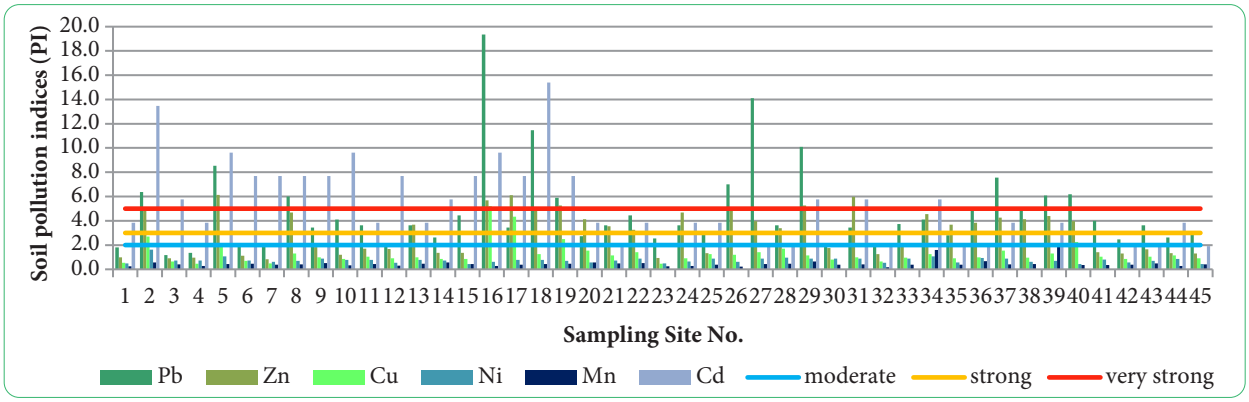

Figure 8. Soil *PI* for heavy metals in 2016

Source: compiled by the authors

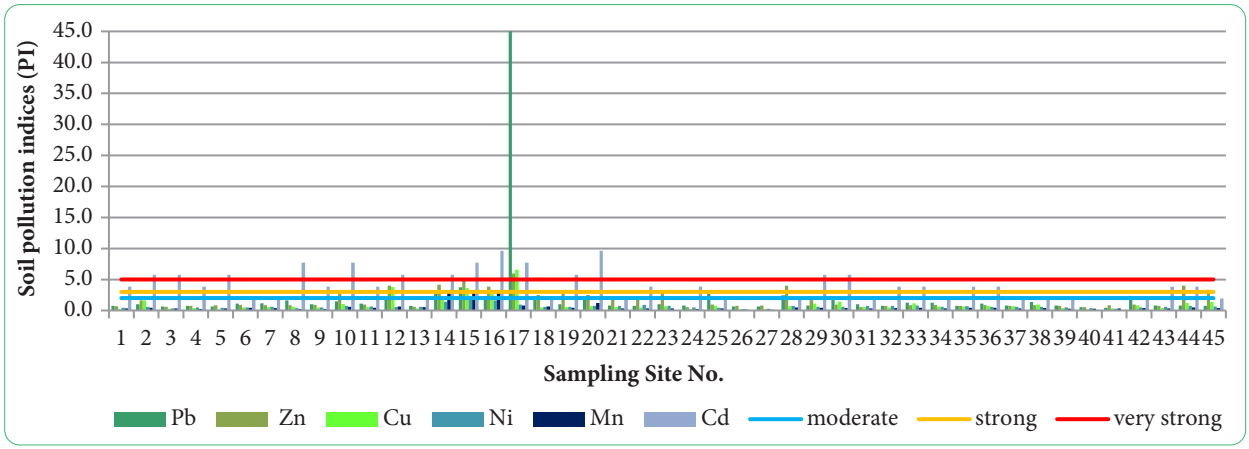

Figure 9. Soil *PI* for heavy metals in 2021

Source: compiled by the authors

Particularly high *PI* values ($PI > 5$) were observed in 2016 for Cd (40% of sites) and Pb (31%). By 2021, the number of sites with very high pollution levels decreased, with Cd exceeding $PI > 5$ at 33% of sites. For Pb, a very high *PI* was observed only at site 17 ($PI = 45$). According to the *PLI* for all heavy metals (Fig. 10), a high level of contamination ($PLI = 4.7$) was observed at site 17 in 2021. Moderately contaminated soils accounted for 22% of samples (sites 2, 3, 16-19, 29, 34, 39) in 2016 and 9% (sites 14, 15, 16) in 2021. At the remaining locations, soils were classified as uncontaminated ($PLI \leq 1$). $PI_{Nemerow}$ were slightly higher than the *PLI*. Soils exhibited a high level of contamination at 33% and 13% of the sites, and a medium level at 60% and 18% of the sites in 2016 and 2021, respectively (Fig. 11).

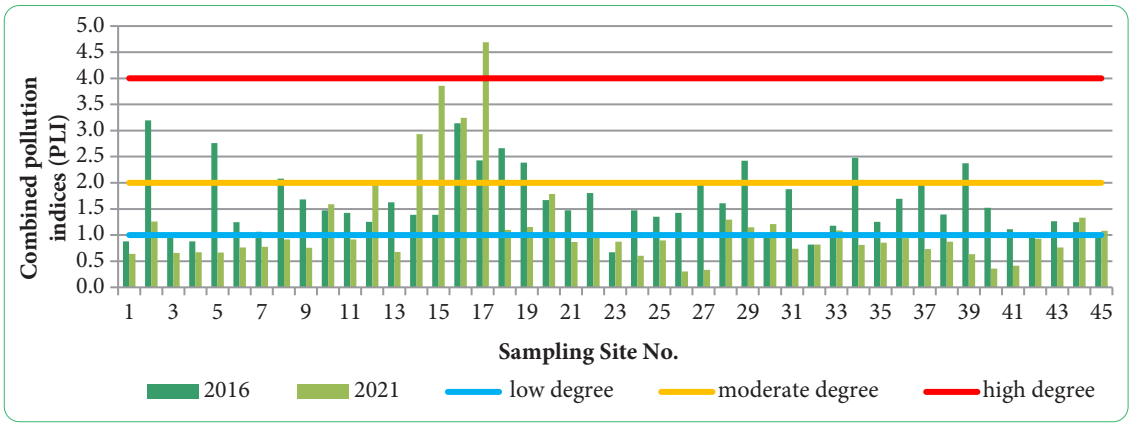

Figure 10. *PLI* of heavy metals in soils

Source: compiled by the authors

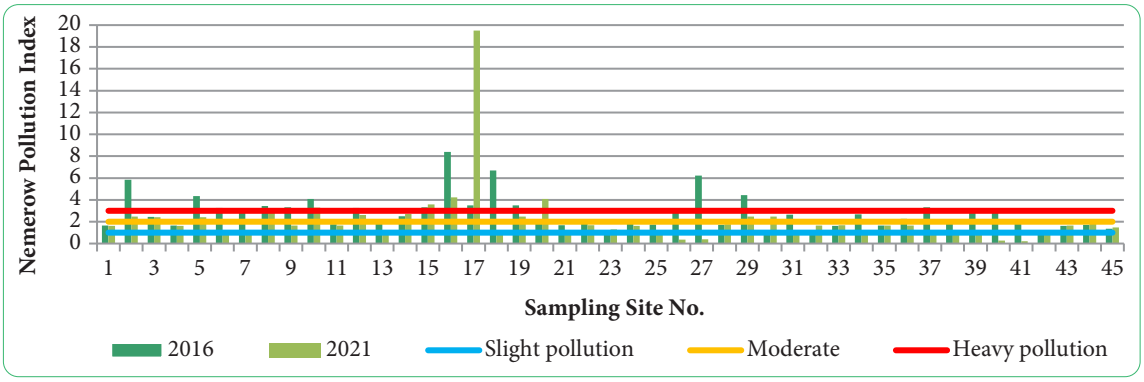

Figure 11. Levels of combined soil contamination by heavy metals according to the $PI_{Nemerow}$
Source: compiled by the authors

The results of the assessment of ecological risks associated with soil contamination by individual heavy metals, as well as the integrated potential ecological risk, are presented in Table 8 and Figures 12-14.

Table 8. Ecological risk indices for soil contamination in the city of Cherkasy: individual heavy metal risk (*Er*) and integrated potential ecological risk (RI)

Sampling Site No.	Er												RI	
	Pb		Zn		Cu		Ni		Mn		Cd			
	2016	2021	2016	2021	2016	2021	2016	2021	2016	2021	2016	2021	2016	2021
1	9.1	3.6	1.0	0.7	2.8	1.3	2.5	2.1	0.2	0.3	115.4	115.4	131	123
2	31.8	5.0	5.0	1.6	13.5	8.0	8.1	3.1	0.6	0.4	403.8	173.1	463	191
3	5.9	3.2	0.9	0.6	3.3	1.5	3.7	1.7	0.4	0.3	173.1	173.1	187	180
4	6.8	3.6	1.0	0.8	2.3	2.0	3.7	2.3	0.3	0.2	115.4	115.4	129	124
5	42.7	3.2	6.1	0.9	9.3	1.0	5.4	2.1	0.4	0.3	288.5	173.1	352	181
6	9.5	5.5	1.1	0.9	3.5	2.5	3.7	2.5	0.4	0.4	230.8	57.7	249	69
7	10.0	5.9	0.8	0.8	2.5	2.8	3.1	2.9	0.4	0.4	230.8	57.7	248	70
8	30.0	8.2	4.7	0.8	6.5	3.0	3.5	1.9	0.4	0.2	230.8	230.8	276	245
9	17.3	5.0	1.8	0.9	5.0	2.5	4.4	2.3	0.5	0.2	230.8	115.4	260	126
10	20.5	7.3	1.2	3.0	4.3	5.3	3.8	3.8	0.3	0.6	288.5	230.8	319	251
11	18.2	5.5	1.7	0.9	5.3	2.8	3.8	3.3	0.4	0.4	115.4	115.4	145	128
12	10.5	10.5	1.7	4.0	4.5	19.0	2.7	2.7	0.3	0.6	230.8	173.1	250	210
13	18.2	3.6	3.7	0.6	5.0	1.8	3.8	3.1	0.5	0.5	115.4	57.7	147	67
14	13.2	13.6	1.3	4.1	4.3	10.5	3.7	7.1	0.6	3.3	173.1	173.1	196	212
15	22.3	18.6	1.4	5.0	4.3	18.3	2.1	9.6	0.4	3.3	230.8	230.8	261	286
16	96.8	11.4	5.7	3.8	26.0	13.3	3.1	8.1	0.3	3.3	288.5	288.5	420	328
17	17.3	231.8	6.1	6.0	21.8	33.0	3.8	4.8	0.4	0.8	230.8	230.8	280	507
18	57.3	10.0	4.8	2.5	6.3	2.5	3.8	2.9	0.4	0.6	461.5	57.7	534	76
19	29.5	5.0	5.3	2.8	12.5	2.8	3.5	3.1	0.4	0.4	230.8	173.1	282	187
20	13.6	10.5	4.1	2.5	7.8	3.5	2.9	3.8	0.6	1.2	115.4	288.5	144	310
21	18.2	4.1	3.5	1.8	5.8	2.8	3.7	3.8	0.5	0.3	57.7	57.7	89	71
22	22.3	3.6	3.3	1.9	7.0	2.5	4.4	4.6	0.5	0.3	115.4	115.4	153	128
23	12.7	5.0	0.9	3.0	2.3	3.5	2.5	3.8	0.3	0.3	0.0	0.0	19	16
24	18.2	4.1	4.7	0.6	4.5	1.3	3.3	2.3	0.3	0.2	115.4	115.4	146	124
25	14.5	13.6	1.3	0.9	6.3	3.8	4.4	2.1	0.4	0.3	115.4	57.7	142	78
26	35.0	3.2	4.8	0.8	6.0	1.0	3.1	1.2	0.2	0.1	0.0	0.0	49	6
27	70.5	3.2	4.0	0.8	7.0	1.3	4.4	1.3	0.4	0.1	57.7	0.0	144	7
28	18.2	12.3	3.4	4.0	8.5	3.5	4.8	3.7	0.4	0.5	57.7	57.7	93	82
29	50.5	4.1	5.3	1.7	5.8	5.5	4.4	2.9	0.6	0.5	173.1	173.1	240	188
30	9.5	8.6	1.8	1.0	4.0	7.0	4.4	3.1	0.4	0.4	0.0	173.1	20	193
31	17.3	5.0	6.0	0.6	5.0	2.8	4.4	3.8	0.4	0.4	173.1	57.7	206	70
32	10.5	3.6	1.3	0.8	3.3	2.5	2.7	3.8	0.2	0.4	57.7	115.4	76	126
33	18.6	6.4	1.9	0.8	4.8	5.8	4.4	4.0	0.4	0.4	0.0	115.4	30	133
34	20.5	6.4	4.5	0.9	6.3	3.3	5.4	3.1	1.6	0.3	173.1	57.7	211	72
35	14.1	3.6	3.7	0.8	4.5	3.3	2.9	3.5	0.4	0.4	57.7	115.4	83	127

Table 8. Continued

Sampling Site No.	Er												RI	
	Pb		Zn		Cu		Ni		Mn		Cd			
	2016	2021	2016	2021	2016	2021	2016	2021	2016	2021	2016	2021	2016	2021
36	25.5	5.5	3.8	0.9	5.0	3.8	4.6	2.9	0.7	0.4	57.7	115.4	97	129
37	37.7	4.1	4.3	0.8	7.8	3.5	4.4	2.9	0.4	0.3	115.4	57.7	170	69
38	25.5	6.8	4.1	0.8	4.8	4.8	3.1	2.9	0.4	0.4	0.0	57.7	38	73
39	30.5	4.1	4.4	0.8	6.5	2.0	3.5	2.5	1.9	0.3	115.4	57.7	162	67
40	30.9	2.7	4.0	0.6	11.3	1.0	2.1	1.9	0.3	0.3	0.0	0.0	49	6
41	20.0	2.3	1.4	0.8	5.3	1.8	4.0	1.3	0.4	0.3	0.0	0.0	31	7
42	12.3	11.8	1.3	0.9	4.3	4.3	2.9	2.3	0.4	0.4	57.7	57.7	79	77
43	18.2	4.1	1.7	0.8	5.3	2.0	3.5	3.1	0.5	0.3	57.7	115.4	87	126
44	13.2	4.1	1.3	4.0	5.8	6.0	4.2	3.8	0.3	0.5	115.4	115.4	140	134
45	15.0	3.6	1.3	3.3	4.5	6.8	2.1	3.3	0.4	0.4	57.7	57.7	81	75
min	5.9	2.3	0.8	0.6	2.3	1.0	2.1	1.2	0.2	0.1	0.0	0.0	19	6
max	96.8	231.8	6.1	6.0	26.0	33.0	8.1	9.6	1.9	3.3	461.5	288.5	534	507
mean	23.5	11.3	3.0	1.7	6.5	4.9	3.7	3.3	0.5	0.6	138.5	112.8	176	135

Source: compiled by the authors

The potential ecological risk factor (Eri) for Pb, Zn, Cu, Ni, Mn, and Cd in 2016 ranged from 5.9-96.8 (mean 23.5), 0.8-6.1 (mean 3.0), 2.3-26.0 (mean 6.5), 2.1-8.1 (mean 3.7), 0.2-1.9 (mean 0.5), and 0.0-461.5 (mean 138.5), respectively. In 2021, Eri varied as follows: Pb – 2.3-231.8 (mean 11.3), Zn – 0.6-6.0 (mean 1.7), Cu – 1.0-33.0 (mean 4.9), Ni – 1.2-9.6 (mean 3.3), Mn – 0.1-3.3 (mean 0.6), and Cd – 0-288 (mean 113), respectively. The main environmentally hazardous metal present in the soils of the studied area was Cd. The ecological risk level of soil contamination by this toxicant in 2016 was assessed as moderate (20%), considerable (24%), high (41%), very high (2%), while 13% of the soils were uncontaminated by this toxic metal. In 2021, 31% of the soil samples fell into the moderate ecological risk category, 27% – considerable, 31% – high, and 11% were uncontaminated.

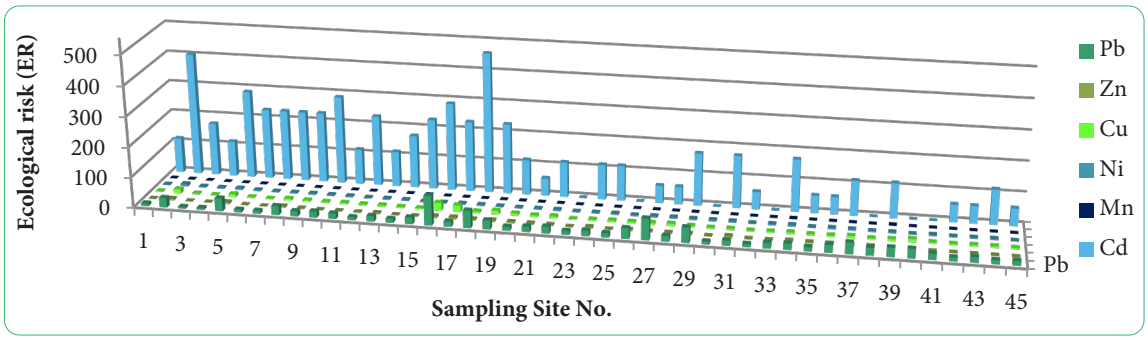

Figure 12. *Er* levels in 2016

Source: compiled by the authors

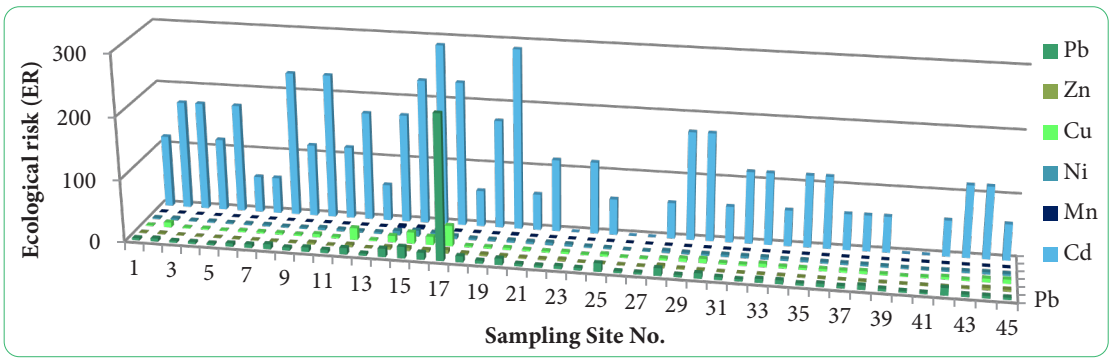

Figure 13. *Er* levels in 2021

Source: compiled by the authors

The ecological risk level of Pb contamination in 2016 was low for 89% of the soils, moderate for 9%, and considerable for 2%. In 2021, only one soil sample (site 17) exhibited a high ecological risk, while all other locations were low. For the other heavy metals, the ecological risk of soil contamination remained low. Based on the cumulative ecological risk (Fig. 14), in 2016, 53% of soil samples were classified as having a low contamination level, 36% as moderate, and 11% as high. In 2021, these proportions were 69%, 24%, and 7%, respectively.

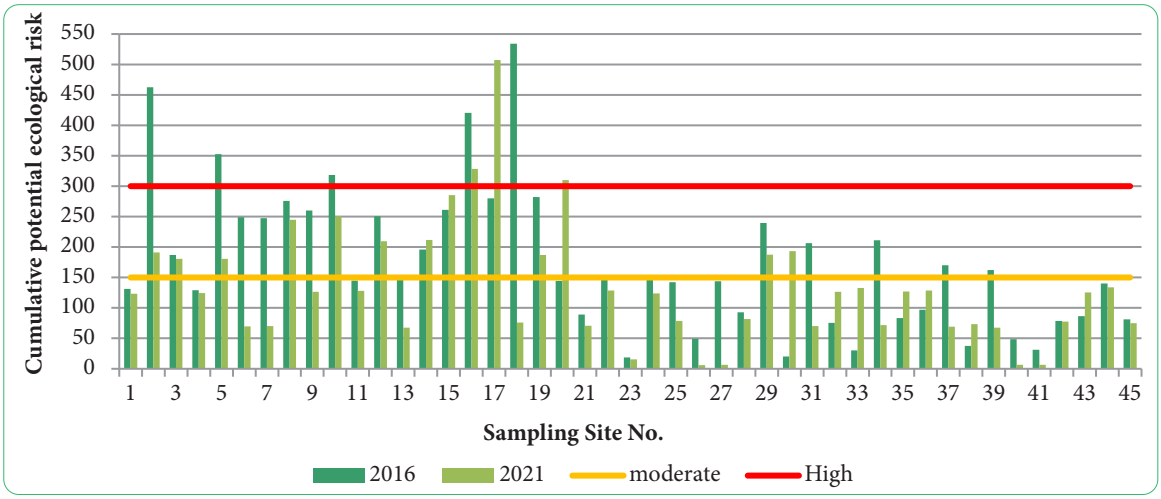

Figure 14. Cumulative potential ecological risk of heavy metal contamination in soils
Source: compiled by the authors

The most critical situations in 2016 were observed at sites 2, 5, 10, 16, and 18, whereas in 2021 the highest risk was recorded at sites 16 and 17. None of the samples exhibited an extremely high level of risk; however, in 2016, sites 2, 5, 10, 16, and 18 showed values exceeding 300, indicating a significant cumulative heavy metal load and a high potential ecological risk. In 2021, the number of such sites decreased (Fig. 13).

The study summarised and statistically processed the results of soil quality monitoring in Cherkasy for Pb, Zn, Cu, Ni, Mn, and Cd using both single-factor and multi-factor soil quality indices. Variations in heavy metal concentrations in the soil primarily depend on the parent material and geological background, but human economic activity also has a significant influence (Yang *et al.*, 2018). The study demonstrated notable spatial differences in the concentrations of the metals analysed. It was found that Mn had the highest content, while Cd had the lowest. The average concentrations decreased in the order Mn > Zn > Pb > Cu > Ni > Cd. High Mn concentrations in the city's soils are attributed to its geological background, as confirmed by pollution indices remaining below 1 across almost all sampling sites. Statistical analysis of the Cherkasy urban soil monitoring data revealed significant spatial and temporal variability in the concentrations of all heavy metals (Table 5), indicating localized enrichment patterns and heterogeneity. The uneven distribution of heavy metals is likely influenced by differences in soil texture (sandy vs. clayey) and industrial emissions, which create artificial and often uneven element concentrations. The coefficient of variation (CV) for Mn, Zn, Pb, Cu, and Cd across different sampling sites in 2016 indicated high variability ($50\% < CV \leq 100\%$), suggesting strong spatial heterogeneity. In 2021, these values significantly exceeded 100% (Pb – 300%, Mn – 130%, Cu – 120%), indicating an even higher degree of spatial variability in heavy metal distribution. This considerable variability in heavy metal concentrations may be associated with localised anthropogenic impacts or similar migration patterns (Rahman *et al.*, 2022; Wu *et al.*, 2025).

Extremely high values of the coefficient of variation for Pb were caused by a very high concentration of this metal at local site 17 (c = 510 mg/kg), against a background of sites with low Pb content. Such elevated lead levels may be attributed to paint fragments, battery residues, and technogenic microparticles. The high degree of variation in Mn and Cu was associated with elevated concentrations of these metals at sites 14-16 (for Mn) and site 17 (for Cu), which may have been caused by local contamination from waste generated by machine-building industries or by changes in the soil's mechanical composition at these sites. In contrast, the coefficient of variation (CV) for Ni across different sampling sites showed moderate variability ($21\% < CV \leq 50\%$), indicating that the sources of Ni may be both natural (geogenic influences) and anthropogenic (emissions from industrial enterprises and vehicles, as well as subsequent atmospheric transport). The strong correlation between Pb and Cu identified in the correlation analysis suggests common pollution sources, likely related to human activities. Potential industrial sources of these metals in the environment include materials used in battery production, electricity generation, and paints (Swain, 2024). In the study area, the shared sources of Pb and Cu contamination in the landscapes are the thermal

power plant (TPP), enterprises producing paint and electrical engineering products, and motor transport (exhaust gases, brake pad wear). High correlation values between Ni and Mn also suggest common sources, but these are likely predominantly natural (e.g., weathering of rocks, wind erosion) and partially anthropogenic, considering the moderate coefficient of variation for Ni and the weak correlations of Mn with all other metals. Manganese is typically present in soils at relatively high natural concentrations. Therefore, limited human activity in the study area may not significantly affect its concentration. Consequently, its presence in the investigated soils may not be directly related to anthropogenic activities (Taghavi *et al.*, 2022). Potential anthropogenic sources of Ni and Mn contamination in Cherkasy include mechanical engineering and chemical industries, thermal power generation (combustion of fossil fuels), and motor transport.

The complex interaction between natural and anthropogenic factors that regulate the distribution and accumulation patterns of heavy metals has also been noted in previous studies (Wu *et al.*, 2025). Differentiating natural versus anthropogenic contributions and identifying human-derived inputs of chemical elements into soils was facilitated by the I_{geo}, which is used to assess the intensity of technogenic contamination. The predominantly natural origin of Mn, Ni, and Cu is confirmed by the strongly negative values of this index. More than 93% of the investigated soils were found to be uncontaminated by these elements. I_{geo} values for Pb and Cd indicate a significant impact of anthropogenic pollution, with only some locations showing lightly or moderately contaminated soils where Pb content was low. The obtained I_{geo} values for Zn suggest a mixed natural-anthropogenic origin for the input and accumulation of this metal. Like the I_{geo} values, *PI* showed high variability, ranging from uncontaminated to very heavily contaminated soils, depending on the specific metals analysed. *PI* values above 1 for all metals except Ni and Mn indicate elevated concentrations due to anthropogenic influence. $PI_{Nemerow}$ were higher than the *PLI* values, which can be explained by the calculation algorithm of $PI_{Nemerow}$ as it accounts for both the average and the maximum values of single-metal *PI*.

A detailed analysis of potential ecological risk, which predominates in assessing the extent of heavy metal contamination in soils and the associated ecological consequences for soil ecosystems, shows that Cd posed mainly moderate, considerable, or high ecological risk and was the main contributor to the overall risk. Only in one location was a high ecological risk observed for Pb in 2021, while all other heavy metals posed a negligible ecological risk. Z. Wang *et al.* (2015) presented the results of a study on soil contamination by metals conducted using geochemical indices and multivariate statistical methods, which enabled the identification of possible sources and pathways of pollutants, as well as the assessment of their potential impact on soil quality and human health. The multi-index analysis of soil quality across different urban sites revealed that the most critical situation was observed in the southeastern and eastern industrial zones. In residential-industrial areas, urban soils generally exhibited low to moderate levels of contamination.

Similar findings have been reported in numerous other studies examining the impact of anthropogenic activities on urban ecosystems. For example, Y. Kuang *et al.* (2024) demonstrated that intensive human activity directly affects soil contamination levels-samples from industrial zones exhibited elevated potential ecological risk, posing a threat to public health. Statistical analyses confirmed that intensive industrial operations significantly influence the degree of soil pollution. A principal component analysis of urban soil contamination, presented by Ghosh *et al.*, 2023, revealed clear patterns of metal covariation, indicating likely sources such as industrial emissions, vehicular traffic, and natural factors. Comparing soil monitoring data from 2016 and 2021 showed certain trends. Most metals exhibited a positive dynamic, with decreasing concentrations: Pb decreased on average by 28%, Cd by 21%, and Zn by 15%. Concentrations of other elements remained largely unchanged, with Cu fluctuating within ±5% and Ni showing a slight decline of 8%. Some elements experienced localised increases, with Mn content rising by 12%.

The spatiotemporal and multi-index geochemical assessment of urban soils in Cherkasy provides critical insights into the dynamics of technogenic pressure and associated ecological hazards. Contextualising these findings within both national baselines and international literature allows for a comprehensive understanding of anthropogenic intervention and environmental risk patterns. The high spatial heterogeneity observed for manganese (Mn), zinc (Zn), lead (Pb), copper (Cu), and cadmium (Cd), indicated by coefficients of variation (CV) ranging from 51% to 100%, confirms that these elements are strongly influenced by localised point sources rather than uniform natural distribution. This high variability in urban zones aligns with the global observations compiled by Q. Yang *et al.* (2018), who noted that industrialisation and intense agricultural practices create highly fragmented soil pollution profiles across diverse geographical regions. In Cherkasy, the concentration of the highest pollution levels within the southeastern and eastern industrial hubs reflects patterns identified by Y. Zhou *et al.* (2022), who demonstrated that areas surrounding long-standing industrial complexes with extensive production histories act as primary sinks for heavy metal accumulation. Conversely, the moderate variation of nickel (Ni), with a coefficient of variation between 21% and 50%, suggests a more balanced interplay between geogenic baselines and diffuse anthropogenic inputs, matching the urban soil characteristics documented by Y. Kuang *et al.* (2024), where intermediate variability typically signified a dual natural-anthropogenic origin. Geochemical Relationships and Source Apportionment Statistical correlation analysis revealed a robust relationship between lead

(Pb) and copper (Cu), pointing toward a shared suite of anthropogenic vectors. In urban environments, this geochemical pairing is frequently driven by the combustion of fossil fuels, vehicular emissions, and discharges from paint and electrical manufacturing. This signature corresponds closely with the long-term urban soil dynamics described by S.G. Papadimou *et al.* (2023), where vehicular traffic and municipal infrastructure served as persistent sources of concurrent Pb and Cu accumulation over extended monitoring periods. In contrast, the strong correlation between nickel (Ni) and manganese (Mn) highlights a mixed geogenic-anthropogenic pathway. While natural soil erosion contributes significantly to the baseline presence of these metals, their concentrations are augmented by machinery manufacturing, chemical processing, and thermal power generation. This dual-origin behaviour is well-documented in the methodological frameworks reviewed by J.B. Kowalska *et al.* (2018), which emphasise that moderate-to-strong correlations among elements like Ni and Mn often reflect underlying lithogenic properties that are partially masked by widespread, low-intensity industrial fallout. Ecological Risk Assessment and Methodological Efficacy The identification of cadmium (Cd) as the primary contributor to potential ecological risk within Cherkasy is a critical outcome of the multi-index approach. Under the foundational framework established by L. Hakanson & S. Charlesworth (1980), elements are evaluated not merely by absolute concentration, but by their biological toxicity weighting factors. Because Cd possesses an exceptionally high toxic-response coefficient, even minor elevations above the natural Ukrainian regional baselines established by A.I. Fateiev & Ya.V. Pashchenko (2003) trigger severe risk classifications. The utilisation of both single-factor indices I_{geo}, contamination/ *PI*, *Er* and composite indices *PLI*, $PI_{Nemerow}$, and RI proved essential for preventing the underestimation of localised threats. As discussed by Ferreira *et al.* (2022), single-factor indices can occasionally overemphasise isolated anomalies, whereas composite models provide a holistic overview of the total pollution burden. In Cherkasy, while $PI_{Nemerow}$ and potential *RI* accurately highlighted the severity of the industrial hubs. This gradient confirms that urban zoning and proximity to heavy infrastructure remain the definitive factors shaping the urban soil profile, mirroring the urban soil indicators evaluated by T.F. Iakovyshyna (2022) across other Ukrainian ecosystems and reinforcing the need for targeted, zone-specific risk management strategies.

Conclusions

The study revealed significant spatial and temporal transformations of urban soils due to the long-term accumulation of heavy metals, resulting in an altered geochemical soil province associated with anthropogenic sources. Spatial analysis of zones with high and low metal concentrations demonstrated clear heterogeneity influenced by both natural and anthropogenic factors. Using various geochemical indices and statistical-correlation analysis, patterns of grouping and associations between the analysed metals were identified, providing insight into potential pollution sources and their interrelationships. The study demonstrated that, based on the average heavy metal content in the city, the following geochemical sequence of urban soil contamination was formed: Mn > Zn > Pb > Cu > Ni > Cd, reflecting a natural-technogenic element association. Most metals showed a decreasing trend in concentrations over the period 2016-2021. For Pb, an average decrease of 28% was observed, with the most pronounced reduction in residential areas. Cadmium concentrations decreased by 21%, and zinc by 15%, while concentrations of other elements remained relatively stable. Strong correlations ($r > 0.7$) were observed between Pb and Cu, as well as between Ni and Mn, indicating similar sources of these elements in urban soils. The applied geochemical indices provided information on the contamination levels of each analysed heavy metal, allowed assessment of the overall scale of pollution and potential ecological risk, enabled identification of probable heavy metal sources, highlighted sites with the highest potential accumulation risk, and characterised the capacity of the surface soil horizon to accumulate heavy metals. The conducted study of urban soils in Cherkasy indicated the formation of localised areas of moderate and high ecological load, posing long-term risks to the ecosystem and human health. A significant potential ecological risk associated with cadmium contamination was identified. Over the period 2016-2021, the proportion of moderately contaminated soils increased 1.4-fold, reaching 31% of the analysed samples, while heavily contaminated soils increased 1.1-fold to 27%. The proportion of uncontaminated soils decreased 1.2-fold. Regarding integrated ecological risk, the proportion of soils with high and moderate contamination decreased 1.6- and 1.5-fold, respectively, while the proportion of soils with low contamination increased 1.3-fold. None of the samples exhibited an extremely high risk level; however, in 2016, sites 2, 5, 10, 16, and 18 exceeded a value of 300, indicating a significant cumulative heavy metal load and a high potential ecological risk. The next stages of the research include assessing the impact of heavy metals on human health; developing cartographic models of the geoecological state of urban soils and identifying areas of significant transformation of urban soils using modern GIS technologies; and addressing the problem of high pollutant concentrations to support sustainable urban development.

Acknowledgements

None.

Funding

None.

Conflict of Interest

None.

References

[1] Cheng, H., Huang, L., Ma, P., & Shi, Y. (2019). Ecological risk and restoration measures relating to heavy metal pollution in industrial and mining wastelands. *International Journal of Environmental Research and Public Health*, 16(20), article number 3985. doi: 10.3390/ijerph16203985.

[2] Fateiev, A.I., & Pashchenko, Ya.V. (2003). *Background content of microelements in the soils of Ukraine*. Kharkiv: Institute for Soil Science and Agricultural Chemistry Research named after O.N. Sokolovsky.

[3] Ferreira, S.L.C., da Silva, J.B., dos Santos, I.F., de Oliveira, O.M.C., Cerda, V., & Queiroz, A.F.S. (2022). Use of pollution indices and ecological risk in the assessment of contamination from chemical elements in soils and sediments – practical aspects. *Trends in Environmental Analytical Chemistry*, 35, article number e00169. doi: 10.1016/j.teac.2022.e00169.

[4] Ghosh, B., Padhy, P.K., Niyogi, S., Patra, P.K., & Hecker, M. (2023). A comparative study of heavy metal pollution in ambient air and the health risks assessment in industrial, urban and semi-urban areas of West Bengal, India. *Environments*, 10(11), article number 190. doi: 10.3390/environments10110190.

[5] Hakanson, L., & Charlesworth, S. (1980). An ecological risk index for aquatic pollution control: A sedimentological approach. *Water Research*, 14(8), 975-1001. doi: 10.1016/0043-1354(80)90143-8.

[6] He, L., Wang, S., Liu, M., Chen, Z., Xu, J., & Dong, Y. (2023). Transport and transformation of atmospheric metals in ecosystems: A review. *Journal of Hazardous Materials Advances*, 9, article number 100218. doi: 10.1016/j.hazadv.2022.100218.

[7] Iakovyshyna, T.F. (2022). Use of environmental risk indicators to assess the degree of danger of metal compounds pollution of urban ecosystem soils. *Environmental Sciences*, 3(42), 67-71. doi: 10.32846/2306-9716/2022.eco.3-42.11.

[8] Jin, M., Tang, M., Liu, J., Zhang, J., & Xiao, R. (2025). Multi-index assessment of heavy metal contamination and ecological risks in paddy soils along national highways in southern Henan Province, China. *Agronomy*, 15(6), article number 1348. doi: 10.3390/agronomy15061348.

[9] Kowalska, J.B., Mazurek, R., Gasiorek, M., & Zaleski, T. (2018). Pollution indices as useful tools for the comprehensive evaluation of the degree of soil contamination – a review. *Environmental Geochemistry and Health*, 40, 2395-2420. doi: 10.1007/s10653-018-0106-z.

[10] Kuang, Y., Chen, X., & Zhu, C. (2024). Characteristics of soil heavy metal pollution and health risks in Chenzhou City. *Processes*, 12(3), article number 623. doi: 10.3390/pr12030623.

[11] Mislyuk, O., Khomenko, E., Yehorova, O., & Zhytska, L. (2023). Assessing risk caused by atmospheric air pollution from motor vehicles to the health of population in urbanized areas. *Eastern-European Journal of Enterprise Technologies*, 1(10), 19-26. doi: 10.15587/1729-4061.2023.274174.

[12] Mustapha, L.S., Obayomi, O.V., & Obayomi, K.S. (2025). A comprehensive review on potential heavy metals in the environment: Persistence, bioaccumulation, ecotoxicology, and agricultural impacts. *Ecological Frontiers*, 46(2), 434-449. doi: 10.1016/j.ecofro.2025.10.009.

[13] Papadimou, S.G., Kantzou, O.D., Chartodiplomenou, M.A., & Golia, E.E. (2023). Urban soil pollution by heavy metals: Effect of the lockdown during the period of COVID-19 on pollutant levels over a five-year study. *Soil Systems*, 7(1), article number 28. doi: 10.3390/soilsystems7010028.

[14] Rahman, M.S., Ahmed, Z., Seefat, S.M., Alam, R., Islam, A.R.M.T., Choudhury, T.R., Begum, B.A., & Idris, A.M. (2022). Assessment of heavy metal contamination in sediment at the newly established tannery industrial estate in Bangladesh: A case study. *Environmental Chemistry and Ecotoxicology*, 4, 1-12. doi: 10.1016/j.enceco.2021.10.001.

[15] Reznikova, O.O., Voitovskyi, K.Ye., & Lepikhov, A.V. (2020). *National risk and threat assessment systems: Best world practices, new opportunities for Ukraine*. Kyiv: NISD.

[16] Rybalova, O.V., Korobkova, H.V., Hudzevich, A.V., Artemiev, S.R., & Bondar, O.B. (2022). Risk assessment for public health from air pollution in the industrial regions of Ukraine. *Visnyk of V.N. Karazin Kharkiv National University, Series "Geology. Geography. Ecology"*, 56, 204-215. doi: 10.26565/2410-7360-2022-56-15.

[17] Swain, C.K. (2024). Environmental pollution indices: A review on concentration of heavy metals in air, water, and soil near industrialization and urbanization. *Discovery Environment*, 2, article number 5. doi: 10.1007/s44274-024-00030-8.

[18] Taghavi, M., Darvishiyan, M., Momeni, M., Eslami, H., Fallahzadeh, R.A., & Zarei, A. (2022). Ecological risk assessment of trace elements pollution and human health risk exposure in agricultural soils used for saffron cultivation. *Research Square*. doi: 10.21203/rs.3.rs-2381307/v1.

[19] Wang, Z., Wang, Y., Chen, L., Yan, C., Yan, Y., & Chi, Q. (2015). Assessment of metal contamination in coastal sediments of the Maluan Bay (China) using geochemical indices and multivariate statistical approaches. *Marine Pollution Bulletin*, 99(1-2), 43-53. doi: 10.1016/j.marpolbul.2015.07.064.

[20] Wu, C., Bao, J., Wang, Z., Chen, Z., Zheng, Y., & Lu, H. (2025). Interplay of natural and anthropogenic factors in source and distribution of heavy metals in Pingtan coastal area, Fujian Province. *Frontiers in Marine Science*, 12, article number 1624141. doi: 10.3389/fmars.2025.1624141.

[21] Yang, Q., Li, Z., Lu, X., Duan, Q., Huang, L., & Bi, J. (2018). A review of soil heavy metal pollution from industrial and agricultural regions in China: Pollution and risk assessment. *Science of The Total Environment*, 642, 690-700. doi: 10.1016/j.scitotenv.2018.06.068.
[22] Yehorova, O., Mislyuk, O., Khomenko, O., & Postryhan, V. (2025). Risk-based assessment of atmospheric air pollution by heavy metals. *Ecological Engineering & Environmental Technology*, 11, 118-128. doi: 10.12912/27197050/211761.
[23] Yu, Z., Liu, E., Lin, Q., Zhang, E., Yang, F., Wei, C., & Shen, J. (2021). Comprehensive assessment of heavy metal pollution and ecological risk in lake sediment by combining total concentration and chemical partitioning. *Environmental Pollution*, 269, article number 116212. doi: 10.1016/j.envpol.2020.116212.
[24] Zhou, Y., Jiang, D., Ding, D., Wu, Y., Wei, J., Kong, L., Long, T., Fan, T., & Deng, S. (2022). Ecological-health risks assessment and source apportionment of heavy metals in agricultural soils around a super-sized lead-zinc smelter with a long production history, in China. *Environmental Pollution*, 307, article number 119487. doi: 10.1016/j.envpol.2022.119487.

Багатоіндексний геохімічний аналіз забруднення урбоземів в умовах техногенного навантаження

Ольга Мислюк
Кандидат хімічних наук, доцент
Черкаський державний технологічний університет
18006, бульв. Шевченка, 460, м. Черкаси, Україна
https://orcid.org/0000-0003-0401-9836
Оксана Єгорова
Кандидат технічних наук, доцент
Черкаський державний технологічний університет
18006, бульв. Шевченка, 460, м. Черкаси, Україна
https://orcid.org/0000-0002-7801-5582
Олена Хоменко
Кандидат хімічних наук, доцент
Черкаський державний технологічний університет
18006, бульв. Шевченка, 460, м. Черкаси, Україна
https://orcid.org/0000-0001-9329-0577
Олександр Лобода
Доктор хімічних наук, доцент
Черкаський державний технологічний університет
18006, бульв. Шевченка, 460, м. Черкаси, Україна
https://orcid.org/0000-0001-5524-3251

Анотація. Забруднення ґрунтів важкими металами стає дедалі серйознішою проблемою в усьому світі. З цих причин комплексна кількісна оцінка якісного стану урбоземів, які знаходяться під техногенним навантаженням, є важливою для розуміння закономірностей забруднення та потенційних екологічних ризиків. Метою проведення дослідження був просторово-часовий аналіз вмісту і оцінка впливу важких металів на стан урбоземів м. Черкаси, ідентифікація джерел забруднення для прийняття обґрунтованих управлінських рішень. Оцінювання ризиків проводили за допомогою багатоіндексного геохімічного аналізу з використанням однофакторних (індекс геоакумуляції I_{geo}, індекс забруднення PI, індекс екологічного ризику *Er*) і комплексних індексів (індекс забруднення PLI, індекс забруднення Немерова та потенційний екологічний ризик RI). Для виявлення імовірних джерел забруднення використовували статистично-кореляційний аналіз. Проведений аналіз продемонстрував значні просторові відмінності в концентраціях досліджених металів. Коефіцієнт варіації для Mn, Zn, Pb, Cu **та** Cd мав високу (51 % < CV ≤ 100 %) мінливість на різних ділянках, що свідчить про сильну просторову гетерогенність. Натомість значення коефіцієнтів варіації Ni були помірними (21 % < CV ≤ 50), що вказує на його природно-антропогенне походження у ґрунті. Сильний зв'язок для Pb і Cu, виявлений при кореляційному аналізі, свідчить про спільні джерела забруднення, ймовірно, теплоелектроцентраль, підприємства з виробництва лакофарбової та електротехнічної продукції, автотранспорт. Високі значення коефіцієнта кореляції між Ni і Mn вказують на змішаний вплив геогенних (ерозія ґрунтів) і антропогенних джерел (підприємства машинобудівної та хімічної промисловості, теплоелектроцентраль та автотранспорт). Значний потенційний екологічний ризик для ґрунтових екосистем при забрудненні ґрунтів на дослідженій території

виявлений для Cd. Багатоіндексний підхід до оцінки впливу забруднення важкими металами досліджених ґрунтів на різних локаціях міста показав, що найбільш небезпечна ситуація склалася в південно-східному і східному промислових вузлах. В селітебно-промислових районах урбоземи мали переважно незначний та помірний рівень забруднення. Основним потенційно екологічно небезпечним важким металом виявився Cd. Результати цього дослідження можуть бути основою для розробки та впровадження цілеспрямованих методів управління ризиками

Ключові слова: важкі метали; міські ґрунти; кореляційні залежності; просторова мінливість; екологічний ризик; антропогенний вплив

Vol. 17, No. 1
2026

Ecological Safety and Balanced Use of Resources

ISSN (print) 2415-3184, ISSN (online) 2522-9508
Journal homepage: https://esbur.com.ua/en

Received: 17.11.2025. Revised: 05.05.2026. Accepted: 12.06.2026. Published: 30.06.2026.

UDC 338.48:502.131.1

DOI: 10.63341/esbur/1.2026.49

International experience in managing the environmentally safe development of tourism and recreational activities: Models, trends, and assessment tools

Liudmyla Tranchenko
Doctor of Economic Sciences, Professor
Uman National University
20301, 1 Institutska Str., Uman, Ukraine
https://orcid.org/0000-0003-0900-5484

Liudmyla Arkhypova*
Doctor of Technical Sciences, Professor
Ivano-Frankivsk National Technical University of Oil and Gas
76019, 15 Karpatska Str., Ivano-Frankivsk, Ukraine
https://orcid.org/0000-0002-8725-6943

Oleksandr Tranchenko
PhD in Economic Sciences, Associate Professor
Uman National University
20301, 1 Institutska Str., Uman, Ukraine
https://orcid.org/0000-0002-0639-5109

Uliana Andrusiv
PhD in Economic Sciences, Associate Professor
Ivano-Frankivsk National Technical University of Oil and Gas
76019, 15 Karpatska Str., Ivano-Frankivsk, Ukraine
https://orcid.org/0000-0003-1793-0936

Tetiana Dolishnia
PhD in Economic Sciences, Associate Professor
Ivano-Frankivsk National Technical University of Oil and Gas
76019, 15 Karpatska Str., Ivano-Frankivsk, Ukraine
https://orcid.org/0000-0003-0972-4219

Abstract. At the present stage, the environmentally safe development of tourism and recreational activities in Ukraine is gaining strategic importance as a priority area of sustainable development. It promotes the rational use of natural areas, contributes to the formation of environmental awareness, and requires systematic regulation to prevent environmental degradation. The aim of this study was to generalise international experience in managing the environmentally safe development of tourism and recreational activities and to establish an analytical framework for its adaptation to Ukrainian conditions. The study systematises international management approaches and identifies eight typological models of ecotourism development characterised by institutional architecture, the role of local communities, visitor flow management instruments, the application of environmental standards, and collaborative governance mechanisms. Based on a comparative case-study analysis, the key trends were identified, including the

Suggested Citation: Tranchenko, L., Arkhypova, L., Tranchenko, O., Andrusiv, U., & Dolishnia, T. (2026). International experience in managing the environmentally safe development of tourism and recreational activities: Models, trends, and assessment tools. *Ecological Safety and Balanced Use of Resources*, 17(1), 49-68. doi: 10.63341/esbur/1.2026.49.

*Corresponding author (*konsevich@ukr.net*)

intensification of environmental certification, the expansion of community-based tourism, the digitalisation of visitor management in protected areas, and the development of low-impact tourism practices. Particular attention was paid to rankings and composite indices as instruments for enhancing national competitiveness in international tourism and as elements of contemporary geopolitical positioning. The structure of the Global Wildlife Travel Index was analysed, and the positions of Australia, Canada, the United States, and Ukraine were compared using selected indicators and overall index values. The study revealed several methodological limitations of the index, including its sensitivity to indicator selection and aggregation procedures, which reduces the validity of final assessments and necessitates its critical application in scientific research. The findings substantiate the need for further refinement of tourism sustainability indices in order to improve the transparency, reproducibility, and comparability of assessment results and to enhance their applicability in evidence-based tourism policy and environmental management

Keywords: ecotourism; nature-based tourism; environmentally safe tourism practices; international experience; models of environmentally safe tourism and recreational development; tourism indices and rankings

Introduction

Several major trends can be identified in the contemporary tourism industry, among which the orientation toward sustainability and environmental balance has become particularly significant. While the emergence of nature-based tourism was initially driven by the intensification of the environmental crisis, ecotourism itself has gradually evolved into a mass phenomenon and is increasingly regarded as a potential risk factor for environmental safety, ecosystem stability, and the functioning of natural complexes. Consequently, countries that occupy leading positions in the global tourism sector in terms of tourist arrivals and revenues, as well as recognised leaders in ecotourism development, have actively introduced systematic approaches to tourism governance. These approaches are based on the principles of consistency, effectiveness, and environmental responsibility aimed at ensuring an adequate level of environmental safety within tourist destinations.

According to the findings of K. Matiyiv *et al.* (2022), the tourism sector is gradually undergoing a process of "greening", reflected in increasing attention to the environmental characteristics of resorts and destinations, the conservation of natural landscapes, and the protection of biodiversity. As a result, a growing number of tourists prefer destinations located in natural areas that have experienced minimal anthropogenic disturbance and have retained their ecological authenticity. At the current stage of tourism industry transformation, a persistent global shift toward sustainability, environmentalisation, and responsible natural resource use can be observed, as confirmed by N.V. Anistratenko & A.V. Malchenko (2022). In contemporary literature, the focus is moving away from declarative discussions of "green tourism" toward the analysis of tourism governance as a system of managerial rationalities, institutional norms, and decision-making practices that directly determine the environmental quality of tourism and recreational development. Consequently, the environmentally safe development of tourism and recreational activities is increasingly viewed as a function of governance effectiveness and the capacity of institutions to establish the "rules of the game" for visitors and stakeholders, as emphasised by R. Sharpley *et al.* (2023) and A. Lundén *et al.* (2025).

As noted by M. Rogowski *et al.* (2025), the paradigm of tourism environmentalisation does not eliminate one of the key contemporary contradictions: nature-based travel, despite being positioned as environmentally acceptable, may generate increasing pressure on ecosystems precisely because of the growing popularity of natural destinations. Empirical studies by Z.A. Atamanchuk *et al.* (2020) and M. Medina-Chavarría *et al.* (2024) demonstrate that the concentration of tourist flows within national parks and other environmentally sensitive areas intensifies manifestations of overtourism, resulting in spatial and temporal unevenness of visitation, user conflicts, and localised environmental degradation. In this context, environmentally safe tourism development should not be interpreted as an inherently "ecological" sector but rather as a socio-ecological-economic system in which environmental outcomes depend on governance regimes and the quality of regulation. A. Lundén *et al.* (2025) and M. Rogowski *et al.* (2025) emphasise that sustainability cannot be automatically guaranteed even within protected areas, since visitor management is influenced by institutional constraints, evolving governance rationalities, and tensions between nature conservation objectives and commercial interests. Moreover, contemporary international discussions increasingly extend beyond the concept of sustainable tourism toward the notion of regenerative tourism, which focuses not only on minimising impacts but also on restoring natural and social systems. J. Iddawala & D. Lee (2026) argue that the regenerative approach becomes particularly relevant during periods of systemic crisis, as it prioritises the restoration of territorial adaptive capacity, community engagement, and long-term ecosystem value.

Accordingly, visitor management instruments – such as zoning, seasonality control, mobility regulation, and route management – are gaining strategic importance, enabling natural areas to be transformed from mere "objects of consumption" into managed systems of recreational use. Lessons learned from the post-pandemic period further demonstrate that changes in mobility patterns and abrupt shifts in visitor behaviour require adaptive governance solutions based on flow analysis and scenario planning, as noted by A. Mandić *et al.* (2025). Thus, the

environmentally safe development of tourism and recreational activities should be understood as an institutionally supported process that integrates environmental constraints, visitor flow management, and the financial and organisational capacity necessary to maintain conservation regimes. Emerging scientific approaches also highlight the importance of integrating ecosystem integrity, visitation dynamics, and financing mechanisms to enhance the resilience of nature-based tourism systems. The aim of this study was to systematise international models of governance for the environmentally safe development of tourism and recreational activities, evaluate contemporary instruments for sustainable tourism management, and substantiate approaches to their adaptation within the Ukrainian context.

Materials and Methods

The object of the study comprised the processes of development and governance regulation of ecotourism within global and national tourism systems, as well as the mechanisms for the formation and application of international rankings and composite indices used to assess the ecological and tourism potential of countries. Ranking and indexing instruments were considered as analytical and managerial resources that not only reflect the current state of ecotourism but also influence tourism policy priorities, territorial competitiveness, and the international positioning of destinations. The methodological framework was based on the principles of interdisciplinarity, systems thinking, and evidence-based research. The study employed methods of analysis and synthesis, comparative and structural-functional approaches, statistical processing of data from the Global Wildlife Travel Index (2019), case-study analysis, and critical analysis to identify governance practices, methodological limitations of tourism indices, and their potential application in strategic planning. This approach enabled the interpretation of tourism indices as instruments of evidence-based tourism policy that support the measurement, interpretation, and justification of management decisions using internationally comparable data.

To assess the role of US federal agencies in ensuring the environmentally safe development of tourism, an expert evaluation method was applied. This approach was selected due to the absence of standardised quantitative indicators that would allow for the direct measurement of the contribution of individual institutions to regulatory, environmental protection, educational, monitoring, and infrastructure-related functions. The expert panel consisted of 12 specialists who met at least two of the following criteria: possession of an academic degree in tourism, ecology, environmental management, or public administration; a minimum of five years of research or professional experience in the management of protected areas, sustainable tourism, or environmental policy; and at least three scientific publications on sustainable tourism or environmental management published during 2020-2025. The evaluation was conducted individually. Each expert was asked to assess the intensity with which a specific institution performs a particular function using a three-level scale:

- High level (H) – the function represents one of the institution's core responsibilities and directly determines its principal management outcomes;
- Medium level (M) – the function is implemented systematically but plays a supporting or partially specialised role;
- Low level (L) – the function is performed indirectly or does not belong to the institution's primary areas of activity.

To ensure the reproducibility of results, qualitative assessments were quantified by assigning numerical values: H = 3 points, M = 2 points, and L = 1 point. For each "institution-function" combination, the arithmetic mean of expert scores was calculated. The final category was determined according to the following intervals: 2.50-3.00 points – High level (H); 1.50-2.49 points – Medium level (M); 1.00-1.49 points – Low level (L).

The consistency of expert judgments was assessed using Kendall's coefficient of concordance (W). A value of W greater than 0.70 was interpreted as indicating a high level of agreement among experts and, consequently, the reliability of the obtained results. The proposed approach enables comparative analysis of institutional models for environmentally safe tourism governance and ensures the reproducibility of the assessment procedure for other countries and tourism governance systems. For the analysis of tourism and recreational activities under wartime threats, the concept of wartime adaptive tourism is proposed. This concept is defined as the ability of a tourism system to maintain functionality, ensure visitor safety, and adapt to crisis conditions. The adaptability of tourism destinations can be assessed using an integrated index incorporating four groups of indicators.

1. Security Dimension: distance from active combat zones; frequency of air raid alerts; number of recorded emergency events; availability of shelters and warning systems.

2. Infrastructure Resilience: accessibility of transport connections; stability of energy supply; operational status of accommodation facilities; availability of digital infrastructure.

3. Tourism Market Adaptability: changes in tourist flows compared with the pre-war period; share of domestic tourism; diversification of tourism products; speed of tourism service recovery following crisis events.

4. Socio-Institutional Resilience: participation of local communities; existence of crisis-management programs; level of inter-institutional coordination; implementation of sustainable development principles.

Each indicator was assessed using a five-point scale, after which the integrated adaptability index was calculated:

$$AI = \frac{(S + I + M + R)}{4}, \quad (1)$$

where *AI* – Adaptability Index of the tourism system; *S* – Security Dimension score; *I* – Infrastructure Resilience score; *M* – Tourism Market Adaptability score; *R* – Socio-Institutional Resilience score. Depending on the obtained value, three levels of tourism system adaptability can be distinguished: high adaptability ($AI > 4.0$); moderate adaptability ($AI = 3.0\text{-}4.0$); low adaptability ($AI < 3.0$). The proposed approach enables the comparative assessment of tourism regions under wartime risks, facilitates the analysis of tourism flow recovery dynamics, and supports the development of recommendations aimed at enhancing the resilience and adaptive capacity of tourism destinations.

Results and Discussion

In constructing the Global Wildlife Travel Index (2019), the international agency True Luxury Travel employs eight key indicators, some of which are composite (aggregated) measures incorporating several interrelated factors. On the one hand, this system of indicators enables the assessment of natural-resource endowments and institutional mechanisms for biodiversity conservation. On the other hand, it provides a basis for comparing countries according to their potential for nature-based tourism development, a segment of the tourism industry that is particularly sensitive to environmental constraints and conservation requirements (Table 1).

Table 1. Indicator system of the global wildlife travel index

No.	Indicator	What It Measures	Category / Rationale
1	Megafauna Conservation	Proportion of extant megafauna species (>40 kg) relative to historically native species	Biodiversity conservation
2	Wildlife Species Richness	Number of recorded wildlife species (mammals, birds, fish, reptiles, and amphibians)	Biodiversity
3	Prevalence of National Parks	Number of national parks within a country	Conservation infrastructure
4	National Park Pioneering	Year of establishment of the first national park (historical benchmark)	Institutional tradition
5	Protected Natural Areas	Area of protected territories (fully or partially protected) per 1,000 ha	Nature protection coverage
6	Forest Area	Share of forests in the total land area of a country (%)	Landscape resources
7	Environmental Sustainability	Composite indicator including renewable energy use, recycling practices, eco-friendly accommodation, sustainable products, and related environmental measures	Sustainable development
8	Environmental Prosperity	Composite indicator reflecting environmental quality, reduction of anthropogenic pressures, and effectiveness of conservation efforts	Sustainable development

Source: summarised by the authors based on P. Wight (2001), M. Saayman *et al.* (2012), A.L. Stronza *et al.* (2019)

The Megafauna Conservation indicator reflects the proportion of extant megafauna species (adult animals weighing more than 40 kg) relative to the historically native assemblage of such species within a given territory. In essence, this indicator captures the degree of biocenotic integrity of ecosystems and demonstrates the extent to which a country has succeeded in preventing the degradation of trophic chains critically dependent on large mammals. Importantly, the megafauna conservation indicator reflects not only contemporary conservation policies but also the historical scale of anthropogenic transformation and colonisation-driven land-use processes. Consequently, the indicator may partially penalise countries with a long history of industrialisation even when current conservation efforts are highly effective. The Wildlife Species Richness indicator represents the recorded number of animal species, including mammals, birds, fish, reptiles, and amphibians. However, species richness alone constitutes an insufficient measure of wildlife tourism attractiveness. Not all species are accessible for observation, and many possess limited tourism visibility. A more informative approach would involve a composite indicator incorporating endemism, the proportion of rare species, biogeographical uniqueness, and accessibility for ecotourism activities.

The Prevalence of National Parks indicator measures the total number of national parks within a country. Nevertheless, the number of parks does not necessarily correspond to the quality of the conservation system. From a scientific perspective, greater validity could be achieved by introducing a coefficient integrating park area, funding levels, accessibility for ecotourism, the existence of management plans, staffing capacity, and monitoring systems. The National Park Pioneering indicator is determined by the year in which the first national park was established. Methodologically, this variable has primarily historical and symbolic significance rather than practical relevance for evaluating contemporary ecotourism potential. An early start in the development of a protected area system does not automatically guarantee its current effectiveness. Therefore, this indicator should be interpreted as a marker of conservation tradition rather than as an equivalent factor within the ranking framework.

The Protected Natural Areas category accounts for the area of protected territories (fully or partially protected) standardised per 1,000 hectares of land. The authors of the index correctly acknowledge that large countries with low population density often contain extensive ecologically valuable territories that remain effectively conserved even

without formal protected status. This reveals a structural bias within the methodology: large countries require alternative scaling approaches, while legal protection status does not necessarily reflect the actual level of ecosystem conservation. Greater differentiation according to protection regimes – strict nature reserves, managed resource-use areas, buffer zones, ecological corridors, and similar categories – would improve the robustness of the assessment.

The Forest Area indicator measures the proportion of forest cover within the total land area of a country. Although forest cover is an important factor for ecotourism development, it is not universally applicable. For wildlife safaris, desert tourism, and arid-region destinations, its relevance is substantially lower. Consequently, this indicator would benefit from weighting adjustments that account for the landscape and biogeographical characteristics of individual regions. The composite Environmental Sustainability indicator reflects the development of environmental technologies and practices, including environmentally friendly products, eco-accommodation, renewable energy use, recycling systems, and related sustainability measures. For scientific applications, it is essential that the methodology relies on verifiable international statistical databases (e.g., UNEP, OECD, World Bank, Environmental Performance Index) rather than opaque expert assessments. The Environmental Prosperity indicator evaluates a country's performance across three dimensions: environmental quality, reduction of anthropogenic pressures, and the effectiveness of conservation efforts. The principal scientific limitation of this indicator lies in the absence of a clearly measurable operationalisation. The lack of transparent criteria reduces the representativeness of the index for academic analysis because it limits the reproducibility of results.

For each of the eight criteria, countries are ranked in descending order according to indicator performance. The highest-ranked country receives five points, whereas the lowest-ranked country receives one point. Intermediate scores range from 1.1 to 4.9 depending on the country's position within the ranking. The scoring interval is determined by the total number of countries included in the assessment (107 countries in the 2019 edition). The composite index is calculated by summing the scores obtained across all eight indicators. The theoretical maximum score is 40 points. In cases where countries achieve identical overall scores, priority is given to the country with the higher Environmental Sustainability score, thereby emphasising environmental modernisation as a fundamental prerequisite for sustainable tourism development.

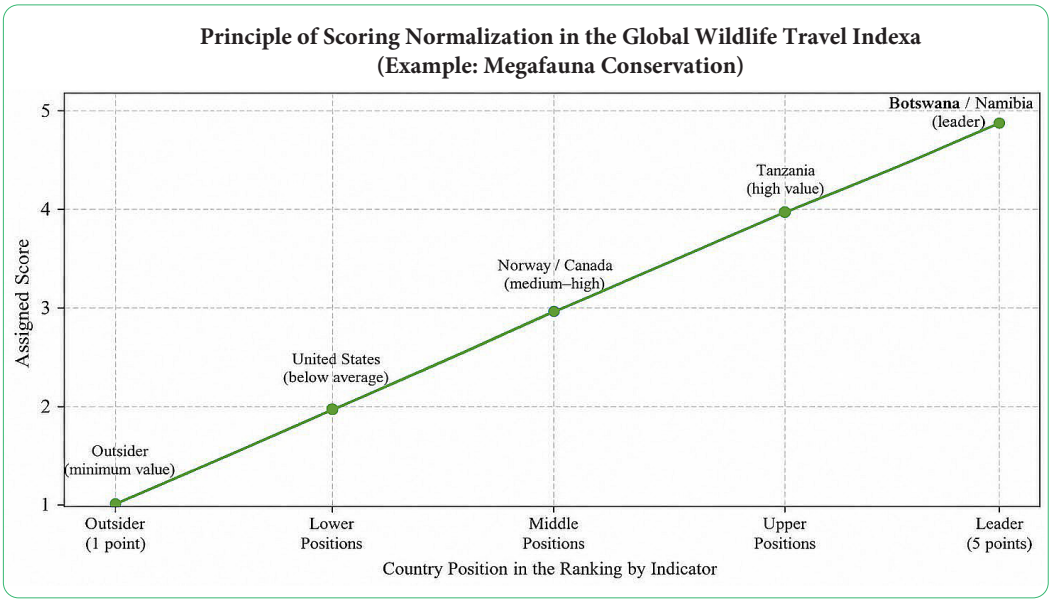

Figure 1. Principles of normalisation of Global wildlife travel index scores
Note: countries are given as illustrative examples according to the ranking description in the index methodology
Source: summarised by the authors based on Global wildlife travel index (2019)

The conducted analysis demonstrates that the True Luxury Travel Index can be regarded as a supplementary composite instrument for measuring the ecological and tourism potential of countries, as it integrates parameters relevant to both biodiversity conservation and nature-based tourism development. Its principal advantage lies in its multidimensional character, which partially reduces subjectivity and expands opportunities for international comparisons of destinations according to their prospects for travel-to-nature tourism segments. Thus, the index may serve as a preliminary analytical framework for benchmarking and stratifying countries according to their ecotourism prerequisites.

Simultaneously, the logic of tourism demand continues to evolve. Environmentally sensitive motivations, preferences for natural destinations, and expectations regarding the ecological integrity of tourism destinations are becoming increasingly prominent. However, the growing demand

for "pristine" natural environments creates a risk of transforming these areas into zones of critical ecological pressure when governance systems fail to keep pace with visitation growth (Bansal & Kumar, 2011). Studies addressing carrying capacity, including its social dimension, demonstrate that exceeding acceptable visitation thresholds affects not only environmental conditions but also the social quality of visitor experiences, thereby necessitating quantitative regulation and continuous monitoring (Rogowski *et al.*, 2025; Pulido-Fernández *et al.*, 2025).

In Ukraine, this issue is becoming increasingly relevant due to the continuous expansion of domestic nature-based tourism and the structural transformation of the tourism system under wartime conditions. The growth of nature-oriented tourist flows and the incorporation of previously undisturbed areas into recreational use may generate a new category of risks, including insufficient infrastructure capacity, inadequate visitor control mechanisms, weak monitoring systems, and imbalances between conservation objectives and commercial exploitation. International experience in the management of protected areas demonstrates that institutional constraints – financial, regulatory, and organisational – often determine the upper limits of sustainability, even when appropriate strategic frameworks are in place (Bezuglyi *et al.*, 2019; Sharpley *et al.*, 2023; Lundén *et al.*, 2025).

These circumstances reveal an important research gap. Despite the rapid expansion of studies devoted to tourism governance, visitor management, and overtourism, insufficient attention has been paid to the institutional adaptation of contemporary environmentally safe tourism governance models to countries characterised by uneven infrastructure development, crisis-related challenges, and highly volatile tourism demand. In particular, further methodological refinement is required regarding the integration of carrying-capacity assessment (including social carrying capacity), adaptive management of visitor flows and seasonality, financial mechanisms supporting conservation regimes, and resilience criteria for tourism destinations (Medina-Chavarría *et al.*, 2024; Pulido-Fernández *et al.*, 2025; Mandić *et al.*, 2025).

The sustainability of the tourism industry has become a strategic priority because tourism simultaneously generates economic value while increasing pressure on ecosystems and local communities. In this context, environmental safety in tourism should not be interpreted as an additional conservation component but rather as an integrated indicator of sustainability that reflects the balance between tourism development, ecological carrying capacities, and the socio-economic needs of host territories. However, environmental safety can only be achieved through scientifically grounded governance, including the determination of ecological thresholds, regulation of recreational pressures, and implementation of ecosystem restoration mechanisms. Consequently, one promising instrument for reducing pressure on wilderness areas is the managed redistribution of visitor flows toward anthropogenic and semi-natural attractions – such as parks, botanical gardens, cultural landscapes, and urban green spaces – which can function as buffer zones and reduce pressure on biodiversity hotspots.

Comparative analysis of tourism models demonstrates that natural resources generate different logics of destination positioning and governance. In Northern European countries, natural landscapes constitute the basis of a high-quality tourism product, with emphasis placed on infrastructure development and regulatory support for environmentally responsible practices, including route management, green mobility, and waste management systems. In contrast, in many countries of Africa and Southeast Asia, natural resources are often utilised according to a short-term profit maximisation logic, increasing the risks of overexploitation and social vulnerability. Consequently, the principal differentiating factor is not the mere presence of natural resources but rather the quality of institutions, namely their capacity to regulate visitor pressure, ensure equitable benefit distribution, and maintain trust among local communities.

This observation is particularly relevant for Ukraine, where natural landscapes remain a key tourism asset and the increasing orientation toward domestic tourism strengthens the need for rational-use regulations and institutional protection mechanisms. Although the tourism sector demonstrated considerable adaptability following the decline of 2020-2021, structural problems remain unresolved. Overtourism has temporarily disappeared from public discourse; however, as mobility recovers, the familiar causal cycle re-emerges: unchanged regulatory mechanisms, growing demand, environmental degradation, infrastructure overload, social tensions, and declining destination quality. Consequently, the central scientific challenge is how to transform the concept of "sustainable tourism" from a normative declaration into a measurable and operational governance framework.

This transition is reflected in the approaches promoted by the World Tourism Organization (2026), which interprets overtourism risks not merely as a matter of local destination management but as an issue of broader global governance involving standards, coordination platforms, monitoring systems, and comparative analytical frameworks. A practical step in this direction has been the Measuring the Sustainability of Tourism (MST) initiative, designed to establish a universal statistical framework integrating economic, environmental, and social indicators. Its significance lies in the fact that sustainability cannot serve as a basis for management decisions without standardised metrics. The absence of comparable data often results in fragmented policies and the substitution of actual constraints with symbolic measures. Consequently, MST has the potential to strengthen evidence-based planning, support intersectoral dialogue among tourism, environmental, transport, and urban planning stakeholders, and provide a robust foundation for measuring progress toward sustainable development goals. Within this framework, the International Network of Sustainable Tourism Observatories

(INSTO) functions as an institutionalised monitoring system at the destination level, enabling continuous assessment of tourism impacts and facilitating the transition from policy intentions to indicator-based governance.

Within contemporary conservation strategies, protected areas increasingly assume a dual role: they serve simultaneously as biodiversity conservation cores and as platforms for environmentally responsible tourism, provided that ecological limits are respected. A prominent example is the activity of EUROPARC and its European Charter for Sustainable Tourism in Protected Areas, which offers a practical methodology for reconciling tourism development with conservation objectives and community interests. Structurally, the approach is implemented through three interconnected modules: sustainable destination management (rules, limits, spatial planning, and visitor behaviour standards), sustainable partners and businesses (environmental standards for services and resource use), and sustainable tour operators (responsibility for mobility and group management practices). In this way, the Charter institutionalises a governance compromise by permitting recreation while subordinating it to long-term principles of responsibility and stakeholder participation.

At the same time, global conservation management standards are increasingly shaped by the International Union for Conservation of Nature (IUCN), particularly through its classification of protected area management categories and the IUCN Green List certification framework. The principal value of this approach for ecotourism lies in shifting attention from the mere existence of protected areas to measurable conservation outcomes. These outcomes ultimately determine the acceptable limits and forms of tourism use. Equally important are global monitoring systems and databases such as Protected Planet and the World Database on Protected Areas (WDPA/OECM), which enable protected areas to be understood as components of a planetary environmental security system rather than isolated local entities.

Tourism sustainability rankings and destination indices constitute another important mechanism influencing competitiveness. These instruments simultaneously perform marketing functions and act as forms of "soft regulation," shaping tourist flows and investment decisions. The Global Wildlife Travel Index (2019) illustrates how attractiveness for wildlife tourism depends not only on resource endowments such as biodiversity and protected areas but also on institutional conservation capacities and risks associated with species decline.

The leading positions occupied by certain countries provide an important practical insight: environmental policy should be viewed not as a cost but as a source of competitive advantage within markets characterised by environmentally conscious demand. However, the results of the 2025 Global Wildlife Travel Index (Best countries for wildlife…, n.d.) indicate relatively weak positions for Ukraine, where the principal limiting factor is the ongoing full-scale war, which undermines tourism capacity through security risks, infrastructure destruction, and ecosystem degradation. Therefore, competitiveness in ecotourism is determined by a triad consisting of natural capital, institutional quality of governance, and resilience to risks (security, infrastructure, and public trust). This triad forms the conceptual framework for further analysis of environmental safety in tourism as a measurable foundation for the long-term sustainability of tourism destinations.

The identified methodological limitations – including the ambiguity of certain indicators, potential inaccuracies in primary statistical data, and insufficient transparency regarding weighting coefficients – reduce the scientific reliability of the ranking as a stand-alone source of evidence. Therefore, the application of the index in academic research should be critical and verification-oriented, requiring the validation of underlying data and the comparison of results with established international assessment systems such as the Environmental Performance Index (EPI), the SDG Index, Protected Planet, and the FAO Forest Resources Assessment. From a methodological perspective, further validation of the instrument is possible only through greater transparency in calculation procedures, refinement of weighting schemes, and stronger data quality control mechanisms. Such improvements would facilitate the transformation of the ranking from a marketing-oriented analytical product into a robust measurement tool for sustainable tourism research.

Additional empirical evidence confirming the decisive role of military and political factors in shaping Ukraine's tourism system is provided by the results of the Global Peace Index 2025 (Institute for Economics & Peace, 2025), which place the country among the lowest-ranked states in terms of security. However, in this context, security should not be regarded merely as a background condition; rather, it constitutes a structural constraint on tourism recovery. Thus, for Ukraine, security has become a fundamental regulator of tourism development, determining the economic feasibility of international tourist flows and particularly constraining wildlife and nature-based tourism, which critically depends on transport accessibility, environmental predictability, and social stability.

Low positions in international tourism rankings should not be interpreted as a complete reflection of Ukraine's actual tourism potential, since ranking systems often overemphasise infrastructure and security indicators while underestimating socio-cultural and behavioural determinants of tourism demand. Particularly illustrative in this regard are the findings of a large-scale international study demonstrating that Ukrainians exhibit one of the highest levels of psychological connectedness to nature among populations of 61 countries. From an applied perspective, this finding indicates a stable domestic demand for nature-based recreational activities even under conditions of restricted inbound tourism. Furthermore, it suggests the existence of a behavioural foundation for responsible ecotourism that, with appropriate support through environmental education, interpretation

services, and regulatory incentives, could evolve into sustainable patterns of domestic tourism demand.

The heterogeneity of Ukraine's international tourism positioning should also be taken into account. In 2025, two Ukrainian rural settlements were included among the world's best tourism villages according to UN Tourism. Even under crisis conditions, local "growth points" remain capable of meeting international standards within rural, nature-based, and sustainable tourism segments. From a scientific perspective, this strengthens the argument for policies focused on pilot destinations where recovery models can be tested through the integration of conservation instruments, spatial planning, and destination marketing strategies.

In 2025, ecotourism in Ukraine has naturally assumed a predominantly domestic character, giving rise to a model of wartime adaptive tourism focused on short-distance travel and relatively safe natural regions such as the Carpathians and Polissia. Nevertheless, the dominance of domestic tourism flows cannot fully compensate for the loss of the international tourism segment without a transition toward systemic recovery measures. Ukraine's return to leading positions in global nature-based tourism rankings will be realistic only under conditions of improved security, restoration of international air connectivity, comprehensive ecological reconstruction measures (including renaturalisation and biodiversity restoration), and infrastructure modernisation in accordance with sustainability and accessibility principles.

Contemporary ecotourism development is increasingly accompanied by the emergence of a comprehensive set of supranational governance instruments aimed at promoting sustainable tourism. However, the effectiveness of their implementation at the national level remains uneven: in some countries these instruments act as catalysts for transformation, whereas in others they remain largely declarative. Consequently, it is scientifically justified to move beyond describing global initiatives and instead focus on the analysis of national governance models that directly shape tourism development trajectories and their environmental consequences.

International experience demonstrates the dual nature of ecotourism. Under effective governance, ecotourism can mitigate the negative effects of mass tourism and support biodiversity conservation. Under weak regulatory frameworks, however, it may contribute to ecosystem degradation and territorial overuse. Therefore, the principal scientific and practical challenge is the identification of governance models capable of balancing tourism attractiveness with ecological sustainability. To achieve this objective, it is useful to compare countries recognised as leaders in environmentally safe tourism development (Australia, the United Kingdom, Germany, Norway, the United States, and Canada) with countries undergoing active ecotourism expansion (Kenya, Botswana, Brazil, China, Malaysia, Mongolia, among others), moving beyond simple comparison toward the development of a typology of governance models.

Such a typology can logically be based on several key dimensions: the institutional role of the state; the spatial and ecological characteristics of natural areas; the role of nature-based tourism within the national tourism product and destination promotion strategies; the structure of tourism demand (domestic versus inbound tourism, seasonality); visitor management regimes (soft, strict, or absent); the role of protected areas; and the quality of infrastructure and interpretation services, including accessibility, digital technologies, and socio-cultural programs. The synthesis of these criteria enabled the identification of eight principal models of ecotourism development among leading countries in this field. The subsequent analysis of these models makes it possible not only to describe governance practices but also to demonstrate their influence on ecological sustainability, destination competitiveness, and the reproduction of natural capital as a strategic foundation of tourism development.

Model 1: Large Territories, High Urbanisation, and Strong Natural Capital

The first model is characteristic of countries with extensive territories, high levels of urbanisation, and populations concentrated in major metropolitan areas, including the United States, Canada, and Australia. This spatial-demographic configuration generates uneven recreational pressure: large natural areas remain relatively undeveloped, while resource-extraction regions, agricultural clusters, and metropolitan peripheries experience intensive anthropogenic transformation. These areas are frequently affected by environmental imbalances such as ecosystem degradation, pollution, habitat fragmentation, waste accumulation, and biodiversity loss. Under such conditions, environmental safety becomes not only a conservation priority but also an indicator of quality of life and social stability. Consequently, ecotourism assumes an instrumental role by combining recreation with environmental education, support for conservation management, and the promotion of environmentally responsible behaviour. The principal drivers of development within this model include extensive natural resources supported by networks of protected areas and national parks, together with strong social demand for nature-based recreation stimulated by local environmental concerns.

In these countries, nature-based tourism occupies a strategic niche within the tourism product. Visitor flows are generated both by domestic demand and by international tourists attracted by the high symbolic and image value of natural heritage. Protected areas – particularly national parks with recreational and educational functions – constitute the primary spatial framework of ecotourism development. The combination of long-standing ecotourism traditions and extensive territories enables relatively soft visitor management through spatial dispersion, diversification of routes and recreational activities, and sophisticated logistical systems. At the same time, accessible protected areas are typically characterised by a high level of infrastructure development, including marked trails, tourist information centres (TICs), environmental education facilities, digital navigation systems, inclusive recreational infrastructure,

and public awareness programs. Protected areas are generally administered by public institutions, although patterns of interaction with the private sector and non-governmental organisations vary according to administrative traditions and public management models.

The United States represents a particularly illustrative example of this first model. Environmental safety is developed within a system of lands managed by multiple jurisdictions, including federal agencies, subnational authorities, and private stakeholders. The existence of one of the world's oldest national park systems has fostered governance practices aimed at preventing overcrowding, minimising the impacts of mass tourism, and optimising visitor flows through logistical planning. The regulatory framework is multi-level, encompassing federal, state, and municipal governance. State authorities frequently play the decisive role in regulating tourism activities, providing flexibility and adaptation to local conditions while simultaneously creating significant interregional variation in regulatory approaches. The environmental effects of regulation are achieved through zoning mechanisms, restrictions on construction and infrastructure development, licensing requirements, penalties for environmental violations, user fees, and resource-use regulations.

An additional factor is the influence of case law, which encourages the adoption of advanced management practices within environmentally sensitive areas. This legal framework is complemented by foundational environmental legislation – including acts related to clean water, clean air, and endangered species protection – which establishes the broader system of environmental standards and conservation obligations. Regulations for individual protected areas are generally designed to minimise localised impacts such as noise, soil erosion, disturbance of nesting and migration processes, and the removal of biological materials. Importantly, since the 1970s the United States has experienced increasing deregulation within the tourism sector. As a result, responsibility for the management of tourism enterprises has shifted substantially toward state governments, while the federal level performs primarily strategic and coordinating functions, including through institutions such as the US Travel and Tourism Advisory Board. Notably, sustainable development and environmental safety are not always explicitly articulated as central priorities within national tourism strategies. Instead, ecotourism is often promoted indirectly through support for small businesses, environmental education initiatives, and interagency cooperation (Table 2).

Table 2. US federal authorities in the national ecotourism management system: categories of functions and impact indicators

Federal Agency	Regulatory Function	Conservation Function	Educational Function	Monitoring Function	Infrastructure Function	Analytical Impact Indicators
National Park Service (NPS)	Visitor regulations, access rules, and restrictions	Protection of ecological, cultural, and landscape integrity	Environmental interpretation and visitor education	Monitoring visitor pressure and tourism flows	Maintenance of parks, trails, and visitor facilities	Reduced environmental degradation; biodiversity stabilisation; controlled visitor flows; increased ecosystem carrying capacity
U.S. Forest Service (FS)	Regulation of recreational activities in national forests	Sustainable forest and wilderness management	Large-scale educational programs and stakeholder engagement	Assessment of ecosystem conditions under recreational pressure	Trails, roads, logistics infrastructure, and zoning regulations	Public-private partnerships (6,000+ guides); improved accessibility without compromising sustainability; managed expansion of ecotourism routes
U.S. Fish and Wildlife Service (FWS)	Regulation of refuge visitation and permitted activities	Biodiversity conservation in wildlife refuges and wetlands	Environmental education programs and outreach events	Monitoring of species, habitats, and migratory birds	Controlled access to protected areas under conservation regimes	Ecotourism supports conservation objectives; development of birdwatching tourism; increased environmental awareness and social value of protected areas
Bureau of Land Management (BLM)	Regulation of recreation and resource use on federal lands	Stewardship and conservation of natural ecosystems	Promotion of responsible behaviour through "Leave No Trace" standards	Spatial monitoring of recreation zones	Designation and maintenance of observation sites and recreation areas	Expansion of ecotourism through approximately 300 recreation areas; responsible visitor behaviour; reduced anthropogenic impacts
Environmental Protection Agency (EPA)	Environmental standards and impact regulations	Reduction of environmental risks through EIA and environmental assessment procedures	Guidelines and technical information for communities and businesses	Environmental and socio-economic impact assessment models	Indirect support through software tools, methodologies, and technical assistance	Evidence-based planning; prevention of overuse; integration of environmental KPIs into tourism planning

Table 2. Continued

Federal Agency	Regulatory Function	Conservation Function	Educational Function	Monitoring Function	Infrastructure Function	Analytical Impact Indicators
Bureau of Reclamation	Regulation of recreation in water-management systems	Protection and sustainable use of aquatic and landscape resources	Education on aquatic ecosystems and scientific outreach programs	Monitoring recreational impacts on aquatic and riparian ecosystems	Access infrastructure for water-based recreation and support facilities	Reduced vulnerability of aquatic ecosystems; development of educational and scientific ecotourism

Source: developed by the authors based on P.F.J. Eagles *et al.* (2002), C.M. Hall *et al.* (2010), J. Coria & E. Calfucura (2012), B. Lane & E. Kastenholz (2015), T.B. Dangi & J.F. Petrick (2021), E. Falko & V. Mateichuk (2023)

Thus, according to Table 2, the management of ecotourism in the USA is characterised by a multi-level institutional architecture, where federal services perform complementary functions of nature protection, access regulation, eco-education, monitoring and infrastructure provision. The qualitative categories presented in Table 3 are based on the procedure of quantitative expert assessment. The mechanism of the model is based on a combination of regime nature use (zoning, restrictions, control) with program-analytical support and partnership involvement of stakeholders. As a result, ecotourism functions as a managed socio-ecological-economic system that reduces the risks of excessive recreational pressure and ensures long-term environmental protection effects. The high intensity of regulatory and environmental protection instruments confirms that the preservation of ecosystems is considered a basic prerequisite for the competitiveness of eco-destinations.

Table 3. Functional importance, weighting categories, and impact indicators of US federal agencies in the system of environmentally safe tourism governance

Federal Agency	Regulatory Function	Conservation Function	Educational Function	Monitoring Function	Infrastructure Function	Key Analytical Impact Indicators
National Park Service (NPS)	H	H	M	M	H	Control of recreational pressure and visitor-use regimes; preservation of ecological, historical, and landscape integrity; improved management of tourist flows
U.S. Forest Service (FS)	M	H	H	M	H	Scaling environmentally safe tourism development through sustainable recreation management; partnerships with the private sector; maintenance of trail networks and accessibility without compromising ecosystem resilience
U.S. Fish and Wildlife Service (FWS)	M	H	H	H	M	Environmentally safe tourism as a tool for biodiversity conservation; development of birdwatching and nature interpretation; support for conservation regimes within wildlife refuge networks
Bureau of Land Management (BLM)	H	M	M	M	H	Spatial expansion of environmentally safe tourism across federal lands through recreation and observation areas; implementation of "Leave No Trace" principles; reduction of anthropogenic impacts
Environmental Protection Agency (EPA)	H	M	M	H	M	Enhancement of evidence-based governance through environmental data, models, and software tools; integration of environmental-economic assessments into tourism planning; prevention of ecosystem overloading
Bureau of Reclamation	M	M	M	M	H	Managed recreation within water-resource systems; development of educational and scientific ecotourism; reduction of degradation risks in sensitive aquatic ecosystems through regulated visitor activities

Note: H – High importance (3 points); M – Medium importance (2 points); L – Low importance (1 point). Categories are derived from expert assessment and subsequent quantification using the methodology described in the Materials and Methods section

Source: summarised by the author based on P.F.J. Eagles et al. (2002), C.M. Hall et al. (2010), J. Coria & E. Calfucura (2012), B. Lane & E. Kastenholz (2015), T.B. Dangi & J.F. Petrick (2021), E. Falko & V. Mateichuk (2023)

Australia represents a prominent example of a country where environmentally safe tourism constitutes the core of tourism specialisation and where nature is treated as a strategic intangible asset requiring a dedicated conservation regime. This approach is supported by a well-developed legislative framework, particularly the Environment Protection and Biodiversity Conservation Act (1999) and the Great Barrier Reef Marine Park Act (1975). Institutionally, tourism is integrated with the environmental and natural resource management sector, reflecting the strategic importance of natural capital within the national tourism product.

The central policy framework is provided by the National Ecotourism Strategy (NES), implemented since 1994, which establishes a comprehensive policy architecture

encompassing environmental sustainability, spatial planning, resource management, regulation and infrastructure development, impact monitoring, destination marketing, certification and accreditation systems, environmental education, and Indigenous participation. From both scientific and practical perspectives, Australia exemplifies a model in which ecotourism functions as a system-forming economic sector governed through an integrated strategic framework rather than fragmented regulatory interventions.

At the state level, individual legal regimes govern protected areas, including mechanisms for the establishment of privately protected lands. To coordinate responsibilities between federal and state authorities, bilateral agreements are widely employed. A partnership-based approach is implemented through the National Reserve System Program, under which the government may compensate up to two-thirds of the acquisition costs incurred by private investors purchasing conservation lands. Revenues generated from these arrangements are accumulated within the Australian National Parks Fund. Additional conservation instruments include conservation covenants, which are voluntary agreements between governments and landowners restricting land-use activities for environmental purposes.

The institutional framework consists of the responsible federal ministry, Tourism Australia (international promotion and strategic tourism development), and the Director of National Parks (management of federally protected areas). Notably, Australia's ecotourism certification system has served as a methodological foundation for numerous international certification frameworks, demonstrating the country's role as a global exporter of environmental governance practices and a leader in ecotourism management.

Model 2: Nordic Sustainable Nature-Based Tourism

The second model is characteristic of Norway, Sweden, Finland, and Iceland and is based on the combination of high urbanisation levels and institutionally mature environmental policies. Unlike many other highly urbanised countries, the Nordic states have systematically minimised environmental risks through effective waste management, decarbonisation policies, energy-efficiency measures, and the large-scale implementation of green technologies. Consequently, sustainability in tourism functions not as a marketing concept but as a normative foundation for sectoral development. A critical feature of this model is that, despite advanced economic modernisation, Nordic countries have preserved extensive areas of minimally disturbed natural landscapes that constitute the primary resource base for ecotourism. Competitiveness is therefore achieved not through intensive recreational development but through the capitalisation of environmental quality combined with high transport accessibility, advanced infrastructure, and environmental certification systems. Their leading positions in international sustainability rankings should be interpreted as the outcome of deliberate public policy that shapes ecotourism as a managed system while minimising land-use conflicts.

A distinctive characteristic of the Nordic model is its cross-sectoral nature. Environmental safety criteria are integrated not only into traditional nature-based tourism but also into ski tourism and cultural-heritage destinations. Sweden operates the Nature's Best certification scheme under the leadership of the Swedish Ecotourism Society, while Norway actively promotes environmental certification programs such as Ecotourism Norway and Green Travel, institutionalising environmental responsibility within the tourism business sector. Finland supports national ecotourism initiatives that strengthen its position in the global nature-based tourism market. Consequently, the promotion of Nordic tourism products is closely aligned with state strategic priorities aimed at ensuring long-term competitiveness.

Since 2017, Norway has formally embedded sustainability, responsibility, and competitiveness into national tourism policy while increasing investments in environmentally sustainable tourism infrastructure. This reflects a transition from declarative environmental commitments to environmentally conditioned planning, where sustainability constitutes a prerequisite for tourism development. An important institutional foundation is the legally and culturally embedded principle of allemannsretten (the right of public access to nature), codified in the Outdoor Recreation Act (1957). While the Act permits a broad range of recreational activities – including hiking, camping, and gathering wild berries and mushrooms – it is balanced by a high level of environmental awareness and effective visitor-flow management.

The dominant governance approach is soft management. Rather than restricting access, public authorities invest in optimising the spatial organisation of tourism through trail construction and reinforcement, expansion of route networks, and the creation of alternative visitor pathways. Additional regulatory support is provided by the Nature Diversity Act and the Environmental Information Act, which institutionalise the principles of environmental democracy through public access to environmental information and citizen oversight. Arctic tourism, particularly in Svalbard, is governed through stricter conservation regimes supported by substantial penalties, illustrating a principle of zero tolerance toward environmentally harmful practices in fragile ecosystems. A key role in tourism development is played by Innovation Norway, which combines product development with international destination branding. National parks are managed by governmental conservation agencies and supported by specialised inspection and directorate structures.

The effectiveness of the Nordic model is further strengthened through partnerships with civil society organisations, particularly the Norwegian Trekking Association (DNT). This influential network simultaneously maintains trail infrastructure, provides visitor information, promotes environmental stewardship, and reinforces social norms of environmentally responsible behaviour. The model is complemented by a comprehensive environmental

certification system, including Nordic Swan, Eco-Lighthouse, Green Key, ISO 14001, and Blue Flag, whose requirements frequently exceed minimum legislative standards. Norway additionally operates the Sustainable Destinations certification program, which requires reassessment every three years and transforms sustainability from a one-time declaration into a continuously verified process. Overall, the Nordic model represents a benchmark of managed ecotourism development, combining strong environmental policy, regulated public access to nature, state coordination, partnerships with non-governmental organisations, certification as a quality standard, and soft visitor-flow management. As a result, ecotourism functions not merely as a tourism segment but as an instrument of environmental policy and socio-economic modernisation through the sustainable use of natural capital.

Model 3: The Western European Integrated Eco-Destination Model

The third model is characteristic of leading Western European countries and has emerged under conditions of high population density, long-term economic transformation of landscapes, and a relative scarcity of wilderness areas. Consequently, ecotourism is primarily based on partially modified or renaturalised ecosystems and integrates natural heritage with cultural landscapes and local community practices. Ecotourism within this model therefore represents a hybrid product combining nature, culture, and local economic activities rather than a strictly nature-centred tourism experience. During the initial establishment of protected areas, conflicts frequently arose between conservation objectives and the interests of landowners and agricultural stakeholders. Contemporary protected areas are therefore the result of negotiated compromises and legal balancing among three objectives: environmental and biodiversity conservation, support for local economies and traditional land-use practices, and the provision of recreational access and tourism attractiveness. As a consequence, many protected areas simultaneously contain conservation zones, agricultural land, settlements, and cultural heritage sites.

This spatial configuration directly shapes the tourism product, which typically combines hiking and cycling routes with cultural-nature excursions, agritourism, gastronomic tourism, and wine tourism experiences. Ecotourism consequently performs a dual function: environmental education and economic diversification of rural areas. The compact geographical structure of Europe and the transboundary nature of many ecosystems have encouraged institutional cooperation, including joint environmental monitoring, harmonisation of visitor-capacity regulations, coordinated planning of eco-infrastructure, and the development of transnational route networks, particularly within mountain and border regions such as the Alps. The model is characterised by a large number of stakeholders and complex land-tenure arrangements. This necessitates a system of multi-level governance involving national governments, regional and local authorities, non-governmental organisations, and private businesses. While multiple actors participate in management processes, the state retains a central role in strategic planning, regulation, and enforcement of environmental standards, thereby preventing excessive commercialisation of natural heritage.

The United Kingdom provides an illustrative example of this model. Tourism development is institutionally supported by the Development of Tourism Act, which established the organisational foundations for state support through national tourism institutions, financial incentives, and registration procedures. Simultaneously, a comprehensive environmental and spatial-planning framework has evolved, including legislation related to wildlife conservation, land-use planning, public access to rural areas, and protected-area management. A distinctive feature of British national parks is their orientation toward the recreational needs of a highly urbanised population. This explains the predominance of domestic tourism and short-duration visits, often limited to a single day. Historically, British national parks were established after World War II primarily as instruments of social policy. Consequently, greater emphasis was placed on landscape protection and public accessibility than on the conservation of untouched wilderness ecosystems.

The integration of private land ownership, agricultural holdings, and permanent settlements has led to the interpretation of national parks as cultural landscapes, thereby increasing management complexity and intensifying the classical "conservation versus recreation" dilemma. The response to this challenge involved the institutionalisation of conservation priorities in situations of acute conflict through the well-known Sandford Principle, as well as the strengthening of the autonomy of park management authorities, particularly through reforms implemented during the 1990s. Contemporary British national parks often deviate from the traditional model of strictly protected wilderness areas. Instead, they remain living landscapes where people reside and engage in economic activities, while the National Park designation simultaneously performs a territorial development and destination-branding function.

Management discipline is reinforced through the mandatory revision of management plans every five years and through the environmentalisation of tourism products via green certification schemes and support for environmentally friendly accommodation facilities. Consequently, the third (Western European) model may be characterised as ecotourism within an integrated cultural landscape system, where natural values are conserved, recreational access is maintained, and the viability of rural communities is supported through the managed diversification of local economies.

Model 4: The Eastern European Transitional Model – Ecotourism as an Instrument of Regional Transformation

The fourth model emerged in Eastern European countries, where ecotourism performs not only a recreational function but also a structural one by supporting the transformation of natural resource use, regional economic diversification, and local employment. In countries such as Poland, Hungary, and the Czech Republic, this model has

reached a relatively high level of institutional maturity. Ecological trails are integrated into national tourism products, supported by basic infrastructure – including signage systems, service nodes, and visitor information centres – and promoted alongside cultural and urban tourism. In contrast, ecotourism in Romania and Bulgaria develops under conditions characterised by socio-economic tensions, including structural unemployment and informal resource markets. These circumstances often generate resistance to conservation initiatives, as the expansion of protected areas is frequently perceived as a restriction on access to natural resources. The resulting conflict is therefore dual in nature, reflecting competition between a "survival economy" and a "conservation economy". Empirical evidence demonstrates that when effective communication and tangible economic benefits are provided, ecotourism gradually becomes an acceptable alternative to unsustainable resource exploitation.

Educational programs implemented in regions such as the Rhodope Mountains illustrate how ecological trails, small-scale accommodation facilities, and local tourism services can generate employment and stimulate local income circulation. International organisations frequently provide additional support and institutional momentum. The principal barrier to the successful functioning of this model is the lack of trust between local communities and conservation institutions. Consequently, instruments such as community-based tourism, co-management of protected areas, and equitable benefit-sharing mechanisms (e.g., allocating a share of ticket revenues and service fees to local budgets) become critically important. These mechanisms transform ecotourism from a perceived restriction into a development opportunity.

Model 5: The Southern European Diversification Model – Ecotourism as a Response to Seasonality and Overtourism

The fifth model is characteristic of Southern European countries traditionally oriented toward mass coastal tourism. The excessive concentration of tourist flows within coastal tourism hubs generates pronounced seasonality, infrastructure overload, landscape degradation, and conflicts over spatial resource use. Consequently, ecotourism acquires strategic importance as a mechanism for the spatial and temporal redistribution of tourists and for restructuring national tourism products toward greater sustainability. From an organisational perspective, this model closely resembles the Western European approach. Ecotourism is integrated with gastronomic and rural tourism, supported by infrastructure and visitor information centres, and systematically promoted in both domestic and international markets. However, in certain destinations ecotourism itself has expanded to a mass-tourism scale, as illustrated by the case of Plitvice Lakes National Park. Coastal destinations increasingly adopt the integrated formula of "sea + nature + culture". The principal risk associated with this model is greenwashing, whereby ecotourism functions primarily as a marketing label rather than as a genuinely sustainable tourism practice. Consequently, effective governance requires visitor quotas, zoning regulations, carrying-capacity controls, sustainability standards for tourism facilities, and continuous monitoring of environmental impacts.

Model 6: The Eco-Resort Model – Comfortable Nature Experiences for High-Value Tourism Demand

The sixth model is typical of countries and territories where ecotourism is marketed as a comfortable and aesthetically enhanced interaction with nature within a resort-oriented framework. Examples include Costa Rica, the Maldives, Seychelles, parts of the Caribbean region, and several destinations in Oceania. The model is fundamentally oriented toward high-spending visitors and environmentally branded premium tourism services. Costa Rica represents a particularly illustrative example of a successful transition from extensive deforestation to institutionally supported forest restoration, which subsequently became the resource foundation of a globally recognised ecotourism industry. Alongside small-scale ecolodges, large destination-oriented resorts have also emerged. Nevertheless, the model reveals an important paradox: visitor concentration within national parks may transform ecotourism into a form of mass tourism, where commercial objectives gradually overshadow environmental protection goals. The principal conclusion associated with this model is that ecotourism is not inherently sustainable. Sustainability is achieved only when visitor management systems, visitation limits, environmental standards, and conservation practices extend beyond protected areas into broader destination management frameworks. Otherwise, environmental responsibility remains largely rhetorical.

Model 7: High Potential, Low Capacity – The Early Institutionalisation Model

The seventh model encompasses countries possessing substantial natural tourism resources but relatively weak tourism systems. Under such conditions, environmentally safe tourism development often occurs spontaneously, while governance remains limited due to political instability, economic imbalances, low-income levels, and inadequate infrastructure. Within this model, it is useful to distinguish between Latin American and African sub-models. In Latin America, tourism development is constrained by security concerns, limited transport accessibility, and institutional instability. Although natural attractions generate tourism demand, systemic risks significantly reduce competitiveness. In Africa, by contrast, growth is frequently supported by extensive networks of protected areas and strong international demand for safari tourism. Common features include transboundary conservation areas, the integration of public protected areas with private lodges, and the growing importance of privately managed reserves. The key lesson of the seventh model is that without institutional capacity – including effective governance, anti-corruption mechanisms, security policies, and basic infrastructure – environmentally safe tourism remains a localised phenomenon. Nevertheless, African experiences demonstrate that successful ecotourism development is possible even under constrained conditions when a functional core exists,

combining protected areas, public-private partnerships, certification systems, and community participation.

Model 8: The Asian State-Led and Network-Based Ecotourism Model

The eighth model encompasses countries of East and Southeast Asia, including China, Malaysia, Indonesia, and Vietnam. Within this framework, natural capital is integrated into national tourism products as a strategic source of competitiveness rather than as a supplementary attraction. Its defining characteristics include strong state involvement in tourism governance, program-based institutionalisation through strategies and action plans, and participation in regional and transnational initiatives that harmonise destination branding and environmental management approaches. China illustrates the transition from a predominantly domestic ecotourism market toward the use of ecotourism as an instrument of international positioning through destination marketing, infrastructure investment, and the expansion of protected-area networks. However, China cannot yet be considered an unequivocal leader because several challenges remain, including fragmented regulatory frameworks, zoning violations within protected areas, the predominance of group-tour formats, limited route diversity, and accessibility constraints affecting key destinations. These factors contribute to visitor overcrowding, localised environmental degradation, waste accumulation, and increasing pressure on natural resources.

Simultaneously, ecotourism in China generates substantial socio-economic benefits by stimulating domestic tourism demand, creating employment opportunities for local residents (guides, service providers, and hospitality workers), and promoting ethno-ecological tourism products. Nevertheless, infrastructure expansion is frequently accompanied by environmental and socio-cultural costs, including waste-management deficiencies, localised ecosystem degradation, commercialisation of traditional cultures, and risks of cultural assimilation. This duality represents the defining characteristic of the model: the coexistence of significant development potential and persistent governance imbalances.

Countries within the region typically emphasise national ecotourism plans and professional capacity building. Malaysia, for example, has incorporated ecotourism into national strategic planning through the National Ecotourism Plan 2016-2025, which integrates economic growth objectives with environmental sustainability goals. A particularly important indicator of institutional maturity is investment in the training of local guides as providers of environmental interpretation and environmental education. In the Philippines, ecotourism has been formalised through a national strategy and action plan focused on competitive tourism products, infrastructure accessibility, and institutional capacity within the broader framework of "tourism for development". In South Asia, particularly Nepal and Bhutan, strict demand-management instruments such as visitor quotas and high tourism fees prioritise ecological limits over visitor-number maximisation. Japan, by contrast, represents a more network-oriented variant in which non-governmental organisations and regional ecotourism councils play central roles, while government involvement is primarily expressed through grants, promotional activities, and oversight of environmental compliance.

The eighth model conceptualises ecotourism as an instrument of state policy or network governance in which nature simultaneously supports recreation, national branding, and the socio-economic integration of peripheral regions. Its central governance challenge is the reconciliation of three objectives: economic efficiency, social equity in benefit distribution, and ecological carrying capacity. The ability to transform tourism growth into a regime of managed sustainability ultimately determines whether the Asian model becomes an international benchmark or remains an example of substantial potential constrained by chronic governance imbalances.

The analysis of international models of environmentally safe tourism and recreational development demonstrates that their direct replication under Ukrainian conditions would be inappropriate due to differences in institutional environments, levels of environmental financing, structures of tourism demand, and contemporary security challenges. Nevertheless, many governance mechanisms and practical instruments may be successfully adapted to support the sustainable development of Ukraine's tourism and recreational sector. One of the most promising directions for Ukraine is the implementation of visitor management systems within protected areas. The experiences of the United States, Canada, Norway, and New Zealand demonstrate the effectiveness of zoning approaches, visitor quotas for sensitive sites, electronic reservation systems, and digital monitoring of recreational pressure. Such instruments are particularly relevant for the Ukrainian Carpathians, national nature parks, and other destinations characterised by high visitor concentrations, where increasing anthropogenic pressure is progressively contributing to the degradation of natural ecosystems.

Another important area for adaptation is the development of collaborative governance models and the expansion of local community participation in decision-making processes related to tourism and recreational resource management. The experiences of Scandinavian countries, Canada, and Kenya indicate that community involvement in destination governance enhances the effectiveness of conservation measures, promotes a more equitable distribution of economic benefits, and creates additional incentives for environmental stewardship. The introduction of environmental certification systems for tourism services and destinations also represents a promising avenue for Ukraine. International certification schemes such as Green Key, Blue Flag, and the Global Sustainable Tourism Council (GSTC) standards provide transparent benchmarks for environmental responsibility within the tourism industry and contribute to the international competitiveness of tourism destinations. In the postwar period, such instruments may become an important

component of Ukraine's tourism branding and international image-building efforts.

Particular attention should also be given to the implementation of regenerative tourism approaches, which extend beyond minimising environmental impacts and actively contribute to the restoration of natural and social capital. In the context of Ukraine's post-war recovery, these approaches could be integrated into programs for the rehabilitation of protected areas, the development of ecological trail networks, and support for local communities. Of growing relevance for Ukraine is the adaptation of the concept of wartime adaptive tourism. Unlike most international tourism governance models developed under relatively stable operating conditions, the contemporary Ukrainian context requires consideration of security risks, potential infrastructure damage, disruptions in tourism flows, and the necessity for rapid responses to crisis events. Consequently, a promising direction involves the integration of security indicators into destination management systems, the establishment of digital risk-monitoring platforms, and the development of mechanisms enabling the rapid adaptation of tourism products to changing external conditions.

International experience demonstrates that the effective governance of environmentally safe tourism and recreational development is based on the combination of institutional coordination, community participation, systematic monitoring of visitor flows, environmental certification, and advanced digital management technologies. Their adaptation to Ukrainian conditions may become a key component in the formation of a competitive, environmentally responsible, and resilient tourism and recreational system capable of supporting both post-war recovery and adaptation to climate change. The pilot application of the proposed methodology (Table 4) revealed significant spatial differentiation in the adaptability of Ukraine's tourism and recreational system under wartime conditions. The highest Tourism System Adaptability Index (AI) was recorded in the Western macro-region (AI = 4.20), which can be attributed to relatively favourable security conditions, a high concentration of domestic tourist flows, developed recreational infrastructure, and the active involvement of local communities.

The Central and Northern macro-regions demonstrate a moderate level of adaptability, reflecting the coexistence of substantial tourism potential with elevated security and infrastructure-related risks. In contrast, the Southern and Eastern macro-regions exhibit low adaptability, primarily due to their proximity to active conflict zones, infrastructure damage, instability of tourism demand, and restrictions affecting nature-based tourism development. The obtained results indicate that, under wartime conditions, the development of environmentally safe tourism in Ukraine should be based on a differentiated regional approach that accounts for variations in security conditions, infrastructure resilience, market adaptability, and institutional capacity.

Table 4. Expert-analytical application of the Wartime Tourism Adaptability Index for the macro-regions of Ukraine

Macro-Region of Ukraine	Security Dimension (S)	Infrastructure Resilience (I)	Tourism Market Adaptability (M)	Socio-Institutional Resilience (R)	Adaptability Index (AI)	Adaptability Level
Western Ukraine	4.0	4.1	4.5	4.2	4.20	High
Central Ukraine	3.0	3.5	3.1	3.4	3.25	Moderate
Northern Ukraine	2.7	3.2	2.8	3.3	3.00	Moderate
Southern Ukraine	2.0	2.6	2.4	2.8	2.45	Low
Eastern Ukraine	1.3	2.0	1.5	2.2	1.75	Low

Note: S – Security Dimension; I – Infrastructure Resilience; M – Tourism Market Adaptability; R – Socio-Institutional Resilience; AI – Adaptability Index calculated as the arithmetic mean of the four component dimensions

Source: compiled by the authors based on expert-analytical assessment using the proposed Wartime Tourism Adaptability Index methodology

The proposed adaptability index should be regarded as a pilot methodological framework that requires further empirical validation at the regional level using statistical indicators of security, tourism flows, and infrastructure resilience. The rapid growth in the popularity of ecotourism within the global tourism landscape has intensified scientific interest in this phenomenon among both academic researchers and practitioners in tourism governance and the tourism industry. Over recent decades, ecotourism has evolved from a niche recreational activity into a distinct segment of the tourism market characterised by its own ideology, institutional logic, and normative-value framework (Jacobson & Robles, 1992). This transformation has stimulated the emergence of a broad body of scientific literature addressing various aspects of ecotourism development, functioning, and governance (Yeoman, 2001; Newsome *et al.*, 2012; Mamotenko *et al.*, 2022).

Within the scientific discourse, several major thematic directions of ecotourism research can be distinguished. A substantial body of literature focuses on theoretical and methodological issues, including the refinement of conceptual definitions, the typology of ecotourism forms, the characterisation of specific ecotourism segments, and the examination of boundaries between ecotourism, nature-based tourism, and sustainable tourism, as well as the challenges associated with measuring sustainability in this field (Munévar-Chauta, 2024; Fennell, 2025). Another important research stream addresses international experiences

in ecotourism governance, examining public policies, regulatory models, institutional mechanisms, and visitor-management practices in natural areas (Munévar-Chauta, 2024). A separate line of inquiry investigates environmental safety and tourism sustainability, focusing on ecosystem degradation risks, recreational carrying capacity, the environmentalisation of tourism infrastructure, and systems for monitoring anthropogenic impacts (Smyk & Arkhypova, 2025). Research devoted to Ukrainian ecotourism destinations is also expanding, with particular attention given to the potential of protected areas, regional practices, and prospects for post-crisis tourism recovery (Wight, 2001).

An important component of the scientific understanding of tourism as a sector competing for resources, visitor flows, and investments concerns approaches to ranking territories according to their tourism potential. Among foreign scholars addressing issues of destination positioning within the international tourism space, particular attention should be given to G. Harris & K.M. Katz (1999). Based on extensive practical experience, these authors proposed a strategic framework for stimulating tourism development in countries with different levels of tourism maturity. According to their approach, a central element of tourism development strategy is the identification, public demonstration, and evidence-based justification of a destination's competitive advantages through comparative benchmarking against competing destinations – that is, through ranking procedures, destination positioning, and tourism branding strategies (Bansal & Kumar, 2011). In contemporary conditions, this approach has become even more relevant, as tourism flows are increasingly influenced not only by service quality but also by environmental standards, security risks, and the reputational stability of destinations.

At the same time, the Ukrainian academic discourse demonstrates different methodological emphases. Most Ukrainian studies are not directly focused on calculating or validating the indicators of the Global Wildlife Travel Index. Instead, researchers extensively employ internationally recognised tourism rankings such as the Travel & Tourism Competitiveness Index (TTCI) and the Travel & Tourism Development Index (TTDI). These indices effectively function as global benchmarks for evaluating the performance of tourism systems. Within Ukrainian scholarship, they are applied in three principal directions: assessing the competitiveness of Ukraine's tourism sector through international comparisons; analysing the methodological foundations and structural components of tourism indices, including institutional conditions, transport infrastructure, cultural resources, and regulatory policies; and developing practical recommendations for tourism policy and regional strategic planning.

In contemporary tourism research, the analysis of international tourism indices such as TTCI and TTDI occupies an increasingly important place because these instruments serve not merely as comparative rankings but also as tools of managerial diagnostics capable of identifying structural imbalances, infrastructure deficits, and institutional constraints within tourism systems. Significant contributions in this area have been made by Ukrainian scholars investigating Ukraine's position within the global tourism landscape. In particular, H. Haponenko *et al.* (2020) conducted a comprehensive analysis of the Ukrainian tourism market in comparison with global tourism competitiveness indicators. Using statistical data from the World Economic Forum (WEF) and the World Travel & Tourism Council (WTTC), the authors identified key factors constraining tourism development as well as potential directions for the growth of Ukraine's tourism system. An important contribution was also made by N. Shcherbakova (2021), who systematised major international tourism indices and conducted a comparative analysis of their methodological foundations. Within her research, TTCI and TTDI are interpreted as composite indicators encompassing a broad range of tourism-development dimensions, including institutional, infrastructural, and socio-economic factors, thereby providing a basis for evaluating tourism policies.

The work of S.O. Polkovnychenko & A.O. Murai (2018) focused on assessing Ukraine's competitive position within the European tourism market. By combining TTCI/TTDI indicators with economic and mathematical modelling approaches, the authors identified promising directions for enhancing the attractiveness of Ukraine as a tourism destination within the broader context of European integration. Another important contribution was made by B. Kovalov *et al.* (2017), who employed TTCI indicators to assess regional tourism potential. Their differentiation of Ukraine's 24 regions according to tourism development levels has substantial practical significance, providing a basis for regional tourism governance, investment prioritisation, and territorial development programs.

A significant contribution to the scientific understanding of index-based approaches was also made by H.O. Gorina (2016), who analysed infrastructure, human-capital, and institutional dimensions of tourism indices as fundamental determinants of tourism competitiveness. The value of her approach lies in the interpretation of tourism competitiveness not as a final ranking outcome but rather as a multidimensional system of causal relationships shaping tourism development. Thus, existing studies demonstrate the active and systematic use of international tourism indices as analytical tools for evaluating tourism competitiveness and supporting evidence-based policy recommendations. At the same time, an important methodological gap remains. Despite the extensive body of literature devoted to specific aspects of ecotourism, there is still no comprehensive comparative analysis of national governance models for environmentally safe tourism development that systematically integrates international best practices, institutional instruments, and environmental safety mechanisms across different countries.

Conclusions

The study demonstrated that the environmentally safe development of tourism and recreational activities is increasingly determined not by the mere availability of natural

resources but by the quality of institutional governance, the capacity to regulate visitor flows, maintain conservation regimes, and balance economic, social, and environmental interests. The analysis of international experience confirms the transition from the traditional understanding of ecotourism as a specific tourism segment toward its interpretation as a complex socio-ecological system whose sustainability depends on effective governance arrangements, visitor management practices, and the regulation of recreational carrying capacity.

As a result of the research, international approaches to the management of environmentally safe tourism and recreational development were systematised, and eight typological models of ecotourism development were identified. These models differ in terms of institutional architecture, the role of government and local communities, the degree of visitor-flow regulation, environmental certification mechanisms, and the integration of conservation objectives into tourism policy. The findings indicate that the most effective models combine multi-level governance, active community participation, systematic visitor monitoring, and environmental responsibility mechanisms implemented by tourism businesses.

The analysis of international tourism rankings and indices, particularly the Global Wildlife Travel Index, confirmed their value as instruments for comparative assessment and tourism policy design. At the same time, several methodological limitations were identified, including insufficient transparency of certain indicators, weighting procedures, and data aggregation methods. Consequently, such indices should be applied as supportive instruments within evidence-based tourism governance and interpreted in conjunction with other internationally recognised statistical and environmental datasets.

A significant contribution of this study is the development of the concept of wartime adaptive tourism, which considers tourism systems through the prism of their ability to maintain functionality, ensure visitor safety, and adapt to external shocks and crisis conditions. To operationalise this concept, an integrated Tourism System Adaptability Index (AI) was proposed, incorporating four dimensions of resilience: security conditions, infrastructure resilience, tourism market adaptability, and socio-institutional resilience. The pilot application of the methodology revealed substantial regional disparities in the adaptability of Ukraine's tourism system under wartime conditions, with the Western macro-region demonstrating the highest level of resilience and the Eastern and Southern regions exhibiting the greatest vulnerability.

The results suggest that the most promising directions for adapting international experience to Ukraine include the implementation of visitor-flow monitoring and management systems, the expansion of environmental certification schemes, the strengthening of community participation in destination governance, the incorporation of recreational carrying-capacity assessment tools, and the integration of regenerative tourism principles into post-war recovery strategies. The implementation of these approaches may contribute to enhancing the competitiveness of the tourism sector, preserving natural capital, and fostering a more resilient and environmentally responsible model of tourism development. Future research should focus on the empirical validation of the proposed Tourism System Adaptability Index at regional and destination levels, the quantitative modelling of recreational pressure on natural ecosystems, and the development of integrated indicators for assessing environmental safety and resilience of tourism systems under conditions of post-war transformation and climate change.

Acknowledgements
None.

Funding
None.

Conflict of Interest
None.

References
[1] Anistratenko, N.V., & Malchenko, A.V. (2022). The role of the World Tourism Organization in the restoration of tourist flows in the post-pandemic world. *Efficient Economy*, 1. doi: 10.32702/2307-2105-2022.1.82.
[2] Atamanchuk, Z.A. (2020). Global trends of international tourism development in the structure of the world market of services. *Business Inform*, 4, 21-27. doi: 10.32983/2222-4459-2020-4-21-27.
[3] Bansal, S., & Kumar, J. (2011). Ecotourism for community development: A stakeholder's perspective in Great Himalayan National Park. *International Journal of Social Ecology and Sustainable Development*, 2(2), 31-40. doi: 10.4018/978-1-4666-3613-2.ch007.
[4] Best countries for wildlife travel in the world (2026 guide). (n.d.). Retrieved from https://true.travel/journal/wildlife-travel-index/.
[5] Bezuglyi, V.V., Boiko, Z.V., & Yarotska, A.A. (2019). Current state of tourism industry development in India. *Geography and Tourism*, 53, 61-68. doi: 10.17721/2308-135X.2019.53.61-68.
[6] Coria, J., & Calfucura, E. (2012). Ecotourism and the development of indigenous communities: The good, the bad, and the ugly. *Ecological Economics*, 73, 47-55. doi: 10.1016/j.ecolecon.2011.10.024.
[7] Dangi, T.B., & Petrick, J.F. (2021). Enhancing the role of tourism governance to improve collaborative participation, responsiveness, representation and inclusion for sustainable community-based tourism: A case study. *International Journal of Tourism Cities*, 7(4), 1029-1048. doi: 10.1108/IJTC-10-2020-0223.

[8] Eagles, P.F.J., McCool, S.F., & Haynes, C.D. (2002). *Sustainable tourism in protected areas: Guidelines for planning and management*. Gland: The World Commission on Protected Areas (WCPA).
[9] Falko, E., & Mateichuk, V. (2023). Prospects of using cultural heritage objects in the development of international tourism. *Market Infrastructure*, 70, 209-215. doi: 10.32782/infrastruct70-37.
[10] Fennell, D.A. (2025). *Ecotourism* (6th ed.). London: Routledge. doi: 10.4324/9781003565635.
[11] Global wildlife travel index. (2019). Retrieved from https://web.archive.org/web/20250131210444/https://www.true.travel/global-wildlife-travel-index/.
[12] Gorina, H.O. (2016). *Market of tourist services: Development management under conditions of spatial polarization*. Kryvyi Rih: FOP Cherniavskyi D.O.
[13] Hall, C.M. (2010). Tourism and biodiversity: More significant than climate change? *Journal of Heritage Tourism*, 5(4), 253-266. doi: 10.1080/1743873X.2010.517843.
[14] Haponenko, H., Shamara, I., & Yevtushenko, O. (2020). The tourist market in Ukraine: Trends and hidden opportunities. *Ukrainian Journal of Applied Economics and Technology*, 1, 64-72. doi: 10.36887/2415-8453-2020-1-8.
[15] Harris, G., & Katz, K.M. (1999). *Promoting international tourism: To the year 2000 and beyond*. New Delhi: Atlantic Publishers and Distributors.
[16] Iddawala, J., & Lee, D. (2026). Regenerative tourism: Context and conceptualisations. *Tourism Planning & Development*, 23(2), 185-215. doi: 10.1080/21568316.2025.2527614.
[17] Institute for Economics & Peace. (2025). *Global peace index 2025: Identifying and measuring the factors that drive peace*. Sydney: Institute for Economics & Peace.
[18] Jacobson, S.K., & Robles, R. (1992). Ecotourism, sustainable development, and conservation education: Development of a tour guide training program in Tortuguero, Costa Rica. *Environmental Management*, 16(6), 701-713. doi: 10.1007/BF02645660.
[19] Kovalov, B., Burlakova, I., & Voronenko, V. (2017). Evaluation of tourism competitiveness of Ukraine's regions. *Journal of Environmental Management and Tourism*, 8(2(18)), 460-466. doi: 10.14505/jemt.v8.2(18).19.
[20] Lane, B., & Kastenholz, E. (2015). Rural tourism: The evolution of practice and research approaches. *Journal of Sustainable Tourism*, 23(8-9), 1133-1156. doi: 10.1080/09669582.2015.1083997.
[21] Lundén, A., Saarinen, J., & Hall, C.M. (2025). Institutional limits of sustainability in tourism governance: Changing governance rationalities in protected area tourism in Finland. *Journal of Ecotourism*, 24(4), 461-481. doi: 10.1080/14724049.2025.2458536.
[22] Mamotenko, D., Hres-Yevreinova, S., & Shelemetieva, T. (2022). World tourism services market monitoring system. *Market Infrastructure*, 66, 23-28. doi: 10.32843/infrastruct66-4.
[23] Mandić, A., Spenceley, A., & Leung, Y.-F. (2025). Toward resilient nature-based tourism in the post-pandemic era: Integrating governance, visitor dynamics, finance, and ecosystem integrity. *Tourism Planning & Development*, 22(5), 617-631. doi: 10.1080/21568316.2025.2553500.
[24] Matiyiv, K., Klymchuk, I., Arkhypova, L., & Korchemlyuk, M. (2022). Surface water quality of the Prut River basin in a tourist destination. *Ecological Engineering & Environmental Technology*, 23(4), 107-114. doi: 10.12912/27197050/150311.
[25] Medina-Chavarría, M.E., Gutiérrez, A., & Saladié, Ò. (2024). Managing visitor flows in protected areas in a context of changing mobilities: An analysis of challenges, responses, and learned lessons during the pandemic in Tarragona Province (Spain). *International Journal of Geoheritage and Parks*, 12(1), 135-146. doi: 10.1016/j.ijgeop.2024.01.005.
[26] Newsome, D., Moore, S.A., & Dowling, R.K. (2012). *Natural area tourism: Ecology, impacts and management*. Bristol: Channel View Publications.
[27] Polkovnychenko, S.O., & Murai, A.O. (2018). Assessment of Ukraine's competitiveness in the European market of tourist services. *Efficient Economy*, 12. doi: 10.32702/2307-2105-2018.12.112.
[28] Pulido-Fernández, J.I., Carrillo-Hidalgo, I., López-Sánchez, Y., & Casado-Montilla, J. (2024). Assessing social carrying capacity of tourists in protected natural areas. *Current Issues in Tourism*, 28(7), 1062-1078. doi: 10.1080/13683500.2024.2320865.
[29] Rogowski, M., Zawilińska, B., & Hibner, J. (2025). Managing tourism pressure: Exploring tourist traffic patterns and seasonality in mountain national parks to alleviate overtourism effects. *Journal of Environmental Management*, 373, article number 123430. doi: 10.1016/j.jenvman.2024.123430.
[30] Saayman, M., Rossouw, R., & Krugel, W. (2012). The impact of tourism on poverty in South Africa. *Development Southern Africa*, 29(3), 462-487. doi: 10.1080/0376835X.2012.706041.
[31] Sharpley, R. (2023). Sustainable tourism governance: Local or global? *Tourism Recreation Research*, 48(5), 809-812. doi: 10.1080/02508281.2022.2040295.
[32] Shcherbakova, N. (2021). Assessment of the competitiveness level of the tourism industry of countries worldwide (TTCI). *Visnyk of Kyiv National Linguistic University (KNLU). Series History. Economics. Philosophy*, 26, 57-71. doi: 10.32589/2412-9321.26.2021.269895.

[33] Smyk, I., & Arkhypova, L.M. (2025). Environmental assessment of water resources in the tourist zones of Ivano-Frankivsk region: A case study. *Ecological Engineering & Environmental Technology*, 26(9), 263-277. doi: 10.12912/27197050/209739.
[34] Stronza, A.L., Hunt, C.A., & Fitzgerald, L.A. (2019). Ecotourism for conservation? *Annual Review of Environment and Resources*, 44, 229-253. doi: 10.1146/annurev-environ-101718-033046.
[35] Wight, P. (2001). *Integration of biodiversity and tourism: Canada case study*. Nairobi: The UNEP Biodiversity Planning Support Programme.
[36] World Tourism Organization. (2026). *World Tourism Barometer and statistical annex, May 2026*. Madrid: World Tourism Organization. doi: 10.18111/wtobarometereng.2026.24.1.
[37] Yeoman, J. (2001). Ecotourism and sustainable development: Who owns paradise? *Tourism Management*, 22(2), 206-208. doi: 10.1016/S0261-5177(00)00045-5.

Міжнародний досвід управління екологічно безпечним розвитком туристично-рекреаційної діяльності: моделі, тенденції та інструменти оцінювання

Людмила Транченко
Доктор економічних наук, професор
Уманський національний університет
20301, вул. Інститутська, 1, м. Умань, Україна
https://orcid.org/0000-0003-0900-5484
Людмила Архипова
Доктор технічних наук, професор
Івано-Франківський національний технічний університет нафти і газу
76019, вул. Карпатська, 15, м. Івано-Франківськ, Україна
https://orcid.org/0000-0002-8725-6943
Олександр Транченко
Кандидат економічних наук, доцент
Уманський національний університет
20301, вул. Інститутська, 1, м. Умань, Україна
https://orcid.org/0000-0002-0639-5109
Уляна Андрусів
Кандидат економічних наук, доцент
Івано-Франківський національний технічний університет нафти і газу
76019, вул. Карпатська, 15, м. Івано-Франківськ, Україна
https://orcid.org/0000-0003-1793-0936
Тетяна Долішня
Кандидат економічних наук, доцент
Івано-Франківський національний технічний університет нафти і газу
76019, вул. Карпатська, 15, м. Івано-Франківськ, Україна
https://orcid.org/0000-0003-0972-4219

Анотація. На сучасному етапі екологічно безпечний розвиток туристично-рекреаційної діяльності в Україні набуває стратегічного значення як пріоритетний напрям сталого розвитку, що сприяє використанню природних територій, формуванню екологічної свідомості та потребує системного регулювання для запобігання їх деградації. Метою даного дослідження було узагальнення міжнародного досвіду управління екобезпечним розвитком туристично-рекреаційної діяльності та формування аналітичної основи для його адаптації до українських умов. У роботі здійснено систематизацію зарубіжних управлінських підходів і виокремлено вісім типологічних моделей розвитку екологічного туризму, охарактеризованих за параметрами інституційної архітектури, ролі місцевих громад, інструментів контролю туристичних потоків, застосування екологічних стандартів та механізмів партнерського управління. На основі порівняльного аналізу кейсів було визначено ключові тренди: інтенсифікацію екологічної сертифікації, поширення community-based tourism, цифровізацію управління відвідуванням охоронюваних територій та розвиток low-impact tourism. Окрему увагу було приділено рейтингам та інтегральним індексам як інструментам формування конкурентоспроможності держав

у міжнародному туризмі та елементам сучасної геополітики. Проаналізовано структуру «Глобального індексу країн для подорожей дикою природою», здійснено порівняння позицій Австралії, Канади, США та України за окремими індикаторами й інтегральними значеннями. Виявлено методологічні обмеження індексу (чутливість до вибору показників та процедур агрегування), що знижує валідність підсумкових оцінок і потребує критичного використання у наукових дослідженнях. У дослідженні було обґрунтовано доцільність подальшого вдосконалення індексу з метою підвищення прозорості, відтворюваності та порівнюваності результатів

Ключові слова: екологічний туризм; природоорієнтований туризм; екологічно безпечні туристичні практики; міжнародний досвід; моделі екологічно безпечного розвитку туристично-рекреаційної діяльності; туристичні індекси та рейтинги

Vol. 17, No. 1
2026

Ecological Safety and Balanced Use of Resources

ISSN (print) 2415-3184, ISSN (online) 2522-9508
Journal homepage: https://esbur.com.ua/en

Received: 20.01.2026. Revised: 20.04.2026. Accepted: 12.06.2026. Published: 30.06.2026.

UDC 628.4/504.06

DOI: 10.63341/esbur/1.2026.69

Environmental assessment of the impact of a residential building's heat sources on air pollution

Olena Savchenko
PhD in Technical Sciences, Associate Professor
Lviv Polytechnic National University
79013, 12 Stepan Bandera Str., Lviv, Ukraine
https://orcid.org/0000-0003-3767-380X

Orest Voznyak
Doctor of Technical Sciences, Professor
Lviv Polytechnic National University
79013, 12 Stepan Bandera Str., Lviv, Ukraine
https://orcid.org/0000-0002-6431-088X

Ivan Liubuska
Engineer
Lviv Municipal Utility Enterprise "Lvivteploenerho"
79040, 1 Danylo Apostol Str., Lviv, Ukraine
https://orcid.org/0009-0009-4E753-7597

Nataliia Moskalchuk*
PhD in Technical Sciences, Associate Professor
Ivano-Frankivsk National Technical University of Oil and Gas
76019, 15 Karpatska Str., Ivano-Frankivsk, Ukraine
https://orcid.org/0000-0003-4838-7972

Vasyl Sheketa
Doctor of Technical Sciences, Professor
Ivano-Frankivsk National Technical University of Oil and Gas
76019, 15 Karpatska Str., Ivano-Frankivsk, Ukraine
https://orcid.org/0000-0002-1318-4895

Abstract. The implementation of energy efficiency measures is crucial for low-carbon development, a reliable energy supply and the country's energy security. One of the steps in implementing such measures is the introduction of new and modernisation of existing district heating systems, which allow for balanced resource use, a reduction in greenhouse gas emissions into the environment, and simplified operation and maintenance of buildings. The aim of the study was to compare the quantities of pollutant and greenhouse gas emissions generated during the production of thermal energy by individual and centralised heat supply systems in a residential building. A 72-apartment residential building was examined, the building envelope of which meets modern thermal engineering requirements. In the autonomous heating supply scenario, the heat sources were individual gas-fired double-circuit boilers, whereas in the centralised heating supply system, thermal energy was generated by a gas-fired boiler house. The amount of emissions released into the environment under individual heat supply was calculated in accordance with the Methodology for determining emissions of pollutants and greenhouse gases into the air from the use of fuel for domestic purposes in

Suggested Citation: Savchenko, O., Voznyak, O., Liubuska, I., Moskalchuk, N., & Sheketa, V. (2026). Environmental assessment of the impact of a residential building's heat sources on air pollution. *Ecological Safety and Balanced Use of Resources*, 17(1), 69-78. doi: 10.63341/esbur/1.2026.69.

*Corresponding author (*nataliia.moskalchuk@nung.edu.ua*)

households. The amount of emissions released into the environment under centralised heat supply was calculated in accordance with the Sectoral Methodology for Calculating Harmful Emissions from Heat-Generating Installations of the Municipal Heat and Power Sector. The pollutants and greenhouse gases whose emissions are accounted for by these methodologies include carbon monoxide, carbon dioxide, nitrogen oxides, nitrogen dioxide, sulphur dioxide, methane and non-methane volatile organic compounds. It has been established that individual heat supply to a residential building generates 881.78 t/year of anthropogenic emissions, of which 879.96 t/year are greenhouse gases, whilst centralised heating generates 707.27 t/year of anthropogenic emissions, of which 703.52 t/year are greenhouse gases. The research results show that the use of centralised heat supply in a residential building generates 176.44 t/year less greenhouse gases than individual heat supply, i.e. a 20.0% reduction in emissions is observed

Keywords: energy efficiency; heating system; gas boiler; natural gas; emissions; greenhouse gases; pollutants

Introduction

One of the strategic priorities of state policy in Ukraine is energy efficiency. As of 2026, Ukraine has developed and adopted a legislative framework aimed at developing the energy efficiency sector, and the National Energy Efficiency Action Plan for the period up to 2030 has been approved. Improving the energy efficiency of buildings is being carried out in accordance with Ukraine's obligations under international and intergovernmental agreements, in particular the Association Agreement between Ukraine and the European Union. Adherence to the principles of energy efficiency is crucial for low-carbon development, a reliable energy supply and the country's energy security. At the same time, state policy is aimed not only at reducing energy consumption but also at cutting emissions and mitigating the effects of climate change.

According to S. Adamenko *et al.* (2024) and L. Arkhypova *et al.* (2025), climate change is leading to a reduction in snow cover in the Carpathians, which increases the risks of extreme weather events, whilst meteorological factors complicate the forecasting and control of pollutant concentrations from stationary sources, in particular such as district heating systems. In this context, energy efficiency is viewed not as an end in itself, but as a tool for achieving environmental and climate goals, in particular reducing the release into the atmosphere of greenhouse gases, pollutants or mixtures thereof, i.e. anthropogenic emissions. The energy efficiency of buildings depends directly on the efficiency of their building services systems.

Thermal energy for heating and hot water supply systems can be generated by individual or district heating systems. F. Vranay *et al.* (2025) described the advantages and disadvantages of implementing district and individual heating systems. In district heating systems, heat is generated at a single centralised heat source and then distributed via a heating network to multiple consumers for heating and hot water supply. In individual heating systems, heat sources are installed in each flat within multi-unit residential buildings. Many researchers, notably A. Mastrucci *et al.* (2025), believed that centralised heat supply systems should be used to improve the energy efficiency of buildings. Centralised heat supply diversifies and strengthens energy supply by utilising renewable energy sources and industrial surplus heat, enabling a balance in resource use and a reduction in greenhouse gas emissions. Economies of scale allow for cost savings by serving many users per metre of pipe, and simplify the operation and maintenance of buildings. Heating boilers, combined heat and power (CHP) plants, and cogeneration units – the operation of which was studied by N.S. Ganesha & M. Omprakash (2022), large-scale heat pumps, and solar thermal power plants, in particular the operation of hybrid solar collectors, which was studied by I. Venhryn *et al.* (2021). In this context, the heat source may utilise alternative energy sources, including biomass, waste heat, wastewater and geothermal water. Schematics of district heating systems using geothermal water were presented by O. Savchenko *et al.* (2023).

In Ukraine, district heating systems serve approximately 50% of consumers. Thermal energy is generated predominantly in heating plants (≈65%) and combined heat and power plants (≈25%). In the energy balance, as of December 2024, the main fuel for heat-generating enterprises was natural gas, which accounted for an average of 92% of thermal energy production. Despite Ukraine's national climate policy, the issue of emissions in district heating systems and their impact on the environment has received little attention in scientific publications. Most publications claim a reduction in energy consumption when using various heat sources, largely without support from analytical or experimental studies. For example, Yu. Selikhov *et al.* (2023) stated that replacing obsolete boiler equipment with modern boiler units allows for a 30% reduction in energy consumption, yet they do not provide supporting calculations. O. Savchenko *et al.* (2025) described the refurbishment of heat supply systems, which reduces heat loss from heating networks by 30%, leading to a reduction in greenhouse gas emissions; however, quantifying these emissions was not the aim of the publication.

With regard to individual heating systems, the energy efficiency of gas condensing boilers in such systems, compared to gas heating boilers, was examined by G. Luzhanska *et al.* (2025). They found that the gas fuel saving per 1 kW of thermal energy is 0.023 m^3/h, which corresponds to a 19% reduction in gas consumption. Yu. Selikhov *et al.* (2025) compared the energy efficiency of single-circuit solar systems for domestic hot water supply and space heating with that of gas heating boilers. The results of the

studies showed that the use of 210 m^2 of solar collectors reduces harmful emissions by 300 kg. As can be seen from the sources cited, the existing literature pays insufficient attention to determining anthropogenic emissions during the operation of heat supply systems. Furthermore, there is no environmental assessment of the choice of heat source in heat supply systems based on the amount of greenhouse gases and pollutants released into the atmosphere. Therefore, the aim of this study was to conduct an environmental assessment of the choice of heat source and to compare the amount of anthropogenic emissions generated during the production of thermal energy by individual and centralised heat supply systems in a residential building.

Materials and Methods

The study presents an analytical comparison of pollutant and greenhouse gas emissions for individual and centralised heating systems in a multi-unit residential building. Greenhouse gases are gases in the Earth's atmosphere that are capable of absorbing thermal radiation from the planet's surface and clouds and reflecting it back, thereby heating the atmosphere. Water vapour (H_2O), which accounts for about 1% of the atmosphere by volume, plays the greatest role in the excessive greenhouse effect on Earth. The concentration of water vapour in the atmosphere is not directly dependent on human activity and varies by region. However, human activity indirectly increases global temperatures and water vapour production, thereby intensifying atmospheric warming. According to Annex A of the Kyoto Protocol… (2006), six main greenhouse gases have been identified as having the greatest impact on climate change, namely carbon dioxide (CO_2), methane (CH_4), nitrous oxide (N_2O), hydrofluorocarbons (HFCs), perfluorocarbons and sulphur hexafluoride (SF_6). Greenhouse gas emissions are equal to the sum of emissions of these gases. Globally, greenhouse gas emissions are increasing every year and, as of 2024, according to H. Ritchie *et al.* (2024), amount to 54.43 billion tonnes of carbon dioxide equivalent (CO_2e). In Ukraine, greenhouse gas emissions have been decreasing over the last 35 years; however, this is not due to the use of energy-efficient technologies and production processes, but rather to a decline in population and industrial capacity. Figure 1 shows greenhouse gas emissions in Ukraine between 1990 and 2023, as determined by the Ministry of Environmental Protection and Natural Resources of Ukraine & the Budget Institution "National Centre for GHG Emission Inventory" (2025).

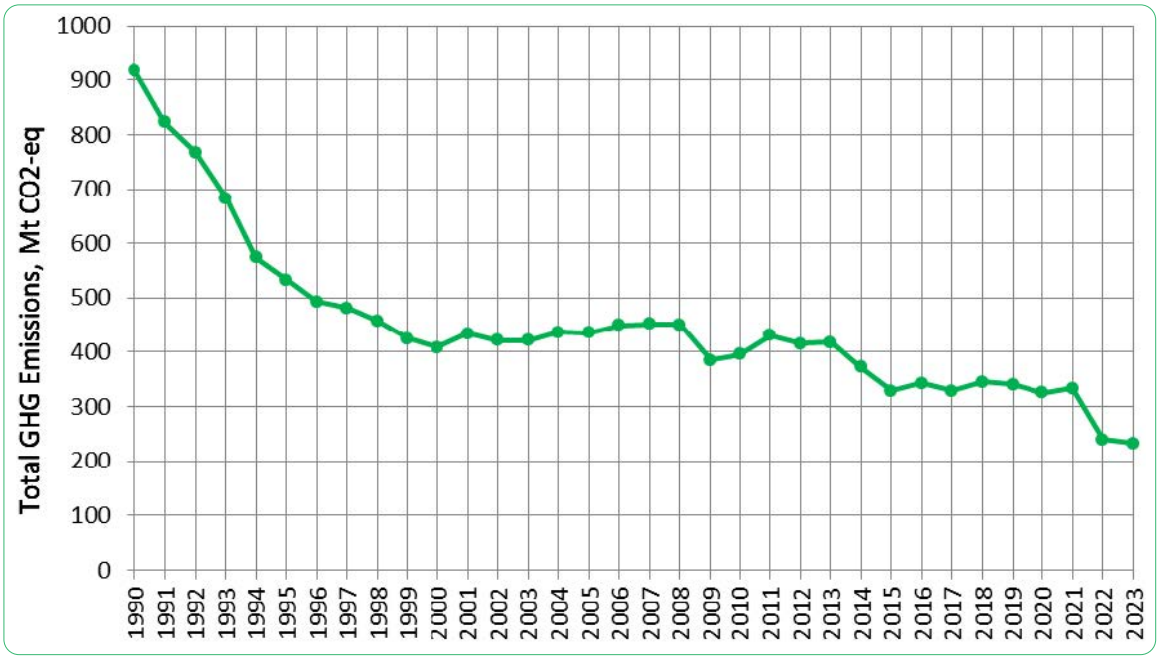

Figure 2. GHG emissions in Ukraine (including LULUCF), Mt CO_2-eq
Source: Ministry of Environmental Protection and Natural Resources of Ukraine & the Budget Institution "National Centre for GHG Emission Inventory" (2025)

Each gas contributes differently to global greenhouse gas emissions; thus, as of 2024, according to H. Ritchie *et al.* (2024), carbon dioxide accounts for 77.2% of global greenhouse gas emissions, methane for 17.5%, and nitrous oxide for 5.4%. Consequently, carbon dioxide has the greatest impact on the greenhouse effect and climate change, a significant amount of which is emitted as a result of human activity. The quantity of pollutants emitted during the operation of heat supply systems is determined using two different methodologies, depending on the type of building's heat supply system – centralised or individual.

To determine the amount of pollutants emitted by heat-generating plants in Ukraine's municipal heating sector (centralised heat supply systems), the Sectoral methodology for calculating harmful emissions is used (Order of the Ministry of Construction of Ukraine No. 67, 2006). In

this methodology, the determination of gross emissions of pollutants from the combustion of natural gas in municipal sector boilers is based on the calculation of the pollutant emission factor. The emission factor characterises the mass of the pollutant per unit of energy released during gas combustion. When calculating emissions of pollutants into the atmosphere during the combustion of natural gas in boiler houses, the following emission factors are used:,;;, . The gross emission of a pollutant, in tonnes, is then determined by the formula:

$$E = k_i \cdot Q_{low} \cdot B, \quad (1)$$

where k_i is the emission factor for the i-th pollutant; Q_{low} is the lower heating value of natural gas; B is the mass flow rate of natural gas per year. The mass flow rate of natural gas is determined by the formula:

$$B = q \cdot \rho, \quad (2)$$

where q is the annual volumetric flow rate of natural gas; ρ is the density of natural gas (mass density). The annual volumetric flow rate of natural gas is determined from the known value of the calculated natural gas flow rate q_h and the number of operating hours of the heat supply system . The calculated flow rate of natural gas burned in the heat supply system boiler is determined by the formula:

$$q_h = \frac{Q \cdot 3{,}600}{Q_{low} \cdot (\eta/100)}, \quad (3)$$

where Q – nominal thermal capacity of the boiler; Q_{low} – lower heating value of natural gas; η – boiler efficiency.

The nominal thermal output of the boiler Q is determined by the thermal load on the heat supply system Q_{DHS}. As mentioned above, the heat supply system for residential buildings covers the requirements of the heating Q_{HS} and hot water supply Q_{DHW} systems, with the heating system operating only during the heating season and the hot water supply system operating all year round. In calculations, the number of operating hours for the hot water supply system is taken as $N = 365$ days $\times$ 24 hours = 8,760 hours per year. The operating duration of the heating system depends on the city of construction, and the duration of the heating season for the selected city zop is determined from DSTU-N B V.1.1-27:2010 (2010). Then Nw = zw days $\times$ 24 hours, and the annual volume consumption of natural gas required for heat generation at the centralised heat supply source is determined by the formula, m³/year:

$$q = N_w \cdot q_h^{HS} + N \cdot q_h^{DWH}, \quad (4)$$

where q_h^{HS} and q_h^{DWH} are the calculated natural gas consumption rates required, respectively, for the heating system and the hot water supply system, determined using formula (3) for the heat load values Q_{HS}, and Q_{DHW}, respectively. The calculation of the heat load for the heating requirements of premises, groups of premises, flats and buildings is determined in accordance with DSTU EN 12831-1:2017 (2017). Since gas-fired boilers are manufactured in specific increments of nominal heat output, the boiler model and, consequently, its Q are selected based on the nearest, not lower, value of the heat load on the heating system Q_{DHS}, i.e. $Q \geq Q_{DHS}$.

To determine emissions of pollutants and greenhouse gases into the air from the use of fuel for domestic purposes in households (for example, in individual heating systems), the Methodology for calculating emissions of pollutants and greenhouse gases is used (Order of the State Statistics Committee of Ukraine No. 98, 2011). The methodology provides for the determination of emissions from the combustion of coal and coal briquettes, peat and peat briquettes, firewood, natural gas and liquefied petroleum gas. The calculation of emissions of pollutants and greenhouse gases from the use of fuel for domestic purposes in households is carried out using the formula:

$$B_j = M_{gi} \cdot A_j, \quad (5)$$

where B_j – emissions of the j-th pollutant and greenhouse gas from the use of the i-th type of fuel in households in settlements; M_{gi} – volumes of gas used in households by settlement; A_{ij} – average specific emissions of the j-th pollutant and greenhouse gas from the use of the i-th the j-th type of fuel in households; j – number of the pollutant and greenhouse gases. For centralised heating systems, the quantity of pollutants is determined using formula (1), and for individual heating systems – using formula (5).

The simplifications and assumptions made when determining pollutant emissions depend on the purpose and subject of the research. In such studies, the site is always linked to the construction location, so the duration of the heating season in that area is known. The characteristics of the heating system that influence the determination of emission quantities include the type of heating system (individual or centralised), the capacity of the heating system, the presence of systems served by the heating system (heating, hot water supply, ventilation, process requirements), their thermal load and operating duration, the type of heat-generating equipment, and the methods of regulating heat output in the heat supply system. The parameters of heat-generating equipment taken into account when determining the quantity of pollutant emissions are the amount of fuel used and the boiler's efficiency (efficiency coefficient).

The amount of fuel used to generate thermal energy depends on the fuel's physical and chemical properties, whilst the boiler's efficiency depends on its design and technical condition. Depending on the purpose of the study, the physical and chemical properties of the fuel may be taken as known average values for the industry, or determined in detail depending on its type, place of extraction, composition, etc. As can be seen from Equations (1), (2) and (3), the physicochemical parameters used in methodologies for calculating pollutant emissions are the lower heating value of the fuel and its density. In actual calculations of pollutant emissions, the type of heat-generating equipment is known, and consequently, the type of fuel it uses is known.

In theoretical calculations, particularly for selecting a heat source in heat supply systems, different types of heat-generating equipment using different types of fuel may be compared. Given the large number of determining factors that influence the thermal load of a heat supply system, and consequently the quantity of pollutant emissions, analytical studies require simplifications and assumptions to streamline the calculations.

It should be noted that the aforementioned methodologies use different terminology regarding emissions. In particular, the Sectoral Methodology for Calculating Harmful Emissions from Heat-Generating Plants of Ukraine's Municipal Heat and Power Sector uses the term "emissions of pollutants", whereas the Methodology for Calculating Emissions of Pollutants and Greenhouse Gases into the Air from the Use of Fuel for Domestic Needs in Households uses a broader definition – "emissions of pollutants and greenhouse gases". In accordance with the definition in the Law of Ukraine No. 3991-IX (2024), the generalised term "anthropogenic emissions" is used in this study to unify approaches.

Results and Discussion

An environmental assessment is carried out to describe and evaluate the consequences of the choice of heat source for a 9-storey residential building. The building has two entrances, with 36 flats in each entrance, making a total of 72 flats in the building. There are eight flats on each floor: two one-bedroom flats, one two-bedroom flat, three three-bedroom flats and two four-bedroom flats. The building's envelope complies with the requirements of DBN V.2.6-31:2021 (2021). The heating supply system is designed to provide thermal energy for the building's heating and hot water supply systems. Heat flows for the heating and hot water supply of the residential building, as mentioned above, were determined in accordance with DBN V.2.5-64:2012 (2012) and DSTU EN 12831-1:2017 (2017). Preliminary calculations have established that heat losses in flats range from 1,483 to 3,531 W, depending on the number of rooms, the floor on which they are located, and so on. The total heat loss of the building is 193.415 kW. The maximum heat flux to the flat's hot water supply system was taken to be equal to the heat loss of that flat, and for the building it amounted to 237.581 kW. The total heat load on the building's centralised heat supply system is 430.996 kW.

The article considers two options for the building's heating system. The first option is individual heating from gas-fired combi boilers, which are installed in the kitchens of the building's flats. The boiler's heat output is taken as the sum of the flat's heat loss and the maximum heat flow to the hot water supply system. Since the standard sizes of combi boilers are available in specific increments, for one- and two-bedroom flats a boiler with the nearest nominal heat output of 6 kW was selected, and for three- and four-bedroom flats – with an output of 9 kW. Thus, the calculation established that the building is equipped with 27 boilers with a capacity of 6 kW and 45 boilers with a capacity of 9 kW. The second option is district heating, with the heat source being a boiler room equipped with a gas boiler, the capacity of which must be no less than the total heat load of the heating system. The gas boiler with a nominal heat output of 450 kW is the closest in terms of capacity.

The following simplifications and assumptions were taken into account in the studies. The city of construction is Lviv; therefore, according to DSTU-N B V.1.1-27:2010 (2010), the duration of the heating season, i.e. the duration of the heating system's operation, is 179 days, which equals $179 \times 24 = 4{,}296$ hours/year. During this period, the heat supply system provides thermal energy to the heating and hot water supply systems. The hot water supply system operates year-round; the duration of the non-heating period is $8{,}760 - 4{,}296 = 4{,}464$ hours/year. There is no regulation of heat transfer fluid flow, i.e. the boilers operate at their rated thermal load. Natural gas is used for combustion in the boilers, with a lower heating value of 33,078 kJ/m^3 and a density of 0.723 kg/m^3. The efficiency (η) of boilers for individual and district heating is 90%.

According to formula (3), the calculated natural gas consumption for individual heat supply, for combustion in boilers with a rated thermal output of 6 kW, is 0.72 m3/h, and for those with a rated thermal output of 9 kW, it is 1.08 m3/h. Taking into account the operating duration of the heating and hot water supply systems, as well as the calculated natural gas consumption, the gas consumption required by the building to generate thermal energy, according to formula (4), is 444,165.12 m^3/year. For the specified quantity of natural gas, the volumes of anthropogenic emissions generated during its combustion were determined using formula (5). The results of the calculations of pollutant gas emissions for individual heat supply to a residential building are summarised in Table 1.

Table 1. Volumes of anthropogenic emissions from individual heat supply to a building

Pollutant / greenhouse gas	Average specific emissions A_{ij}, kg/1000$^{m^3}$	Emissions, kg/year	Emissions, t/year
CO	1.8	799.4972	0.799497
NO_2	2.088	927.4168	0.927417
SO_2	0.036	15.98994	0.01599
NMVOC	0.18	79.94972	0.07995
SN_4	0.108	47.96983	0.04797
N_2O	0.036	15.98994	0.01599
CO_2	1,981	879,891.1	879.8911

Source: compiled by the authors based on data from Order of the State Statistics Committee of Ukraine No. 98 (2011)

As shown in Table 1, the total amount of anthropogenic emissions generated annually from individual heat supply to flats is 881.78 t/year, including greenhouse gas emissions (CO_2, CH_4, N_2O) – 879.96 t/year. The main component of anthropogenic emissions from individual heat supply is carbon dioxide (CO_2), accounting for 879.89 t/year, or over 99.8% of total emissions. This is because natural gas consists mainly of methane (CH_4), and upon its complete combustion, the primary reaction product is CO_2. In addition to carbon dioxide, other pollutants and greenhouse gases are produced in small quantities. Nitrogen oxides (NO_x, accounted for as NO_2 in this study) are formed as a result of the oxidation of atmospheric nitrogen at high temperatures in the combustion zone. Carbon monoxide (CO) and non-methane volatile organic compounds (NMVOCs) are products of the incomplete combustion of natural gas. Methane (CH_4) in emissions indicates losses of unburned fuel, whilst nitrous oxide (N_2O) is formed in negligible quantities during high-temperature combustion. Sulphur dioxide (SO_2) is present in minimal concentrations due to the low sulphur content in natural gas.

For a district heating system during the heating season, the calculated natural gas consumption for combustion in a boiler with a rated thermal output of 450 kW, in accordance with formula (3), is 54.42 m^3/h. Additionally, the amount of gas required for the hot water supply system during the non-heating season is also taken into account, which is determined by formula (3) for a heat load of 237.581 kW. Taking into account the duration of operation of the heating and hot water supply systems over the year, the annual volume of natural gas for heat production in the district heating system is 36,2024 m^3/year. The mass flow rate of natural gas for district heating is determined by formula (2) and equals $B = 261{,}745$ t/year. The lower heating value of natural gas is determined as:

$$0.723 \cdot 38{,}078 = 45{,}751\ MJ/kg.$$

Gross emissions of pollutants into the environment from district heating are determined separately for each pollutant using formula (1). The results of the calculations are summarised in Table 2.

Table 2. Volumes of anthropogenic emissions from district heating of a building

Pollutant / greenhouse gas	Emission factor, g/GJ	Emissions, t/year
CO	$248.75 \cdot 10^{-6}$	2.97879278
NO_x	$64.311 \cdot 10^{-6}$	0.7701272
CH_4	$1 \cdot 10^{-6}$	0.01197505
N_2O	$0.1 \cdot 10^{-6}$	0.0011975
CO_2	$58{,}748.13 \cdot 10^{-6}$	703.511579

Source: compiled by the authors based on data from Order of the Ministry of Construction of Ukraine No. 67 (2006)

As can be seen from Table 2, the total amount of anthropogenic emissions generated annually by the central heating boilers of the building is 707.27 t/year, of which greenhouse gas emissions (CO_2, CH_4, N_2O) account for 703.52 t/year. The calculation results show that when using district heating for a multi-apartment residential building, there are 881.78 – 707.27 = 174.51 t/year fewer anthropogenic emissions, in particular greenhouse gases (CO_2, CH_4, N_2O) are reduced by 879.96 – 703.52 = 176.44 t/year, i.e. emissions are reduced by 20.0%. A similar emission profile is observed with district heating. Carbon dioxide also accounts for the largest share of total anthropogenic emissions, whilst the contribution of other gases is comparatively insignificant. This is due to the fact that the mass of CO_2 produced during the complete combustion of natural gas exceeds the mass of other emission components by several orders of magnitude. Thus, the observed reduction in total anthropogenic emissions from district heating is primarily due to lower CO_2 emissions resulting from lower annual natural gas consumption compared to individual heating.

To determine the impact of the efficiency of district heating boilers on the quantity of pollutant emissions, anthropogenic emissions were calculated for efficiency values in the range of 70-90% in 5% increments. To this end, when determining the calculated gas consumption in Equation (3), the value of η was varied, whilst subsequent calculations using Equations (4), (2) and (1) were carried out without change. Figure 2 shows the values of anthropogenic emissions for district heating (DHS) depending on the boiler efficiency in the range of 70-90%, as well as the volume of anthropogenic emissions for individual heating (IHS) using boilers with an efficiency of 90%.

As can be seen from Figure 2, the efficiency of centralised heat supply boilers significantly influences the amount of pollutants generated during the combustion of natural gas in them. The lower the boiler efficiency, the greater the amount of anthropogenic emissions generated. Within this efficiency range, the highest level of anthropogenic emissions occurs at an efficiency of 70%, specifically 909.35 t/year. However, as can be seen from Figure 2, district heating systems with boilers having an efficiency of 75-90% produce fewer emissions than individual heating systems with boilers having an efficiency of 90%. This is because as boiler efficiency decreases, the natural gas consumption required to produce the same amount of thermal energy increases. Since carbon dioxide accounts for over 99% of anthropogenic emissions, an increase in natural gas consumption leads to a practically proportional increase in total emissions.

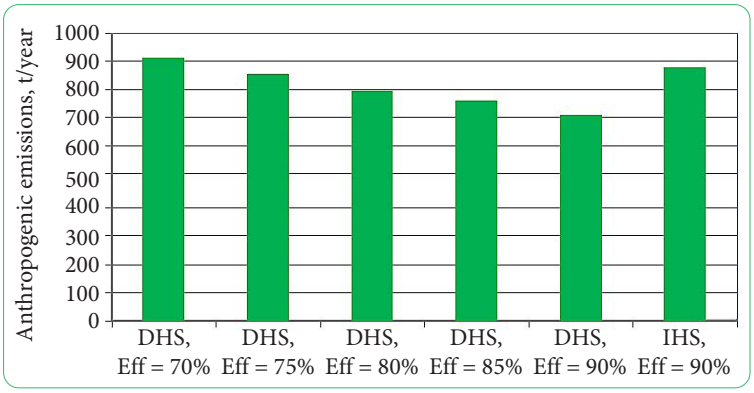

Figure 2. Volumes of anthropogenic emissions generated during the production of thermal energy by district heating (DH) and individual heating (IH) systems with different boiler efficiency values
Source: developed by the authors using Order of the Ministry of Construction of Ukraine No. 67 (2006) and Order of the State Statistics Committee of Ukraine No. 98 (2011)

It has been established that when the efficiency of a district heating boiler exceeds 72%, total anthropogenic emissions are lower than in the case of individual heating from gas boilers with an efficiency of 90%. The threshold value obtained is of practical significance in the preliminary assessment of the feasibility of using district heating and determines the minimum level of energy efficiency of boiler equipment at which a district heating system has an environmental advantage. The results presented were obtained for the assumed modelling conditions, which did not take into account heat losses in heating networks, variable boiler operating modes, and weather-dependent heat supply regulation. Taking these factors into account may affect the absolute emission values, but does not alter the established pattern of decreasing anthropogenic emissions as the efficiency of boiler equipment increases.

A comparison of the results obtained with studies by other authors confirms the advantages of centralised heat supply systems in reducing anthropogenic emissions, particularly greenhouse gases, compared to individual gas boilers, although efficiency depends on energy sources, regional and other factors. According to Q. Cai *et al.* (2024), energy consumption during the operation of a building's engineering systems – specifically heating, cooling, hot water supply and electricity supply systems – accounts for 94.4% of primary energy consumption over the building's life cycle. A.X. Malcher *et al.* (2025) noted that in the European Union, heating systems account for 42% of primary energy consumption and 15% of global pollutant emissions. Therefore, reducing the use of energy resources and, consequently, reducing anthropogenic emissions during the operation of a building's engineering systems is a key challenge for energy efficiency and decarbonisation.

In the work by A.X. Malcher *et al.* (2025), based on an analysis of 42 life-cycle assessment studies for 160 heating configurations, it is shown that cogeneration plants reduce emissions by 16-70% compared to traditional boilers, and heat pumps by an average of 64% compared to gas-fired ones. This is consistent with the results obtained, in particular the 20% reduction in anthropogenic emissions when switching to a centralised boiler plant with 90% efficiency, but highlights the greater potential when integrating renewable sources, which have not been taken into account in our case. Similarly, L. Balode *et al.* (2023), when analysing the potential for using renewable energy sources in one of Latvia's municipalities, found that district heating powered by gas has CO_2 emissions of 202 g/kWh, similar to individual gas boilers, but when renewable components, such as heat pumps, are added, the reduction reaches 72%. This indicates that the estimate obtained is a baseline scenario without decarbonisation, where the benefit of 176.44 t/year is lower than what is possible with the use of renewable energy sources.

In a study by S. O'Brien *et al.* (2025) for the Baltic region, a biogas cogeneration plant in a district heating system reduces annual emissions by 72.9% compared to natural gas cogeneration plants, with a focus on the life cycle, where embodied emissions are higher for waste heat (402,000 kg CO_2 eq versus 256,000), but operational emissions are lower. This complements the calculations of gross emissions obtained without a life-cycle assessment, demonstrating the potential for further reductions in the Ukrainian context. L. Ho (2022), in a UK context, reports a 3.2-fold reduction in emissions for district heating compared to individual gas boilers, citing the example of Nottingham, where emissions avoided amounted to 27,000 tonnes of CO_2 per year due to centralised energy generation from waste. Y. Ju *et al.* (2022) assessed the CO_2 reduction potential in district heating for a German demand-response system (a mechanism for flexible management of heat demand in district heating systems), focusing on savings, although without a direct comparison with individual systems.

J. Rey-Hernández *et al.* (2023) achieved a 92.69% reduction in CO_2 emissions for a Spanish campus with a biomass-fired district heating system, alongside a 96.19% saving in non-renewable primary energy. Due to the use of biomass, this significantly exceeds our 20%, but illustrates the potential for Ukraine with alternative fuels. H. Dorotić *et al.* (2021) highlighted the importance of allocation in cogeneration plants, where district heating reduces

emissions to 0.04-0.09 t CO_2/MWh compared to 0.23 for individual gas boilers, i.e. almost five times less. Finally, in their study, F. Neirotti *et al.* (2020) conducted a life-cycle assessment for Italian networks, which showed that emissions from district heating amount to 0.10-0.47 kg CO_2 eq/kWh depending on allocation, compared to 0.27 for individual gas boilers. The authors emphasise the need to account for gas imports and other factors, but do not take network losses into account. Overall, the available studies confirm the findings regarding a reduction in anthropogenic emissions when using district heating, but point in particular to greater potential with alternative energy sources, which should be taken into account in future work for the Ukrainian context.

Conclusions

In Ukraine, roughly the same number of consumers use individual and district heating systems for heat production. To confirm the environmental sustainability of centralised heat supply systems compared to individual heat supply systems, an environmental assessment was carried out. The environmental assessment was conducted for heat supply systems that met the heating and hot water supply needs of a 72-apartment residential building. Individual gas-fired double-circuit boilers, installed in each flat of the residential building, were adopted as the heat source in individual heat supply systems, whilst in the centralised heat supply system, a single gas boiler was used in the heating plant.

The main components of anthropogenic emissions during the operation of heat supply systems, specifically during the combustion of natural gas in boilers, are carbon monoxide, carbon dioxide, nitrogen oxides, nitrogen dioxide, sulphur dioxide, methane and non-methane volatile organic compounds. The quantities of pollutant emissions and greenhouse gases released into the environment were determined using Ukrainian state methodologies. The environmental assessment found that individual heating of a residential building generates 881.78 t/year of anthropogenic emissions, of which 879.96 t/year are greenhouse gases, whereas centralised heat supply generates 707.27 t/year of anthropogenic emissions, of which 703.52 t/year are greenhouse gases. Consequently, the use of district heating in a residential building results in 176.44 t/year fewer greenhouse gas emissions than with individual heating, i.e. a 20.0% reduction in emissions is observed.

Lower greenhouse gas emissions from district heating compared to individual heating are also observed when the efficiency of the gas boiler in the boiler room decreases. A reduction in the boiler efficiency of the boiler house below 72% leads to an increase in greenhouse gas emissions compared to individual heat supply from gas boilers with an efficiency of 90%. When using district heating from gas boilers with an efficiency >73%, greenhouse gas emissions are lower than with individual heating from gas boilers with an efficiency of 90%. Therefore, in order to reduce the environmental impact when designing new and modernising existing heat supply systems, it is advisable to opt for centralised heat supply systems. Further research should involve an environmental assessment of centralised heat supply systems using alternative fuels.

Acknowledgements

None.

Funding

None.

Conflict of Interest

None.

References

[1] Adamenko, S.Y., Arkhipova, L.M., Adamenko, Y.O., Moskaliuk, N.M., Hlibovytska, N.I., & Chupa, V.M. (2024). Patterns of PM10 particle changes in the atmospheric air of Ivano-Frankivsk city. *IOP Conference Series: Earth and Environmental Science*, 1415, article number 012002. doi: 10.1088/1755-1315/1415/1/01200.

[2] Arkhypova, L.M., Adamenko, S.Y., Adamenko, Y.O., Kachala, T.B., & Kachala, S.V. (2025). Modelling the dependence of ambient air pollution on meteorological factors: A case study from Ukraine. *Journal of Physics: Conference Series*, 3153, article number 012021. doi: 10.1088/1742-6596/3153/1/012021.

[3] Balode, L., Zlaugotne, B., Gravelsins, A., Svedovs, O., Pakere, I., Kirsanovs, V., & Blumberga, D. (2023). Carbon neutrality in municipalities: Balancing individual and district heating renewable energy solutions. *Sustainability*, 15(10), article number 8415. doi: 10.3390/su15108415.

[4] Cai, Q., Li, B., He, W., & Guo, M. (2024). Energy consumption calculation of civil buildings in regional integrated energy systems: A review of characteristics, methods and application prospects. *Sustainability*, 16, article number 5692. doi: 10.3390/su16135692.

[5] DBN V.2.5-64:2012. (2012). *Internal water supply and sewerage. Part I. Design. Part II. Construction. With amendment No. 1*. Retrieved from https://online.budstandart.com/ua/catalog/doc-page.html?id_doc=29848.

[6] DBN V.2.6-31:2021. (2021). *Thermal insulation and energy efficiency of buildings*. Retrieved from https://online.budstandart.com/ua/catalog/doc-page.html?id_doc=98037.

[7] Dorotić, H., Pukšec, T., Schneider, D.R., & Duić, N. (2021). Evaluation of district heating with regard to individual systems – importance of carbon and cost allocation in cogeneration units. *Energy*, 221, article number 119905. doi: 10.1016/j.energy.2021.119905.

[8] DSTU EN 12831-1:2017. (2017). *Energy performance of buildings. Method for calculation of the design heat load. Part 1. Space heating load, Module M3-3*. Retrieved from https://surli.cc/nzhvjg.

[9] DSTU-N B V.1.1-27:2010. (2010). *Protection against hazardous geological processes, harmful operational impacts and fire. Building climatology.* Retrieved from https://online.budstandart.com/ua/catalog/doc-page.html?id_doc=26655.
[10] Ganesha, N.S., & Omprakash, M. (2022). Comprehensive review on cogeneration systems for low and medium temperature heat recoveries. *Energy Sources, Part A: Recovery, Utilization and Environmental Effects*, 44(3), 6404-6432. doi: 10.1080/15567036.2022.2098420.
[11] Ho, L. (2022). *How district heating can cut carbon emissions*. Retrieved from https://surl.li/wbiftm.
[12] Ju, Y., Lindholm, J., Verbeck, M., Jokisalo, J., Kosonen, R., Janßen, P., Li, Y., Schäfers, H., & Nord, N. (2022). Cost savings and CO2 emissions reduction potential in the German district heating system with demand response. *Science and Technology for the Built Environment*, 28(2), 255-274. doi: 10.1080/23744731.2021.2018875.
[13] Kyoto Protocol to the United Nations Framework Convention on Climate Change. (2006). Retrieved from https://zakon.rada.gov.ua/laws/show/995_801#Text.
[14] Law of Ukraine No. 3991-IX "On the Basic Principles of State Climate Policy". (2024, October). Retrieved from https://zakon.rada.gov.ua/laws/show/3991-20#Text.
[15] Luzhanska, G., Diachenko, G., Bessatyan, Y., Tarasiuk, O., & Sergeiev, I. (2025). Energy efficiency analysis of water heating system gas condensing boilers. *Proceedings of Odessa Polytechnic University*, 1(71), 89-97. doi: 10.15276/opu.1.71.2025.10.
[16] Malcher, X., Tenorio-Rodriguez, F.C., Finkbeiner, M., & Gonzalez-Salazar, M. (2025). Decarbonisation of district heating: A systematic review of carbon footprint and key mitigation strategies. *Renewable and Sustainable Energy Reviews*, 215, article number 115602. doi: 10.1016/j.rser.2025.115602.
[17] Mastrucci, A., Boza-Kiss, B., & van Ruijven, B. (2025). Towards net-zero emissions in global residential heating and cooling: A global scenario analysis. *Climatic Change*, 178, article number 85. doi: 10.1007/s10584-025-03923-6.
[18] Ministry of Environmental Protection and Natural Resources of Ukraine & the Budget Institution "National Centre for GHG Emission Inventory". (2025). *Ukraine's greenhouse gas inventory 1990-2023. Annual national inventory report for submission under the United Nations Framework Convention on Climate Change and the Paris Agreement*. Kyiv: Ministry of Environmental Protection and Natural Resources of Ukraine.
[19] Neirotti, F., Noussan, M., & Simonetti, M. (2020). Evaluating the emissions of the heat supplied by district heating networks through a life cycle perspective. *Clean Technologies*, 2(4), 392-405. doi: 10.3390/cleantechnol2040024.
[20] O'Brien, S., Ul Abdeen Qureshi, Z., & Aghamolaei, R. (2025). Comparative life cycle assessment of district heating supply pathways: Insights from waste heat and CHP configurations. *Results in Engineering*, 28, article number 107718. doi: 10.1016/j.rineng.2025.1037718.
[21] Order of the Ministry of Construction of Ukraine No. 67 "On Approval of the sectoral methodology for Calculating Harmful Emissions from Heat-Generating Installations of communal heat energy in Ukraine". (2006, March). Retrieved from https://zakon.rada.gov.ua/rada/show/v0067667-06.
[22] Order of the State Statistics Committee of Ukraine No. 98 "On Approval of the Methodology for Calculating Emissions of Pollutants and Greenhouse Gases into the Air from Fuel Use for Household Needs". (2011, April). Retrieved from https://ukrstat.gov.ua/metod_polog/metod_doc/2011/98/98.htm.
[23] Rey-Hernández, J.M., Rey-Martínez, F.J., Yousif, C., & Krawczyk, D. (2023). Assessing the performance of a renewable district heating system to achieve nearly zero-energy status in renovated university campuses: A case study for Spain. *Energy Conversion and Management*, 292, article number 117439. doi: 10.1016/j.enconman.2023.117439.
[24] Ritchie, H., Rosado, P., & Roser, M. (2024). *Greenhouse gas emissions*. Retrieved from https://archive.ourworldindata.org/20251204-133820/greenhouse-gas-emissions.html.
[25] Savchenko, O., Yurkevych, Yu., Liubuska, I., & Spodyniuk, N. (2025). Ways to reduce heat losses in district heating systems: Case study. In Z. Blikharskyy, D. Katunský & L. Lichołai (Eds.), *Proceedings of CEE 2025. Lecture notes in civil engineering* (pp. 376-388). Cham: Springer. doi: 10.1007/978-3-032-06850-7_37.
[26] Savchenko, O., Yurkevych, Yu., Zhelykh, V., & Voznyak, O. (2023). Review of geothermal district heating schemes and recommendations for their use in the Lviv region. In Z. Blikharskyy (Ed.), *Proceedings of ecocomfort 2022. Lecture notes in civil engineering* (pp. 344-354). Cham: Springer. doi: 10.1007/978-3-031-14141-6_35.
[27] Selikhov, Yu., Gorbunov, K., Nagorniy, E., Pilnyk, I., & Rys, V. (2025). Energy efficiency of thermal power plant operation based on solar collectors using programming in the MATHCAD application environment. *Integrated Technologies and Energy Saving*, 1, 12-24. doi: 10.20998/2078-5364.2025.1.02.
[28] Selikhov, Yu., Rishchenko, I., & Gorbunov, K. (2023) Integration of heating system operation. *Integrated Technologies and Energy Saving*, 4, 3-16. doi: 10.20998/2078-5364.2023.4.01.
[29] Venhryn, I., Shapoval, S., Voznyak, O., Datsko, O., & Gulai, B. (2021). Modelling of optical characteristics of the thermal photovoltaic hybrid solar collector. In *IEEE16th international conference on computer sciences and information technologies* (pp. 255-258). Lviv: Lviv Polytechnic National University. doi: 10.1109/csit52700.2021.9648738.
[30] Vranay, F., Kaposztasova, D., & Vranayova, Z. (2025). Dynamic regulation and renewable integration for low-carbon district heating networks. *Sustainability*, 17(23), article number 10713. doi: 10.3390/su172310713.

Екологічна оцінка впливу джерел теплоти житлового будинку на забруднення атмосферного повітря

Олена Савченко
Кандидат технічних наук, доцент
Національний університет «Львівська політехніка»
79013, вул. Степана Бандери, 12, м. Львів, Україна
https://orcid.org/0000-0003-3767-380X

Орест Возняк
Доктор технічних наук, професор
Національний університет «Львівська політехніка»
79013, вул. Степана Бандери, 12, м. Львів, Україна
https://orcid.org/0000-0002-6431-088X

Іван Любуська
Інженер
Львівське міське комунальне підприємство «Львівтеплоенерго»
79040, вул. Данила Апостола, 1, м. Львів, Україна
https://orcid.org/0009-0009-4E753-7597

Наталія Москальчук
Кандидат технічних наук, доцент
Івано-Франківський національний технічний університет нафти і газу
76019, вул. Карпатська, 15, м. Івано-Франківськ, Україна
https://orcid.org/0000-0003-4838-7972

Василь Шекета
Доктор технічних наук, професор
Івано-Франківський національний технічний університет нафти і газу
76019, вул. Карпатська, 15, м. Івано-Франківськ, Україна
https://orcid.org/0000-0002-1318-4895

Анотація. Реалізація заходів з енергоефективності має вирішальне значення для низьковуглецевого розвитку, надійного енергозабезпечення та енергетичної безпеки країни. Одним з кроків реалізації таких заходів є впровадження нових та модернізація існуючих систем централізованого теплопостачання, які дозволяють збалансувати ресурсокористування, зменшити викиди парникових газів у довкілля, спростити експлуатацію та технічне обслуговування будівель. Метою роботи було порівняння кількості викидів забруднюючих речовин та парникових газів, які утворюються при виробництві теплової енергії індивідуальною та централізованою системами теплопостачання житлового будинку. Розглянуто 72-квартирний житловий будинок, огороджувальні конструкції якого відповідають сучасним теплотехнічним вимогам. У варіанті автономного теплопостачання джерелами теплоти були індивідуальні газові двоконтурні котли, тоді як у централізованій системі теплопостачання теплова енергія вироблялася газовою котельнею. Кількість викидів, які надходили у довкілля при індивідуальному теплопостачанні, було розраховано відповідно до Методики визначення викидів забруднюючих речовин та парникових газів у повітря від використання палива на побутові потреби в домогосподарствах. Кількість викидів, які надходили у довкілля при централізованому теплопостачанні було розраховано відповідно до Галузевої методики розрахунку шкідливих викидів, які надходять від теплогенеруючих установок комунальної теплоенергетики. До забруднюючих речовин та парникових газів, викиди яких враховують вказані методики, належать оксид вуглецю, діоксид вуглецю, оксиди азоту, діоксид азоту, діоксид сірки, метан та неметанові леткі органічні сполуки. Встановлено, що при індивідуальному теплопостачанні житлового будинку утворюється 881,78 т/рік антропогенних викидів, з них 879,96 т/рік парникових газів, а при централізованому теплопостачанні утворюється 707,27 т/рік антропогенних викидів, з них 703,52 т/рік парникових газів. Результати досліджень свідчать, що при використанні централізованого теплопостачання житлового будинку утворюється на 176,44 т/рік парникових газів менше, ніж при індивідуальному теплопостачанні, тобто спостерігається зменшення викидів на 20,0 %

Ключові слова: енергоефективність; система теплопостачання; газовий котел; природний газ; викиди; парникові гази; забруднюючі речовини

Vol. 17, No. 1
2026

Ecological Safety and Balanced Use of Resources

ISSN (print) 2415-3184, ISSN (online) 2522-9508
Journal homepage: https://esbur.com.ua/en

Received: 03.12.2025. Revised: 04.05.2026. Accepted: 12.06.2026. Published: 30.06.2026.

UDC 69.059.7:502

DOI: 10.63341/esbur/1.2026.79

Short- and long-term ecological consequences of methodological discrepancies in building energy efficiency calculations

Volodymyr Chupa*
Doctor of Philosophy, Associate Professor
Ivano-Frankivsk National Technical University of Oil and Gas
76019, 15 Karpatska Str., Ivano-Frankivsk, Ukraine
https://orcid.org/0000-0001-5658-1877

Iryna Vashchyshak
PhD in Technical Sciences, Associate Professor
Ivano-Frankivsk National Technical University of Oil and Gas
76019, 15 Karpatska Str., Ivano-Frankivsk, Ukraine
https://orcid.org/0000-0002-9078-6726

Serhii Maksymiuk
Doctor of Philosophy, Associate Professor
Ivano-Frankivsk National Technical University of Oil and Gas
76019, 15 Karpatska Str., Ivano-Frankivsk, Ukraine
https://orcid.org/0000-0002-6312-7047

Kyrylo Novytskyi
Executive Secretary, Lead Engineer
Ivano-Frankivsk National Technical University of Oil and Gas
76019, 15 Karpatska Str., Ivano-Frankivsk, Ukraine
https://orcid.org/0009-0001-3383-1973

Abstract. In the context of global decarbonisation, the accuracy of assessing building energy efficiency has become a critical factor for predicting environmental impacts and achieving vital climate goals. Existing discrepancies between national and international calculation methodologies have created significant risks during the planning of large-scale thermal modernisation strategies. This article aimed to quantitatively assess the ecological consequences of methodological discrepancies between quasi-stationary and hourly dynamic approaches to calculating building energy consumption. A comprehensive approach was developed, including hierarchical modelling and a detailed methodology for converting energy consumption into carbon emission mass with a thorough assessment. It was established that the key sources of methodological discrepancy are the choice of the time model, the format of presenting climatic data, the description of thermal inertia, and the algorithm for interpreting internal heat gains. Research proved that the difference in annual energy demand when changing calculation methods reaches several tens of percent. This was equivalent to deviations in carbon dioxide emission mass in the range of hundreds of kilograms. To address this, the concept of a "zone of discrepancy" was proposed, introducing a threshold T to determine the feasibility of using simplified methodologies depending on the required accuracy. A methodology for aggregating individual deviations to the building stock level, based on a deterministic comparison of representative scenarios, is justified. These mathematical dependencies for quantitative assessment increase environmental

Suggested Citation: Chupa, V., Vashchyshak, I., Maksymiuk, S., & Novytskyi, K. (2026). Short- and long-term ecological consequences of methodological discrepancies in building energy efficiency calculations. *Ecological Safety and Balanced Use of Resources*, 17(1), 79-87. doi: 10.63341/esbur/1.2026.79.

*Corresponding author (*volodymyr.chupa@nung.edu.ua*)

monitoring reliability, allowing specialists to develop precise regulatory requirements and reduce the construction sector's carbon footprint

Keywords: decarbonisation; thermal modernisation; carbon footprint; fuel and energy resources; regulatory framework; dynamic modelling

Introduction

Improving building energy efficiency is a key decarbonisation tool, but the accuracy of assessing the environmental load critically depends on the chosen energy demand calculation model. The use of different methodological approaches when harmonising national and international standards causes significant discrepancies in determining the annual volumes of pollutant emissions. In the long term, such methodological uncertainty accumulates, leading to systemic distortions in predicting environmental effects at the level of the entire building stock. Consequently, a quantitative analysis of the consequences of applying different methodologies is necessary for the formation of optimal energy modernisation strategies and ensuring the sustainable development of the sector.

The problem of methodological differences in building energy efficiency calculations has been studied by numerous scientists. The existing scientific heritage has outlined both the theoretical foundations of calculation models and applied approaches to assessing energy consumption and related ecological consequences. A number of studies emphasised that the key discrepancy between Ukrainian (DSTU) and international (ISO/EN) approaches lies in different approximations of time characteristics (quasi-stationary monthly models versus hourly dynamic models) which, as I.M. Dashko & D.V. Krylov (2021) pointed out, stems from fundamentally different approaches to the assessment of enclosing structures, engineering systems, and operational features. This difference is clearly observed when comparing DSTU 9190:2022 (2022) with the international standard ISO 52016-1:2017 (2017), moreover, the international normative document provides a more accurate dynamic approach and allows accounting for hourly temperature fluctuations, solar radiation, and the inertial properties of building masses.

The practical consequences of such methodological differences result in differing calculation outcomes, which can lead to incorrect classification of the building's energy class, erroneous ranking of thermal modernisation measures, and making unjustified investment decisions. O.V. Komelina & A.A. Komelina (2022) argued that the lack of methodology unification complicates data integration and distorts the assessment of environmental risks at the national level, which is critical for achieving climate goals. At the same time, T.D. Kosova & A.D. Titarenko (2021) were confident that for Ukraine, the problem of improving the legislative framework and finding effective financial incentives is critically relevant. The current regulations often do not meet modern international standards, and business support mechanisms, such as tax benefits and lending, are insufficiently effective and limited. The absence of adequate incentives hinders investments in energy-saving technologies and restrains the development of the relevant market. H. Farenyuk & Ye. Farenyuk (2025) also noted a pragmatic approach: quasi-stationary methods (embedded in individual DSTUs or national codes) are recognised as justified for mass screening and rapid design, whereas hourly dynamic models according to ISO 52016-1 are appropriate for detailed engineering analysis and complex operating modes. Accordingly, such a dichotomy highlights the need for formalised criteria for choosing a methodology depending on the calculation purpose, project scale, and expected accuracy.

Considering the above, the current scientific discussion focuses on three interrelated areas: refinement and unification of input data and assumptions to ensure comparability; development of procedures for selecting an adequate methodology for specific classes of objects; quantitative assessment of the impact of methodological discrepancies on environmental indicators (in particular, predicted emission volumes) and the economic feasibility of energy modernisation. Accordingly, further research should be aimed at developing practically oriented tools for harmonising methodologies (including recommendations on applying simplified or detailed approaches) and formalising procedures for recalculating indicators between different approaches in order to correctly assess the ecological consequences of energy efficiency measures. The aim of the study was to quantitatively assess the short- and long-term ecological consequences of methodological discrepancies between quasi-stationary and hourly dynamic approaches to calculating building energy efficiency, as well as to identify the key factors causing these differences.

Materials and Methods

Representative types of building premises were used as calculation materials: a residential apartment, an office, and an educational classroom. They were purposefully selected according to criteria of typicality, prevalence in the building stock, and differences in functional purpose, allowing for a comparison of results for objects with different thermal load profiles. The choice of materials was determined by their availability, regulatory validity, and suitability for comparing results obtained using different calculation methodologies. To demonstrate the application of the proposed approach, three representative building types (a residential apartment, an office, and a classroom) were selected as illustrative cases for visualisation and aggregation. A set of simplified scenarios was developed to

estimate greenhouse gas emissions using emission factors (*EF*), with the corresponding coefficients adopted from the Green Transition Office database (Shlapak *et al*., 2024). For the residential case study, annual energy demand was calculated using two alternative methodologies: ISO 52016-1:2017 (2017) and DSTU 9190:2022 (2022). The annual energy demand of a typical apartment was estimated at 17,200 kWh according to DSTU 9190 and 12,717 kWh according to ISO 52016-1. The difference between the calculated values was determined as:

$$\Delta Q = QDSTU - QISO = 4{,}483\ kWh.$$

The relative deviation between the methods was calculated as a percentage of the ISO-based estimate. To assess the environmental implications of methodological differences, the obtained energy demand deviation was converted into CO_2 emissions using the natural gas emission factor (*EFgas* = 0.201 kg CO_2/kWh) reported by M. Shlapak *et al*. (2024). The resulting difference in annual emissions was calculated according to the following equation:

$$\Delta mCO_2 = \Delta Q \times EFgas, \quad (1)$$

where ΔmCO_2 – the difference in annual CO_2 emissions (kg/year); ΔQ – the difference in calculated annual energy demand (kWh/year); *EFgas* – the natural gas emission factor (kg CO_2/kWh).

The theoretical basis of the article was based on combining a formal dynamic energy balance model as a basic description of the physical process; a comparative analysis of DSTU and ISO/EN standards, as well as evaluating the differences between the results of quasi-stationary and hourly dynamic approaches and practical implementation through modelling to develop rules for recalculating results between methodologies. The methodological framework combined the formalisation of physical building energy balance models with a clear procedure for converting energy results into environmental indicators and quantitatively assessing the uncertainty of such conversions.

According to S.B. Smereka & S.M. Lifyrenko (2025) two complementary classes of energy demand calculations are fundamental: quasi-stationary (monthly, as in national methodologies according to DSTU) and hourly dynamic (ISO 52016-1). Based on them, a sequential chain of transformations was formed: formalisation of energy calculation → linear conversion of energy into emissions → aggregation by energy carrier classes and equipment → analysis of the "zone of discrepancy" in environmental impact indicators → study of consequences in the context of the building stock. To perform the comparative analysis, normative-methodological documents regulating the calculation of building energy efficiency in Ukraine and internationally were used, namely ISO 52016-1:2017 (2017), DBN V.2.6-31:2021 (2021), and DSTU 9190:2022 (2022). To convert energy consumption into greenhouse gas emissions, emission factors listed in open official and reference sources were applied. According to DBN V.2.6-31 (2021), building energy efficiency calculations are based on formalised mathematical models of energy balance, where the key components are temporal climate characteristics, internal heat gains, parameters of enclosing structures, and operating modes of engineering systems. In its basic form, the dynamic energy balance is described by a differential equation of the form:

$$C_{int} \cdot \frac{d\theta_{int}(t)}{dt} = \Phi_{tot}(t), \quad (2)$$

where C_{int} – the effective heat capacity of the building; $\frac{d\theta_{int}(t)}{dt}$ – the time derivative of the internal temperature; $\Phi_{tot}(t)$ – the sum of all heat fluxes at time *t*.

The formalisation of the energy calculation consists in selecting input data and typical objects – a set of parameters and scenarios necessary for the a priori systematisation of the physical model, so this stage prepares the tools and initial data for the further implementation of calculation procedures. Without a clear description of the geometry, thermal characteristics, and climatic profiles, it is impossible to correctly apply either the monthly or the hourly algorithm. The indicator $\Phi_{tot}(t)$ from formula 1 can be detailed. Then the general dynamic energy balance equation takes the form:

$$C_{int} \cdot \frac{d\theta_{int}(t)}{dt} = \Phi_{HC}(t) + \Phi_{int}(t) + \Phi_{sol}(t) - \\ - H_T \cdot [\theta_{int}(t) - \theta_e(t)] - H_V \cdot [\theta_{int}(t) - \theta_e(t)], \quad (3)$$

where $\Phi_{HC}(t)$ – the heat flux from heating and cooling systems; $\Phi_{int}(t)$ – internal heat gains; $\Phi_{sol}(t)$ – solar gains; H_T – the transmission heat transfer coefficient of the enclosures; H_V – the ventilation heat loss coefficient; $\theta_{int}(t)$ – the internal temperature at time *t*; $\theta_e(t)$ – the external temperature at the same moment.

To transition from the instantaneous energy balance described by equations 1-2 to the annual energy demand indicator, integration of the thermal load over the calculation period was used. For the quasi-stationary methodology, this period corresponded to the heating year, and the annual energy demand was determined as the sum (integral) of the time values of the heat flux over the entire calculation interval. In the hourly dynamic model, integration was performed with a time step of 1 hour, which allowed accounting for the diurnal variability of climatic conditions, internal gains, and the operation of engineering systems. Formally, the annual energy demand was determined as the integral of the thermal load over the period $0 \le t \le T$, where T is the duration of the calculation year or heating season depending on the methodology. The difference in temporal discretisation and the duration of the calculation period is one of the key sources of discrepancy between the results of DSTU- and ISO-oriented approaches:

$$E_p = \sum_{k=1}^{N} \Phi_{tot}(t_k)\Delta t,\ \Delta t = 1\ \text{hour}. \quad (4)$$

After implementing both types of calculations (monthly and hourly), it is necessary to obtain numerical values

of energy demand E in comparable units (hourly, seasonal, annual). It is these results that form the basis for further linear and advanced transformations into environmental indicators: only by having comparable E values is it possible to apply primary energy coefficients α and emission factors EF to obtain the emission mass. The standard operational approximation for converting energy consumption into CO_2 emission mass has a linear form:

$$m_{CO_2} = E \cdot EF, \quad (5)$$

where E – the annual amount of energy to be recalculated (kWh); EF – the emission factor (kg CO_2/kWh) for the corresponding energy carrier or generating unit. It is important to distinguish the types of the indicator E: consumed final energy E_{cons}; primary energy E_p; system heat output E_{heat}. The dependencies between them can be presented linearly:

$$E_p = \alpha \cdot E_{cons}; \quad (6)$$

$$m_{CO_2} = E_p \cdot EF_p = E_{cons} \cdot (\alpha \cdot EF_p), \quad (7)$$

where α – the conversion factor to primary energy; EF_p – the emission factor calculated per primary energy. The result of this stage are numerical bases that can be transformed into emission mass indicators.

At the stage of aggregation by energy carrier classes and equipment, it is necessary to foresee the breakdown of the emission mass into components by sources:

$$m_{CO_2}^{(tot)} = \sum_j E_{cons}^{(j)} \cdot \alpha^{(j)} \cdot EF_p^{(j)}, \quad (8)$$

where the index j – the type of energy carrier or generation method (gas boiler, centralised heat, electrical grid with a specific generation component, etc.). This will make it possible to assess the sensitivity of the output result to changes in the energy supply structure (for example, replacing a gas boiler with a heat pump or changing the power grid to photovoltaic generation). The choice of matrices $EF_p^{(j)}$ and $\alpha^{(j)}$ should be made based on the information provided in the methodological guidelines and national normative documents.

The initial construct was the explicit representation of an individual deviation in the mass of greenhouse emissions due to the methodological choice: for each unit of the stock i the value is introduced:

$$\Delta m_i = (E_{DSTU,i} - E_{ISO,i}) \cdot EF_i, \quad (9)$$

which underscores the dual nature of the problem – the combination of a methodological discrepancy in assessing energy demand and the variability of the emission intensity of the heat supply source. The cumulative effect was determined by the sum of individual deviations:

$$\Delta M = \sum_{i-1}^{N} \Delta m_i. \quad (10)$$

This formula reflects the deterministic core of aggregation. The concept of the "zone of discrepancy" is formalised. In other words, knowing which sources of uncertainty dominate allows determining the criteria for selecting the threshold T and for constructing a rule for the parameter's inclusion in the zone of discrepancy. As a criterion for defining the zone of discrepancy, a pragmatic threshold T is introduced (for example, T = 10% relative to the annual heat demand). The set of parameters x (climate, U-values, C_{int}, occupancy profile, etc.) for which the condition is met:

$$\left|\frac{E_{DSTU}(x) - E_{ISO}(x)}{E_{ISO}(x)}\right| \geq T, \quad (11)$$

defines the zone of discrepancy. The translation of this criterion to the ecological scale is carried out through the corresponding EF, meaning the zone of discrepancy generates a set of scenarios with a deviation in emission mass:

$$\Delta m_{CO_2}(x) = (E_{DSTU}(x) - E_{ISO}(x)) \cdot EF(x). \quad (12)$$

Quantitative localisation of such zones can be performed using parametric scanning, followed by building "parameter/climate" heat maps. Implementing this approach allows formulating practical rules: provided it falls within the zone of discrepancy, using a quasi-stationary methodology is considered inappropriate for the purpose of environmental assessment. Once the zone of discrepancy is defined and localised in the parameter space, the next logical step is to assess its consequences at a higher aggregation level: at the building stock level. Information about the share of buildings falling into the zone of discrepancy and the magnitudes of individual deviations Δm_{CO_2} allows transitioning from individual cases to assessments of the cumulative impact on the municipal or national building stock. The cumulative effect is estimated as the sum of individual deviations over the number of buildings:

$$\Delta M_{CO_2}^{(tot)} = \sum_{i-1}^{N} (E_{DSTU,i} - E_{ISO,i}) \cdot EF_i. \quad (13)$$

In practical application, N is formed taking into account typology, distribution of technical characteristics, and the frequency of distinct building classes. This approach allows modelling short- (1-5 years) and long-term (10-30 years) scenarios of the impact of choosing the methodology for calculating energy efficiency indicators on the volume of emissions. The temporal dynamics of aggregation are introduced via the time parameter t, which allows formalising the integral effect over the forecast horizon T:

$$\Delta M_{[0,T]} = \sum_i \int_0^T (E_{DSTU,i}(t) - E_{ISO,i}(t)) \cdot EF_i(t) dt. \quad (14)$$

Formula 14 was used in the study as a general scenario dependency for evaluating the accumulated effect over the forecast horizon T. Since the actual calculations within the research were performed for one year, the annual value is taken as the basic step for extrapolation over a longer period. For this transition, it is assumed that the

annual difference between the methodologies remains constant over time, and the structure of energy consumption and emission factors do not change. Accordingly, for a representative group of three types of objects, the total annual deviation is 3,754.28 kg CO_2/year for natural gas, 7,527.24 kg CO_2/year for centralised heat supply, and 8,108.94 kg CO_2/year for electricity supply, which over 10 years corresponds to values of 37,542.8; 75,272.4, and 81,089.4 kg CO_2, respectively, over 20 years – 75,085.6; 150,544.8, and 162,178.8 kg CO_2, and over 30 years – 112,628.4; 225,817.2, and 243,268.2 kg CO_2. Thus, even under the conservative assumption about the constancy of the annual difference, the methodological effect accumulates into very significant quantities over the medium- and long-term planning horizons. The quantitative analysis within this study had a deterministic comparative nature and was aimed at juxtaposing the results obtained using quasi-stationary and hourly dynamic methodologies. The assessment was performed by calculating the absolute and relative deviations between the annual energy demand values and corresponding CO_2 emissions for representative scenarios. Therefore, the results presented below should be interpreted as deterministic scenario estimates obtained for typical objects and fixed emission factors.

Results

The energy efficiency of buildings and structures is a fundamental factor in ensuring the energy security, sustainable development, and economic growth of Ukraine. It is recognised as a key priority at the current stage of development, encompassing both national economies and individual structures. This is driven by the strategic need to respond to global limitations – the depletion of natural non-renewable energy resources. From a technological point of view, energy efficiency is viewed as a consequence of the implementation of modern technologies and equipment that make it possible to reduce the volume of energy required to produce goods and provide services. Within the framework of the economic approach, energy efficiency is treated as the economic expediency of reducing energy consumption volumes. It manifests itself in a reduction of energy costs per unit of GDP or for the production of goods and provision of services (Sovacool & Griffiths, 2020). In the context of ecology, energy efficiency is one of the key mechanisms for minimising the anthropogenic load on the environment, achieved by limiting greenhouse gas emissions and reducing the consumption of non-renewable energy resources (Hossin *et al*., 2023). The interdisciplinary approach to energy efficiency defined it as a generalised complex indicator combining economic, technological, and environmental dimensions of energy resource utilisation processes.

N. Kryshtof (2017) emphasised that building energy efficiency serves as an effective mechanism for ensuring energy security and the structural modernisation of the economy, which in turn requires precise and unified calculation approaches. A. Menegaki (2014) emphasised that improving the energy efficiency of buildings simultaneously solves several tasks: reduces greenhouse gas emissions, lowers household energy poverty, increases energy security, and creates new jobs in the construction and renovation sector. In practical terms, this means transitioning to the deep renovation of existing buildings, modernisation of heating and ventilation systems, comprehensive insulation of facades and roofs, replacement of windows, and implementation of automation and energy management systems. The Commission, forming policy in the field of energy consumption, highlights that buildings are the largest energy consumer in the EU and at the same time possess the greatest potential for reducing final consumption without losing comfort, which warrants special attention to energy efficiency as a strategic priority for the period up to 2050.

According to A. Bahaterenko *et al*. (2013) currently, the real estate sector in Ukraine consumes about 40% of all energy, while a significant part of it is lost due to the use of outdated construction and exploitation technologies. The vast majority of the residential and public building stock is characterised by a low level of thermal insulation and the inefficiency of heating and ventilation systems, leading to excessively high costs for energy resources. The situation has also been complicated by military hostilities, which have significantly damaged the country's energy infrastructure, causing systemic interruptions in the supply of gas, electricity, and heat. Thus, the regulatory and legal field of the study at the level of Ukraine is represented by the respective DSTUs, in particular DSTU 9190 (2022), whereas the international methodology is represented by the ISO 52016-1:2017 (2017). The discrepancies between the DSTU and ISO approaches have a systemic character and are caused by differences in assumptions, model structure, and the interpretation of input parameters. This provision explains why indicators identical in name can be "incomparable values" in a direct comparison without methodological correction.

Specific sources of methodological discrepancy include: the choice of the time model (monthly averaged versus hourly with a 1-hour step), the format of climatic data (average monthly temperatures versus hourly profiles), different approaches to describing the thermal inertia of a building (effective heat capacities of different aggregation levels), the discretisation and logic of heating/cooling systems operation (set-points, time schedules), and the interpretation of internal gains and solar gains. Thus, for the very same object, applying the DSTU and ISO methodologies can yield significantly different values of the annual heat demand and, accordingly, different estimates of operational emissions. According to M. Shovkalyuk (2018), special attention in the development of state stimulation programs must be given to the correct assessment of energy indicators. The absence of adequate baseline calculations can lead to systemic errors when justifying investments in energy efficiency improvements at the municipal level. Based on similarity, a representative sample was created for different premises. It is presented in Table 1.

Table 1. Annual energy demand (kWh)

	Q_{DSTU}, kWh	Q_{ISO}, kWh	ΔQ, kWh	Δ% (Q_{ISO})
Residential apartment	17,200	12,717	4,483	35.3%
Average office room	32,000	24,271	7,729	31.8%
Educational classroom	25,000	18,534	6,466	34.9%

Source: developed by the authors

It is important to emphasise that the given values are the result of deterministic scenario comparisons and do not contain statistical characteristics of variability. Consequently, these data are used to illustrate the systematic difference between calculation methodologies, and not for assessing the probabilistic distribution of outcomes (Table 2).

Table 2. Ecological indicators of emission conversion

	ΔQ	$\Delta m_{CO_2}(gas), kg$	$\Delta m_{CO_2}(ch), kg^*$ *ch – central heating	$\Delta m_{CO_2}(electr), kg$
conversion factor		0.201	0.403	0.430
Residential apartment	4,483	901.08	1,806.65	1,927.69
Average office room	7,729	1,553.53	3,114.79	3,323.47
Educational classroom	6,466	1,299.67	2,605.80	2,857.78

Source: developed by the authors

Accordingly, for all three cases, the emissions associated with central heating and electricity supply approximately doubled the emissions from gas given the same ΔQ, with electricity contributing a somewhat larger share than central heating (coefficient 0.430 > 0.403). This indicated that a decrease in demand for electricity and heat supply created a greater effect in reducing CO_2 per unit of saved energy than an equivalent reduction in gas consumption. Hence, priorities for energy efficiency measures should consider both the function of the building (which determines ΔQ) and the relative emission intensity by energy type when making decisions regarding the reduction of short- and long-term environmental consequences. To illustrate the aggregation of individual deviations at the group level of buildings, a pilot calculation was performed for a representative set of three types of objects listed in Table 2. Assuming equal weight for each case, the total deviation was: for natural gas – 3,754.28 kg CO_2/year, for centralised heat supply – 7,527.24 kg CO_2/year, for electricity supply – 8,108.94 kg CO_2/year. The average deviation per object within this sample was 1,251.43, 2,509.08, and 2,702.98 kg CO_2/year, respectively. The obtained values confirm that even on a small group of typical buildings, methodological discrepancies form a noticeable cumulative effect, which grows as the number of objects increases. In broader application for a block, district, or city, the aggregated effect should be calculated taking into account the number of buildings in each typological stratum, their area, operating modes, and the share of connection to a specific energy source. Within the scope of this article, such data were not available, so the presented calculation has a demonstrative nature and shows the principle of transition from an individual case to the group level.

Such a general expression serves as a basis for formalising different scenarios: a baseline scenario that fixes the existing calculation practice and modernisation rates; a scenario of gradual methodology harmonisation with a time profile of correction factors; a technological transformation scenario in which emission factors $EF_i(t)$ change as a result of power system decarbonisation or the widespread adoption of low-carbon technologies. The discrepancies obtained in the work between the DSTU and ISO/EN results have not an accidental, but a systemic nature: for a typical apartment, the annual energy demand differs by 35.3%, which in conversion to natural gas corresponds to roughly 901 kg CO_2/year; for an office and an educational classroom, the absolute deviation is even greater. In the article, the results are presented as a deterministic scenario comparison without confidence intervals and statistical characteristics of variability, so it is appropriate to interpret them as an estimate of methodological bias, and not as a probabilistic forecast. This type of gap between the calculated and actual or alternatively calculated energy consumption is well known in international literature regarding the performance gap and the sensitivity of models to input data and the level of detail.

The most important conclusion of the work is that the time scale of the model itself is the source of the systematic difference. This aligns with the study by H. Zhang *et al.* (2024) who showed that the results of a global sensitivity analysis for annual, monthly, and daily building energy consumption differ substantially, and finer time steps require more complex computations and provide a different picture of parameter influence. L. Zhu *et al.* (2022) demonstrated the feasibility of the Monte Carlo approach in combination with building simulation and global sensitivity for forecasting loads at the planning stage. A similar focus on the role of temporal discretisation and behavioural scenarios is also found in the scientific work of S. Norouziasl *et al.* (2024), where occupancy density and simulation step size significantly influenced the energy consumption of an office building. E. Kang *et al.* (2024) additionally showed that occupancy schedules and physiological characteristics of users can change office energy consumption even

within a single scenario. Therefore, the thesis regarding the key role of the time model is quite well-founded, but in this work, it is currently confirmed only by comparing two regulatory approaches, and not by current modelling. During the preparation of the study, V. Chupa *et al.* (2024) encountered the problem of selecting a methodology that would allow objectively comparing fundamentally different objects: certified biofuel (pellets) and morphologically heterogeneous municipal solid waste (MSW). In parallel, I. Vashchyshak *et al.* (2025) developed an improved methodology for energy auditing of underground heating networks, which ensures a more accurate identification of energy losses during transport.

For the practice of thermal modernisation, the conclusions of the current work also align with papers dedicated to renovation risk and the choice of measures. C. Carpino *et al.* (2022) showed that uncertainty and sensitivity analysis can reduce investment risk when applying energy performance contracts in the renovation of residential neighbourhoods. Also, Y. Deng *et al.* (2023) applied Morris's analysis to 14 enclosure parameters of an old residential district in Beijing and used it to select priority solutions considering climate change. M. Nasouri & N. Delgarm (2025) proposed a more formalised SBSA approach combining point and global sensitivity with Sobol metrics for a residential building in Iran, thereby showing a way to shift from descriptive comparison to quantitative ranking of factors. All these works confirm the validity of the idea that the calculation method influences reconstruction priorities and managerial decisions; however, they analyse uncertainty within a single modelling framework, whereas this study compares two different regulatory logic for energy efficiency calculations.

Publications on calibration and the performance gap additionally reinforce that part of the conclusions concerning the limits of permissible simplification. G. Chiesa *et al.* (2025) proved that weather data, occupancy profiles, internal heat gains, and ventilation can change the magnitude of the performance gap by up to 50% and more; This value is close to the discrepancy obtained between the approaches, although the reason for its occurrence is different – the article is not about measurement error, but about the methodological divergence between the standards. F. Johari *et al.* (2022) concluded that simplified building energy models can maintain acceptable calibration accuracy for urban-scale analysis if the purpose matches the level of detail. Q. Xue *et al.* (2025) determined that an approximate Bayesian approach is capable of calibrating uncertainty parameters significantly more accurately for a nearly-zero energy building, provided a sufficient dataset is available. Collectively, this means that this article convincingly reveals a systematic bias between DSTU and ISO/EN, but for complete scientific thoroughness, it lacks a real component, or rather a narrower, purely deterministic formulation of methods. Overall, this opinion corresponds to modern international practice in building energy efficiency modelling.

Conclusions

Methodological discrepancies between quasi-steady-state (DSTU) and dynamic (ISO/EN) approaches lead to systematic and quantitatively significant differences in the determination of annual thermal energy demand for various building types. Practical examples demonstrate differences on the order of tens of percent, resulting in substantial deviations in CO_2 emission estimates. These findings show that methodological inconsistency at the individual building level may propagate errors to national scales, particularly when results are aggregated at the city or country level. The aggregation analysis presented in this study indicates that the cumulative effect of methodological differences depends on building stock typology, the distribution of technical characteristics, and the structure of energy supply. The formulation of the "mismatch zone" concept and the proposed pragmatic threshold T provide an operational basis for identifying classes of objects for which the application of simplified methodologies is inappropriate. This establishes a clear criterion for distinguishing cases where a quasi-steady-state approach is sufficient from those requiring hourly dynamic simulations.

Quantitative assessment combined with the conversion of energy results into environmental indicators, confirm that correct interpretation of the impact of methodological choice requires simultaneous consideration of uncertainties in energy demand and variability in emission factors. The proposed analytical framework forms a practical platform for the quantitative justification of decisions and for the verification of national building stock assessments. In light of the results obtained, priority practical actions include: formalising procedures for recalculating results between methodologies to ensure harmonised reporting; developing criteria for methodology selection based on building typology and the mismatch zone concept; and creating representative statistical databases (stratified by building type and technical condition) to calibrate prior parameter distributions for simulations. Further research prospects concern several directions. An initial priority is to extend the analysis to a broader sample of real buildings with diverse climatic and technical characteristics, enabling refinement of mismatch zone topology and the development of regionally adapted methodological application rules. Furthermore, the approaches considered should be integrated with life-cycle assessment and energy system decarbonisation scenarios to link methodological discrepancies with long-term changes in emission factors.

Acknowledgements

None.

Funding

None.

Conflict of Interest

None.

References

[1] Bahaterenko, A.O., *et al.* (2013). Problems and prospects of Ukraine's European integration. *Scientific Bulletin of the Institute of International Relations NAU. Series: Economics, Law, Political Science, Tourism*, 1(1), 1-14.

[2] Carpino, C., Bruno, R., Carpino, V., & Arcuri, N. (2022). Uncertainty and sensitivity analysis to moderate the risks of energy performance contracts in building renovation: A case study on an Italian social housing district. *Journal of Cleaner Production*, 379, article number 134637. doi: 10.1016/j.jclepro.2022.134637.

[3] Chiesa, G., Pizzuti, S., & Zinzi, M. (2025). A new approach to assess the building energy performance gap: Achieving accuracy through field measurements and input data analysis. *Journal of Building Engineering*, 102, article number 111941. doi: 10.1016/j.jobe.2025.111941.

[4] Chupa, V., Adamenko, Y., Boychuk, V., & Kotsyubynska, Y. (2024). Comparative assessment of the content of heavy metals in the ash of solid fuel pellets and different types of sorted and unsorted solid domestic waste. *Ecological Engineering & Environmental Technology*, 25(5), 25-31. doi: 10.12912/27197050/184236.

[5] Dashko, I.M., & Krylov, D.V. (2021). Energy efficiency: Problems of assessment and current state. *Bulletin of Khmelnytskyi National University*, 3, 108-112. doi: 10.31891/2307-5740-2021-294-3-17.

[6] DBN V.2.6-31:2021. (2022). *Thermal insulation and energy efficiency of buildings*. Retrieved from https://online.budstandart.com/ua/catalog/doc-page.html?id_doc=98037.

[7] Deng, Y., Zhou, Y., Wang, H., Xu, C., Wang, W., Zhou, T., Liu, X., Liang, H., & Yu, D. (2023). Simulation-based sensitivity analysis of energy performance applied to an old Beijing residential neighbourhood for retrofit strategy optimisation with climate change prediction. *Energy and Buildings*, 294, article number 113284. doi: 10.1016/j.enbuild.2023.113284.

[8] DSTU 9190:2022. (2022). *Energy performance of buildings: Method for calculating energy use for heating, cooling, ventilation, lighting and domestic hot water*. Retrieved from https://surl.li/vqnbcj.

[9] Farenyuk, H.H., & Farenyuk, Ye.H. (2025). Implementation of the parametric method in modern building energy efficiency standards. *Science and Construction*, 35(1), 3-8. doi: 10.33644/2313-6679-1-2023-1.

[10] Hossin, M.A., Alemzero, D., Wang, R., Kamruzzaman, M.M., & Mhlanga, M.N. (2023). Examining artificial intelligence and energy efficiency in the MENA region: The dual approach of DEA and SFA. *Energy Reports*, 9, 4984-4994. doi: 10.1016/j.egyr.2023.03.113.

[11] ISO 52016-1:2017. (2017). *Energy performance of buildings – energy needs for heating and cooling, internal temperatures and sensible and latent heat loads – part 1: Calculation procedures*. Retrieved from https://www.iso.org/standard/65696.html.

[12] Johari, F., Munkhammar, J., Shadram, F., & Widén, J. (2022). Evaluation of simplified building energy models for urban-scale energy analysis of buildings. *Building and Environment*, 211, article number 108684. doi: 10.1016/j.buildenv.2021.108684.

[13] Kang, E., Lee, H., Yoon, J., Cho, H., Chaichana, C., & Kim, D. (2024). Investigating the influence of uncertainty on office building energy simulation through occupant-centric control and thermal comfort integration. *Energy and Buildings*, 322, article number 114741. doi: 10.1016/j.enbuild.2024.114741.

[14] Komelina, O.V., & Komelina, A.A. (2022). Environmental risks in implementing a sustainable development model: A scientific and practical approach. In *Monitoring of geological processes and ecological condition of the environment: 16th international conference* (pp. 1-5). Bunnik: European Association of Geoscientists & Engineers. doi: 10.3997/2214-4609.2022580268.

[15] Kosova, T.D., & Titarenko, A.D. (2021). Problems of forming integrated sustainable development reporting in the energy sector. In *Development of economy and business administration: Scientific trends and solutions* (pp. 211-212). Kyiv: National Aviation University.

[16] Kryshtof, N.S. (2017). Energy efficiency – an effective mechanism for ensuring energy security and structural modernisation of Ukraine's economy. *Investments: Practice and Experience*, 6, 104-110.

[17] Menegaki, A. (2014). On energy consumption and GDP studies: A meta-analysis of the last two decades. *Renewable and Sustainable Energy Reviews*, 29, 31-36. doi: 10.1016/j.rser.2013.08.081.

[18] Nasouri, M., & Delgarm, N. (2025). A new method for simulation-based sensitivity analysis of building efficiency for optimal building energy planning: A case study of Iran. *Energy, Ecology and Environment*, 10(2), 202-224. doi: 10.1007/s40974-024-00338-4.

[19] Norouziasl, S., Vosoughkhosravi, S., Jafari, A., & Pang, Z. (2024). Assessing the influence of occupancy factors on energy performance in US small office buildings. *Energies*, 17(21), article number 5277. doi: 10.3390/en17215277.

[20] Shlapak, M., *et al.* (2024). *Greenhouse gas emission factor for electricity production and consumption*. Kyiv: NGO "DIXI GROUP".

[21] Shovkalyuk, M.M. (2018). Development of programs to stimulate building energy efficiency improvement in Ukraine. In *Energy management: Status and prospects – PEMS* (pp. 116-117). Kyiv: National Technical University of Ukraine "Igor Sikorsky Kyiv Polytechnic Institute".

[22] Smereka, S.B., & Lifyrenko, S.M. (2025). Peculiarities of regulatory and legal support for energy efficiency. *Visnik of the Volodymyr Dahl East Ukrainian National University*, 289(3), 87-92. doi: 10.33216/1998-7927-2025-289-3-87-92.

[23] Sovacool, B.K., & Griffiths, S. (2020). Culture and low-carbon energy transitions. *Nature Sustainability*, 3(9), 685-693. doi: 10.1038/s41893-020-0519-4.

[24] Vashchyshak, I., Tsykh, V., Chernetska, I., & Dotsenko, Y. (2025). Improving the energy inspection methodology of the underground heating networks. In Y. Zabulonov, I. Peer & M. Zheleznyak (Eds.), *Liquid radioactive waste treatment: Ukrainian context* (pp. 249-259). Cham: Springer. doi: 10.1007/978-3-031-95663-8_25.
[25] Xue, Q., Gu, M., Yang, Y., Bai, P., Wang, Z., Jiang, S., & Duan, P. (2025). Calibration study of uncertainty parameters for nearly-zero energy buildings based on a novel approximate Bayesian approach. *Energy*, 322, article number 135823. doi: 10.1016/j.energy.2025.135823.
[26] Zhang, H., Tian, W., Tan, J., Yin, J., & Fu, X. (2024). Sensitivity analysis of multiple time-scale building energy using Bayesian adaptive spline surfaces. *Applied Energy*, 363, article number 123042. doi: 10.1016/j.apenergy.2024.123042.
[27] Zhu, L., Zhang, J., Gao, Y., Tian, W., Yan, Z., Ye, X., Sun, Y., & Wu, C. (2022). Uncertainty and sensitivity analysis of cooling and heating loads for building energy planning. *Journal of Building Engineering*, 45, article number 103440. doi: 10.1016/j.jobe.2021.103440.

Коротко- та довгострокові екологічні наслідки методологічних розбіжностей у розрахунках енергоефективності будівель

Володимир Чупа
Доктор філософії, доцент
Івано-Франківський національний технічний університет нафти і газу
76019, вул. Карпатська, 15, м. Івано-Франківськ, Україна
https://orcid.org/0000-0001-5658-1877
Ірина Ващишак
К.т.н, доцент
Івано-Франківський національний технічний університет нафти і газу
76019, вул. Карпатська, 15, м. Івано-Франківськ, Україна
https://orcid.org/0000-0002-9078-6726
Сергій Максим'юк
Доктор філософії, доцент кафедри ІВТЕМ
Івано-Франківський національний технічний університет нафти і газу
76019, вул. Карпатська, 15, м. Івано-Франківськ, Україна
https://orcid.org/0000-0002-6312-7047
Кирило Новицький
Відповідальний секретар, провідний інженер
Івано-Франківський національний технічний університет нафти і газу
76019, вул. Карпатська, 15, м. Івано-Франківськ, Україна
https://orcid.org/0009-0001-3383-1973

Анотація. В умовах глобальної декарбонізації точність оцінювання енергоефективності будівель стала критично важливим чинником прогнозування екологічних наслідків та досягнення ключових кліматичних цілей. Наявні розбіжності між національними та міжнародними методологіями розрахунку створюють суттєві ризики під час планування масштабних стратегій термомодернізації. Метою статті було кількісне оцінювання екологічних наслідків методологічних розбіжностей між квазістаціонарним та погодинним динамічним підходами до розрахунку енергоспоживання будівель. Розроблено комплексний підхід, що включає ієрархічне моделювання та детальну методику перетворення показників енергоспоживання в масу викидів вуглецю з ґрунтовним оцінюванням результатів. Встановлено, що основними джерелами методологічних розбіжностей є вибір часової моделі, формат подання кліматичних даних, опис теплової інерції та алгоритм інтерпретації внутрішніх тепловиділень. Доведено, що різниця в річній потребі в енергії при зміні методики розрахунку сягає кількох десятків відсотків. Це еквівалентно відхиленням маси викидів діоксиду вуглецю в межах сотень кілограмів. Для розв'язання цієї проблеми запропоновано концепцію «зони розбіжності», яка вводить порогове значення T для визначення доцільності використання спрощених методик залежно від необхідної точності. Обґрунтовано методику агрегування індивідуальних відхилень до рівня фонду будівель на основі детермінованого порівняння репрезентативних сценаріїв. Запропоновані математичні залежності для кількісного оцінювання підвищують надійність екологічного моніторингу, даючи змогу розробляти більш точні нормативні вимоги та зменшувати вуглецевий слід будівельного сектору

Ключові слова: декарбонізація; термомодернізація; вуглецевий слід; паливно-енергетичні ресурси; нормативно-правова база; динамічне моделювання

Vol. 17, No. 1
2026

Ecological Safety and Balanced Use of Resources

ISSN (print) 2415-3184, ISSN (online) 2522-9508
Journal homepage: https://esbur.com.ua/en

Received: 27.10.2025. Revised: 11.05.2026. Accepted: 12.06.2026. Published: 30.06.2026.

UDC 504.4:551.588.7:004.9

DOI: 10.63341/esbur/1.2026.88

Interactive system for analysis of climatic and ecological processes of urban areas

Vitalii Hrytsuliak
Student
Ivano-Frankivsk National Technical University of Oil and Gas
76019, 15 Karpatska Str., Ivano-Frankivsk, Ukraine
https://orcid.org/0009-0003-9257-2638

Sofia Kachala*
PhD in Technical Sciences, Associate Professor
Ivano-Frankivsk National Technical University of Oil and Gas
76019, 15 Karpatska Str., Ivano-Frankivsk, Ukraine
https://orcid.org/0000-0003-1084-2968

Taras Kachala
PhD in Technical Sciences, Associate Professor
Ivano-Frankivsk National Technical University of Oil and Gas
76019, 15 Karpatska Str., Ivano-Frankivsk, Ukraine
https://orcid.org/0000-0002-2178-6781

Abstract. The relevance of the study is driven by the growing impact of climate change on the functioning of urbanised areas, manifested in rising temperatures, uneven precipitation patterns, increasing frequency of extreme hydrometeorological events, and the formation of urban heat islands. In the context of intensive urbanisation and transformation of the natural environment, the need for a comprehensive analysis of climatic and ecological processes at the local level becomes particularly significant. The aim of the study was to develop an interactive information-analytical system for comprehensive analysis of climatic and ecological processes in urban areas. The research methodology was based on statistical analysis of climatic data, geoinformation analysis, three-dimensional modelling, and software development of an interactive application. As a result of the study, the software application "EcoData" was developed, integrating modules for the analysis of temperature, precipitation, water bodies, green infrastructure, and urban heat islands. Tools for building interactive charts and three-dimensional models were implemented to analyse climatic indicators for the period 1990-2024. A trend of increasing temperature values and the presence of local thermal anomalies in the central part of the city were identified. Years with anomalously high and low precipitation levels were detected. The positive effect of green plantings on reducing the thermal load of the urban environment was demonstrated. The obtained results can be applied in scientific research, educational processes, the development of urban climate strategies, greening programs, and climate change adaptation measures

Keywords: environmental monitoring; temperature regime; urban heat island; 3D modelling; urbanised areas

Introduction

Climate change and urbanisation significantly affect the functioning of urban ecosystems. Rising air temperatures, increasing frequency of extreme weather events, transformation of green zone structures, and changes in water

Suggested Citation: Hrytsuliak, V., Kachala, S., & Kachala, T. (2026). Interactive system for analysis of climatic and ecological processes of urban areas. *Ecological Safety and Balanced Use of Resources*, 17(1),88-100. doi: 10.63341/esbur/1.2026.88.

*Corresponding author (*pernerolik@gmail.com*)

regimes require the application of modern digital tools for environmental monitoring and support of managerial decision-making. Contemporary digital platforms provide access to large volumes of climatic data; however, they are predominantly oriented toward global or regional scales, are complex to use, and do not account for the specific characteristics of individual cities. At the same time, traditional analytical methods fail to provide sufficient clarity and operational efficiency for informed managerial decision-making. In this regard, the development of integrated digital tools that combine the processing of long-term climatic data, spatial analysis, 3D visualisation, and assessment of urban factor impacts within a unified system becomes particularly relevant. Such solutions contribute to improving the effectiveness of environmental monitoring, forecasting climate risks, and shaping sustainable development strategies for urban areas.

In the study by V. Zatserkovnyi *et al.* (2024), the potential of Earth remote sensing for monitoring urban heat islands was analysed. The researchers applied Landsat satellite data and Google Earth Engine tools to assess temperature anomalies in cities, particularly Kyiv and European urbanised areas. The results demonstrated a clear relationship between building density, green space coverage, and the intensity of heat islands. The authors concluded that geoinformation technologies represent an effective tool for assessing the ecological condition of urban areas and forecasting climate risks. G. Rees *et al.* (2024) investigated spatiotemporal changes in surface temperature within urbanised environments. The authors analysed long-term satellite data and established that land use transformation and urban expansion directly contribute to the growth of temperature anomalies.

The study confirmed the importance of integrating remote sensing data and geoinformation systems for urban environment monitoring. L. Lishchenko & O. Kudryashov (2021) analysed the spatiotemporal dynamics of surface temperature in one of the largest industrial cities of Ukraine based on Landsat and Sentinel-2 satellite data. The authors examined the formation of the urban heat island, determined its spatial boundaries, and established the relationship between land use patterns and temperature anomalies. The results confirmed the effectiveness of Earth remote sensing for monitoring urbanised areas and identifying zones of elevated thermal load. In the work of N. Pazynych (2020), the influence of natural landscape complexes on the formation of the temperature regime of the city of Kyiv was investigated. Based on long-term Landsat satellite data, the author established the role of valley complexes in reducing surface temperature and mitigating the manifestations of the urban heat island effect. The findings confirmed the significant importance of natural elements of the urban environment in regulating local microclimate and maintaining the ecological resilience of urbanised areas. J. Hofierka & T. Fedor (2025) developed an approach to three-dimensional modelling of urban climate using digital elevation and building models. The study demonstrated that 3D-GIS modelling enables more detailed assessment of the spatial distribution of temperature and the effectiveness of urban climate adaptation measures.

The analysis of scientific sources indicates significant advances in methods of environmental monitoring, Earth remote sensing, geoinformation analysis, and urban heat island modelling. This confirms the feasibility of developing a localised digital tool for territorial communities that integrates long-term climatic analysis, 3D modelling, heat island assessment, water body analysis, and the evaluation of green infrastructure impact within a unified interactive system (Vasylieva *et al.*, 2024; Hramchuk, 2025; Voronkova *et al.*, 2025). The majority of existing studies focus on individual aspects of environmental analysis, particularly temperature changes, satellite monitoring, or geoinformation mapping. Insufficient attention has been given to the development of unified interactive software systems that would combine automated acquisition of climatic data, their processing, statistical analysis, three-dimensional modelling, and clear visualisation of results within a single software environment. The aim of the present study was to develop a software application for the collection of climatic data, their processing, construction of informative charts, analysis of changes over time, and identification of long-term trends in temperature regime and precipitation patterns – including determination of the direction and intensity of climate change, detection of anomalously warm or cold periods, drought-affected and excessively humid years, as well as assessment of the influence of the urbanised environment on the formation of local climatic characteristics.

Materials and Methods

The study employed a combination of general scientific and specialised research methods. Statistical analysis was applied to examine the long-term dynamics of air temperature and atmospheric precipitation. The identification of climatic trends and patterns of indicator changes over time was carried out using the time series method. Elements of geoinformation analysis were used to assess the spatial distribution of temperature anomalies and to investigate urban heat islands. Visualisation of the temperature field, water bodies, and thermal anomalies was performed using three-dimensional modelling methods. The assessment of the influence of green infrastructure on the temperature regime of the urban environment was conducted through comparative analysis. For the development of the "EcoData" software application, software engineering methods were applied, encompassing software architecture design, integration of functional modules, user interface development, and system performance testing.

Within the scope of this study, the "EcoData" software application was developed, enabling the collection, processing, and interactive analysis of historical atmospheric precipitation data. A key element of the system is an interactive precipitation chart featuring zooming functionality, display of precise values, and analysis of peak and

anomalous periods (Meteostat, n.d.; IQAir, 2026). The user interface of the application is presented in the Ukrainian language, which is determined by its orientation toward local use within the framework of research on climatic and ecological indicators of the urban environment. The "EcoData" application is implemented in the Python programming language following a modular architecture. The system structure includes modules for loading climatic data, their processing and statistical analysis, two-dimensional and three-dimensional visualisation, as well as a graphical user interface. For the implementation of individual functions, the following libraries were utilised: Pandas and NumPy for data processing and analysis, Matplotlib and mpl_toolkits.mplot3d for chart construction and three-dimensional modelling, FuncAnimation for the creation of animated visualisations, mplcursors for interactive engagement with charts, and Meteostat (n.d.) for retrieving historical climatic data via API.

The primary source of information was open climatic data from the Meteostat platform (n.d.) for the territory of the city of Ivano-Frankivsk covering the period 1990-2024, including indicators of mean, maximum, and minimum air temperature, atmospheric precipitation amounts, and relative humidity. Following data import, missing values were removed, time series were constructed, data were aggregated by month and year, and the dataset was prepared for subsequent modelling and visualisation. The study was conducted in stages and encompassed analysis of the subject domain, formulation of software requirements, connection of data sources, data collection and cleaning, construction of mathematical models, development of visualisation tools, and interpretation of the obtained results. To evaluate the performance of the software application, functional testing was carried out, during which the accuracy of climatic data loading and processing, the operation of interactive interface elements, and the generation of charts and three-dimensional models were verified. Thus, the development of a digital tool for comprehensive analysis of climatic indicators is aimed at improving the effectiveness of environmental monitoring, forming scientifically grounded managerial decisions, and ensuring the sustainable development of the urban environment (Pernerovska, 2014; Arkhypova & Pernerovska, 2015; Hutnyk & Kachala, 2025).

Results and Discussion

The "EcoData" software application is constructed as an integrated multifunctional system that combines several interrelated analytical modules within a unified interface. The program structure incorporates a climatic data loading module, which ensures the import and preparation of information for subsequent analysis; a temperature analysis module for examining seasonal and long-term dynamics of temperature indicators; and an atmospheric precipitation analysis module, which enables assessment of annual and seasonal changes in precipitation amounts and identification of anomalous periods. The system also includes a 3D temperature model module, which displays long-term temperature dynamics in three-dimensional space, as well as a dedicated annual 3D temperature model module, providing the capability for detailed analysis of daily temperature fluctuations for a specific year. Spatial analysis is further complemented by a water bodies map, which displays the hydrographic structure of the city and allows examination of its influence on microclimatic conditions. An important component is the 3D heat map module, aimed at detecting and visualising urban heat islands formed under the influence of dense urban development and reduction of green space coverage. A dedicated urban greening analysis module was also implemented, enabling assessment of the role of green plantings in regulating the temperature regime and shaping a favourable urban environment. All the aforementioned modules are integrated into a unified software shell with an interactive research period management system, allowing the user to independently select the temporal boundaries of analysis within a defined range. This structure ensures a comprehensive approach to the study of climatic processes within the city and enables both temporal and spatial analysis of ecological indicators. The identification of anomalously rainy or drought-affected years is essential for forecasting climate risks, planning climate change adaptation measures, and shaping sustainable development strategies for communities. Thus, the development of a software application for the collection, processing, and interactive visualisation of atmospheric precipitation data represents a timely and scientifically grounded step that contributes to improving the effectiveness of environmental monitoring, enhancing the urban environment management system, and ensuring the ecological security of the territory (Fig. 1). A key element of the system is the interactive charts, which enable analysis of the annual dynamics of indicator changes, mean monthly values, peak periods, and other ranges. Drought periods, excessive moisture periods, and long-term trends can be tracked and analysed. Interactive features include hover tooltips displaying the precise date and precipitation values in mm, chart zooming, and navigation along the timeline (Fig. 2). The urban heat island module implements spatial analysis of thermal load distribution within the city of Ivano-Frankivsk and displays the results in the form of a three-dimensional heat map (Fig. 3). The constructed model demonstrates the variation of the temperature field depending on geographical coordinates (longitude and latitude), while the Z-axis reflects the temperature increment (ΔT, °C) relative to a conditional background value. This approach enables quantitative assessment of the intensity of local thermal overheating of areas and determination of the spatial structure of the urban heat island. Within the model, the main districts of the city were identified, namely the Center, Pasichna, Naberezhna, BAM, and Kaskad. The highest temperature increment values are observed in the central part of the city, indicating heat concentration in the zone of dense urban development, high traffic load, and a significant proportion of artificial surfaces that accumulate and slowly release heat. In districts with a greater share of green plantings and lower building density, a gradual decrease in temperature indicators is observed.

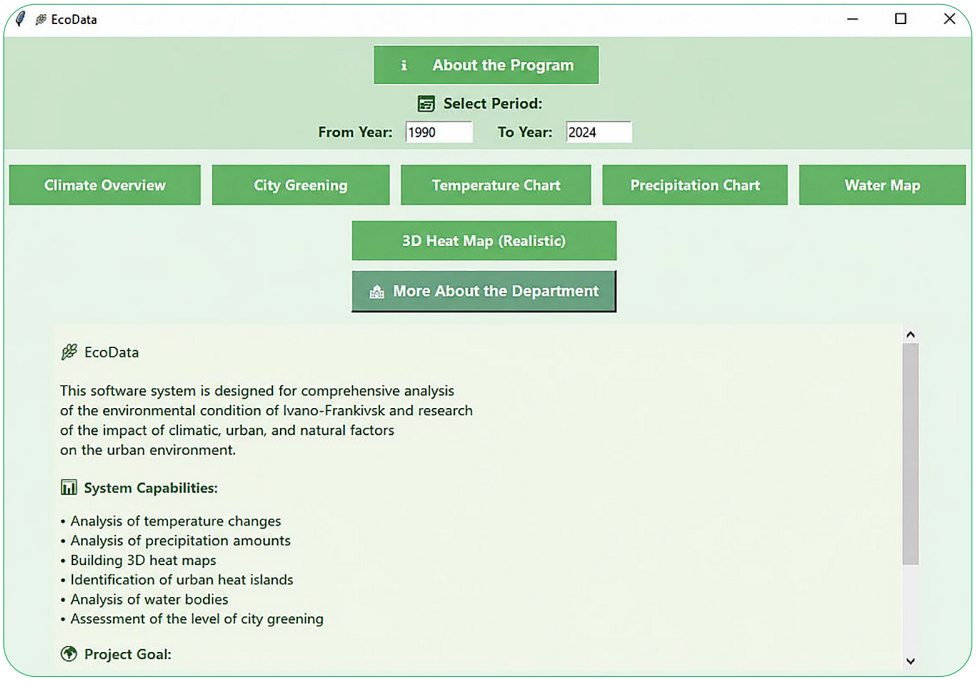

Figure 1. Main screen of the "EcoData" application

Note: the figure presents the main window of the developed EcoData software, designed for analysing the ecological condition of the city of Ivano-Frankivsk and assessing the influence of climatic, urban, and natural factors on the urban environment. The interface includes fields for selecting the research period, specifically the start and end year, as well as functional buttons for loading climatic data, analysing urban green infrastructure, constructing temperature and precipitation charts, generating a water bodies map, and producing a 3D heat map. The lower section of the window provides a brief description of the system's capabilities, explaining its core analytical functions

Source: compiled by the authors based on the results of the "EcoData" application

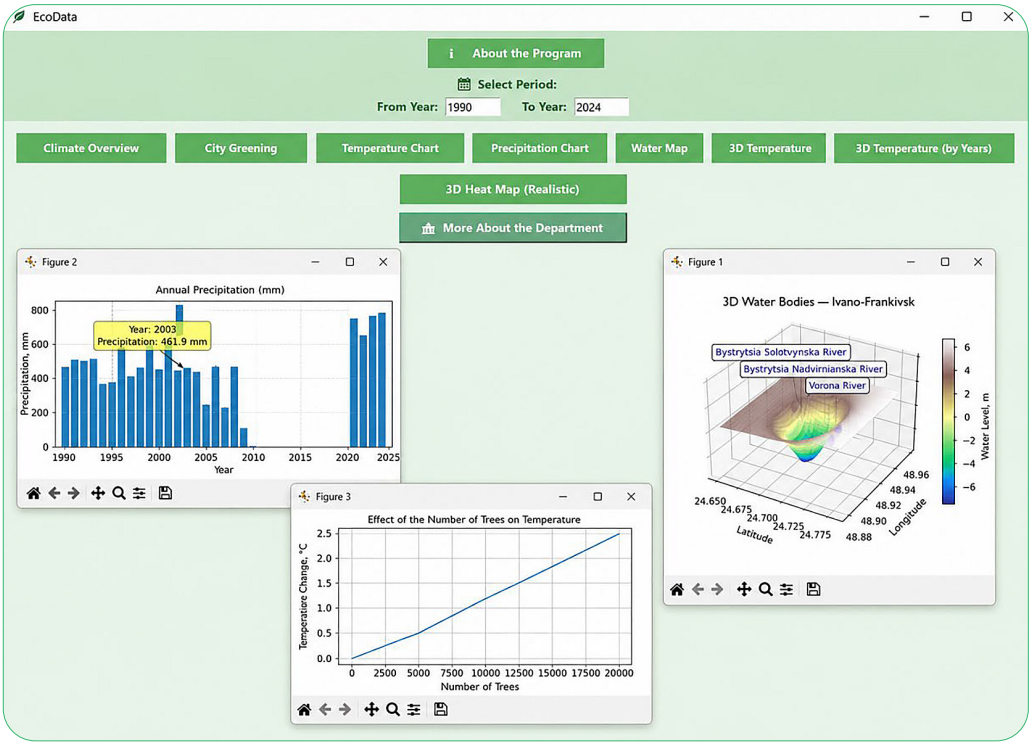

Figure 2. Example of graphical data display in the application

Source: compiled by the authors based on the results of the "EcoData" application

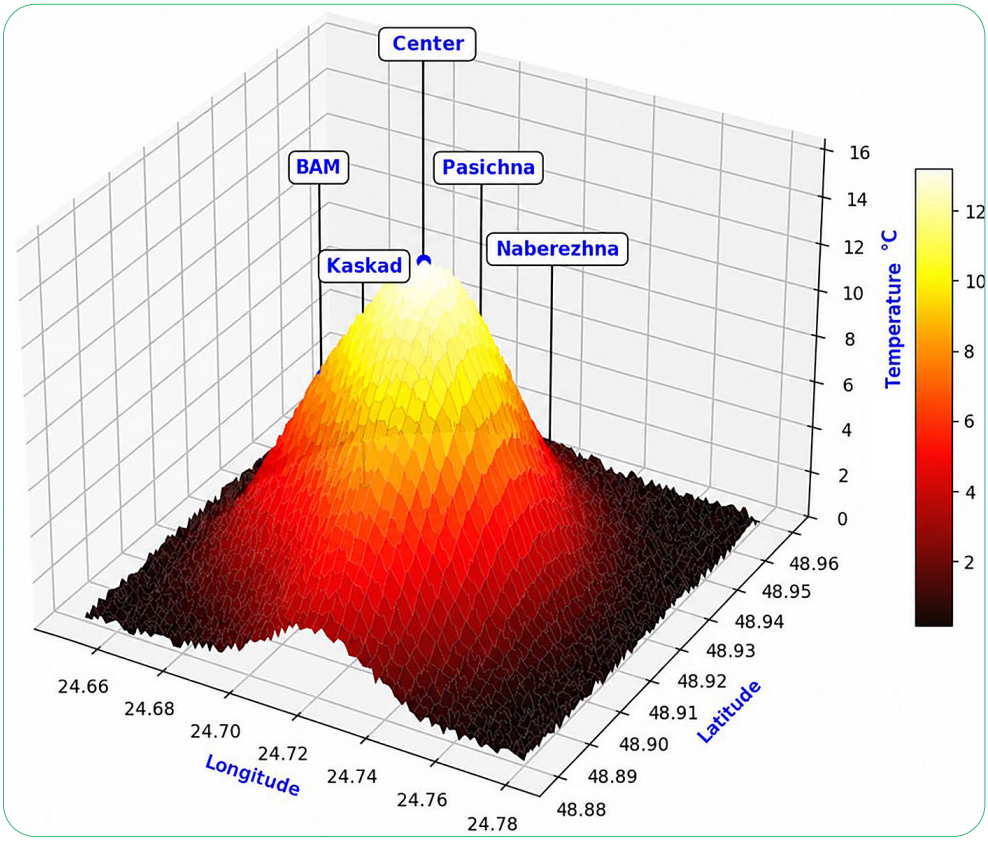

Figure 3. 3D heat islands of the city of Ivano-Frankivsk
Source: compiled by the authors based on the results of the "EcoData" application

The three-dimensional thermal model demonstrates the influence of urban factors on the formation of local temperature anomalies and confirms the manifestation of the urban heat island effect. The visualisation enables tracing of the temperature gradient from the central part to the periphery of the city, which is a characteristic feature of urbanised areas. Thus, the model provides the capability to comprehensively assess the interrelationship between building density, green infrastructure coverage, and the temperature regime. The practical significance of the module lies in the potential application of the obtained results for planning measures to expand green zones, optimise urban development policy, and form climate-adapted infrastructure. The 3D heat map data can be applied in the development of programs aimed at reducing thermal load, improving the energy efficiency of urban development, and enhancing the quality of the urban environment in accordance with the principles of sustainable development.

The "3D Water Bodies – Ivano-Frankivsk" module is designed for spatial analysis of the hydrographic structure of the city and its influence on the formation of the local microclimate (Fig. 4). Within this module, a three-dimensional terrain model was constructed incorporating the locations of the main water bodies, namely the Bystrytsya Solotvynska, Bystrytsya Nadvirnyanska, and Vorona rivers. The model displays spatial coordinates (longitude and latitude) along the horizontal axes, while the Z-axis characterises elevation or depth, enabling assessment of the terrain features and hydrological structure of the territory. The central part of the model demonstrates a surface depression corresponding to the river channel and floodplain areas. The colour scale enhances the visualisation: darker and cooler shades correspond to deeper areas, while lighter shades represent higher elevations. The three-dimensional visualisation enables tracing of the interrelationship between terrain, water body locations, and potential water accumulation zones. This is particularly important for assessing flood risk, analysing the hydrological regime, and forecasting possible changes under the influence of intensive precipitation. The presence of water bodies also affects the formation of the local microclimate, in particular contributing to temperature reduction in adjacent districts during the warm season through evaporation and air mass circulation. The practical significance of the module lies in the potential application of its results for planning water resource management measures, flood prevention, optimisation of development in coastal zones, and formation of ecologically balanced urban infrastructure. The model can be integrated with precipitation and temperature data for comprehensive analysis of the interaction between climatic and hydrological processes within the urbanised territory.

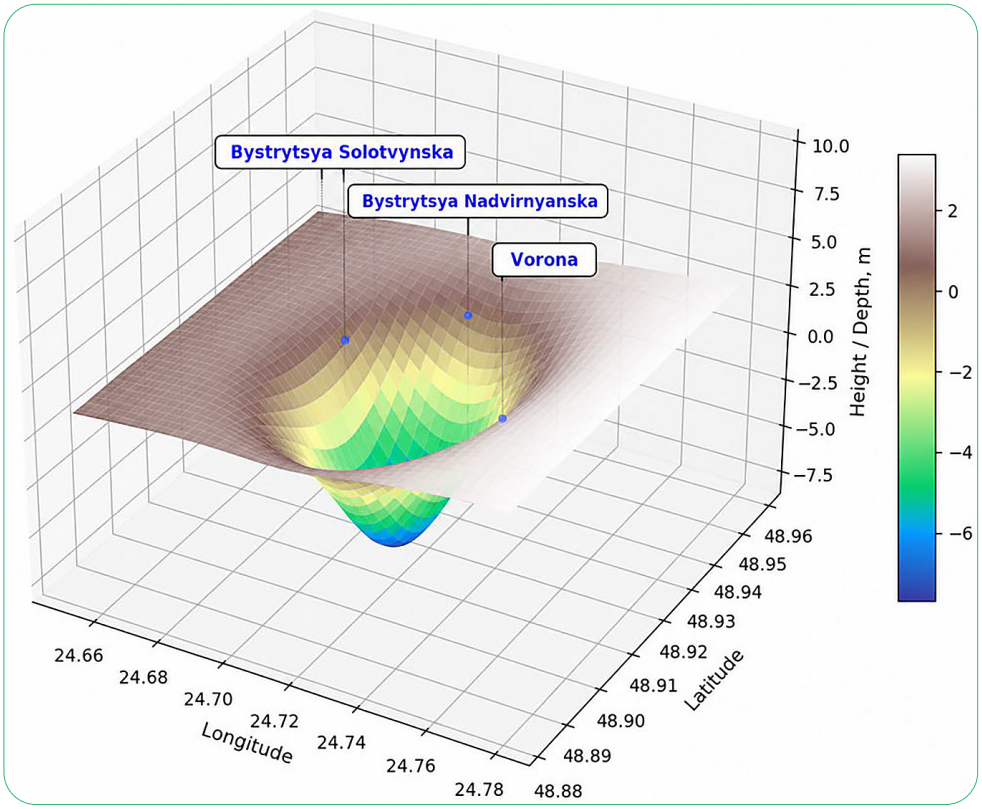

Figure 4. 3D Water Bodies – city of Ivano-Frankivsk
Source: compiled by the authors based on the results of the "EcoData" application

The module for assessing the influence of green infrastructure on the urban temperature regime demonstrates the relationship between changes in air temperature and the number of planted trees. Within this module, a chart was constructed in which the X-axis displays the number of trees and the Y-axis represents the change in air temperature (°C) (Fig. 5). The linear relationship presented in the chart shows a gradual temperature decrease with an increasing number of green plantings. The model illustrates that even a moderate increase in tree count leads to a noticeable reduction in thermal load. With an expansion of the green stock to 20,000 trees, a conditional temperature decrease of approximately 2-2.5°C is observed, which represents a significant indicator for an urbanised environment. This effect is explained by the processes of transpiration, surface shading, reduction of heat accumulation by artificial materials, and improvement of air circulation.

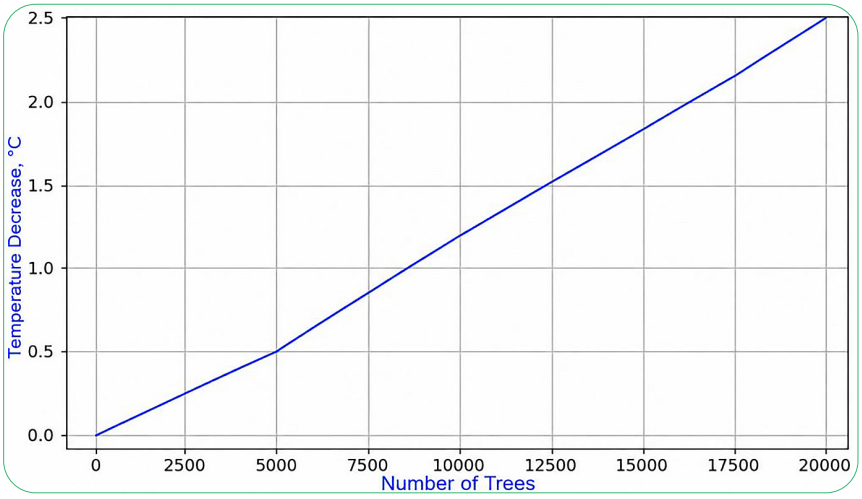

Figure 5. Influence of green infrastructure on the urban temperature regime
Source: compiled by the authors based on the results of the "EcoData" application

The chart enables assessment of the potential ecological effect of implementing mass greening programs and serves as an important tool for strategic urban development planning. Through this model, it is possible to forecast the degree to which the intensity of the heat island effect will diminish with an increase in green space coverage. The practical significance of the module lies in the potential application of the obtained results in the formulation of ecological restoration programs, development of "green city" concepts, improvement of residential comfort for the population, and adaptation of the urban environment to climate change. It can also serve as a justification for investment in the development of green plantings as one of the most effective and nature-based approaches to reducing thermal load.

The daily temperature analysis module displays the dynamics of temperature regime changes in Ivano-Frankivsk for the period 1990-2024 in the form of a continuous time series chart (Fig. 6). The horizontal axis represents the calendar scale (dates), while the vertical axis displays air temperature values in degrees Celsius. This format enables tracing not only the overall long-term trend but also detailed temperature fluctuations within each individual year. The chart clearly demonstrates the cyclical nature of temperature changes, corresponding to seasonal processes: regular peaks during the summer period and temperature decreases in winter. The recurrence of the wave-like structure indicates the stability of the seasonal rhythm, while individual deviations are also evident – sharp temperature decreases or increases that may be associated with anomalous weather events. Analysis of the long-term data array enables assessment of the frequency of extremely low temperatures during the winter period and high temperatures during the summer season. In certain years, significant temperature amplitudes are observed, which may indicate an increase in climatic variability. A gradual shift of temperature maxima toward higher values in more recent years can also be traced, which is consistent with the global warming trend. The practical significance of this module lies in the capability to identify extreme temperature periods, analyse the duration of warm and cold seasons, assess the thermal load on urban infrastructure and the population. The obtained results can be applied for forecasting climate risks, planning energy consumption, developing climate change adaptation measures, and enhancing the resilience of the urban environment to temperature extremes.

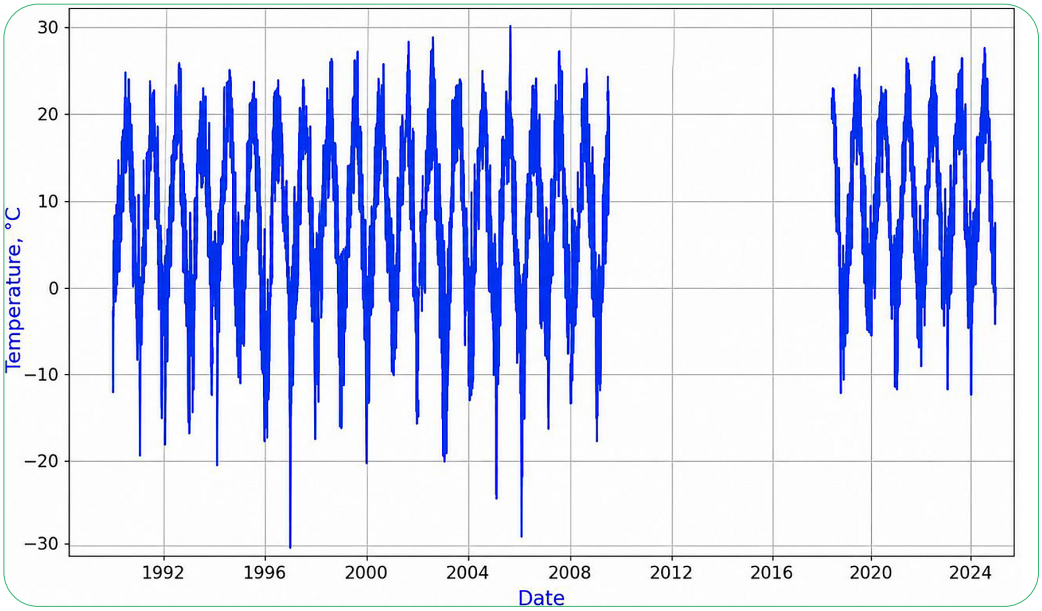

Figure 6. Analysis of daily temperature in the city of Ivano-Frankivsk for the period 1990-2024
Source: compiled by the authors based on the results of the "EcoData" application

The precipitation analysis module is one of the key components of the software system and is aimed at investigating the long-term dynamics of atmospheric precipitation within Ivano-Frankivsk (Fig. 7). Within this module, the system automatically generates a bar chart of annual precipitation totals in millimetres, covering the study period from 1990 to 2024. The visualisation enables clear tracing of changes in annual precipitation sums, assessment of their inter-annual variability, and identification of years with maximum and minimum values. The chart displays peak values that may indicate anomalously rainy years, as well as periods of reduced precipitation characterised as anomalously dry. This approach makes it possible to identify the long-term trend of changes in territorial moisture levels and assess whether a tendency toward increase or decrease in annual precipitation totals is observed in the context of climate change.

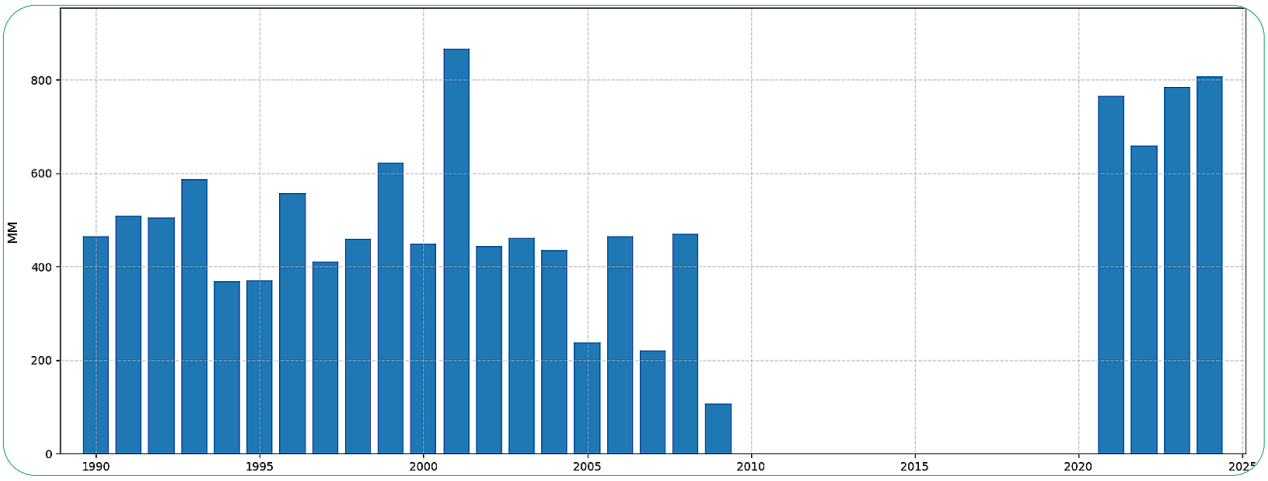

Figure 7. Annual precipitation totals – city of Ivano-Frankivsk
Source: compiled by the authors based on the results of the "EcoData" application

The analytical capabilities of the module enable comparison of any years with one another, identification of periods of elevated flood risk resulting from excessive precipitation, as well as assessment of moisture deficit periods that may negatively affect green plantings and the city's water resources. In addition, the system provides detection of climatic anomalies that are significant for ecological planning and the development of climate change adaptation measures. An important advantage of the module is its interactivity. The user has the capability to obtain precise precipitation values in millimetres through hover tooltips, zoom the chart for detailed analysis of individual periods, navigate along the timeline, and drill down into specific years. This format of data presentation enhances the usability of the system and makes the analysis process more intuitive and effective.

The module presented in Figure 8 provides comprehensive spatiotemporal analysis of the temperature regime of the city of Ivano-Frankivsk over an extended observation period (1990-2024). Within this module, a three-dimensional surface was constructed in which the X-axis represents the day of the year (from 1 to 365), the Y-axis represents the observation year, and the Z-axis displays air temperature values in degrees Celsius. This format enables simultaneous assessment of both seasonal dynamics and long-term changes in temperature indicators. The model surface demonstrates a characteristic wave-like form corresponding to the cyclical nature of seasonal processes: temperature increase during the spring-summer period and its decrease during the autumn-winter season. Through the use of a colour scale ranging from blue to red shades, temperature contrasts are clearly visualised: blue tones correspond to negative values during winter months, while red tones represent maximum summer temperatures.

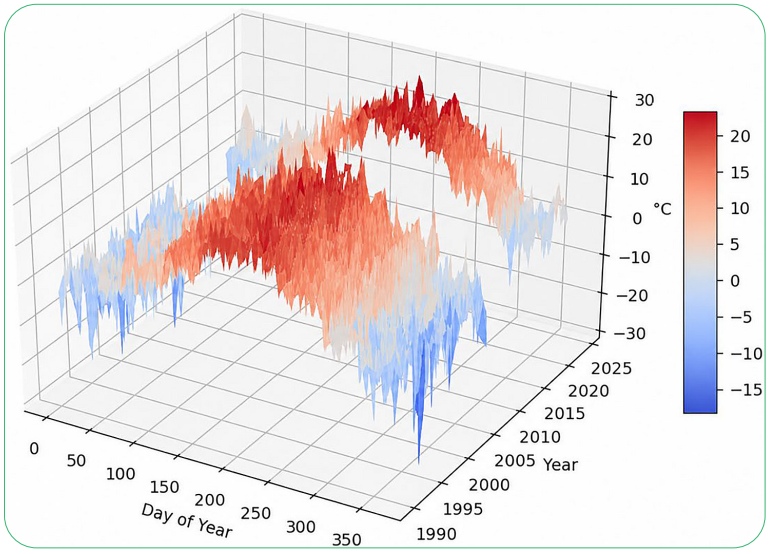

Figure 8. 3D temperature – Ivano-Frankivsk
Source: compiled by the authors based on the results of the "EcoData" application

Analysis of the model enables tracing of long-term temperature change trends, in particular the gradual increase in mean annual values in more recent observation years. Periods of extreme temperatures can also be identified – both anomalously cold winters and exceptionally hot summers. The three-dimensional visualisation assists in detecting changes in the duration of warm and cold periods, which serves as an important indicator of climatic transformations. The practical significance of the module lies in the potential application of the obtained results for assessing the impact of temperature changes on urban infrastructure, energy consumption, the condition of green plantings, and residential comfort of the population. The model represents an effective tool for scientific analysis of climatic trends and the formulation of urban adaptation measures in response to global warming conditions.

The "3D Temperature by Year" module (Fig. 9) is designed for detailed analysis of the temperature regime of an individual year with the capability of spatiotemporal visualisation. Within this tool, a three-dimensional model is generated in which the X-axis represents the day of the year (from 1 to 365), the Y-axis corresponds to the selected study year, and the Z-axis displays air temperature values in degrees Celsius. This approach enables representation of daily temperature dynamics within a specific year and tracing of the character of seasonal fluctuations. Using 1992 as an example, a gradual temperature increase from winter negative values to summer maxima is clearly visible, followed by a characteristic temperature decrease during the autumn-winter period. The colour scale ranging from blue to red shades enhances the clarity of analysis: cold periods are represented by blue tones, while warm periods are depicted in orange-red hues. This enables rapid visual identification of temperature peak periods, cold waves, or atypical seasonal deviations.

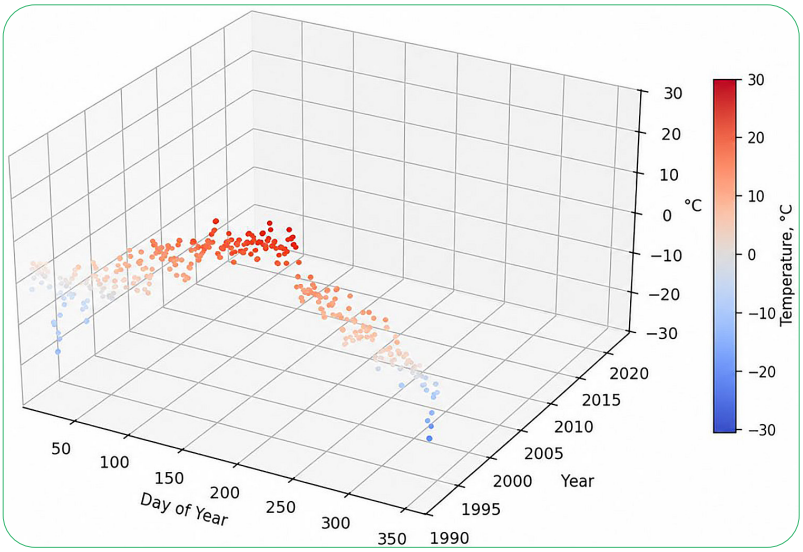

Figure 9. Temperature by years – 1992-2025

Source: compiled by the authors based on the results of the "EcoData" application

This form of data presentation makes it possible to identify anomalously warm or cold periods, analyse the duration of seasons, assess the intensity of summer maxima and winter minima, and compare the characteristics of the temperature regime across different years. The model serves as an important tool for investigating long-term climatic trends and confirming the manifestations of global warming at the local level. From a practical standpoint, the module can be utilised for climate risk analysis, assessment of thermal load on the urban environment, investigation of the impact of temperature extremes on public health, and planning of climate change adaptation measures. Three-dimensional visualisation significantly enhances the informativeness of the analysis and renders the results comprehensible to both researchers and representatives of local government authorities.

The results obtained through the three-dimensional temperature field analysis module confirm the presence of a pronounced urban heat island effect in the central part of Ivano-Frankivsk. Similar patterns were established in the study by D. Lauwaet *et al.* (2024), who demonstrated through high-resolution modelling across one hundred European cities that the greatest intensity of heat islands is characteristic of areas with high building density and a significant proportion of artificial surfaces. Similar conclusions were also presented in the work of M. Possega *et al.* (2022), which proved the intensification of thermal load in urbanised districts during extreme temperature events. The results obtained in the present study regarding the positive influence of green infrastructure on the urban temperature regime are consistent with the findings of T. Iungman *et al.* (2023), who established that increasing green space coverage represents one of the most effective nature-based approaches to reducing thermal load and improving the quality of the urban environment. Studies

by C. Andrade *et al.* (2023) and N. Krupa (2025) also confirmed that the development of green infrastructure is one of the key instruments for adapting cities to climate change. Furthermore, contemporary research indicates that even a modest increase in green space coverage can provide a noticeable cooling effect in central urban districts.

The precipitation analysis and long-term temperature dynamics modules constructed in the present study confirmed the growth of climatic variability and the increasing frequency of extreme weather events. Similar trends were described in the work of C. Reis *et al.* (2022), where, based on large climatic datasets from the Copernicus service (n.d.), a substantial intensification of temperature anomalies in cities of Southern Europe was established. The study by K. Koutroumanou-Kontosi *et al.* (2022) also demonstrated the necessity of combining regional and local climate modelling for identifying the characteristics of urban microclimate formation and forecasting future climate risks.

Of particular interest are the results of applying three-dimensional visualisation within the "EcoData" system. A similar approach was described in the works of G. Lobaccaro *et al.* (2021) and S. Dimitrov *et al.* (2024), who emphasised that the application of GIS technologies, unmanned remote sensing systems, and three-dimensional modelling significantly enhances the analytical capabilities for examining the spatial structure of thermal anomalies and improves the informativeness of environmental monitoring. The results of these studies confirmed the feasibility of the approach implemented in the present work, which combines temporal and spatial analysis within a unified software environment.

The results of the analysis of spatiotemporal variability of the urban temperature regime are consistent with contemporary approaches to urban climate modelling. In particular, K. Koutroumanou-Kontosi *et al.* (2022) emphasised the necessity of combining regional and local climate models for accurate representation of the characteristics of the urban thermal environment. The methodology of integrating multi-scale climatic simulations proposed by the authors confirms the feasibility of employing long-term climatic data in combination with local spatial analysis within the developed "EcoData" application, as precisely this approach enables the identification of local temperature anomalies and assessment of potential risks for the urban environment.

The importance of applying high-resolution climatic data is confirmed by the study of G. Frustaci *et al.* (2022), in which a high-resolution air temperature dataset was created for the city of Milan. The authors demonstrated that the use of detailed spatial temperature data substantially improves the capabilities for identifying urban heat islands and analysing intra-urban temperature heterogeneity. A similar approach is implemented in the three-dimensional visualisation module of the "EcoData" application, which provides clear representation of the spatial distribution of temperature indicators and enables identification of areas with elevated thermal load. The obtained results regarding the influence of temperature anomalies on the urban environment are also consistent with the conclusions of D. Hidalgo-García & H. Rezapouraghdam (2023), who investigated the spatial variability of heat stress in the city of Seville using the UrbClim climate model and proposed measures for its mitigation. The authors demonstrated that the most effective adaptation measures include expansion of green space coverage, reduction of the proportion of artificial surfaces, and implementation of continuous temperature regime monitoring tools. This confirms the practical significance of the developed software application, which can be utilised as a decision-support tool for planning urban environment adaptation measures in response to climate change and minimising the negative consequences of urban heat islands.

Thus, the results of the study confirm global trends in the development of digital environmental monitoring systems and demonstrate the effectiveness of integrating long-term climatic data, spatial analysis, and three-dimensional visualisation for investigating climatic and ecological processes in urban areas. The developed "EcoData" application can be regarded as a promising decision-support tool in the field of urban environment management, planning of climate change adaptation measures, and implementation of sustainable urban development strategies. The conducted study confirmed that contemporary approaches to urban climate analysis are increasingly oriented toward the integration of long-term climatic data, geoinformation analysis, three-dimensional modelling, and interactive visualisation tools. Comparison of the obtained results with current international research indicates that the trends identified for Ivano-Frankivsk are consistent with pan-European processes of temperature increase, intensification of climatic variability, and formation of urban heat islands. In contrast to the majority of existing studies, which predominantly focus on individual aspects of urban environment monitoring, the developed "EcoData" software application provides a comprehensive combination of temperature regime analysis, atmospheric precipitation, water bodies, green infrastructure, and spatial thermal anomalies within a unified interactive software environment. This allows the proposed system to be regarded as a promising instrument for supporting managerial decision-making aimed at enhancing the climatic resilience of cities and implementing the principles of sustainable development of urbanised territories.

Conclusions

As a result of the conducted work, the "EcoData" software application was developed – an interactive information-analytical system designed for investigating climatic, ecological, and urban-ecological processes at the local level, particularly for the city of Ivano-Frankivsk. The system ensures the integration of long-term meteorological data, their analytical processing, and multi-level visualisation in the form of charts and three-dimensional models. The software tool combined the processing of climatic data (temperature and precipitation), analysis of ecological factors (territorial

green infrastructure), spatial modelling of natural objects (water resources), and 2D and 3D visualisation of results.

Analysis of long-term climatic data for the city of Ivano-Frankivsk over the period 1990-2024 confirmed a trend toward increasing mean annual temperatures, growing frequency of extremely warm periods, and anomalous precipitation years, which is consistent with general regional and global climate change patterns. The atmospheric precipitation analysis module enabled identification of years with anomalously high and low precipitation amounts, indicating an increase in climatic variability. The three-dimensional urban heat island modelling module revealed the concentration of elevated temperatures in areas of dense urban development and transport hubs, while territories with a high proportion of green plantings are characterised by lower temperature values, confirming the role of green infrastructure in reducing thermal load. The water bodies analysis module demonstrated the positive influence of the urban lake and river network on the formation of the local microclimate. The obtained results indicate the feasibility of comprehensive consideration of climatic, hydrological, and urban-ecological factors in the development of sustainable urban development strategies. Prospects for further research lie in expanding the functionality of the system through integration of satellite data, application of artificial intelligence-based forecasting algorithms, and development of a web-oriented version of the platform for broader application in sustainable urban development management practice.

Acknowledgements

None.

Funding

None.

Conflict of Interest

None.

References

[1] Andrade, C., Fonseca, A., & Santos, J.A. (2023). Climate change trends for the urban heat island intensities in two major Portuguese cities. *Sustainability*, 15(5), article number 3970. doi: 10.3390/su15053970.

[2] Arkhypova, L.M., & Pernerovska, S.V. (2015). Forecasting hydrological parameters of water bodies using singular spectrum analysis. *Scientific Bulletin of National Mining University*, 2, 45-50.

[3] Copernicus. (n.d.). Retrieved from https://cds.climate.copernicus.eu.

[4] Dimitrov, S., Iliev, M., Nedkov, S., & Borisova, B. (2024). A methodological framework for high-resolution surface urban heat island mapping: Integration of UAS remote sensing, GIS, and the local climate zone concept for surface urban heat island assessment. *Remote Sensing*, 16(21), article number 4007. doi: 10.3390/rs16214007.

[5] Frustaci, G., Onorati, G., Malatesta, L., & Bisignano, A. (2022). High-resolution gridded air temperature data for the urban environment: The Milan data set. *Forecasting*, 4(1), 238-261. doi: 10.3390/forecast4010014.

[6] Hidalgo-García, D., & Rezapouraghdam, H. (2023). Variability of heat stress using the UrbClim climate model in the city of Seville: Mitigation proposal. *Environmental Monitoring and Assessment*, 195, article number 1164. doi: 10.1007/s10661-023-11768-8.

[7] Hofierka, J., & Fedor, T. (2025). Modelling and visualisation of heat stress in urban areas using high-resolution geospatial data. *Abstracts of the ICA*, 10, article number 107. doi: 10.5194/ica-abs-10-107-2025.

[8] Hramchuk, M. (2025). Integrated "Smart City" model as a factor of digitalization and eco-balanced development: A socio-philosophical analysis. *Humanities Studies*, 23(100), 35-45. doi: 10.32782/hst-2025-23-100-04.

[9] Hutnyk, V., & Kachala, S.V. (2025). Biodiversity conservation under climate change: Challenges and prospects for Ukraine. In *Proceedings of the regional conference "Youth ecoforum – 2025"* (pp. 25-26). Ivano-Frankivsk: Ivano-Frankivsk National Technical University of Oil and Gas.

[10] IQAir. (2026). Retrieved from https://www.iqair.com.

[11] Iungman, T., *et al.* (2023). Cooling cities through urban green infrastructure: A health impact assessment of European cities. *The Lancet*, 401(10376), 577-589. doi: 10.1016/S0140-6736(22)02585-5.

[12] Koutroumanou-Kontosi, K., Cartalis, C., & Santamouris, M. (2022). A methodology for bridging the gap between regional- and city-scale climate simulations for the urban thermal environment. *Climate*, 10(7), article number 106. doi: 10.3390/cli10070106.

[13] Krupa, N. (2025). Integrated models of urban ecosystems: A systems approach to sustainable development planning. In *Current problems, ways and prospects of development of landscape architecture, horticulture, urban ecology and phytomelioration* (pp. 152-154). Bila Tserkva: Bila Tserkva National Agrarian University. doi: 10.33245/25-09-2025.

[14] Lauwaet, D., Berckmans, J., Hooyberghs, H., Wouters, H., Driesen, G., Lefebre, F., & De Ridder, K. (2024). High resolution modelling of the urban heat island of 100 European cities. *Urban Climate*, 54, article number 101850. doi: 10.1016/j.uclim.2024.101850.

[15] Lishchenko, L., & Kudryashov, O. (2021). The results of the study of spatio-temporal changes in surface temperatures of Zaporizhzhia based on satellite data. *Ukrainian Journal of Remote Sensing*, 8(3), 27-36. doi: 10.36023/ujrs.2021.8.3.198.

[16] Lobaccaro, G., Acero, J.A., Martín-García, D., Kennedy, C., & Galatioto, A. (2021). Applications of models and tools for mesoscale and microscale thermal analysis in mid-latitude climate regions: A review. *Sustainability*, 13(22), article number 12385. doi: 10.3390/su132212385.
[17] Meteostat. (n.d.). Retrieved from https://meteostat.net.
[18] Pazynych, N. (2020). Valley complexes as ecosystem assets of heat island of urban agglomerations (on the example of the right-bank part of Kyiv). *Ukrainian Journal of Remote Sensing*, 26, 38-47. doi: 10.36023/ujrs.2020.26.181.
[19] Pernerovska, S.V. (2014). Determination of the degree of hydroecological risk as the main parameter of sustainable development of a hydroecosystem. *Ecological Safety and Balanced Use of Resources*, 5(3), 23-28.
[20] Possega, M., Baklanov, A., Lhotka, O., Plavcová, E., & Belda, M. (2022). Observational evidence of intensified nocturnal urban heat island during heatwaves in European cities. *Environmental Research Letters*, 17(12), article number 124013. doi: 10.1088/1748-9326/aca3ba.
[21] Rees, G., Hebryn-Baidy, L., & Belenok, V. (2024). Temporal variations in land surface temperature within an urban ecosystem: A comprehensive assessment of land use and land cover change in Kharkiv, Ukraine. *Remote Sensing*, 16(9), article number 1637. doi: 10.3390/rs16091637.
[22] Reis, C., Lopes, A., & Nouri, A.S. (2022). Assessing urban heat island effects through local weather types in Lisbon's metropolitan area using big data from the Copernicus service. *Urban Climate*, 43, article number 101168. doi: 10.1016/j.uclim.2022.101168.
[23] Vasylieva, N., Vasylieva, O., Prylipko, S., & Shevchenko, N. (2024). Public management of recreational nature use on the principles of sustainable inclusive development under urbanization conditions. *Scientific Bulletin: Public Administration*, 2(16), 90-100. doi: 10.33269/2618-0065-2024-2(16)-90-100.
[24] Voronkova, V.H., Nikitenko, V.O., & Metelenko, N.H. (2025). "Green" digital transformation as a driver of sustainable regional development in post-war recovery. *Educational Discourse: Collection of Scientific Papers*, 52(1-2), 22-30. doi: 10.33930/ed.2019.5007.52(1-2)-4.
[25] Zatserkovnyi, V., De Donatis, M., Plichko, L., Sakhniuk, S., Odarchuk, N., & Mironchuk, T. (2024). Using remote sensing technologies for monitoring urban heat islands. *Bulletin of Taras Shevchenko National University of Kyiv: Geography*, 3(106), 99-106. doi: 10.17721/1728-2713.106.13.

Інтерактивна система для аналізу кліматичних та екологічних процесів міських територій

Віталій Грицуляк
Студент
Івано-Франківський національний технічний університет нафти і газу
76019, вул. Карпатська, 15, м. Івано-Франківськ, Україна
https://orcid.org/0009-0003-9257-2638
Софія Качала
Кандидат технічних наук, доцент
Івано-Франківський національний технічний університет нафти і газу
76019, вул. Карпатська, 15, м. Івано-Франківськ, Україна
https://orcid.org/0000-0003-1084-2968
Тарас Качала
Кандидат технічних наук, доцент
Івано-Франківський національний технічний університет нафти і газу
76019, вул. Карпатська, 15, м. Івано-Франківськ, Україна
https://orcid.org/0000-0002-2178-6781

Анотація. Актуальність дослідження зумовлена зростаючим впливом кліматичних змін на функціонування урбанізованих територій, що проявляється у підвищенні температури, нерівномірності атмосферних опадів, збільшенні частоти екстремальних гідрометеорологічних явищ та формуванні міських теплових островів. В умовах інтенсивної урбанізації та трансформації природного середовища особливої значущості набуває необхідність комплексного аналізу кліматичних і екологічних процесів на локальному рівні. Метою дослідження була розробка інтерактивної інформаційно-аналітичної системи для комплексного аналізу кліматичних та екологічних процесів міських територій. Методологія дослідження ґрунтувалася на використанні методів статистичного аналізу кліматичних даних, геоінформаційного аналізу, тривимірного моделювання та програмної розробки інтерактивного застосунку. У результаті дослідження розроблено програмний застосунок «EcoData», який інтегрує модулі аналізу температури, атмосферних опадів, водних об'єктів, озеленення та міських теплових островів. Реалізовано інструменти побудови інтерактивних графіків і тривимірних моделей для аналізу кліматичних показників за період 1990-2024 рр. Встановлено тенденцію до підвищення температурних показників та наявність локальних теплових аномалій у центральній частині міста. Виявлено роки з аномально високою та низькою кількістю опадів. Показано позитивний вплив зелених насаджень на зниження температурного навантаження міського середовища. Отримані результати можуть бути використані у наукових дослідженнях, освітньому процесі, при розробці міських кліматичних стратегій, програм озеленення та заходів адаптації до змін клімату

Ключові слова: екологічний моніторинг; температурний режим; тепловий острів; 3D-моделювання; урбанізовані території

Vol. 17, No. 1
2026

Ecological Safety and Balanced Use of Resources

ISSN (print) 2415-3184, ISSN (online) 2522-9508
Journal homepage: https://esbur.com.ua/en

Received: 03.02.2026. Revised: 01.05.2026. Accepted: 12.06.2026. Published: 30.06.2026.

UDC 504.06:614.7:711.4

DOI: 10.63341/esbur/1.2026.101

Ambient air quality assessment in the Kremenchuk Territorial Community based on the environmental risk concept

Tetiana Ryhas*
PhD in Technical Sciences, Associate Professor
Mykhailo Ostrohradsky Kremenchuk National University
39600, 20 University Str., Kremenchuk, Ukraine
https://orcid.org/0000-0001-9297-2787

Volodymyr Shmandii
Doctor of Technical Sciences, Professor
Mykhailo Ostrohradsky Kremenchuk National University
39600, 20 University Str., Kremenchuk, Ukraine
https://orcid.org/0000-0002-8811-4824

Abstract. Under conditions of urban transformation and increasing anthropogenic pressure, the assessment of ambient air quality and associated environmental risks is becoming increasingly important. A significant role in the formation of environmental hazards is played by short-term peaks in pollutant concentrations, which are often not taken into account by conventional monitoring methods. The aim of this study was to substantiate an approach to the operational assessment of environmental hazard states of ambient air at the territorial community level, taking into account natural and anthropogenic factors. The study employed methods of logical analysis of scientific research findings, system analysis of factors influencing air quality formation, elements of mathematical modelling of pollutant dispersion processes, and a risk-oriented approach to assessing the impact of pollution on the population. The concept of natural-anthropogenic fluctuations in ambient air quality within a territorial community was substantiated, taking into account natural factors, emergency and war-related events, and anthropogenic hazard sources. An Increased Environmental Risk Index (IER) was introduced as an analytical indicator for assessing the short-term effects of air pollution on public health. An integrated model for environmental assessment was proposed, combining mathematical modelling (Gaussian, jet, and energy models) with instrumental measurements. Regularities in the formation of local zones of ingredient and acoustic pollution under conditions of intensive use of individual power generators were identified. The proposed approach makes it possible to promptly identify periods of increased risk and assess the spatial heterogeneity of environmental hazards. The obtained results may be used by local authorities to improve ambient air monitoring systems, develop measures for managing anthropogenic pressure, and implement early warning mechanisms for informing the population about increased levels of environmental hazard

Keywords: ambient air quality; environmental risk; anthropogenic pressure; natural-anthropogenic fluctuations; mathematical modelling

Introduction

Under conditions of increasing anthropogenic pressure, ensuring adequate ambient air quality has become an important area of environmental safety management. The impact of emergency and war-induced factors leads to the emergence of new types of environmental hazards. This necessitates the assessment of ambient air quality within territorial

Suggested Citation: Ryhas, T., & Shmandii, V. (2026). Ambient air quality assessment in the Kremenchuk Territorial Community based on the environmental risk concept. *Ecological Safety and Balanced Use of Resources*, 17(1), 101-114. doi: 10.63341/esbur/1.2026.101.

*Corresponding author (*office@kdu.edu.ua*)

communities based on the concept of a health-oriented environment, which is interpreted by T.Ye. Ryhas (2026) as a dynamic socio-ecological-economic system capable of adapting to external challenges, including climate change, anthropogenic threats, and crisis situations, by enhancing environmental safety, increasing the resilience of urban ecosystems, and improving the quality of life of the population. In this context, environmental safety serves not only as a prerequisite for environmental protection but also as a fundamental basis for health-oriented urban development.

Contemporary studies focus not only on annual average concentrations of air pollutants but also on short-term pollution episodes, which may cause significant adverse health effects. B. Hoffmann *et al.* (2021) analysed current scientific evidence regarding the impact of air pollution on human health, which formed the basis for updating the World Health Organization air quality guidelines. The study demonstrated that adverse health effects associated with fine particulate matter ($PM_{2.5}$), nitrogen dioxide, and other air pollutants may occur even at concentrations previously considered relatively safe. The authors emphasised the need to revise existing approaches to ambient air quality management in light of current knowledge regarding risks to public health.

S. Khomenko *et al.* (2021) assessed the impact of air pollution on premature mortality in nearly one thousand European cities. The analysis revealed that a substantial proportion of premature deaths could be prevented if the recommended air quality levels were achieved. The authors also identified significant intercity differences in environmental risk levels, highlighting the need to develop localised air quality management strategies. In a subsequent study, S. Khomenko *et al.* (2023) analysed the spatial and sector-specific contributions of various emission sources to ambient air pollution and associated mortality in European cities. Using a health impact assessment approach, the authors evaluated the contribution of individual economic sectors to particulate matter pollution and related health risks. The results demonstrated that the structure of emission sources varies considerably among cities, while the effectiveness of environmental protection measures largely depends on the appropriate identification of priority emission sources.

Particular attention has recently been paid to the concept of short-term exposure, which focuses on assessing the health effects associated with short-term episodes of elevated pollutant concentrations. Unlike traditional approaches based mainly on annual average pollutant concentrations, contemporary studies indicate that short-term pollution peaks play a significant role in environmental risk formation and the occurrence of acute adverse health outcomes. Thus, W. Yu *et al.* (2024) performed a global assessment of mortality associated specifically with short-term exposure to air pollution. Based on data analysis from more than 13,000 cities worldwide, the authors estimated that short-term exposure to fine particulate matter is associated with approximately one million premature deaths annually, accounting for nearly 2% of total global mortality. These findings confirmed that short-term pollution episodes make a substantial contribution to the global burden of disease and should therefore be considered in environmental risk assessment.

Y. Ma *et al.* (2024) analysed the relationship between short-term changes in particulate matter and NO_2 concentrations and mortality based on nearly nine million death records from four countries. Using advanced causal modeming methods, the authors identified a statistically significant association between increased pollutant concentrations and higher all-cause mortality. The findings emphasised the importance of considering short-term variations in ambient air quality when assessing environmental risks. C. Demoury *et al.* (2024) investigated the effects of short-term exposure to $PM_{2.5}$, PM_{10}, NO_2, O_3, and black carbon on natural mortality in Belgium. The study demonstrated a significant association between increased pollutant concentrations and the risk of death from natural causes. Particular attention was paid to the identification of vulnerable population groups for whom short-term pollution episodes pose an increased health risk.

Therefore, the findings of contemporary studies convincingly demonstrate that short-term peaks in pollutant concentrations represent an important factor in the formation of public health risks. However, most existing approaches focus primarily on the epidemiological and statistical assessment of the consequences of short-term exposure, whereas the integration of short-term pollution indicators, meteorological conditions, local emission sources, and the natural self-purification capacity of a territory into a unified environmental risk assessment framework remains insufficiently explored. This necessitates the development of risk-oriented approaches to ensuring adequate ambient air quality at the territorial community level.

The aim of this study was to apply the environmental risk concept to the operational assessment of ambient air quality in the Kremenchuk Territorial Community (KTC) under the influence of natural and anthropogenic factors contributing to environmental hazards. To achieve this aim, the following objectives were addressed: to analyse the factors affecting ambient air quality formation in an urbanised area; to assess the influence of short-term pollution peaks on the level of environmental risk to the population; and to substantiate approaches to ambient air quality management, taking into account anthropogenic pressure and the bioregulatory potential of the territory.

Materials and Methods

The KTC, characterised by a specific structure of environmental hazards, was selected as the study area. The urban environment should be considered as a complex urban geosystem in which natural conditions, features of spatial organisation, and anthropogenic pressures determine the course of ecological processes (Serohin & Kostrikov, 2024). The uniqueness of the environmental situation in the KTC is determined by the combination of natural conditions,

transformation of natural landscapes during urbanisation, and the presence of numerous anthropogenic facilities. The interaction of these factors forms a complex system of environmental risks manifested in changes in ambient air quality, soils, surface and groundwater quality, as well as in the formation of noise pollution within the community. The combination of valley relief, the extensive water surface of the Kremenchuk Reservoir, and temperature inversions creates air stagnation zones where pollutants accumulate. Thus, the natural environment of the territory is not only affected by anthropogenic impacts but also actively contributes to their manifestation. These conditions determine the occurrence of natural-anthropogenic fluctuations in ambient air quality.

The study employed methods of analysis and synthesis of scientific findings, system analysis of factors influencing air quality formation, elements of mathematical modelling of pollutant dispersion processes, and a risk-oriented approach to assessing the impact of pollution on the population. Current approaches to assessing the impact of air pollution on public health are based on the concept of short-term exposure. Quantitative methods for assessing health risks associated with ambient air pollution rely on the use of Relative Risk (RR) and Population Attributable Fraction (PAF) indicators, as well as AirQ and AirQ+ software tools recommended by the World Health Organization (Amini *et al*., 2024). Quantitative assessment of such impacts at the territorial community level was performed using the Relative Risk (RR) indicator of adverse health outcomes, which is widely applied in epidemiological studies investigating the effects of ambient air pollution on public health (Khomenko *et al*., 2021):

$$RR = e^{\beta \Delta C}, \tag{1}$$

where β is the population sensitivity coefficient to changes in pollutant concentration (for $PM_{2.5}$, approximately 0.0008-0.0012 per 1 μg/m³); ΔC is the increase in pollutant concentration relative to the background level, μg/m³.

To assess the proportion of health risk attributable to ambient air pollution, the Population Attributable Fraction (PAF) indicator was used:

$$PAF = \frac{RR-1}{RR}. \tag{2}$$

The reduction in the increase of pollutant concentrations in the near-surface atmospheric layer under the influence of natural purification mechanisms can be described by the following generalised relationship:

$$\Delta C_{adj} = \Delta C - \frac{M_{dep}}{V_{mix}}, \tag{3}$$

where ΔC_{adj} is the adjusted increase in pollutant concentration taking into account natural deposition processes; M_{dep} is the mass of pollutant particles deposited by vegetation (kg); V_{mix} is the volume of air within the atmospheric mixing layer (m³).

For the operational assessment of environmental hazard levels in the near-surface atmospheric layer under conditions of short-term fluctuations in pollutant concentrations, the Increased Environmental Risk Index (IER) was applied:

$$IER = \frac{\Delta C \cdot F_{met} \cdot F_{src}}{B_{reg}}, \tag{4}$$

where F_{met} is an indicator characterising the atmospheric dispersion capacity and accounting for meteorological conditions (wind speed, the occurrence of temperature inversions, and the height of the atmospheric mixing layer); F_{src} is an indicator of anthropogenic pressure intensity reflecting the cumulative impact of major emission sources (transport, stationary sources, autonomous diesel generators, emergency and war-induced emissions); B_{reg} is an indicator of the bioregulatory potential of the territory characterising the ability of green infrastructure to reduce pollutant concentrations in the near-surface atmospheric layer (the main contributing factors include the area of green spaces, leaf surface area, and the capacity of vegetation to deposit fine particulate matter).

The structure of the index is based on the principles of risk-oriented assessment, according to which the level of environmental risk increases with increasing pollutant concentrations, unfavourable meteorological conditions, and the intensity of local emission sources. At the same time, the presence of green spaces and other natural ecosystem elements contributes to the self-purification of ambient air and reduces the level of risk, which is accounted for through the indicator of the territory's bioregulatory potential. The proposed approach makes it possible to consider the specific features of urbanised areas, where local short-term pollution peaks frequently occur and are not always reflected by conventional air quality indices.

The processes of sound wave propagation in ambient air were described using a fragment of the integrated model of ecological safety and sustainable development of a health-oriented urban territorial community developed by the authors (Ryhas, 2026):

$$\frac{\partial^2 P}{\partial t^2} - c^2 \nabla^2 P = 0, \tag{5}$$

where P is the sound pressure (acoustic load); c is the speed of sound in air; and ∇^2 is the Laplace operator.

This equation describes the propagation of acoustic waves in an elastic medium. Its solutions take the form of wave functions characterising the propagation of sound energy in space. However, for practical engineering calculations, a simplified energy-based model is used, which accounts for the attenuation of sound intensity with distance:

$$\frac{dP}{dr} = -\frac{2I}{r} - \alpha I. \tag{6}$$

The solution of this equation is given by:

$$P(r) = P_0 \cdot \frac{1}{r^2} \cdot e^{-\alpha r}. \tag{7}$$

This equation was used to calculate noise pollution levels. The integrated pollution index was determined as the average value of the relative concentrations of the investigated pollutants with respect to their maximum permissible concentrations. This approach makes it possible to comprehensively assess the state of ambient air within the study area and determine the level of anthropogenic pressure. To describe the processes of transport, dispersion, and transformation of pollutants in ambient air, a corresponding fragment of the mathematical model within the concept of environmentally safe functioning of a health-oriented territorial community was employed (Ryhas, 2026):

$$\frac{\partial c}{\partial t} + u\frac{\partial c}{\partial x} + v\frac{\partial c}{\partial y} + w\frac{\partial c}{\partial z} = \frac{\partial}{\partial x}\left(k_x\frac{\partial c}{\partial x}\right) + \\ + \frac{\partial}{\partial y}\left(k_y\frac{\partial c}{\partial y}\right) + \frac{\partial}{\partial z}\left(k_z\frac{\partial c}{\partial z}\right) + S - R, \quad (8)$$

where C denotes the pollutant concentration; u, v, and w represent the components of air flow velocity; K_x, K_y, and K_z are the turbulent diffusion coefficients in the x, y, and z directions, respectively; S is the emission source strength; R represents the rate of chemical transformations and pollutant deposition. One of the most commonly used approaches for solving Equation (8) is the Gaussian plume model, widely applied in atmospheric pollution studies (Johnson, 2022):

$$C(x,y,z) = \frac{S}{2\pi u\sigma_y(x)\sigma_z(x)}\exp\left(-\frac{y^2}{2\sigma_y^2(x)}\right)\exp\left(-\frac{(z-H)^2}{2\sigma_z^2(x)}\right), \quad (9)$$

where the main parameters are the emission rate, wind speed, and dispersion coefficients characterising turbulent air mixing.

Maximum pollutant concentrations are observed along the plume centerline (at $y = 0$) and near the effective source height ($z \approx$ H). As the distance from the source (x) increases, the plume expands, resulting in a decrease in pollutant concentrations. Physically, this model describes the formation of a so-called "plume" – an elongated cloud of pollutants transported by wind and gradually expanding in both horizontal and vertical directions (Khomenko *et al*., 2023).

The following assumptions were adopted when applying the Gaussian plume model: emissions are continuous and stationary over time; wind speed and direction remain constant during the calculation period; atmospheric conditions are homogeneous within the study area; turbulent mixing of pollutants is described by the dispersion coefficients σy and σz; and chemical transformations of pollutants during transport are neglected. The Gaussian model was applied to assess pollutant dispersion at distances greater than 10 m from the emission source.

Despite its widespread applicability, the Gaussian model has several limitations when applied to low-height emission sources, such as power generators. First, the model assumes that pollutants are instantaneously distributed according to a Gaussian profile immediately after release. In real conditions, a generator produces a directed exhaust jet characterised by its own velocity, temperature, and flow structure. Second, the Gaussian model is generally valid at distances ranging from tens to hundreds of meters, whereas the impact zone of generators is typically limited to 1-10 m. Third, the model does not account for the influence of local obstacles (buildings, fences, and trees), which substantially affect turbulence characteristics in the near-surface atmospheric layer.

Thus, the application of the Gaussian model for describing pollutant dispersion from autonomous power generators in the near-field zone is limited. This is because, in the immediate vicinity of the source (within several meters), turbulent mixing processes between the exhaust jet and the surrounding air dominate and are not adequately represented by the classical Gaussian approach. To adequately describe processes occurring in the immediate vicinity of the emission source, the use of a jet model is considered appropriate. In this case, emissions are treated as a turbulent jet that gradually expands due to mixing with the surrounding air (Johnson, 2022). In a simplified form, the solution of Equation (8) can be expressed as:

$$C(x) = \frac{S}{u \cdot A(x)}, \quad (10)$$

where $A(x)$ is the cross-sectional area of the expanding jet.

Typically, $A(x) \sim (\alpha x)^2$; therefore:

$$C(x) \sim \frac{S}{u \cdot x^2}. \quad (11)$$

Unlike traditional approaches, this study proposes the combined use of Gaussian, jet, and energy-based models for assessing natural-anthropogenic fluctuations in ambient air quality. The authors' approach is based on the differentiated application of these models depending on the spatial scale of the process: the jet model is used to describe pollutant dispersion in the near-field zone (up to 10 m) from autonomous power generation sources; the Gaussian model is applied to assess pollutant dispersion at greater distances; and the energy-based model is employed to evaluate acoustic load. In addition, the modelling results are integrated with the Increased Environmental Risk Index (IER), which accounts for meteorological conditions, the intensity of local emission sources, and the bioregulatory potential of the territory. Such an approach makes it possible to consider the specific features of short-term pollution peak formation under the conditions of the KTC.

Instrumental studies within the KTC were carried out in several urban areas characterised by intensive use of electric generators. The study objects included gasoline and diesel generators with a capacity of 2-5 kW, which are most widely used as backup power sources in the residential sector. Ambient air sampling and noise level measurements were performed at distances of 1, 5, 10, and 15 m from an operating generator, taking into account the prevailing wind direction. Monitoring points were located at

a height of 1.5 m above ground level, corresponding to the average height of the human breathing zone. Concentrations of carbon monoxide (CO), nitrogen dioxide (NO_2), sulfur dioxide (SO_2), and fine particulate matter were determined in ambient air. Each measurement cycle lasted 20 min. Measurements were recorded every 2 min, resulting in 10 consecutive readings at each monitoring point. Average values of pollutant concentrations and noise levels were subsequently used for analysis.

Measurements were conducted in the absence of atmospheric precipitation and at wind speeds ranging from 0.5 to 2.0 m/s. The obtained experimental data were used to verify mathematical models of pollutant dispersion and to assess environmental risk. Particular attention was paid to areas characterised by a high concentration of commercial infrastructure facilities, including retail stores, catering establishments, and other service sector enterprises, where generators were used as backup power sources (Fig. 1).

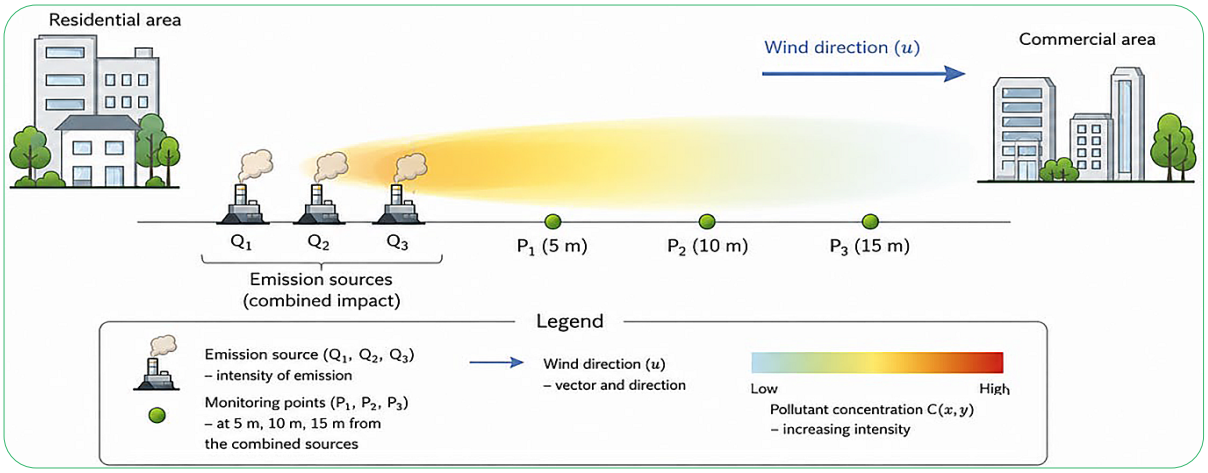

Figure 1. Schematic representation of the spatial arrangement of emission sources and monitoring points with consideration of pollutant dispersion in the near-surface atmosphere

Source: created by the authors

The assessment of acoustic load was carried out at the same monitoring points where pollutant concentration measurements were performed. Noise level measurements were conducted at different distances from the generators, taking into account the spatial arrangement of noise sources and the direction of sound wave propagation. The main parameter determined during the study was the equivalent continuous A-weighted sound pressure level (LAeq, dBA).

Results and Discussion

Contemporary fluctuations in ambient air quality are formed not only under the influence of traditional emission sources (industry, heat and power facilities, and transport) but also as a result of the widespread use of electric generators at critical infrastructure facilities, commercial establishments, healthcare institutions, and in the residential sector due to regular damage to energy infrastructure, as well as emergency- and war-induced fires and the destruction of fuel and energy facilities. A generalised model describing the interaction between natural and anthropogenic factors and emergency events that determine short-term fluctuations in pollutant concentrations in the near-surface atmospheric layer was proposed (Fig. 2).

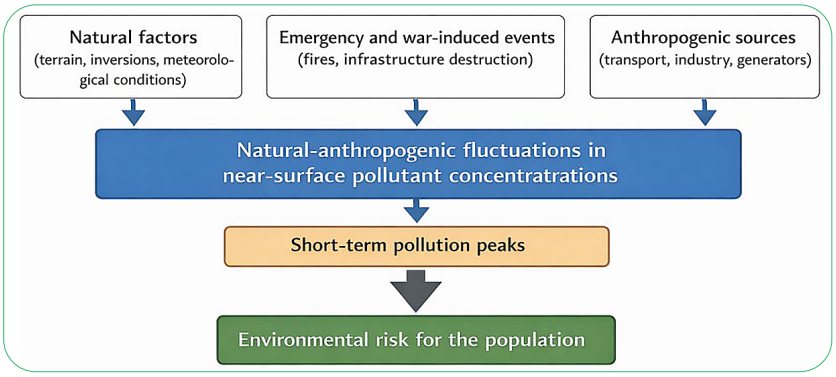

Figure 2. Conceptual scheme of the formation of natural-anthropogenic fluctuations in ambient air quality within a territorial community

Source: created by the authors

An assessment of the Relative Risk (RR) was carried out for the conditions of the KTC. For a short-term increase in $PM_{2.5}$ concentration by 20 μg/m³ relative to the background level and assuming $\beta = 0.001$, Equation (1) yields $RR \approx 1.02$. Thus, the relative risk of adverse health effects may increase by approximately 2% during periods of peak ambient air pollution. For the KTC, with $RR = 1.02$, Equation (2) gives $PAF \approx 0.0196 \approx 1.96\%$, indicating that approximately 2% of adverse health outcomes in the population may be associated with short-term peaks in ambient air pollution. Since the RR value is determined by the concentration increment (ΔC), a key objective of environmental safety management is to reduce the amplitude of peak pollutant concentrations.

One of the natural mechanisms for reducing ΔC is the deposition of pollutants by urban vegetation. Assessment of the bioregulatory potential of vegetation showed that green spaces within the KTC annually remove hundreds of tons of fine particulate matter from the atmosphere. In addition, based on the area characteristics of green spaces and the average biological productivity of vegetation, the integrated bioregulatory potential of urban vegetation was determined. The calculations demonstrated that the annual oxygen production amounts to approximately 130 thousand tonnes per year. This value was used as an integral indicator of the biological activity of vegetation and its potential capacity for phytoremediation of ambient air and does not characterise changes in atmospheric oxygen concentrations. According to J. Liao & H.Y. Kim (2024), urban green spaces contribute to pollutant deposition, regulation of microclimatic conditions, and enhancement of the environmental resilience of urbanised areas. Similar conclusions were reported by P. Kumar *et al.* (2024), who considered green infrastructure as one of the key natural mechanisms for reducing anthropogenic pressure on ambient air quality.

Thus, the presence and spatial distribution of green spaces can significantly affect the concentration regime of ambient air. Through the processes of dry deposition of aerosol particles and the absorption of gaseous pollutants by vegetation, green infrastructure functions as a natural regulator of both the gaseous composition of ambient air and the amplitude of short-term fluctuations in pollutant concentrations, thereby directly influencing the level of environmental risk for the population. Analysis of the spatial distribution of emission sources and green spaces within the KTC revealed pronounced spatial asymmetry. The northern industrial district is characterised by a high concentration of pollution sources and insufficient greening, which enhances concentration increments (ΔC) and, consequently, increases RR values. In contrast, central urban areas with well-developed green infrastructure exhibit lower amplitudes of concentration fluctuations. Therefore, environmental risk within the territorial community is spatially differentiated and depends on the interplay among the following factors: the intensity of anthropogenic emissions, meteorological conditions affecting pollutant dispersion, and the bioregulatory potential of the territory.

Quantitative assessment of RR makes it possible to move from a descriptive analysis of ambient air quality to environmental risk modelling and the development of an early warning system. It should be noted that the actual level of environmental hazard is determined not only by pollutant concentrations but also by the combined influence of natural and anthropogenic factors affecting the formation of short-term pollution peaks. These factors include, in particular, meteorological conditions, the intensity of anthropogenic emissions, the spatial distribution of pollution sources, and the natural self-purification capacity of the environment. The need for an integrated consideration of such factors as ambient air quality, noise exposure, the availability of sufficient green infrastructure, and other characteristics of the urban environment in assessing the condition of territorial communities is confirmed by recent studies on the impact of urban environments on public health (Arriazu-Ramos *et al.*, 2025). For the operational assessment of environmental hazard levels in the near-surface atmospheric layer under conditions of short-term concentration fluctuations, it is advisable to use an integral indicator that summarises the influence of the main natural and anthropogenic risk factors, namely the Increased Environmental Risk Index (IER) (Equation 4).

Existing air quality assessment indices, particularly the Air Quality Index (AQI), are widely used to inform the public about current levels of ambient air pollution. Analysis of contemporary approaches to calculating such indices indicates that they are primarily based on pollutant concentrations and are used for the operational assessment of ambient air quality and the potential health impacts of pollution (Shihab, 2023). However, conventional indices only partially reflect environmental risk under conditions of short-term natural-anthropogenic fluctuations, since they do not account for meteorological dispersion conditions, the intensity of local emission sources, or the natural self-purification capacity of the environment. As demonstrated by recent studies on short-term exposure (Yu *et al.*, 2024; Demoury *et al.*, 2024), the combination of short-term pollutant concentration peaks and unfavourable accumulation conditions may substantially increase health risks.

In this regard, the proposed Increased Environmental Risk Index (IER) should not be considered an alternative to traditional air quality indices but rather as a complementary tool. Unlike AQI, the IER is aimed at assessing the potential environmental risk associated with hazardous short-term pollution episodes and takes into account not only changes in pollutant concentrations but also the conditions governing their accumulation and dispersion in ambient air, the intensity of local emission sources, and the bioregulatory potential of the territory. This approach makes it possible to use the IER for analysing scenarios of environmental change and forecasting periods of elevated environmental hazard at the territorial community level.

As follows from Equation (4), the IER value increases with increasing pollutant concentration increments,

deterioration of meteorological dispersion conditions, and increasing anthropogenic pressure, whereas it decreases with increasing bioregulatory potential of the territory. For the practical application of the IER and the operational assessment of changes in environmental hazard levels under short-term fluctuations in ambient air quality, a tentative risk scale was proposed (Table 1). The boundaries of the proposed categories were determined based on the analysis of typical scenarios characteristic of the KTC, including background conditions, calm weather episodes, temperature inversions, widespread use of autonomous generators, and accidental emissions during fires at fuel and energy facilities.

Table 1. Tentative scale of environmental risk levels under conditions of short-term fluctuations in ambient air quality

IER Value	Environmental Risk Level
IER < 15	Background
15 ≤ IER < 30	Elevated
30 ≤ IER < 60	High
IER ≥ 60	Critical

Note: the proposed scale is tentative and intended for the comparative assessment of environmental risk levels under different ambient air quality scenarios. The threshold values between risk categories were established based on expert analysis of IER calculation results and may be refined during further validation of the methodology in other territorial communities

Source: developed by the authors

Thus, the IER is determined by pollutant concentrations in the near-surface atmospheric layer, meteorological conditions affecting their dispersion, the intensity of anthropogenic pressure, and the bioregulatory potential of the territory. Therefore, it can be considered an integral indicator characterising the cumulative influence of natural and anthropogenic factors on the formation of short-term peaks in ambient air pollution. Analysis of ambient air quality data and meteorological conditions during temperature inversion episodes revealed a short-term increase in PM_{10} concentrations of approximately 20 μg/m³ above the background level (ΔC = 20 μg/m³). Under unfavourable meteorological conditions (low wind speed and temperature inversion), the meteorological coefficient was assumed to be $F_{met} \approx 2$. During periods of intensive use of electric generators and increased traffic load, the anthropogenic pressure coefficient was estimated as $F_{src} \approx 1.5$. The bioregulatory potential of the territory, determined by the presence of green infrastructure, was estimated by the coefficient $B_{reg} \approx 1.2$. According to Equation (4), the calculated value of the Increased Environmental Risk Index was IER ≈ 50. This value indicates a high level of short-term environmental risk resulting from the combined effects of unfavourable meteorological conditions and significant anthropogenic pressure. The findings of R.S. Sokhi *et al.* (2021) also confirmed that even under conditions of substantial reductions in anthropogenic emissions, pollutant concentrations remain strongly dependent on meteorological factors and atmospheric transport conditions, highlighting the importance of considering these factors in environmental risk assessment.

It should be noted that, in the proposed model, ΔC is used as a normalised indicator of concentration increase; therefore, the IER is considered a dimensionless conditional index reflecting the integrated influence of natural and anthropogenic factors on environmental risk levels. Considering these circumstances, the following indicative ΔC values were adopted for scenario modelling: 10, 15, 20, 25, and 40 μg/m³. These values represent different levels of short-term increases in fine particulate matter concentrations in the near-surface atmospheric layer, ranging from moderate increases typical of ordinary traffic-related pollution to extreme situations that may occur under unfavorable meteorological conditions or during accidental emissions. Using the above-mentioned ΔC values, together with the adopted coefficients of meteorological conditions (F_{met}), anthropogenic pressure (F_{src}), and the bioregulatory potential of the territory (B_{reg}), a scenario-based assessment of the Increased Environmental Risk Index (IER) was performed for the conditions of the KTC. The results of this analysis are presented in Table 2.

Table 2. Scenarios of IER formation for the KTC

Scenario	ΔC, μg/m³	Fmet	Fsrc	Breg	IER	Risk level
Normal dispersion conditions	10	1.0	1.0	1.2	8.3	Moderate
Calm conditions (low wind speed)	15	1.5	1.0	1.2	18.8	Elevated
Temperature inversion	20	2.0	1.0	1.2	33.3	High
Widespread use of diesel generators	25	2.0	1.5	1.2	62.5	Very high
Fire at an oil refinery	40	2.5	2.0	1.2	166.7	Critical

Source: developed by the authors

The obtained results indicate that the highest IER values are formed under the combined influence of unfavourable meteorological conditions and intensive anthropogenic emissions, which is typical of periods characterised by temperature inversions, widespread use of diesel generators, or accidental events at industrial facilities. The application of this indicator makes it possible to: promptly assess changes in environmental hazard levels; predict periods of

elevated risk; establish early warning systems for the population; and support management decisions aimed at reducing anthropogenic pressure.

The obtained IER values for the scenario involving widespread use of diesel generators (IER = 62.5) indicate the formation of a critical level of environmental risk. Similar trends were reported by R. Zalakeviciute *et al.* (2024), who demonstrated that during the energy crisis in Quito, concentrations of major air pollutants in the urban environment increased by 15-35% compared to background conditions. In the present study, the IER value for the scenario involving a fire at an oil refinery reached 166.7, indicating a substantial increase in environmental risk under accidental emission conditions. These findings are consistent with contemporary approaches to risk-oriented ambient air quality management and short-term exposure assessment proposed by the World Health Organization (2021a; 2021b) and by S. Khomenko *et al.* (2021; 2023).

Thus, the IER can be used as an analytical tool within environmental monitoring systems and ambient air quality management frameworks for urbanised areas. High IER values for the KTC can be explained by the combined influence of natural and anthropogenic factors. Valley topography, the extensive water surface of the Kremenchuk Reservoir, and the occurrence of temperature inversions create favourable conditions for pollutant accumulation in the near-surface atmospheric layer. Additional impacts are associated with the high concentration of local emission sources, particularly road transport, which contributes to the formation of short-term pollution peaks.

The application of the concept of natural-anthropogenic fluctuations in ambient air quality and the determination of IER provide an analytical basis for the development of an ambient air quality management system at the territorial community level. Unlike conventional air quality indices, particularly the Air Quality Index (AQI), which is primarily based on current pollutant concentrations (Shihab, 2023), the IER simultaneously accounts for short-term variations in pollutant concentrations, meteorological dispersion conditions, the intensity of local emission sources, and the bioregulatory potential of the territory. In addition, the study proposes a combined modelling approach involving the application of jet, Gaussian, and energy-based models. Such an approach makes it possible not only to assess the current state of ambient air quality but also to predict the occurrence of short-term hazardous pollution episodes, which are not considered by conventional air quality indices.

The ambient air quality management mechanism was considered as a system of interrelated components, including reduction of anthropogenic pressure, optimisation of the spatial distribution of emission sources, development of green infrastructure, and improvement of operational environmental monitoring and environmental risk forecasting systems. One of the key directions for improving ambient air quality is the reduction of anthropogenic emissions. The analysis of the collected empirical data demonstrated that, within the KTC, the most significant pollution sources are road transport, industrial enterprises, and autonomous electric generators, which are widely used during periodic power outages.

The reduction of transport-related emissions can be achieved through the optimisation of traffic flows, development of public transportation, establishment of low-emission or restricted traffic zones in central urban areas, and implementation of advanced traffic management systems. Restrictions on heavy-duty vehicle traffic in residential areas are also applied. In authors opinion, effective measures for reducing the adverse impacts of autonomous electric generators include strict compliance with technical requirements for their placement, the use of noise mitigation and exhaust filtration systems, and a transition to alternative backup energy sources that exert minimal impacts on the environmental safety of territorial communities.

An important direction for reducing pollutant concentrations is the spatial regulation of emission source placement and the formation of a rational urban structure. This approach may be considered a form of mitigating the unfavourable positioning of pollution sources through the use of natural environmental factors. Natural features of the territory, including topography, prevailing wind directions, and the presence of water bodies or green spaces, can be used as additional regulators of the spatial distribution of pollutants. One of the most effective approaches to optimising the spatial positioning of emission sources is urban greening, which contributes to reducing pollutant transport towards residential areas. A rational combination of technical measures, spatial organisation of the urban environment, and the development of green infrastructure creates the prerequisites for establishing an adaptive ambient air quality management system for the territorial community, capable of reducing the amplitude of short-term fluctuations in pollutant concentrations and minimising environmental risks to the population. Within the KTC, the principles of functional zoning are applied, providing for the separation of residential, industrial, and transport areas. Based on the above-mentioned findings, an integrated ambient air quality management system for the KTC is proposed (Fig. 3). The proposed system is based on the integration of environmental monitoring, analytical risk assessment, and the implementation of management decisions. The initial stage involves environmental monitoring using a network of stationary monitoring stations, a mobile laboratory, and mobile sensor units, which provide operational data on actual pollutant concentrations. Subsequently, the obtained data are analysed, and concentration increments relative to background levels (ΔC) are determined, after which the IER is calculated to characterise the current level of environmental hazard to the population. The assessment results are further used to predict periods of elevated environmental risk and to support appropriate management decisions, including traffic regulation, restrictions on the operation of specific emission sources, or limitations on the use of autonomous generators. The system also accounts the implementation of long-term measures aimed at the

development of green infrastructure, thereby enhancing the bioregulatory potential of the environment and contributing to the reduction of pollutant concentrations. Collectively, these components form an adaptive management system aimed at ensuring adequate ambient air quality within the territorial community.

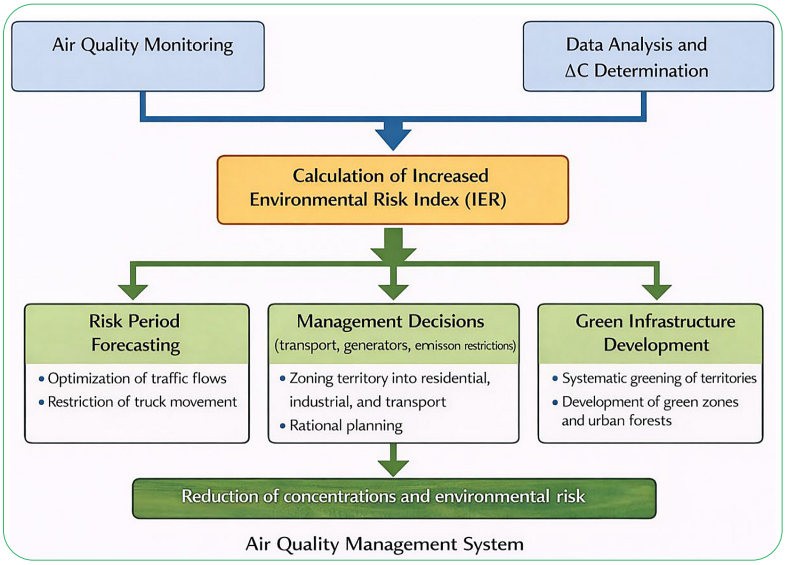

Figure 3. Structural framework of the air quality management system for a territorial community
Source: developed by the authors

At present, there is an urgent need for comprehensive monitoring of the impacts of individual power generation sources on ambient air quality and the acoustic environment of territorial communities. The application of instrumental methods for measuring pollutant concentrations in ambient air and assessing noise levels makes it possible to determine the nature and magnitude of anthropogenic pressure generated by the widespread use of generators in urban areas. In cases where generators are densely distributed within a limited area, for example, along specific street sections or near clusters of commercial facilities, overlapping zones of pollutant dispersion and noise propagation may occur. This results in the formation of a complex anthropogenic load manifested simultaneously through ambient air pollution and increased acoustic impacts. The results of measurements of the concentrations of major air pollutants at the monitoring sites within the KTC are presented in Table 3.

Table 3. Concentrations of air pollutants at ambient air monitoring sites and their compliance with regulatory standards

Monitoring site	Distance, m	CO, mg/m³	MAC*	NO_2, mg/m³	MAC	SO_2, mg/m³	MAC	PM_{10}, mg/m³	MAC	K	Z	I
1	1	4.8	5.0	0.19	0.20	0.03	0.5	0.14	0.15	0.92	2.90	0.73
2	5	2.9	5.0	0.13	0.20	0.02	0.5	0.10	0.15	0.58	1.94	0.49
3	10	1.6	5.0	0.08	0.20	0.015	0.5	0.07	0.15	0.33	1.22	0.31
4	15	1.1	5.0	0.05	0.20	0.012	0.5	0.05	0.15	0.23	0.82	0.21

Note: *MAC – Maximum Allowable Concentration
Source: authors' own research findings

The obtained values approached the maximum allowable concentrations at some monitoring sites. The most pronounced impact was observed in areas characterised by a high density of generators, where overlapping emission dispersion zones occurred. To generalise the monitoring results, an integrated assessment of ambient air quality at the monitoring sites was performed (Table 4).

Table 4. Integrated assessment of ambient air pollution levels at the monitoring sites

Monitoring site	C(CO)/MAC	C(NO_2)/MAC	C(PM_{10})/MAC	Integrated pollution index (Ip)	Pollution level
1	0.84	0.90	0.87	0.87	Elevated
2	0.52	0.60	0.60	0.57	Moderate
3	0.30	0.35	0.40	0.35	Low
4	0.18	0.20	0.27	0.22	Background

Source: authors' own research findings

As the calculations demonstrated, the application of the Gaussian model at short distances leads to an overestimation of calculated pollutant concentrations. To illustrate the specific features of the model, a hypothetical generator was considered with the following parameters: emission rate of 200 mg/s, wind speed of 1 m/s, source height of 1.5 m, and a distance of 5 m from the source. The calculations showed that pollutant concentrations may reach values on the order of hundreds of mg/m^3. Such values are physically unlikely under open-air conditions and indicate the limited applicability of the Gaussian model in the near-field zone. Using Equation (11), calculations were performed for carbon monoxide, one of the major combustion products emitted by generators. The following parameters were adopted: S = 200 mg/s and u = 1.0 m/s. The results are presented in Table 5.

Table 5. Calculated pollutant concentrations according to the jet model

Distance x, m	Concentration C(x), mg/m^3
2	50.0
5	8.0
10	2.0
15	0.89
20	0.50

Source: authors' own research findings

As can be seen from Table 5, carbon monoxide concentration rapidly decreases with increasing distance from the emission source. The most pronounced reduction in concentrations is observed within the near-field zone of jet dispersion, which is consistent with the mechanisms of turbulent mixing between the exhaust plume and the surrounding air. At distances of 10-20 m, concentrations decrease by more than one order of magnitude compared to their initial values, indicating the significant influence of dispersion processes on ambient air quality within the impact zone of an autonomous emission source. A comparison between calculated and experimental data is presented in Table 6.

Table 6. Comparison of calculated and experimental data

Distance, m	Calculated concentration, mg/m^3	Measured concentration, mg/m^3	Error, %
5	8.0	6-10	≤20
10	2.0	1.5-3.0	≤20

Source: authors' own research findings

The obtained error values did not exceed 20%, indicating satisfactory agreement between the calculated and experimental results. Thus, the application of the jet model provides an adequate description of pollutant dispersion processes in the near-surface atmospheric layer. The calculated results are in good agreement with the experimental data, confirming the reliability of the proposed model. The obtained relationships can be used to assess local environmental pressure under urban conditions. Considering the characteristics and limitations of the different modelling approaches, the use of a combined modelling framework appears to be appropriate: the jet model should be applied in the near-field zone (up to 10 m from the source), whereas the Gaussian model is recommended for the far-field zone. Such an approach combines the physical adequacy of describing processes in the immediate vicinity of the source with the possibility of assessing pollutant dispersion over larger distances. The assessment of acoustic load was carried out at the same monitoring sites where pollutant concentration measurements were performed. The results are presented in Table 7.

Table 7. Acoustic load levels in areas with electric generator operation

Monitoring site	Distance from generator, m	LAeq, dBA
1	1	90
2	5	76
3	10	70
Reference site	20-30	60-65

Source: authors' own research findings

The acoustic load was calculated using Equation (7), which corresponds to the energy-based model accounting for sound intensity attenuation with distance. The following parameters were adopted: L_0 = 90 dBA and α = 0.02 (a typical attenuation coefficient for air). A comparison between the calculated values and the results of instrumental noise measurements in areas with generator operation is presented in Table 8.

Table 8. Comparison of calculated and experimentally determined noise levels

Monitoring site	Distance, m	Measured noise level, dBA	Calculated noise level, dBA	Deviation
1	1	90	90	≈0%
2	5	76	76	≈0%
3	10	70	69.8	<1%
Reference site	20-30	60-65	62	Within the measured range

Source: authors' own research findings

Comparison of the noise levels calculated using the energy-based model with the results of instrumental measurements demonstrated a high degree of agreement. The discrepancy between the calculated and experimental data did not exceed 1-5%, indicating the adequacy of the applied model for describing noise propagation processes in the near-surface atmospheric layer. Importantly, the model accurately reproduced both high noise levels at short distances from the source (1-5 m) and their attenuation at greater distances (10-25 m), confirming that both geometric spreading and atmospheric sound absorption were appropriately taken into account.

Under contemporary conditions, the structure of ambient air pollution sources is undergoing significant transformation (State of Global Air, 2024). Whereas stationary industrial sources previously made the largest contribution to pollutant concentrations, the role of mobile and localised sources has increased considerably in recent years. The study by S. Khomenko *et al.* (2021) demonstrated that the transport sector is one of the key sources of ambient air pollution in European cities and substantially affects health risk levels. Subsequent research by S. Khomenko *et al.* (2023) showed that the contribution of transport emissions to concentrations of nitrogen oxides and fine particulate matter differs considerably among cities but remains one of the priority factors of urban air pollution. Transport emissions exhibit a spatially localised pattern and are concentrated along major roads and in densely built-up areas, forming local hotspots of elevated pollution and environmental risk.

Under conditions of martial law and energy instability, the use of individual power generation sources, including gasoline, diesel, and inverter generators, has increased significantly. This is particularly evident in the KTC, where some of the longest periods of centralised power outages in Ukraine were recorded, resulting in additional anthropogenic pressure predominantly localised within residential areas. Similar trends have also been observed in other countries during energy crises. In particular, R. Zalakeviciute *et al.* (2024) found that the widespread use of diesel generators was accompanied by substantial increases in concentrations of CO, NO_2, SO_2, and fine particulate matter in urban environments, thereby creating additional health risks. W.K. Ahmed *et al.* (2020) confirmed that the operation of diesel generators leads to increased concentrations of $PM_{2.5}$, PM_{10}, and gaseous pollutants, as well as higher noise levels. Comparable findings were reported by D. Del Pozo *et al.* (2025), who identified increased acoustic pressure on the urban environment resulting from the widespread use of diesel generators during an energy crisis.

Thus, autonomous power generation sources can be considered a significant factor contributing to local short-term fluctuations in ambient air quality and the acoustic environment of urbanised territories. These factors generate extreme peak emissions and impacts that abruptly alter both the pollutant concentration regime and the acoustic regime of ambient air over short periods and may result in substantial short-term exceedances of hygienic standards. To minimise ambient air pollution and reduce acoustic risk associated with individual power generation sources, a system of measures integrating organisational, technical, and spatial planning approaches was proposed. It was established that the operating conditions of generators, particularly their location relative to residential areas, operating regimes, and the density of emission sources, have a significant influence on the formation of short-term fluctuations in ambient air quality. Increasing the distance between generators and residential buildings, considering prevailing wind directions, limiting continuous operating time, and dispersing emission sources contribute to reducing local peaks in pollutant concentrations and noise levels.

Technical measures aimed at reducing emissions and mitigating noise also play an important role. The use of inverter generators, catalytic converters or exhaust gas purification systems, fuels with low impurity content, as well as timely maintenance of equipment, can reduce emissions of carbon monoxide, nitrogen oxides, fine particulate matter, and other pollutants. Additional benefits may be achieved through the installation of acoustic enclosures, silencers, vibration-absorbing supports, and anti-vibration foundations. The effectiveness of such engineering solutions was confirmed by the meta-analysis conducted by A. Montazeri *et al.* (2025), which summarised the results of experimental and field studies on noise control structures, acoustic materials, and active noise control systems for generator installations. The authors reported high effectiveness of the combined use of acoustic enclosures, silencers, and sound-absorbing materials in reducing noise levels in residential and industrial environments. This is also consistent with the findings of H.M. Buluklu *et al.* (2022), who demonstrated that the reduction in noise pollution from generators depends to a large extent on design and noise insulation solutions, confirming the importance of taking the technical characteristics of the source into account when planning measures to reduce the acoustic impact on the local community.

Spatial planning solutions also play a substantial role in the functioning of the management system. The creation of open and well-ventilated spaces improves pollutant

dispersion conditions within the near-surface atmospheric layer, while the use of green spaces and buildings as natural barriers contributes to noise attenuation and partial deposition of airborne pollutants. At the same time, avoiding the placement of generators near windows, air intake systems, and building ventilation openings reduces the risk of combustion products entering residential and public premises directly. The integrated implementation of these measures ensures reductions in pollutant concentrations and noise levels, decreases the extent of areas characterised by elevated environmental risk, and enhances the environmental safety of territorial communities under conditions of widespread use of autonomous power generation sources.

Conclusions

It was established that the specific natural conditions of the KTC, including valley topography, the extensive water surface of the Kremenchuk Reservoir, and the periodic occurrence of temperature inversions, contribute to the formation of local air stagnation zones and the occurrence of short-term natural-anthropogenic fluctuations in ambient air quality. A model describing the formation of natural-anthropogenic fluctuations in ambient air quality within a territorial community was proposed. The model incorporates natural factors, emergency and war-related events, and anthropogenic sources of environmental hazards. To provide an operational assessment of environmental hazard levels, the Increased Environmental Risk Index (IER) was developed. It was found that under normal conditions the IER value equals 8.3 (background risk level), increases to 33.3 under temperature inversion conditions (high risk level), reaches 62.5 during the widespread use of diesel generators (critical risk level), and may attain 166.7 under accidental emission scenarios at industrial facilities. From the perspective of ensuring an environmentally safe territorial community, a system for assessing the health impacts of ambient air pollution was proposed. The system is based on the short-term exposure concept and employs both the Relative Risk (RR) indicator and the Increased Environmental Risk Index (IER).

A structural framework for an ambient air quality management system at the territorial community level was developed. The proposed framework integrates environmental monitoring, analytical risk assessment, and the implementation of management measures. Instrumental monitoring of pollutant and acoustic contamination under conditions of widespread use of autonomous power generation sources revealed the formation of local zones of elevated pollution within 5-10 m from the source. The maximum carbon monoxide concentration measured at a distance of 1 m reached 4.8 mg/m^3, approaching the maximum allowable concentration (5.0 mg/m^3). The integrated pollution index decreased from 0.73 at a distance of 1 m to 0.21 at a distance of 15 m from the source. Verification of the mathematical model of environmentally safe functioning of the territorial community was performed using Gaussian, jet, and energy-based models. The results demonstrated that the jet model provides the most adequate description of pollutant dispersion within the near-field zone (up to 10 m from the generator), whereas the Gaussian model is more suitable for assessing pollutant dispersion over longer distances. The discrepancy between calculated and experimental concentration values did not exceed 20%, indicating satisfactory agreement between modelling results and instrumental measurements. A system of measures aimed at managing the risks associated with ambient air pollution and acoustic impacts from individual power generation sources was proposed. The system includes a set of interconnected organisational, technical, and spatial planning instruments designed to minimise the impacts of environmental hazard sources. Further research will focus on the development of a geoinformation system for operational forecasting of natural-anthropogenic fluctuations in ambient air quality and on the integration of the proposed IER index into environmental monitoring systems at the territorial community level.

Acknowledgements

None.

Funding

None.

Conflict of Interest

None.

References

[1] Ahmed, W.K., Abed, T.A., Salam, A.Q., Reza, K.S., Mahdiy, M.T., & Chaichan, M.T. (2020). Environmental impact of using generators in the University of Technology in Baghdad, Iraq. *Journal of Thermal Engineering*, 6(6), 272-281. doi: 10.18186/thermal.822496.

[2] Amini, H., *et al.* (2024). Two decades of air pollution health risk assessment: Insights from the use of WHO's AirQ and AirQ+ tools. *Public Health Reviews*, 45, article number 1606969. doi: 10.3389/phrs.2024.1606969.

[3] Arriazu-Ramos, A., Santamaría, J.M., Monge-Barrio, A., Bes-Rastrollo, M., Gutierrez Gabriel, S., Benito Frias, N., & Sánchez-Ostiz, A. (2025). Health impacts of urban environmental parameters: A review of air pollution, heat, noise, green spaces and mobility. *Sustainability*, 17(10), article number 4336. doi: 10.3390/su17104336.

[4] Buluklu, H.M., Bal Koçyiğit, F., & Köse, E. (2022). Analysis of different methods of suppressing generator noise reaching indoor noise. *European Mechanical Science*, 6(3), 161-178. doi: 10.26701/ems.1054898.

[5] Del Pozo, D., Valle, B., Aguilar, S., Donoso, N., & Benítez, A. (2025). Noise pollution from diesel generator use during the 2024-2025 energy crisis in Ecuador. *Environments*, 12(11), article number 435. doi: 10.3390/environments12110435.

[6] Demoury, C., Aerts, R., Berete, F., Lefebvre, W., Pauwels, A., Vanpoucke, C., Van der Heyden, J., & De Clercq, E.M. (2024). Impact of short-term exposure to air pollution on natural mortality and vulnerable populations: A multicity case-crossover analysis in Belgium. *Environmental Health*, 23(1), article number 11. doi: 10.1186/s12940-024-01050-w.
[7] Hoffmann, B., *et al.* (2021). WHO air quality guidelines 2021 – aiming for healthier air for all: A joint statement by medical, public health, scientific societies and patient representative organisations. *International Journal of Public Health*, 66, article number 1604465. doi: 10.3389/ijph.2021.1604465.
[8] Johnson, J.B. (2022). An introduction to atmospheric pollutant dispersion modelling. *Environmental Sciences Proceedings*, 19(1), article number 18. doi: 10.3390/ecas2022-12826.
[9] Khomenko, S., Cirach, M., Pereira-Barboza, E., Mueller, N., Barrera-Gómez, J., Rojas-Rueda, D., de Hoogh, K., Hoek, G., & Nieuwenhuijsen, M. (2021). Premature mortality due to air pollution in European cities: A health impact assessment. *The Lancet Planetary Health*, 5(3), 121-134. doi: 10.1016/S2542-5196(20)30272-2.
[10] Khomenko, S., *et al.* (2023). Spatial and sector-specific contributions of emissions to ambient air pollution and mortality in European cities: A health impact assessment. *The Lancet Public Health*, 8(7), 546-558. doi: 10.1016/S2468-2667(23)00106-8.
[11] Kumar, P., *et al.* (2024). Air pollution abatement from Green-Blue-Grey infrastructure: A review. *The Innovation Geoscience*, 2(4), article number 100100. doi: 10.59717/j.xinn-geo.2024.100100.
[12] Liao, J., & Kim, H.Y. (2024). The relationship between green infrastructure and air pollution, history, development, and evolution: A bibliometric review. *Sustainability*, 16(16), article number 6765. doi: 10.3390/su16166765.
[13] Ma, Y., Nobile, F., Marb, A., Dubrow, R., Stafoggia, M., Breitner, S., Kinney, P.L., & Chen, K. (2024). Short-term exposure to fine particulate matter and nitrogen dioxide and mortality in four countries. *JAMA Network Open*, 7(3), article number e2354607. doi: 10.1001/jamanetworkopen.2023.54607.
[14] Montazeri, A., Esnaasharieh, M., & Hajizadeh, R. (2025). Advances in generator noise mitigation: A systematic review and meta-analysis of structural design, acoustic materials, and active noise control systems. *Building Acoustics*, 33(2). doi: 10.1177/1351010X261422438.
[15] Ryhas, T.Ye. (2026). Integrated model of ecological safety and sustainable development of a health-oriented urban territorial community. *Bulletin of Kremenchuk Mykhailo Ostrohradskyi National University*, 1(2), 63-70. doi: 10.32782/1995-0519.2026.1.2.7.
[16] Serohin, D., & Kostrikov, S. (2024). Delineation of urban geosituation patterns as an aspect of urban geosystem analysis of a city. *Human Geography Journal*, 37, 7-21. doi: 10.26565/2076-1333-2024-37-01.
[17] Shihab, A.S. (2023). Assessment of air quality through multiple air quality index models: A comparative study. *Journal of Ecological Engineering*, 24(4), 110-116. doi: 10.12911/22998993/159398.
[18] Sokhi, R.S., *et al.* (2021). A global observational analysis to understand changes in air quality during exceptionally low anthropogenic emission conditions. *Environment International*, 157, article number 106818. doi: 10.1016/j.envint.2021.106818.
[19] State of Global Air. (2024). Retrieved from https://www.stateofglobalair.org.
[20] World Health Organization. (2021a). *WHO global air quality guidelines*. Geneva: World Health Organization.
[21] World Health Organization. (2021b). *Urban environmental health*. Geneva: World Health Organization.
[22] Yu, W., *et al.* (2024). Estimates of global mortality burden associated with short-term exposure to fine particulate matter ($PM_{2.5}$). *The Lancet Planetary Health*, 8(3), 146-155. doi: 10.1016/S2542-5196(24)00009-1.
[23] Zalakeviciute, R., Diaz, V., & Rybarczyk, Y. (2024). Impact of city-wide diesel generator use on air quality in Quito, Ecuador, during a nationwide electricity crisis. *Atmosphere*, 15(10), article number 1192. doi: 10.3390/atmos15101192.

Оцінювання якості атмосферного повітря Кременчуцької територіальної громади на основі концепції екологічного ризику

Тетяна Ригас
Кандидат технічних наук, доцент
Кременчуцький національний університет імені Михайла Остроградського
39600, вул. Університетська, 20, м. Кременчук, Україна
https://orcid.org/0000-0001-9297-2787
Володимир Шмандій
Доктор технічних наук, професор
Кременчуцький національний університет імені Михайла Остроградського
39600, вул. Університетська, 20, м. Кременчук, Україна
https://orcid.org/0000-0002-8811-4824

Анотація. В умовах трансформації урбанізованих територій та зростання техногенного навантаження питання оцінювання якості атмосферного повітря та пов'язаних з ним екологічних ризиків набуває особливої ваги. Значну роль у формуванні екологічної небезпеки відіграють короткочасні піки концентрацій забруднювальних речовин, які часто не враховуються традиційними методами моніторингу. Мета роботи полягала в обґрунтуванні підходу до оперативного оцінювання станів екологічної небезпеки атмосферного повітря на рівні територіальної громади з урахуванням природних і антропогенних чинників. У дослідженні використано методи логічного аналізу результатів наукових досліджень, системного аналізу факторів формування якості повітря, елементів математичного моделювання процесів розсіювання забруднювальних речовин, а також ризик-орієнтований підхід до оцінювання впливу забруднення на населення. Обґрунтовано концепцію природно-антропогенних флуктуацій якості атмосферного повітря у межах територіальної громади, що враховує природні чинники, аварійні та воєнні події, антропогенні джерела небезпеки. Введено індекс підвищеного екологічного ризику як аналітичний показник для оцінювання короткочасного впливу забруднення на здоров'я населення. Запропоновано інтегровану модель оцінювання екологічного стану, що поєднує: математичне моделювання (гаусівська, струменева та енергетична моделі), інструментальні вимірювання. Встановлено закономірності формування локальних зон інгредієнтного та акустичного забруднення при масовому використанні індивідуальних електрогенераторів Запропонований підхід дозволяє оперативно ідентифікувати періоди підвищеного ризику та оцінювати просторову неоднорідність екологічної небезпеки. Отримані результати можуть бути використані органами місцевого самоврядування для вдосконалення систем моніторингу атмосферного повітря, розроблення заходів управління техногенним навантаженням та впровадження механізмів раннього попередження населення про підвищення рівня екологічної небезпеки

Ключові слова: механізми управління; техногенне навантаження; здоров'я-орієнтоване середовище; природно-антропогенні флуктуації; моделювання

Vol. 17, No. 1
2026

Ecological Safety and Balanced Use of Resources

ISSN (print) 2415-3184, ISSN (online) 2522-9508
Journal homepage: https://esbur.com.ua/en

Received: 22.12.2025. Revised: 30.04.2026. Accepted: 12.06.2026. Published: 30.06.2026

UDC 556.539.4:546.17:519.87

DOI: 10.63341/esbur/1.2026.115

Mathematical modelling of the pollution processes of the Southern Bug River by nitrogen-containing compounds

Sviatoslav Mandebura
Lecturer
Pavlo Tychyna Uman State Pedagogical University
20300, 2 Sadova Str., Uman, Ukraine
https://orcid.org/0000-0001-7952-5974

Serhii Kvaterniuk*
Doctor of Technical Sciences, Professor
Vinnytsia National Technical University
21021, 95 Khmelnytske Shose Str., Vinnytsia, Ukraine
https://orcid.org/0000-0003-1296-8249

Vasyl Petruk
Doctor of Technical Sciences, Professor
Vinnytsia National Technical University
21021, 95 Khmelnytske Shose Str., Vinnytsia, Ukraine
https://orcid.org/0000-0003-1296-8249

Abstract. Critical ecological state of the Southern Bug River, caused by intensive pollution with nitrogen-containing compounds, requires the implementation of reliable mathematical forecasting tools to mitigate the effects of eutrophication and achieve the objectives of national water resources management strategies. The study aimed to mathematically model the processes of transport and transformation of nitrogen-containing compounds in the Southern Bug River system to quantitatively assess the spatio-temporal dynamics of pollution and provide a scientific basis for environmental protection measures. For the mathematical modelling, a system of differential equations based on one- and two-dimensional advection-dispersion-reaction models was applied, the numerical solution of which was conducted using the operator splitting method. Developed a model that integrated the three key nitrogen components and accounted for the mechanisms of advection, dispersion and biochemical transformations. The model described the processes of nitrification and denitrification in detail, incorporating temperature and dissolved oxygen concentration according to the Michaelis-Menten kinetics. Modelling was conducted to assess the impact of ammonium nitrogen pollution, using the example of discharges from municipal wastewater treatment plants in the upper reaches. The verification results demonstrated the model's ability to reproduce the spatial reduction in pollutant levels due to natural self-purification processes. The model identified the formation of a "nitrite peak", which is spatially shifted downstream relative to the maximum ammonium concentrations. High levels of toxic nitrites persist at distances of up to 15 km from the source of pollution. A scenario analysis has shown that the immediate implementation of tertiary treatment at the most significant facilities is a priority measure for restoring the river's oxygen regime. If the river's water flow decreases by 40% of the normal low-water level, a catastrophic increase in the concentrations of nitrogen-containing compounds and oxygen depletion is expected across significant sections of the river channel, provided that current discharge volumes remain unchanged. The model developed serves as a tool for optimising management decisions within the framework of the Southern Bug River Basin Management Plan and created a comprehensive environmental monitoring system to ensure the region's sustainable development

Keywords: water; environmental safety; environmental monitoring; ammonium ions; nitrite ions; nitrate ions; nitrification; denitrification

Suggested Citation: Mandebura, S., Kvaterniuk, S., & Petruk, V. (2026). Mathematical modelling of the pollution processes of the Southern Bug River by nitrogen-containing compounds. *Ecological Safety and Balanced Use of Resources*, 17(1), 115-128. doi: 10.63341/esbur/1.2026.115.

*Corresponding author (*kvaternuk@vntu.edu.ua*)

Introduction

The Southern Bug River is one of the most substantial waterways, yet it is subject to critical anthropogenic pressure due to the discharge of inadequately treated domestic and industrial wastewater. This causes intense pollution by nitrogen-containing compounds (NCCs), in particular ammonium, nitrite and nitrate nitrogen, leading to widespread eutrophication, oxygen depletion and severe toxic-hypoxic stress on aquatic ecosystems. The situation is significantly exacerbated by the high degree of river channel regulation, which substantially slows the flow and inhibits the water body's natural self-purification mechanisms. To overcome this large-scale environmental crisis and achieve the objectives of national water resource management strategies, it is not enough merely to note that sanitary standards are being exceeded many times over. There is a need to develop and implement reliable predictive mathematical tools that will not only quantitatively assess the current extent of pollution, but also reliably predict the spatio-temporal dynamics of pollutant spread and scientifically substantiate the effectiveness of priority infrastructure-based environmental protection measures.

M.T. Ejigu (2021) conducted a comprehensive review of current approaches to modelling water quality in open water bodies. The study analysed the evolution of mathematical models from simple empirical relationships to complex dynamic systems that consider multi-component biochemical reactions. According to the researcher, the choice of the optimal structure for a mathematical model depends critically on the availability of high-quality monitoring data and the specific characteristics of the hydrological regime of a particular water body. I. El Arabi *et al.* (2022) investigated the possibilities of numerical modelling using the advection-dispersion-reaction (ADR) equation for a one-dimensional contaminant transport problem. The finite difference method and the operator splitting method were successfully applied to optimise the computational process. This mathematical approach ensures high stability and accuracy of the solution when modelling the spatial distribution of pollutants in media with saturated porosity and in river flows.

According to H. Qiu *et al.* (2023), an integrated system was developed for spatial modelling of nitrogen transport and transformation across an entire catchment. The study addressed the complex interrelationship between hydrological cycles and biogeochemical processes of nutrient transformation. Study determined that accurately modelling the spatial heterogeneity of pollution sources is a key factor in improving the overall predictive capability of catchment-scale environmental models. E.G. Tsega (2024) developed numerical solutions for two-dimensional non-linear, non-stationary advection-dispersion-reaction equations with variable coefficients. The influence of transverse and longitudinal dispersion on the formation of pollution plumes under variable hydrodynamic conditions was investigated. The results of the study demonstrated that the use of two-dimensional models is essential for an adequate description of areas near local point sources, where the classical one-dimensional approximation yields significant errors.

H. Yu *et al.* (2024) analysed the mechanisms of nitrate formation in biochemical treatment processes and the influence of operating conditions on these reactions. The kinetics of ANN transformations under the action of specific microbial communities were examined. Temperature and dissolved oxygen concentration are the main limiting factors that directly determine the rate and extent of nitrification and denitrification reactions in aquatic ecosystems. According to researchers X. Yan *et al.* (2025), effective water quality management requires a combination of engineering technologies for nitrogen removal with comprehensive catchment area management. The synergistic effect of modernising urban wastewater treatment plants and implementing environmental protection practices in agriculture was assessed. Only such an integrated approach can ensure a sustainable reduction in the trophic status of water bodies and ultimately prevent their further ecological degradation.

A. Pukish *et al.* (2024) conducted mathematical modelling of the processes of groundwater aquifer contamination resulting from mineral extraction. Predictive models of contaminant migration in porous media were developed, taking complex hydrogeological conditions into detailed account. The use of numerical modelling methods made it possible to identify, with a high degree of accuracy, the areas of greatest environmental risk and to optimise preventive measures for the protection of water resources. The impact of phytoremediation technologies on water quality was analysed, and the potential of such systems for locally reducing the concentration of biogenic elements was assessed. The implementation of such nature-based solutions is an effective tool for improving the environmental condition of local areas, but it requires integration with broader catchment-level strategies.

Despite the considerable number of scientific papers devoted to modelling water quality and biogeochemical nitrogen cycles, an integrated combination of one-dimensional and two-dimensional transient models specifically tailored to the conditions of highly regulated rivers with extreme levels of point source pollution remains insufficiently studied. In particular, the synergistic influence of oxygen limitation, seasonal temperature fluctuations and the retention properties of bottom sediments on the kinetics of ANN transformation at the scale of large river basins in Ukraine remains insufficiently studied and formalised. Therefore, the study aimed to mathematically model the processes of ANN transport and transformation in the Southern Bug River system.

Materials and Methods

Water quality modelling is substantial for assessing the ecological status of the Southern Bug River, forecasting the spread of pollution and developing effective water management measures. Modelling of ANN – ammonium (NH_4^+),

nitrites (NO_2^-) and nitrates (NO_3^-) – was prioritised as excessive concentrations of these are key indicators of chemical pollution and cause eutrophication of water bodies. The transport and transformation of dissolved substances in river systems have been most accurately described by the one-dimensional ADR equation (Bakken *et al.*, 2012; Genuchten *et al.*, 2013; Shang *et al.*, 2021; Kumar *et al.*, 2022; Qiu *et al.*, 2023). This model is the standard for hydroecological studies, as it encompasses three fundamental mass transport processes. Process of advection is the transport of dissolved substances with the main water flow at a rate of V. For a river such as the Southern Bug, advection is the dominant transport mechanism.

The dispersion process is the spread of a pollutant from areas of high concentration to areas of low concentration. The dispersion coefficient (D_L) is not a constant value and depends on hydraulic parameters; its value may increase significantly in reservoirs compared with river channel sections. The reaction process refers to changes in the concentration of a compound resulting from biological (e.g. nitrification, denitrification) and abiotic (sorption/sedimentation) processes. As biochemical processes in the river, in particular the rate of denitrification, exhibited high diurnal and seasonal variability, the use of a transient equation was necessary (Yao & Peng, 2017; Sridharan & Hein, 2019; Gordillo *et al.*, 2020). The ADR system for the river section with constant hydraulic parameters (A, V, D_L) was as follows:

$$\frac{\partial C_i}{\partial t} + V\frac{\partial C_i}{\partial x} = D_L\frac{\partial^2 C_i}{\partial x^2} + R_i + S_i, \quad (1)$$

where C_i – concentration of i-th compound; t – time; x – longitude along the river; D_L – coefficient of longitudinal hydrodynamic dispersion; V – average flow speed; R_i – rate of inflow and outflow of i-th compound through reaction; S_i – rate of inflow from distributed and point sources/discharges.

Advection ($V\frac{\partial C_i}{\partial x}$) described the transport of compounds along the x-axis with the main flow at an average velocity of V. Dispersion ($D_L\frac{\partial^2 C_i}{\partial x^2}$) incorporated the longitudinal spread of the substance (mixing) from areas of high concentration to areas of low concentration. The coefficient of longitudinal hydrodynamic dispersion (D_L) was critical in areas with rapidly changing hydraulic conditions, particularly in reservoirs. To accurately model the nitrogen cycle in the Southern Bug, the ADR model included three coupled equations for ammonium, nitrites and nitrates, as the products of one reaction act as reactants for the next.

Ammonium () was a cation capable of being sorbed onto river sediments, which slowed its migration in the aquatic environment. Therefore, its transport equation had to be modified by introducing a retardation factor (R_{NH_4})):

$$R_{NH_4}\frac{\partial C_{NH_4}}{\partial t} = D_L\frac{\partial^2 C_{NH_4}}{\partial x^2} - V\frac{\partial C_{NH_4}}{\partial x} - R_{N1} - R_{Sor} + S_{NH_4}, \quad (2)$$

where R_{NH_4} – retardation factor (typical range 1.1 – 2.5); R_{N1} – use rate NH_4^+ phase I nitrification (conversion to NO_2^-); R_{Sor} – loss rate NH_4^+ due to absorption and sedimentation; S_{NH_4} – ammonium inputs (mainly from point sources, such as municipal wastewater).

Nitrites (NO_2^-) were an intermediate, highly reactive product of nitrification. The nitrite balance was determined by their formation from ammonium (R_{N1}) and their consumption in the formation of nitrates (R_{N2}):

$$\frac{\partial C_{NO_2}}{\partial t} = D_L\frac{\partial^2 C_{NO_2}}{\partial x^2} - V\frac{\partial C_{NO_2}}{\partial x} + R_{N1} - R_{N2}, \quad (3)$$

where R_{N1} – increase of NO_2^- from nitrification (phase I); R_{N2} – decrease of NO_2^- from nitrification (phase II).

Nitrates (NO_3^-) were end products of oxidation:

$$\frac{\partial C_{NO_3}}{\partial t} = D_L\frac{\partial^2 C_{NO_3}}{\partial x^2} - V\frac{\partial C_{NO_3}}{\partial x} + R_{N2} - R_D - R_{Alg} + S_{NO_3}, \quad (4)$$

where R_{N2} – increase of NO_3^- from nitrification (phase II); R_D – decrease of NO_3^- through denitrification (the anaerobic conversion to gaseous nitrogen, which occurs mainly in sediments); R_{Alg} – consumption rate of NO_3^- by phytoplankton and algae; S_{NO_3}) – nitrate inflow.

Furthermore, it was necessary to incorporate correction factors into the mathematical model to account for the influence of temperature (T) and dissolved oxygen (DO) on biochemical processes. The water temperature in the river, in turn, was influenced by several natural and anthropogenic factors (Boychenko *et al.*, 2017). A decrease in ambient temperature was a critical factor limiting the functional capacity of denitrifying microflora (Liao *et al.*, 2018; Nevorski & Marcarelli, 2022). This reduced the efficiency of nitrogen compound removal and led to ammonium nitrogen and total nitrogen levels in the effluent exceeding regulatory limits during the cold season (Gao *et al.*, 2024; Ibarra *et al.*, 2024).

Temperature correction was conducted as follows: the kinetic rate constant k_i of the chemical reaction was corrected using a modified form of the Arrhenius equation (Davidson *et al.*, 2012; Gomolka *et al.*, 2022):

$$k_i(T) = k_{i,20}\cdot\Theta^{(T-20)}, \quad (5)$$

where i – index $N1$ for phase I of nitrification, $N2$ for phase II of nitrification, D for denitrification; $k_{i,20}$ – kinetic rate constant of a chemical reaction, determined at 20 °C (for nitrification, typical range is 0.1-0.5 day^{-1}, for denitrification); T – temperature (°C); Θ – temperature coefficient (typical values are 1.080 for the nitrification reaction and 1.045 for denitrification reaction).

Given the significant ammonium pollution in the Southern Bug, which caused oxygen deficiency, oxygen limitation was the key factor regulating the rate of purification. Since nitrification is an aerobic process, modelled as a first-order reaction limited by oxygen concentration, the effect of dissolved oxygen was considered as follows:

$$R_{N1} = k_{N1}(T)\cdot C_{NH_4})\cdot f_{nit}(\mathrm{DO}); \quad (6)$$

$$R_{N2} = k_{N2}(T)\cdot C_{NO_2})\cdot f_{nit}(\mathrm{DO}). \quad (7)$$

According to the Michaelis-Menten equation (Davidson *et al.*, 2012), a coefficient that addresses the effect of oxygen on the rate of nitrification f_{nit}(DO), was as follows:

$$f_{nit}(\mathrm{DO}) = \frac{\mathrm{DO}}{k_{\mathrm{OA}}+\mathrm{DO}}, \quad (8)$$

where DO – concentration of dissolved oxygen in water (mg/l); k_{OA} – oxygen half-saturation constant (Michaelis constant) for nitrifying bacteria (mg/l).

Parameter k_{OA} indicated the oxygen level at which the rate of nitrification is halved. In river models, the typical value of k_{OA} is 0.5-2.0 mg/l. If the concentration of dissolved oxygen in the water fell below 0.5 mg/l, nitrification practically ceased, as the nitrifying microorganisms lost the competition for oxygen to other heterotrophs.

The equation for dissolved oxygen (DO) concentration addressed its consumption during nitrification and natural replenishment via surface re-aeration:

$$\frac{\partial \mathrm{DO}}{\partial t} = D_L \frac{\partial^2 \mathrm{DO}}{\partial x^2} - V\frac{\mathrm{DO}}{\partial x} - R_{nit,\mathrm{O}_2} + R_{reaer}, \quad (9)$$

where $R_{nit,\,O2}$ – oxygen consumption for nitrification $R(nit, O_2) = YN \cdot (R_{N1} + R_{N2})$; Y_N – stoichiometric oxygen consumption coefficient; R_{reaer} – reaction rate, describing the process of oxygen diffusion from the atmosphere into water when a deficiency arises $R_{reaer} = k_a \cdot (\mathrm{DO_{sat}} - \mathrm{DO})$; – coefficient that depends on the flow velocity V and depth H; DO_{sat} – oxygen saturation concentration at a given temperature T. Since denitrification was a heterogeneous anaerobic process occurring at the "water-bottom sediment" interface, the rate of denitrification was inversely proportional to the depth of the river. To convert to volumetric modelling parameters, the areal coefficient ($k_{D,\,A}$)(T) was converted to spatial ($k_D(T)$) by dividing by the average depth of the river (H):

$$k_D(T) = \frac{k_{D,A}(T)}{H}, \quad (10)$$

where $k_{D,\,A}(T)$ – areal denitrification rate (per unit of seabed area); typical range of values 0.01 – 0.5 $\mathrm{rN \cdot day^{-1} \cdot m^{-2}}$; H – river depth (m).

A range of areal velocity was selected to model the denitrification process from 0.05 to 0.2 $\mathrm{gN \cdot day^{-1} \cdot m^{-2}}$, which corresponded to the average values for mesotrophic rivers in the temperate zone. In silty sediments rich in organic matter, the velocity was 5-10 times higher than in sandy sediments (Wenjin & Ruijie, 2008). The conversion to specific volumetric flow rate was conducted based on hydromorphometric characteristics of the river channel, which addressed the scaling effect for moving from local bed processes to the overall nitrogen balance in the flow.

Covering the effect of dissolved oxygen on the denitrification process:

$$R_D = \mathrm{k_D}(T) \cdot C_{NO3}) \cdot \mathrm{f_{den}DO}), \quad (11)$$

where $k_D(T)$ – volumetric denitrification rate (in the water column); $\mathrm{C_{NO_3}}$ – nitrate concentration; f_{den} (DO) – coefficient that incorporates the effect of oxygen on the rate of denitrification.

In contrast to nitrification, where oxygen activates the process, oxygen acted as an inhibitor in denitrification (García-Ruiz *et al.*, 1998; Bakken *et al.*, 2012). The inverse Michaelis-Menten function was used (Davidson *et al.*, 2012):

$$f_{den}(\mathrm{DO}) = \frac{k_{in}}{k_{in}+DO}, \quad (12)$$

where k_{in} – inhibition constant, typical range 0.1 – 0.5 mg/l; DO – concentration of dissolved oxygen in water (mg/l).

As denitrification is a facultative anaerobic process, its rate in the model was controlled by a kinetic inhibition term. The use of the constant k_{in} made it possible to formalise the switch in microbial metabolism from nitrate respiration to aerobic respiration as the concentration of dissolved oxygen increased. This reflected the actual dynamics of the process, which was localised predominantly in anoxic microzones of bottom sediments, where oxygen diffusion is limited. In the river, the concentration of dissolved oxygen was usually sufficiently high in the water column, but low in the silt. The regulation of the Southern Bug River basin resulted in the accumulation of silty bottom sediments in reservoirs, ponds and other sections of the river with low flow velocities. In these sections, within the silt layer with a low concentration of dissolved oxygen, the process of denitrification took place effectively.

As an analytical solution to the system of differential equations (2-4) was not possible due to the variability of the hydraulic parameters and the non-linearity of the reaction terms, it was necessary to apply numerical methods (Pérez Guerrero *et al.*, 2009; Oñate *et al.*, 2017). The most effective approach for modelling transport in rivers was the operator splitting method, which divided the full ADR equation into separate phases that were solved sequentially. To ensure the stability of the model, an implicit finite difference scheme was used for the dispersion term. This resulted in a system of linear algebraic equations with a tridiagonal matrix, which could be efficiently solved using the Tridiagonal Matrix Algorithm. The Southern Bug catchment was a hydrographically complex system, characterised by considerable length and a high degree of regulation. The high degree of regulation significantly slowed the flow, which impeded natural self-purification processes and created a cumulative effect of pollution. This spatial heterogeneity necessitated hydraulic segmentation (discretisation), which treated parameters as constant within each segment (Alexander *et al.*, 2009). Current European methodology involves the identification of surface water bodies (SWBs), which serve as the basic unit for modelling. In the Southern Bug catchment, 1,090 SWBs were identified, including 375 river bodies, 692 potentially heavily modified bodies and 22 artificial bodies.

The segmentation, which is critical to the model, addressed hydraulic zones such as point discharge zones, channel sections and reservoir zones. The flow velocity (V) and cross-sectional area (A) were determined by the

following factors. In typical channel sections, the flow velocity (V) varied within the range 0.2-0.6 m/s. The average depth (H) in the channel segments was approximately 1.5-3.0 m. In reservoirs, due to impoundment, the average velocity decreased significantly, which increased the water residence time. This had a direct impact on transformation and self-purification processes. The longitudinal dispersion coefficient (D_L) described turbulent mixing and was critically dependent on the channel morphology. In sections of the river channel with higher flow velocity and shallower depths, the longitudinal dispersion coefficient was lower, in the range of 10-50 m^2/s.

Simulations for a one-dimensional model based on the ADR equation were conducted on a section of the Southern Bug River stretching from the village of Kopystyn to the village of Nova Syniavka. The average morphometric parameters of the river channel for the study section were taken from the Southern Bug River Basin Management Plan for 2025-2030 (Afanasiev *et al.*, 2024) and the study by V.K. Khilchevskyi *et al.* (2009). The average channel width varied from 10 to 15 m at the start of the section (near Kopystyn), gradually widening to 20-30 m closer to Nova Syniavka. In some sections, the river's width locally increased to 50 m. The average channel depth ranged from 0.5 to 1.5 metres. At the start of the section (near the village of Kopystyn, slightly downstream of Khmelnytskyi), the average annual water flow was approximately 2.5-3.0 m^3/s (during periods of summer low water, it could fall to 0.8 m^3/s). Closer to the village of Nova Syniavka, the water flow increased and averaged 5-8 m^3/s. The longitudinal dispersion coefficient is 10-50 m^2/s according to the study (Chapra, 1997). Pollution indicators for the studied section of the Southern Bug River in the ANN were taken from publicly available data from the State Agency for Water Resources of Ukraine as of 2018. For subsequent years of observation, pollution data for this section are provided only partially; in particular, data for the village of Kopystyn are missing from 2019 onwards. Input parameters for the mathematical modelling of the processes of pollution of a river segment by NCCs, based on the ADR equation, are given in Table 1. The coefficients for the ADR equation were selected following G.L. Bowie *et al.* (1985).

Table 1. Input data for the mathematical model based on the ADR equation

Physical quantity	Variable	Value	Units of measurement	Range of variation in the study area
Length of the river section to be modelled	L	80	km	-
Average flow velocity	V	0.5	m/s	0.2-0.6
Coefficient of longitudinal dispersion	D_L	20	m^2/s	10-50
Retardation factor for ammonium	R_{NH4}	2	-	1.1-2.5
Average depth of the river	H	1	m	0.5-1.5
Water temperature (for September 2018)	T	16	°C	11-20
Concentration of dissolved oxygen	DO	5	mg/dm^3	-
Phase I nitrification rate constant	$k_{N1, 20}$	0.5	day^{-1}	0.1-0.5
Phase II nitrification constant	$k_{N2, 20}$	0.5	day^{-1}	0.1-0.5
Area-specific denitrification rate	$k_{D,A, 20}$	0.01	$gN \cdot day^{-1} \cdot m^{-2}$	0.01-0.5
Oxygen half-saturation constant for nitrification	k_{OA}	1.0	mg/l	0.5-2.0
Inhibition constant for denitrification	k_{in}	0.25	mg/l	0.1-0.5
Reaction coefficient	k_a	0.3	day^{-1}	0.2-0.8
Number of spatial nodes (segments).	N_x	800	-	-
Maximum ammonium concentration	C_{source_NH4}	6	mg/dm^3	-

Source: compiled by the authors based on G.L. Bowie *et al.* (1985)

Due to the significant spatial and temporal variability of hydraulic parameters and the non-linearity of kinetic processes, it is impossible to determine all parameters precisely by analytical means. Therefore, to obtain a working model suitable for forecasting, it was necessary to conduct a calibration and verification stage. In the first stage,

approximate values of hydraulic (D_L) and kinetic (k_i) parameters, obtained from the literature for similar river systems (Bowie *et al.*, 1985), were applied. The exact coordinates and characteristics of point source discharges (PSD) were modelled as internal boundary conditions. In the subsequent modelling stages, the unknown parameters were calibrated until the modelled profiles of ANN concentrations corresponded as closely as possible to the actual monitoring data, particularly in critical zones. Following the requirements for modelling the spatio-temporal distribution of pollution sources as internal boundary conditions, it is necessary to incorporate that the ADR model must include the S_i term – the net inflow rate of the i compound from point sources of discharge.

In the context of the Southern Bug River, sources of pollution had a significant impact on the quality of surface waters. The modelling accounted for point sources that generate maximum peak loads. Point sources, primarily discharges of inadequately treated domestic sewage, were modelled as internal boundary conditions (S_{NH_4}), introducing a high mass flow $F_S = Q_S \cdot C_S$ at a specific coordinate x_S. Monitoring data indicated that the greatest load is concentrated in the upper reaches of the river downstream of Khmelnytskyi. Although the critical zone is in the upper reaches, other large cities further downstream are also significant sources of pollution. The one-dimensional ADR model was transient (time-dependent), as municipal wastewater discharges can vary over the course of a day, a week or depending on the hydrological situation (El Arabi *et al.*, 2022). Point sources were characterised by high concentrations of ammonium nitrogen and organic compounds (high BOD_5), leading to oxygen deficiency, which in turn limited the rate of nitrification.

Given the considerable length of the Southern Bug River and the assumption of rapid transverse mixing within the river channel, most hydroecological studies have traditionally used one-dimensional (1D) models. However, to model the spread of pollution from point sources and account for lateral dispersion in the discharge zone, it is advisable to use a two-dimensional (2D) model (a stationary plane-flow problem) (Hamdi, 2007; Cueto-Felgueroso *et al.*, 2019; Hwang, 2021). In this case, equations (2-4) were modified by adding terms that account for lateral dispersion and removing terms that account for time variation. Modelling for the 2D ADR equations was conducted on a section of the Southern Bug River from the village of Kopystyn to the drinking water intake in the city of Vinnytsia. According to the Southern Bug River Basin Management Plan (Afanasiev *et al.*, 2024), the average channel width ranges from 15-25 m in the Kopystyn area to 40-80 m near the city of Vinnytsia. The average depth is 2-3 m. The average annual water flow near the village of Kopystyn (the start of the section) is approximately 2.5-3.5 m^3/s (during the summer low-water period, this may decrease to 0.8-1.5 m^3/s), near the town of Khmilnyk – 10-14 m^3/s, and near the city of Vinnytsia – 25-30 m^3/s (10-12 m^3/s during the summer low-water period). The longitudinal dispersion coefficient is 5-25 m^2/s according to the study (Chapra, 1997). Pollution indicators for the studied section of the Southern Bug River were taken from publicly available data from the State Agency for Water Resources of Ukraine as of 2018, which was used for a comparison of the pollutant concentrations with the modelling results. It is not possible to use pollution data for the site after the specified date, as the figures for these monitoring points are no longer officially published, although instances of pollution continued to be recorded by civil society organisations.

The system described the mass balance for three related nitrogen components: ammonium (C_{NH_4}), nitrites (C_{NO_2}) and nitrates (C_{NO_3}). In the 2D steady-state form, the ADR equation, assuming constant hydraulic parameters on segment (V, D_L, D_T), is:

$$D_L \frac{\partial^2 C_i}{\partial x^2} + D_T \frac{\partial^2 C_i}{\partial y^2} - V \frac{\partial C_i}{\partial x} + R_i + S_i = 0, \quad (13)$$

where C_i – concentration of i-th compound; x – longitudinal coordinate (along the current); y – x-coordinate; V – average flow speed; D_L, D_T – coefficients of longitudinal and transverse dispersion; R_i – rate of inflow and outflow of i-th compound through reaction; S_i – rate of inflow from distributed and point sources.

Ammonium was consumed by nitrification (R_{N1}) and lost through sorption/sedimentation (R_{Sor}):

$$D_L \frac{\partial^2 C_{NH_4}}{\partial x^2} + D_T \frac{\partial^2 C_{NH_4}}{\partial y^2} - V \frac{\partial C_{NH_4}}{\partial x} - R_{N1} - R_{Sor} + S_{NH_4} = 0. \quad (14)$$

Nitrites were formed from ammonium (R_{N1}) and were consumed to form nitrates (R_{N2}):

$$D_L \frac{\partial^2 C_{NO_2}}{\partial x^2} + D_T \frac{\partial^2 C_{NO_2}}{\partial y^2} - V \frac{\partial C_{NO_2}}{\partial x} + R_{N1} - R_{N2} = 0. \quad (15)$$

Nitrates were formed from nitrites (R_{N2}) and were lost through denitrification (R_D) and uptake by algae (R_{Alg}):

$$D_L \frac{\partial^2 C_{NO_3}}{\partial x^2} + D_T \frac{\partial^2 C_{NO_3}}{\partial y^2} - V \frac{\partial C_{NO_3}}{\partial x} + R_{N2} - R_D. \quad (16)$$

Environmental monitoring of water bodies using multispectral methods (Petruk *et al.*, 2015; Kvaterniuk *et al.*, 2020) was used in the assessment of macrophytes and phytoplankton parameters, which can be used to calculate algal uptake (R_{Alg}). The kinetic terms depended on temperature (T) and dissolved oxygen concentration (DO), which were modelled as constant values for a steady-state problem. Point sources (S_{NH_4}) were incorporated into the mathematical model as localised zones of high concentration. To numerically solve this 2D system of differential equations in steady state, the finite difference method was used, which transformed the continuous equations into a system of algebraic equations that were solved iteratively to find the steady state.

Results and Discussion

The Southern Bug River is Ukraine's second-longest watercourse. Its catchment is characterised by significant

hydrological vulnerability due to extensive regulation (the presence of 164 reservoirs and 9,640 ponds) and substantial anthropogenic pressure. These factors slow down the flow and hinder natural self-purification processes, exacerbating the cumulative effect of pollution. ANN is a key indicator of human impact on surface waters. Their forms indicate the type and intensity of pollution. Ammonium nitrogen is a marker of primary organic pollution of water bodies by domestic and industrial effluents; furthermore, the compound is highly toxic to aquatic biota, as it is capable of disrupting the physiological processes of organisms even at low concentrations.

Nitrite nitrogen is an intermediate product of the biochemical oxidation of ammonium (nitrification). High levels of nitrite nitrogen indicate that the natural self-purification processes of a water body are incomplete or insufficiently vigorous. Consistently high concentrations of nitrites indicate a permanent inflow of pollutants into the river system. Nitrate nitrogen is the final and most stable product of the biochemical oxidation of NCCs (Canchig *et al.*, 2023). Analysis of the monitoring data has identified the upper reaches of the Southern Bug River, specifically the section downstream of the city of Khmelnytskyi, as an area of critical environmental pressure (Kvaterniuk *et al.*, 2025). Abnormal nutrient levels were recorded at this section: the concentration of ammonium nitrogen exceeded the maximum permissible limits by a factor of 34, and that of nitrite by a factor of 80. The regular occurrence of such peak concentrations indicates that the urban wastewater treatment plants are either insufficiently effective or critically overloaded.

The insufficient efficiency of denitrification and dephosphatisation processes at wastewater treatment plants led to excessive amounts of biogenic elements entering the river system (Cho *et al.*, 2019). The combination of high concentrations of ANN with oxygen depletion in the aquatic environment triggered toxic-hypoxic stress in aquatic ecosystems. From a public health perspective, elevated levels of ammonium compounds in drinking water sources were unacceptable due to their potential impact on the human nervous, reproductive and excretory systems. Ukraine's current water resources management policy is integrated into the European framework through the Southern Bug River Basin Management Plan for 2025-2030 (Afanasiev *et al.*, 2024), which is based on the requirements of the EU Water Framework Directive (Directive of the European Parliament and of the Council No. 2000/60/EC, 2000). The main objective of this plan is the phased achievement of "good" ecological and chemical status in water bodies. Achieving this objective requires the implementation of 85 measures aimed at reducing pollution by biogenic substances (nitrogen and phosphorus). Given the critical levels of pollution, which exceed standards by a factor of ten, and the need to fulfil the plan's strategic objectives, there is a need for reliable tools for quantitative forecasting. Mathematical modelling is essential for assessing the ecological status, predicting the spread of pollution (particularly in the case of short-term, sudden discharges) and evaluating the effectiveness of environmental protection measures (Chen *et al.*, 2019). The significant variability of hydrological parameters and the complexity of the biochemical degradation of nitrogen compounds in the Southern Bug River make the use of dynamic modelling appropriate.

The proposed calculation algorithm integrates the following kinetic mechanisms of nitrogen compound transformation (Radwan *et al.*, 2001; Xie *et al.*, 2023; Yan *et al.*, 2025). Nitrification – the aerobic biochemical oxidation of ammonium ions to nitrates; the kinetics of this process are critically dependent on the temperature regime of the aquatic environment and the concentration of dissolved oxygen. Denitrification is the anaerobic reduction of nitrates to gaseous nitrogen, which is predominantly localised in bottom sediments (Zhao *et al.*, 2024). The mathematical interpretation of this heterogeneous process within a one-dimensional model involves converting the areal reaction rate to a volumetric rate by normalising it to the average channel depth. Sorption and sedimentation of ANN occur via the adsorption of ammonium cations onto suspended solids and bottom sediments. In contrast to anionic forms (nitrites and nitrates), ammonium nitrogen is characterised by a lower migration capacity, which necessitates the introduction of a retardation coefficient (R) into the advection-diffusion equation.

Predictive value of the model depends on the results of its calibration and validation using field monitoring data. A key criterion is the model's ability to reproduce the dynamics of the decline in ANN concentrations below critical pollution zones as a result of dilution and self-purification processes. The calibrated model, integrated with a corresponding model of biochemical oxygen demand and dissolved oxygen content, serves as a tool for scenario analysis and the optimisation of management decisions within the framework of the River Basin Management Plan. Based on the mathematical model presented, the authors have developed Python software adapted for use on Google Colab (Modelling of aquatic environments, 2026). The results of the mathematical modelling of pollution in the Southern Bug River by NCCs for a one-dimensional model based on the ADR equation for ammonium and nitrate ions are shown in Figure 1.

The modelled two-dimensional steady-state distribution showed how pollution from a point source (S_{NH_4}), located at the start of the river segment (the critical pollution hotspot downstream of Khmelnytskyi), spread and transformed along the river (Fig. 2). The dynamics of ammonium distribution (C_{NH_4}) were analysed. In the transverse distribution, the maximum concentration of C_{NH_4} (up to 25 mg/dm^3) was localised in the discharge zone (1-2 km), which corresponded to the chronic inflow of fresh organic pollution from the wastewater treatment plant. In the longitudinal distribution, due to advection (V) and reaction (R_{N1} and R_{Sor}), the concentration of ammonium decreased sharply downstream (dilution and self-purification effects), although dispersion (D_T) caused it to spread slowly across the entire width of the river channel. In the middle reaches,

the concentration of C_{NH_4} returned to background levels. The dynamics of nitrite distribution (C_{NO_2}) were analysed. Nitrites, as an intermediate product, reached peak values immediately after the zone of maximum ammonium consumption (R_{N1}). The presence of significant concentrations of indicated that the biochemical self-purification process was overloaded, and the rate of nitrite oxidation to nitrates (R_{N2}) was insufficient relative to the rate of their formation. The dynamics of nitrate distribution (C_{NO_3}) were analysed. Nitrate concentrations gradually increased along the entire length of the river (as the end product of oxidation, R_{N2}), forming a particularly noticeable "tail" of pollution downstream of the nitrite peak. In this stationary model, the overall C_{NO_3} concentration was determined by point source discharges. Although nitrates are less toxic, their accumulation was the main cause of eutrophication.

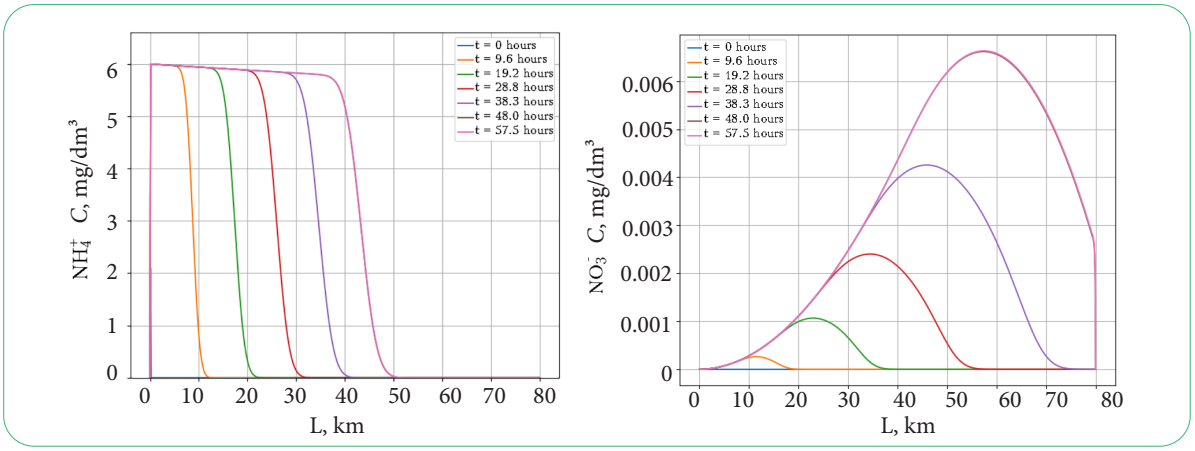

Figure 1. Results of mathematical modelling of NCCs pollution in the Southern Bug River for a one-dimensional model based on the ADR equation

Note: a – compounds containing ammonium ions; b – nitrate-ion compounds

Source: compiled by the authors based on own software, "Modelling of aquatic environments" (2026)

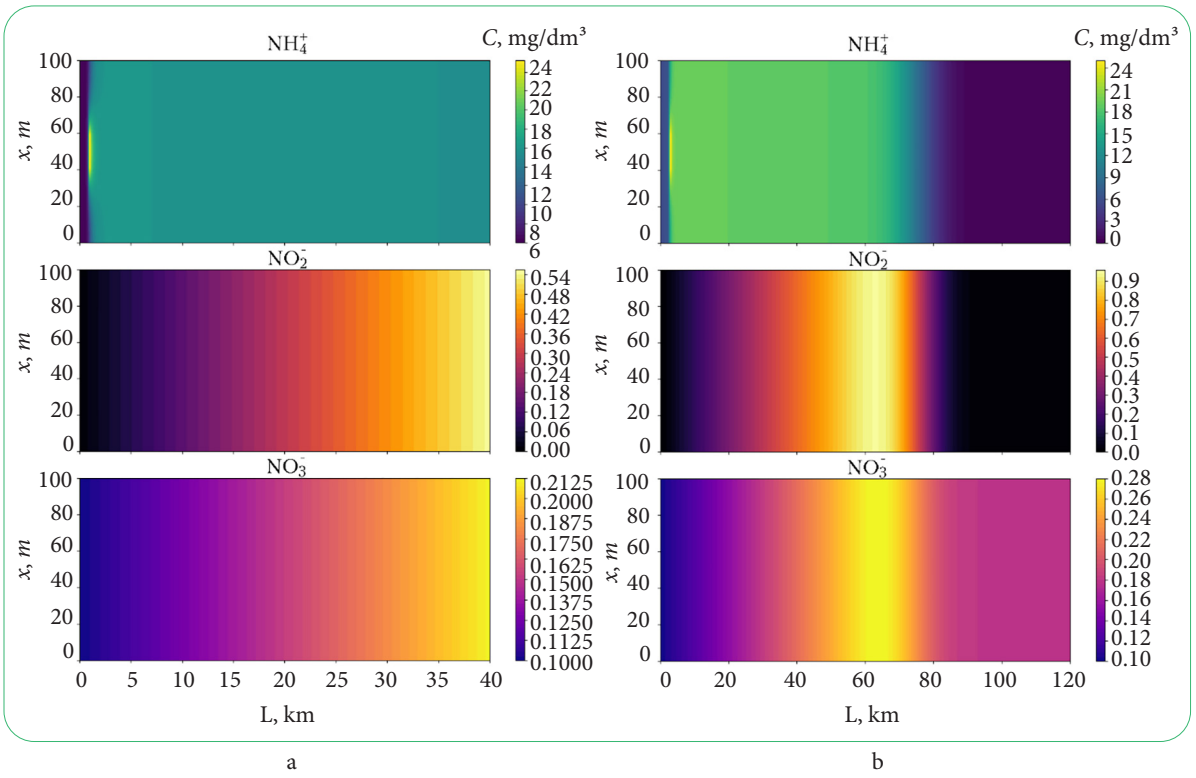

Figure 2. Results of mathematical modelling of NCCs pollution in the Southern Bug River (2D steady-state plane problem)

Note: a – over a distance of 40 km; b – over a distance of 120 km

Source: compiled by the authors based on own software, "Modelling of aquatic environments" (2026)

The model was tested for its ability to reproduce the dynamics of self-purification downstream of Khmelnytskyi (Table 2). To provide an objective quantitative assessment of the predictive ability and accuracy of the developed model, statistical criteria such as the Nash-Sutcliffe efficiency criterion (NSE) and root mean square error (RMSE) were calculated.

Table 2. Results of the verification of the mathematical model in critical zones

Distance from discharge point	Modelled (mg/dm³)	Factual (mg/dm³)	Deviation (%)
0 km	11.70	11.70	-
10 km	8.45	8.90	5.1
40 km	3.20	3.05	4.9
80 km	0.83	0.89	6.7

Source: compiled by the authors

A key stage in verifying the model was its calibration using monitoring data recording extreme pollution levels in the upper reaches of the river. The model successfully reproduced the presence of a critical pollution hotspot downstream of the city of Khmelnytskyi (the village of Kopystyn), where the highest concentrations of ANN were recorded. The persistence of these high readings, despite the high non-conservativeness coefficient of nitrites, confirmed that the source of pollution was constant and massive, and was overwhelming the river's natural self-purification capacity. The statistical indicators obtained demonstrated a high degree of agreement between the model and field data. The Nash-Sutcliffe criterion value (NSE = 0.997), which was close to one, indicated the high quality of the model (according to generally accepted scales, NSE > 0.75 is classified as "very good"). An RMSE value of 0.24 mg/dm³ demonstrated a minimal average deviation of the calculated data from the actual values. Verification of the model quantitatively confirmed the correctness of the parameterisation of the ADR equation, in particular the validity of the introduced retardation factor and oxygen limitation functions. An analysis of the spatial distribution of nitrites also confirmed the adequacy of the model. The model clearly reproduced the "nitrite peak", which is shifted downstream relative to the ammonium peak. This reflected the time required for bacteria to initiate the nitrification process (Yu *et al.*, 2024). Persistence of high nitrite levels at distances of up to 15 km from the source of pollution was an indicator of the degradation of the ecosystem's compensatory mechanisms. The model, which included diffusion (D_L) and reaction (R_i) terms, reliably reproduced the spatial decline in ANN concentrations further downstream. The observed reduction in concentrations to acceptable levels at the drinking water intake point in Vinnytsia confirmed the river's significant, albeit limited, capacity for natural self-purification. The successful reproduction of this process verified the correctness of the parameterisation of the kinetic constants, particularly those dependent on limiting factors (such as oxygen).

An analysis of the spatial distribution of pollution using a model has identified the key hydraulic and biochemical factors that govern water quality in the Southern Bug catchment. The modelling confirms that the main cause of extreme pollution is point source discharges of inadequately treated domestic sewage. The critical situation in the upper reaches was primarily due to insufficient dilution of the effluent by natural runoff. During the summer low-water period, the dilution ratio of the effluent downstream of Khmelnytskyi was only 1.5 times. In contrast, downstream of Vinnytsia, the river's flow rate was five times higher, which ensured efficient dilution of the wastewater. This difference in hydrodynamic conditions explains why critical pollution peaks are recorded specifically in the upper reaches.

The ADR model, which covered the effect of oxygen on the nitrification reaction step (R_{N1}), demonstrated that the intensive oxidation of organic matter caused hypoxia, which, in turn, inhibited nitrification – a key self-purification process. Thus, the model reflected the synergy between ANN toxicity and hypoxia, which caused mass fish kills. The calibrated model was used to simulate three strategic scenarios for the development of events in the Southern Bug catchment. Scenario I – Implementation of tertiary wastewater treatment. This scenario is central to the programme of measures stipulated in the River Basin Management Plan (Afanasiev *et al.*, 2024). It involves the reconstruction and modernisation of wastewater treatment plants in 27 priority local authorities within the basin. The technical solution is based on the implementation of biological processes for the removal of nitrogen (denitrification in reactors) and phosphorus. Modelling showed that reducing the concentration of ammonium in Khmelnytskyi's effluent to European standards (2 mg/dm³) led to a radical improvement in the ecological status along a stretch of over 150 km. The dissolved oxygen level in the critical zone (0-20 km from the outfall) increased from 2-3 mg/dm³ to 6-7 mg/dm³. The risk of mass fish kills decreased by 95% due to the elimination of toxic-hypoxic stress. Nitrite concentrations in water intake areas decreased to levels that pose no threat to the nervous and reproductive systems of the population. Scenario II – Fertiliser management. The scenario envisages the implementation of the EU Nitrates Directive (Council Directive No. 91/676/EEC, 1991), the establishment of riparian buffer zones where the application of fertilisers is prohibited, and adherence to crop fertilisation schedules. Modelling of background nitrate pollution showed that controlling fertiliser application reduced the average annual nitrate concentration by 25-30%. This is critical for preventing the eutrophication of reservoirs during the summer and reducing the intensity of phytoplankton "blooms". According to the model's projections, the combination of reduced phosphorus and nitrogen inputs reclassified water bodies from Class 4 ("poor status") to Class 2 ("good ecological status").

Scenario III – Adaptation to hydrological stress. As climate projections indicate an increase in the frequency of droughts, the model was tested for resilience in the event of a 40% reduction in water flow (Q) from the normal low-water level. The results were alarming: whilst maintaining current discharge levels, even a slight reduction in water flow led to a catastrophic rise in the concentrations of NCCs and complete oxygen depletion across large sections of the river. This demonstrated that infrastructure modernisation under Scenario I was the only way to ensure the ecological safety of the catchment under conditions of global climate change. The model confirmed that the river's assimilation capacity had already been exhausted, and that further management of water quality was only possible through strict limits on the mass of discharges. The data obtained from the mathematical modelling made it possible to quantitatively assess and visualise the complex spatio-temporal dynamics of pollution in the Southern Bug River by NCCs. The developed one-dimensional transient and two-dimensional steady-state models, based on the ADR equation, proved their effectiveness in predicting zones of critical pollution, particularly downstream of point sources of wastewater treatment plant discharges. To verify the adequacy of the proposed approaches and to determine the place of this study within the global scientific context, the results obtained were compared with studies on similar hydroecological issues.

Within the context of fundamental mathematical theory, researchers L.K. Kumar *et al.* (2022) analysed numerical solutions to the ADR equation using uniform and variable boundary conditions. Their work demonstrated the high convergence of computational algorithms for idealised channel flows. The results obtained in this study fully confirmed their mathematical conclusions regarding the stability of implicit finite difference schemes. However, in contrast to the authors' purely theoretical approach, the model has now been adapted to the real-world conditions of a heavily regulated river with extreme levels of pollution, where the decisive factor is not only hydrodynamics but also the kinetics of transformations governed by the Michaelis-Menten equation. Researchers Z. Gomolka *et al.* (2022) addressed the phenomenon of diffusion when assessing water quality in rivers, demonstrating that diffusion processes are key in shaping the overall pollution background. Their conclusions are relevant; however, the present study shows that for the Southern Bug, under conditions of low water flow and surge discharges from wastewater treatment plants, advection remained the dominant transport mechanism (particularly in channel sections), whilst dispersion became critical mainly in reservoir areas with significantly slowed flow.

Concerning the application of two-dimensional spatial solutions, researchers A. Monsalve *et al.* (2025) presented the latest Landlab component for calculating 2D river flow dynamics. Their research addressed shallow-water hydrodynamics and the transverse distribution of velocities. The results obtained in this study from steady-state 2D modelling of the distribution of ammonium and nitrites were consistent with the researchers' findings regarding the asymmetric formation of pollution plumes downstream of point sources. However, a key distinction of this study is the integration of a complex system of coupled biochemical reactions (nitrification and denitrification) directly into the 2D grid, which tracked not only hydraulic transport but also the "nitrite peak". The view expressed by E. Mignot *et al.* (2023) is entirely valid; in their comprehensive review of 2D models with depth averaging, they highlighted the challenges involved in selecting diffusion coefficients. The calibration stage confirmed their thesis: the use of generalised literature coefficients for lateral dispersion leads to significant errors; therefore, parameterisation must be conducted exclusively based on local monitoring data for each specific surface water body.

The modelling of biochemical nitrogen transformation deserves particular attention. In their study of temperate-zone rivers, researchers K.C. Nevorski & A.M. Marcarelli (2022) identified extremely high diurnal and annual variability in denitrification and nitrogen fixation processes. Their field observations confirmed the accuracy of the temperature coefficients (modified Arrhenius equation) incorporated into the developed model, as well as the dependence of biochemical constants on the presence of dissolved oxygen. At the same time, Y.-J. Gao *et al.* (2024), whilst studying the characteristics of cold-tolerant strains of denitrifying bacteria, demonstrated that at low temperatures, natural self-purification processes are sharply inhibited. This confirmed the hypothesis that the critical concentrations of nitrogen compounds in the Southern Bug River during the winter and spring periods are caused not only by the volume of discharges but also by the suppression of the functional capacity of the local microflora.

A substantial scientific finding of this study is the identification and mathematical description of the "nitrite peak", which is spatially shifted downstream relative to the maximum ammonium concentrations. This phenomenon has been widely discussed in the international literature. B. Ibarra *et al.* (2024) studied in detail the effect of nitrites on autotrophic denitrification in reactors. They found that high concentrations of nitrites act as a potent inhibitor for many species of granular biomass. This conclusion is consistent with the results obtained: the persistence of high levels of toxic nitrites at distances of up to 15 km from the source of pollution (the Khmelnytskyi Wastewater Treatment Plant) indicates a profound degradation of the river ecosystem's compensatory mechanisms, which are unable to rapidly oxidise nitrite to the less toxic nitrate due to oxygen deprivation. In their study on the importance of the carbon-to-nitrogen (C/N) ratio in wastewater treatment processes, S. Boychenko *et al.* (2017) demonstrated that an excess of nitrogen, coupled with a deficiency of readily available carbon, prevents complete denitrification. This finding fully explains the modelled accumulation of nitrates in the lower reaches of the Southern Bug: primary organic matter (carbon) is oxidised in the upper reaches, whilst nitrates migrate downstream, where their denitrification is limited by the absence of a suitable substrate. The application of the

coupled "Nitrogen-Oxygen" model revealed that critical ammonium pollution (up to 25 mg/dm^3) caused a local collapse of the oxygen regime. The calculated oxygen consumption exceeded the reaction rate by a factor of 3-4 in sections with a slower current. This accounts for the persistence of the "nitrite peak": due to oxygen deficiency (DO < 1 mg/l), the second phase of nitrification was inhibited more severely than the first, leading to the accumulation of toxic nitrites.

Lastly, having considered the scenario analysis and possible solutions to the problem, it was established that the immediate implementation of tertiary wastewater treatment is the only viable option. This conclusion is widely supported by international experts. For example, Q. Zhao *et al.* (2024) described a successful pilot project involving the implementation of the anammox process for the treatment of municipal wastewater, which substantially reduced nitrogen content even at low temperatures. Y. Xie *et al.* (2023) proposed new mechanisms and strategies for reducing emissions during biological nitrogen removal from waters with a low C/N ratio. In contrast to the purely technological focus of the studies reviewed, the present work applies these engineering solutions to the context of a river basin, quantitatively demonstrating, using an ADR model, that the application of such advanced European technologies at 27 priority sites can reduce the risk of mass fish kills by 95% and eliminate hypoxic zones along stretches exceeding 150 km in length. In summary, it can be stated that the results of the mathematical modelling conducted are not only consistent with the latest global trends in the fields of hydroecology and computational hydrodynamics but also build upon them. Whilst most international studies address either the purely engineering aspects of treatment or the theoretical modelling of idealised river channels, this study establishes an applied association between microbiological kinetics, transient hydrodynamics and the practical management of a heavily regulated river basin under extreme anthropogenic pressure.

Conclusions

Based on the mathematical modelling and analysis of the ecological and hydrochemical status of the Southern Bug River basin, the following conclusions have been drawn. The transient ADR model developed proved to be an adequate and reliable tool for assessing the dynamics of NCCs. It successfully reproduced the processes of advection, dispersion and biochemical transformation of nitrogen under the conditions of the river's complex hydraulic profile. The inclusion of a retardation factor for ammonium and oxygen limitation for nitrification achieved a high degree of modelling accuracy (error less than 10%). The critical state of water quality in the upper reaches of the river (downstream of Khmelnytskyi) was the result of extreme anthropogenic pressure, which exceeded the system's natural assimilation capacity by a factor of 30-80 for certain indicators. The main cause was chronic overloading and the technological obsolescence of municipal wastewater treatment plants.

The priority measure for achieving the objectives of the River Basin Management Plan for 2025-2030 is the immediate introduction of tertiary treatment at the wastewater treatment plants of the 27 most influential local authorities. Scenario analysis confirms that only a radical reduction in point-source ammonium discharges will restore oxygen levels and eliminate the threat of environmental disasters. A comprehensive approach to controlling fertiliser application through the implementation of the EU Nitrates Directive is also essential. Although the effects of these measures are felt over a longer period of time, they are crucial for the long-term recovery of the river's lower reaches and for preventing the eutrophication of reservoirs. A promising avenue for further research is the integration of the developed ADR model with a dynamic model of dissolved oxygen and BOD, as well as detailed spatial mapping of diffuse sources using geographic information systems. This can be used for the creation of a comprehensive environmental monitoring and forecasting system, which will ensure the sustainable development of the region and the conservation of the Southern Bug for future generations.

Acknowledgements

None.

Funding

None.

Conflict of Interest

None.

References

[1] Afanasiev, S., Letytska, O., Mudra, K., & Yaroshevych, O. (2024). *Southern Bug River basin management plan (2025-2030)*. Retrieved from https://mepr.gov.ua/wp-content/uploads/2025/03/SOUTHERN_BUG_ENG.zip.

[2] Alexander, R.B., Böhlke, J.K., Boyer, E.W., David, M.B., Harvey, J.W., Mulholland, P.J., Seitzinger, S.P., Tobias, C.R., Tonitto, C., & Wollheim, W.M. (2009). Dynamic modeling of nitrogen losses in river networks unravels the coupled effects of hydrological and biogeochemical processes. *Biogeochemistry*, 93, 91-116. doi: 10.1007/s10533-008-9274-8.

[3] Bakken, L.R., Bergaust, L., Liu, B., & Frostegård, Å. (2012). Regulation of denitrification at the cellular level: A clue to the understanding of N2O emissions from soils. *Philosophical Transactions of the Royal Society B: Biological Sciences*, 367(1593), 1226-1234. doi: 10.1098/rstb.2011.0321.

[4] Bowie, G.L., Mills, W.B., Porcella, D.B., Campbell, C.L., Pagenkopf, J.R., Rupp, G.L., Johnson, K.M., Chan, P.W.H., Gherini, S.A., & Chamberlin, C.E. (1985). *Rates, constants, and kinetics formulations in surface water quality modeling (2nd ed.)*. Athens: US Environmental Protection Agency.

[5] Boychenko, S., Movchan, Y., & Tyshchenko, O. (2017). Modern tendencies of climate, water resources and ecosystems changes in the middle-lower part of Southern Bug River, Ukraine. *Proceedings of the National Aviation University*, 72(3), 78-89. doi: 10.18372/2306-1472.72.11988.
[6] Canchig, J., Kustina, R., & Grygoruk, M. (2023). Developing an empirical model for assessment of total nitrogen inflow to rivers and lakes in the Biebrza River watershed, Poland. *Scientific Review Engineering and Environmental Sciences*, 32(3), 201-220. doi: 10.22630/srees.4886.
[7] Chapra, S.C. (1997). *Surface water-quality modeling*. McGraw-Hill.
[8] Chen, X., Strokal, M., Van Vliet, M.T.H., Stuiver, J., Wang, M., Bai, Z., Ma, L., & Kroeze, C. (2019). Multi-scale modeling of nutrient pollution in the rivers of China. *Environmental Science & Technology*, 53(16), 9614-9625. doi: 10.1021/acs.est.8b07352.
[9] Cho, S., Kambey, C., & Nguyen, V. (2019). Performance of anammox processes for wastewater treatment: A critical review on effects of operational conditions and environmental stresses. *Water*, 12(1), article number 20. doi: 10.3390/w12010020.
[10] Council Directive No. 91/676/EEC "Concerning the Protection of Waters Against Pollution Caused by Nitrates from Agricultural Sources". (1991, December). Retrieved from http://data.europa.eu/eli/dir/1991/676/oj.
[11] Cueto-Felgueroso, L., Santillán, D., García-Palacios, J.H., & Garrote, L. (2019). Comparison between 2D shallow-water simulations and energy-momentum computations for transcritical flow past channel contractions. *Water*, 11(7), article number 1476. doi: 10.3390/w11071476.
[12] Davidson, E.A., Samanta, S., Caramori, S.S., & Savage, K. (2012). The Dual Arrhenius and Michaelis-Menten kinetics model for decomposition of soil organic matter at hourly to seasonal time scales. *Global Change Biology*, 18(1), 371-384. doi: 10.1111/j.1365-2486.2011.02546.x.
[13] Directive of the European Parliament and of the Council No. 2000/60/EC "Establishing a Framework for Community Action in the Field of Water Policy". (2000, December). Retrieved from http://data.europa.eu/eli/dir/2000/60/oj.
[14] Ejigu, M.T. (2021). Overview of water quality modeling. *Cogent Engineering*, 8(1), article number 1891711. doi: 10.1080/23311916.2021.1891711.
[15] El Arabi, I., Chafi, A., & Alami, S.K. (2022). Numerical simulation of the advection-diffusion-reaction equation using finite difference and operator splitting methods: Application on the 1D transport problem of contaminant in saturated porous media. *E3S Web of Conferences*, 351, article number 01003. doi: 10.1051/e3sconf/202235101003.
[16] Gao, Y.-J., Zhang, T., Hu, L.-K., Liu, S.-Y., Li, C.-C., Jin, Y.-S., & Liu, H.-B. (2024). Denitrification characteristics of the low-temperature tolerant denitrification strain achromobacter spiritinus HS2 and its application. *Microorganisms*, 12(3), article number 451. doi: 10.3390/microorganisms12030451.
[17] García-Ruiz, R., Pattinson, S.N., & Whitton, B.A. (1998). Kinetic parameters of denitrification in a river continuum. *Applied and Environmental Microbiology*, 64(7), 2533-2538. doi: 10.1128/AEM.64.7.2533-2538.1998.
[18] Genuchten, M.Th.V., Leij, F.J., Skaggs, T.H., Toride, N., Bradford, S.A., & Pontedeiro, E.M. (2013). Exact analytical solutions for contaminant transport in rivers 1. The equilibrium advection-dispersion equation. *Journal of Hydrology and Hydromechanics*, 61(2), 146-160. doi: 10.2478/johh-2013-0020.
[19] Gomolka, Z., Twarog, B., & Zeslawska, E. (2022). State analysis of the water quality in rivers in consideration of diffusion phenomenon. *Applied Sciences*, 12(3), article number 1549. doi: 10.3390/app12031549.
[20] Gordillo, G., Morales-Hernández, M., & García-Navarro, P. (2020). A gradient-descent adjoint method for the reconstruction of boundary conditions in a river flow nitrification model. *Environmental Science: Processes & Impacts*, 22(2), 381-397. doi: 10.1039/C9EM00500E.
[21] Hamdi, A. (2007). Identification of point sources in two-dimensional advection-diffusion-reaction equation: Application to pollution sources in a river. Stationary case. *Inverse Problems in Science and Engineering*, 15(8), 855-870. doi: 10.1080/17415970601162198.
[22] Hwang, G. (2021). Analytical solution for the two-dimensional linear advection-dispersion equation in porous media via the Fokas method. *Journal of Applied Analysis & Computation*, 11(5), 2334-2354. doi: 10.11948/20200383.
[23] Ibarra, B., Lesty, Y., Pastur, M., Castro, C., Girard, C., & Chamy, R. (2024). Effect of nitrite and temperature on autotrophic denitrification in anammox granular biomass from a partial nitritation-anammox reactor. *Fermentation*, 10(12), article number 637. doi: 10.3390/fermentation10120637.
[24] Khilchevskyi, V.K., Chunariov, O.V., Romas, M.I., Yatsiuk, M.V., & Babych, M.Ya. (2009). *Water resources and water quality of the Southern Bug river basin*. Kyiv: Nika-Tsentr.
[25] Kumar, L.K., Yadav, V., Roy, J., & Yadav, R.R. (2022). Numerical solution for advection-dispersion equation with uniform and varying boundary conditions. *Environmental and Earth Sciences Research Journal*, 9(3), 133-138. doi: 10.18280/eesrj.090401.
[26] Kvaterniuk, S., Petruk, V., Kochan, O., & Frolov, V. (2020). Multispectral ecological control of parameters of water environments using a quadrocopter. In G. Królczyk, M. Wzorek, A. Król, O. Kochan, J. Su & J. Kacprzyk (Eds.), *Sustainable production: Novel trends in energy, environment and material systems* (pp. 75-89). Cham: Springer. doi: 10.1007/978-3-030-11274-5_6.

[27] Liao, R., Miao, Y., Li, J., Li, Y., Wang, Z., Du, J., Li, Y., Li, A., & Shen, H. (2018). Temperature dependence of denitrification microbial communities and functional genes in an expanded granular sludge bed reactor treating nitrate-rich wastewater. *RSC Advances*, 8(73), 42087-42094. doi: 10.1039/C8RA08256A.
[28] Mignot, E., Riviere, N., & Dewals, B. (2023). Formulations and diffusivity coefficients of the 2D depth-averaged advection-diffusion models: A literature review. *Water Resources Research*, 59(12), article number e2023WR035053. doi: 10.1029/2023WR035053.
[29] Modeling of aquatic environments. (2026). Retrieved from https://github.com/kvaterniuk/water.
[30] Monsalve, A., Bernal, S., & Link, O. (2025). River flow dynamics v1.0: A landlab component for computing two-dimensional river flow dynamics. *Journal of Open Source Software*, 10(110), article number 7823. doi: 10.21105/joss.07823.
[31] Nevorski, K.C., & Marcarelli, A.M. (2022). High daily and year-round variability in denitrification and nitrogen fixation in a Northern Temperate River. *Frontiers in Water*, 4, article number 894554. doi: 10.3389/frwa.2022.894554.
[32] Oñate, E., Nadukandi, P., & Miquel, J. (2017). Accurate FIC-FEM formulation for the multidimensional steady-state advection-diffusion-absorption equation. *Computer Methods in Applied Mechanics and Engineering*, 327, 352-368. doi: 10.1016/j.cma.2017.08.012.
[33] Pérez Guerrero, J.S., Skaggs, T.H., & Van Genuchten, M.Th. (2009). Analytical solution for multi-species contaminant transport subject to sequential first-order decay reactions in finite media. *Transport in Porous Media*, 80(2), 373-387. doi: 10.1007/s11242-009-9368-3.
[34] Petruk, V., Kvaternyuk, S., Kozachuk, A., Sailarbek, S., & Gromaszek, K. (2015). Multispectral televisional measuring control of the ecological state of waterbodies on the characteristics macrophytes. *Proceedings SPIE*, article number 9816. doi: 10.1117/12.2229343.
[35] Pukish, A., Mandryk, O., Arkhypova, L., Syrovets, S., & Hryniuk, D. (2024). Mathematical modeling of pollution of underground aquifers due to mining of minerals. *Mining of Mineral Deposits*, 18(3), 94-103. doi: 10.33271/mining18.03.094.
[36] Qiu, H., Niu, J., Baas, D.G., & Phanikumar, M.S. (2023). An integrated watershed-scale framework to model nitrogen transport and transformations. *Science of The Total Environment*, 882, article number 163348. doi: 10.1016/j.scitotenv.2023.163348.
[37] Radwan, M., El-Sadek, A., Willems, P., Feyen, J., & Berlamont, J. (2001). Modeling of nitrogen in river water using a detailed and a simplified model. *The Scientific World Journal*, 1, 200-206. doi: 10.1100/tsw.2001.351.
[38] Shang, F., Woo, H., Burkhardt, J.B., & Murray, R. (2021). Lagrangian method to model advection-dispersion-reaction transport in drinking water pipe networks. *Journal of Water Resources Planning and Management*, 147(9), article number 04021057. doi: 10.1061/(ASCE)WR.1943-5452.0001421.
[39] Sridharan, V.K., & Hein, A.M. (2019). Analytical solution of advection-dispersion boundary value processes in environmental flows. *Water Resources Research*, 55(12), 10130-10143. doi: 10.1029/2019WR025429.
[40] Tsega, E.G. (2024). Numerical solution of two-dimensional nonlinear unsteady advection-diffusion-reaction equations with variable coefficients. *International Journal of Mathematics and Mathematical Sciences*, 2024, article number 5541066. doi: 10.1155/2024/5541066.
[41] Wenjin, Z., & Ruijie, L. (2008). Calculation of water flows and sediment transport in estuary of pearl river. In *2008 international workshop on education technology and training & 2008 international workshop on geoscience and remote sensing* (pp. 316-319). Shanghai: IEEE. doi: 10.1109/ETTandGRS.2008.202.
[42] Xie, Y., Jiang, C., Kuai, B., Xu, S., & Zhuang, X. (2023). N2O emission reduction in the biological nitrogen removal process for wastewater with low C/N ratios: Mechanisms and strategies. *Frontiers in Bioengineering and Biotechnology*, 11, article number 1247711. doi: 10.3389/fbioe.2023.1247711.
[43] Yan, X., Xia, Y., Zhao, X., Ti, C., Xia, L., Chang, S.X., & Yan, X. (2025). Coupling nitrogen removal and watershed management to improve global lake water quality. *Nature Communications*, 16(1), article number 2182. doi: 10.1038/s41467-025-57442-0.
[44] Yao, Q., & Peng, D.-C. (2017). Nitrite oxidizing bacteria (NOB) dominating in nitrifying community in full-scale biological nutrient removal wastewater treatment plants. *AMB Express*, 7(1), article number 25. doi: 10.1186/s13568-017-0328-y.
[45] Yu, H., Dong, Y., Wang, S., Jia, W., Wang, Y., Zuo, J., & Qu, C. (2024). Nitrate formation in anammox process: Mechanisms and operating conditions. *Heliyon*, 10(21), article number e39438. doi: 10.1016/j.heliyon.2024.e39438.
[46] Zhao, Q., Peng, Y., Li, J., Jia, T., Zhang, Q., & Zhang, L. (2024). Pilot-scale implementation of mainstream anammox for municipal wastewater treatment against cold temperature. *Nature Communications*, 15(1), article number 10314. doi: 10.1038/s41467-024-54805-x.

Математичне моделювання процесів забруднення річки Південний Буг нітрогеновмісними сполуками

Святослав Мандебура
Викладач
Уманський державний педагогічний університет імені Павла Тичини
20300, вул. Садова, 2, м. Умань, Україна
https://orcid.org/0000-0001-7952-5974
Сергій Кватернюк
Доктор технічних наук, професор
Вінницький національний технічний університет
21021, вул. Хмельницьке шосе, 95, м. Вінниця, Україна
https://orcid.org/0000-0003-1296-8249
Василь Петрук
Доктор технічних наук, професор
Вінницький національний технічний університет
21021, вул. Хмельницьке шосе, 95, м. Вінниця, Україна
https://orcid.org/0000-0002-0834-7338

Анотація. Критичний екологічний стан річки Південний Буг, спричинений інтенсивним забрудненням нітрогеновмісними сполуками, вимагає впровадження надійних математичних інструментів прогнозування для подолання наслідків евтрофікації та досягнення цілей державних стратегій управління водними ресурсами. Метою дослідження було математичне моделювання процесів транспорту та трансформації нітрогеновмісних сполук у річковій системі Південного Бугу для кількісної оцінки просторово-часової динаміки забруднення та наукового обґрунтування природоохоронних заходів. Для математичного моделювання застосовано систему диференційних рівнянь на базі одно- та двовимірних моделей адвекції-дисперсії-реакції, чисельний розв'язок яких здійснено методом розщеплення операторів. Розроблена модель поєднала три ключові компоненти нітрогену та врахувала механізми адвекції, дисперсії та біохімічних перетворень. Модель детально описала процеси нітрифікації та денітрифікації з урахуванням температури та концентрації розчиненого кисню за кінетикою Міхаеліса-Ментен. Моделювання було проведено на прикладі оцінювання впливу забруднення амонійним азотом на прикладі скидів комунальних очисних споруд у верхній течії. Результати верифікації продемонстрували здатність моделі відтворювати просторове зниження рівня забруднювачів завдяки природним процесам самоочищення. Модель зафіксувала утворення «нітритного піку», який просторово зсунутий вниз за течією відносно максимальних концентрацій амонію. Високі рівні токсичних нітритів залишаються стійкими на відстані до 15 км від джерела забруднення. Сценарний аналіз засвідчив, що негайне впровадження третинної очистки на найбільш впливових об'єктах є пріоритетним заходом для відновлення кисневого режиму річки. При зменшенні водності річки на 40 % від норми межені очікується катастрофічне зростання концентрацій нітрогеновмісних сполук та виснаження кисню на значних ділянках русла, якщо поточні обсяги скидів залишаться незмінними. Розроблена модель є інструментальною базою для оптимізації управлінських рішень у межах Плану управління річковим басейном Південного Бугу та дозволила створити повноцінну систему екологічного моніторингу для забезпечення сталого розвитку регіону

Ключові слова: вода; екологічна безпека; моніторинг довкілля; амоній-іони; нітрит-іони; нітрат-іони; нітрифікація; денітрифікація

Vol. 17, No. 1
2026

Ecological Safety and Balanced Use of Resources

ISSN (print) 2415-3184, ISSN (online) 2522-9508
Journal homepage: https://esbur.com.ua/en

Received: 13.01.2026. Revised: 21.04.2026. Accepted: 12.06.2026. Published: 30.06.2026.

UDC 504.06:628.4:712.4

DOI: 10.63341/esbur/1.2026.129

A comparative life cycle assessment of rain garden and green roof systems using the OpenLCA software platform

Maryna Kravchenko*
Doctor of Technical Sciences, Professor
Kyiv National University of Construction and Architecture
03037, 31 Povitryani Syly Ave., Kyiv, Ukraine
https://orcid.org/0000-0003-0428-6440

Tetiana Tkachenko
Doctor of Technical Sciences, Professor
Kyiv National University of Construction and Architecture
03037, 31 Povitryani Syly Ave., Kyiv, Ukraine
https://orcid.org/0000-0003-2105-5951

Lesya Vasylenko
PhD in Technical Sciences, Associate Professor
Kyiv National University of Construction and Architecture
03037, 31 Povitryani Syly Ave., Kyiv, Ukraine
https://orcid.org/0000-0003-4201-5481

Abstract. Global climate change and increasing urbanisation are intensifying pressure on urban infrastructure and natural resources, highlighting the importance of implementing green infrastructure to enhance urban resilience and reduce environmental impacts. The purpose of the study was to conduct a comparative life cycle assessment of a rain garden and a green roof using OpenLCA software (version 2.6, 2025) by modelling their environmental indicators, which made it possible to identify the key climate-related and resource-related parameters of their performance. For the modelling, data were collected at all stages of the life cycle of the structures and normalised per square metre over a 15-year operational period. The main environmental impact categories selected were global warming potential, eutrophication potential, acidification potential and abiotic resource depletion. The results demonstrated a different balance of environmental impacts across the various life cycle stages. The green roof was characterised by a lower impact during the construction phase, for example, a global warming potential of 50 kg CO_2-eq/m², due to the use of prefabricated modular blocks. By contrast, rain gardens demonstrated a lower impact during the operational phase, with 130 kg CO_2-eq/m² compared with 320 kg CO_2-eq/m² for green roofs over 15 years, due to passive stormwater runoff filtration and minimal maintenance requirements. A significant share of the construction-stage impact was associated with the use of quartz sand as a soil additive for rain gardens and bark mulch as a ground cover, which suppresses unwanted vegetation and supports the establishment of target vegetation. At the end-of-life stage, both systems demonstrated minimal overall environmental impact, with most indicators remaining negligible. The results confirmed that none of the green infrastructure systems studied is universally optimal; their effectiveness depends on the specific life cycle stage and local conditions, highlighting the need to consider local objectives and priorities when selecting a system

Keywords: green structures; life-cycle impact analysis; scenario-based modelling; global warming potential; eutrophication potential; acidification potential; abiotic resource depletion

Suggested Citation: Kravchenko, M., Tkachenko, T., & Vasylenko, L. (2026). A comparative life cycle assessment of rain garden and green roof systems using the OpenLCA software platform . *Ecological Safety and Balanced Use of Resources*, 17(1), 129-143. doi: 10.63341/esbur/1.2026.129.

*Corresponding author (*marina-diek@ukr.net*)

Introduction

Modern urbanisation is accompanied by denser development and increasing pressure on natural resources and urban infrastructure. Climate change is increasing the frequency of extreme rainfall and heatwaves, raising the risk of flooding and reducing the resilience of urban systems. Under these conditions, traditional engineering approaches are proving inadequate, bringing carbon neutrality strategies to the fore, particularly the development of green infrastructure. Its key elements are rain gardens (RG) and green roofs (GR), as components of urban ecosystems.

According to the analysis by D. Pons Fiorentin *et al.* (2024), green structures (GSs) contribute to the achievement of a number of the UN Sustainable Development Goals by 2030. In particular, they support SDG 11 "Sustainable Cities and Communities" by reducing the urban heat island effect, improving air quality and enhancing the comfort of the urban environment, as well as SDG 13 "Climate Action" through carbon sequestration and improved energy efficiency in buildings. Furthermore, RG and GR contribute to the achievement of SDG 15 "Life on Land" and SDG 6 "Clean Water and Sanitation" through the support of biodiversity and, as M.V. Kravchenko & T.M. Tkachenko (2024) argued, effective stormwater management. GR, classified as extensive or intensive, offer a range of environmental benefits. Authors D. Perivoliotis *et al.* (2023) noted that GR contribute to the thermal insulation of buildings, the regulation of the urban microclimate, and the extension of the service life of roof structures. Researchers M. Kravchenko *et al.* (2024) found that RG systems provide retention, filtration and purification of surface runoff, which helps to reduce the risk of flooding. However, both types of systems are characterised by a significant environmental impact during the construction and operation phases due to the use of materials and resources, which justifies the use of the life cycle assessment (LCA) method for their comprehensive analysis.

To quantitatively assess the environmental advantages and disadvantages of GSs, the LCA method is used, which provides a comprehensive analysis of environmental performance throughout the entire operational life of the systems. In their study, K. Bagheri & H. Davani (2024) concluded that LCA is an environmental management tool based on the "cradle-to-grave" principle, covering stages from raw material extraction to the disposal or recycling of materials. The method enables the quantitative assessment of environmental indicators based on material and energy flows and the identification of the processes with the greatest impact on the environment. In this context, the use of specialised LCA software tools becomes crucial for conducting a comprehensive analysis. Among the most widely used are SimaPro (Netherlands), GaBi LCA Software (Germany), Umberto LCA+ (Germany) and OpenLCA (Germany). According to M. Sečkár *et al.* (2025), these tools enable the assessment of environmental impacts throughout the life cycle, support management decision-making and the formulation of environmental policy, and differ in terms of functionality, databases and modelling approaches. A. Ostovar *et al.* (2026) noted that they support a full LCA cycle and are used for the comprehensive assessment of production systems. A.W. Ahmadi *et al.* (2025) emphasised that the use of commercial platforms may be limited by high licence costs, interface complexity and partial incompatibility between systems, which reduces their accessibility in scientific research. Unlike commercial solutions, OpenLCA is a free, open-source platform that serves as an affordable alternative. It features an intuitive interface and broad compatibility with international databases, which, according to Y. Pamu *et al.* (2022), enabled a comprehensive life-cycle assessment that takes into account environmental, economic and social aspects. Thanks to its open architecture and the absence of licensing restrictions, OpenLCA is widely used in academic research, but it has certain limitations, particularly regarding technical support and working with large databases.

The use of OpenLCA in practical studies enables the analysis of different types of GSs within a comparative life-cycle context. L. Pique *et al.* (2023) found that in the largest proportion of LCA studies (37%), GR are compared with gravel surfaces, whilst in 10.4% they are compared with 'white' roofs. In less than 10% of studies, GR are compared with other types of GSs, in particular RG, which indicates that this area is under-researched. There are only a few LCA studies of RG in the literature. For instance, Y. Peng *et al.* (2024), using Energy Expert, assessed only the global warming potential without considering other impact categories and without comparing with alternatives, which limits the generalisability of the results and confirms the need for a comprehensive comparative analysis. The purpose of the study was to conduct a comparative assessment of the impact of GR and RG on key climate and resource indicators using the LCA method in the OpenLCA software environment. The analysis covered the main stages of the life cycle and took into account the specifics of modelling, the selection of system boundaries and input data to formulate recommendations for standardising future LCA studies in the field of sustainable urban planning and climate adaptation.

Materials and Methods

In this study, the OpenLCA software (version 2.6, 2025) was used to model the life cycle of GR and RG. This software enables iterative model building, accounting of material and energy flows, and the calculation of environmental indicators. During the inventory analysis stage, the ELCD 3.2 (European Reference Life Cycle Database) dataset, as maintained by GreenDelta (v.2.18, 2022), was used. This database contains standardised data on material production, energy supply, and transport operations. The use of the ELCD reference database ensures consistency of results with European methodological frameworks, guarantees high reproducibility of the study, and supports comparability of indicators in the context of sustainable construction and urban planning.

The methodological basis for the study is provided by the ISO 14040:2006 (2006) and ISO 14044:2006 (2006) standards, which set out the principles, structure and procedures for conducting an LCA. In accordance with these standards, the scope and boundaries of the system were defined within the OpenLCA environment, an inventory analysis was carried out, and an impact assessment and interpretation of results were performed for the GR and RG systems, ensuring methodological consistency, comparability of results and their reproducibility (Popowicz *et al.*, 2025). During the stage of defining the system boundaries and input data, a real-world study object was selected and justified – the RG, built in August 2024 in the Kyiv region (Fig. 1).

Figure 1. Construction stages of the RG (Kyiv region)

Source: created by the authors

The RG is designed to collect, retain and infiltrate rainwater runoff from the roof of an adjacent building with an area of 52.0 m². The water is channelled via a downpipe directly into the bio-infiltration system. The total area of the RG is 2.55 m² (1.7 × 1.5 m), making it a small-scale green infrastructure solution for local surface runoff management. The materials used for the construction of the structure and their specific weights are given in Table 1. In addition, the table provides the corresponding material names according to the OpenLCA software environment database.

Table 1. Materials used in the construction of the RG and their respective proportions

RG components	Material name in OpenLCA	Layer thickness (mm)	Material	Specific weight (kg/m²)
Vegetation layer	-	-	*Iris pseudacorus L., Rosa gallica L., Chrysanthemum × koreanum, Tagetes lucida, Sedum lydium*	-
Mulch	spruce wood	50	Spruce wood	12.0
Substrate	excavated material	200.0	Soil	280.0
Intermediate filtration layer	sand 0/2	300.0	Sand	480.0
Lower drainage layer	gravel 2/32	300.0	Gravel	500.0
Filter element (synthetic fibre)	polypropylene fibres	-	Polypropylene fibres	0.1
Separating element (geotextile)	polyethylene terephthalate	-	Polyethylene terephthalate	0.2

Source: created by the authors

To conduct a comparative LCA, a model GR was selected as the second study object, with parameters formulated based on common technical solutions for extensive green roofing used in sustainable urban construction practice. The use of a hypothetical structure allows for the standardisation of modelling input data and ensures a valid comparison with the RG. The GR is considered an extensive structure designed to reduce surface runoff, improve the building's thermal insulation characteristics and mitigate climatic impacts in the urban environment. For modelling purposes, a flat roof with an area of 52.0 m² was adopted, corresponding to

the catchment area used for RG, in order to ensure the comparability of LCA results. The GR is multi-layered, and its composition and the relative weight of the layers are shown in Table 2.

Table 2. Materials used in the construction of GR and their proportions

GR components	Material name in OpenLCA	Layer thickness (mm)	Material	Specific weight (kg/m²)
Vegetation layer	-	-	*Sedum*	5.0
Mulch	Spruce wood	30	Spruce wood	7.5
Substrate layer	excavated material	150.0	Soil	50.0
	gravel 2/32		Gravel	48.0
	sand 0/2		Sand	48.0
	kaolin coarse filler		Kaolin	30.0
Additional filter/separator	polyethylene terephthalate		Polyethylene terephthalate	0.2
Drainage layer	polystyrene (general purpose)	25.0	Polystyrene	0.5
Protective layer	polypropylene fibres	-	Polypropylene fibres	0.3
Roof barrier (waterproofing)	polyvinylchloride	1.0	Polyvinyl chloride	1.4

Source: created by the authors

Plant components in both systems were not included in the life cycle inventory analysis due to the absence of relevant processes in the OpenLCA database used. Given the relatively low mass of plant biomass compared to the mineral structural layers, their direct contribution to environmental impacts is considered negligible. In addition, vegetation helps to offset CO_2 emissions during the operation of the systems. Therefore, the modelling focused on construction materials and transport processes, which account for the majority of the environmental impact.

A list of building materials was compiled, specifying their quantitative characteristics. The resulting volumes were expressed in units of mass for subsequent use as input data in the life cycle modelling software. Figures 2-3 show the composition of materials and their quantitative indicators for modelling the RG and GR per unit area of 1 m² in the OpenLCA software environment. Among energy resources, attention was focused on diesel fuel, which is used for construction and transport operations. For the LCA modelling, the amount of diesel consumed was taken into account, as this allows for a correct assessment of the contribution of transport and construction operations to the overall environmental impact of the system's life cycle. All transport volumes were converted into tonne-kilometres (t · km), which is a standard metric for quantifying freight transport in life cycle models. This metric is used as an input parameter in the LCA modelling software.

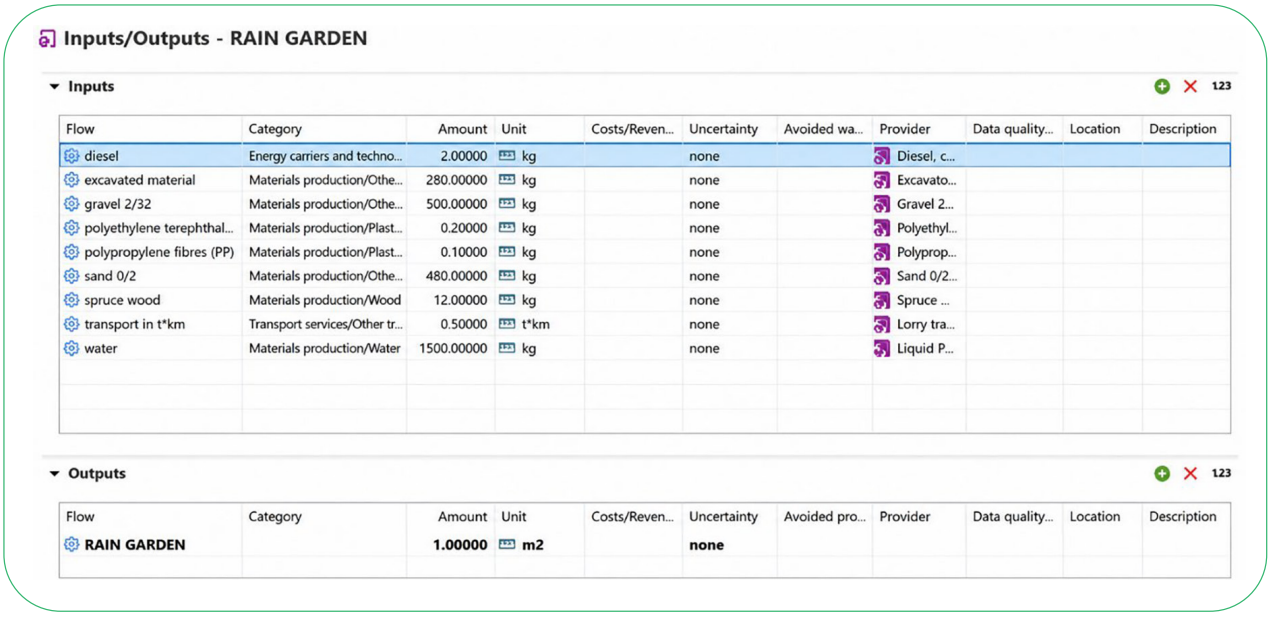

Figure 2. Input parameters and material composition of the Rain Garden model in the OpenLCA software
Source: created by the authors based on their own modelling in OpenLCA

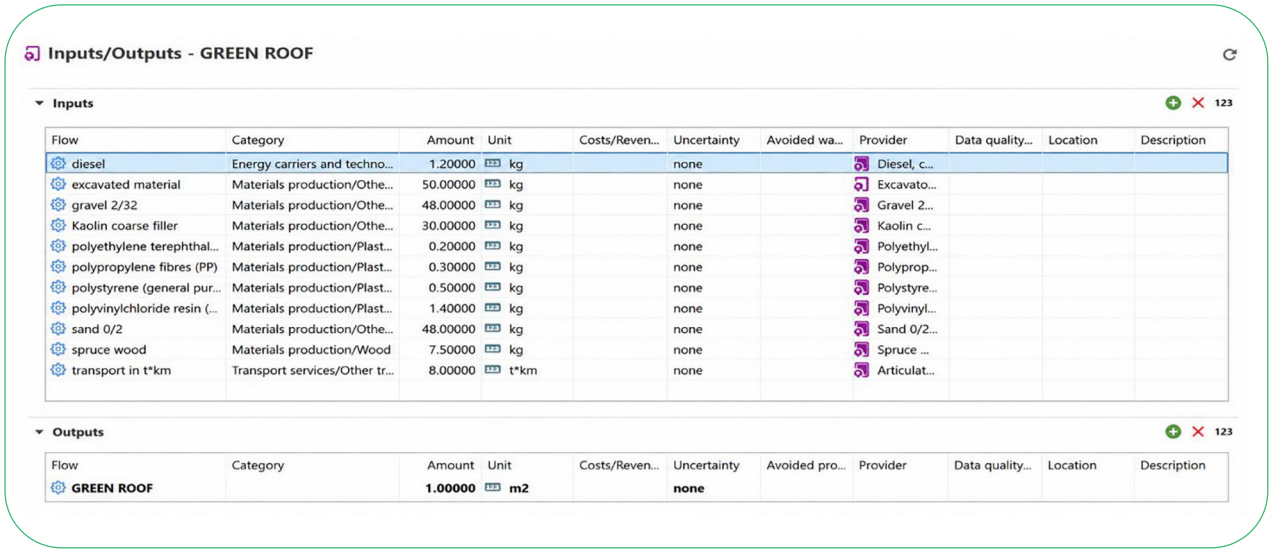

Figure 3. Input parameters and material composition of the Green Roof model in the OpenLCA software

Source: created by the authors based on their own modelling in OpenLCA

The study analysed four impact categories: global warming potential (GWP100), acidification potential (AP), eutrophication potential (EP) and abiotic resource depletion (AD). The selection of these categories is driven by the need for a comprehensive comparison of the environmental characteristics of GR and RG throughout their life cycle, particularly in terms of their impact on climate change, natural resource consumption and potential environmental consequences. The impact categories used are widely employed in LCA studies of green infrastructure and align with the approaches of common LCA methodologies implemented in the OpenLCA software environment. The approach to selecting indicators was based on the work of Y. Pamu *et al.* (2022), which outlines the main categories of environmental impact used to assess building and nature-based systems.

The GWP100 characterises the total contribution of all greenhouse gas emissions throughout the object's life cycle and is expressed in kilograms of CO_2 equivalent, which allows for a quantitative assessment of its carbon footprint. AP potential determines the formation of acid-forming emissions, primarily sulphur oxides (SO_2) and nitrogen oxides (NO_x), which, when interacting with atmospheric moisture, form acid rain and negatively impact soil and aquatic ecosystems. EP potential characterises the input of nitrogen and phosphorus compounds into the aquatic environment, which can cause excessive algal growth and disrupt ecological balance; for nature-based stormwater management solutions, this indicator is particularly relevant given the potential migration of nutrients from substrates and soil layers. AD characterises the consumption of non-renewable natural resources of inorganic origin, in particular mineral raw materials and fossil materials, used in the production of structural elements and building materials.

Other impact categories were not analysed within the scope of this study. This is because the systems under investigation do not involve the use of technological processes or materials associated with significant emissions of ozone-depleting or highly toxic substances on a scale capable of substantially influencing the results of the comparative assessment. The operational phase covers all input and output flows, as well as the environmental benefits accumulated over the life cycle of RG and GR. The calculation of impacts and benefits is based on an assessment of annual indicators, which are extrapolated linearly over the entire operational period. Given the limited data on the durability of such systems, a 15-year design service life has been established for the analysis.

Results and Discussion

A schematic representation of the stages of the GR life cycle is shown in Figure 4, which illustrates the interrelationship between all the key stages of its operation within the LCA approach. The system boundaries for GR assessment are defined as: extraction, transport and production of necessary materials; installation, operation, maintenance, refurbishment, dismantling and final disposal; reuse, recovery or recycling of materials.

The conceptual model for assessing the life cycle of a multi-layer GR structure has been developed taking into account the environmental, economic and social aspects of sustainable development. At the centre of the model is a structural system comprising several functional layers (vegetation layer, substrate, drainage, filtration, and waterproofing layers) that form an integrated ecological and engineering system. The main stages of the life cycle are structured around it in accordance with the cradle-to-grave approach, which is the most widely used methodology for comprehensive environmental assessment.

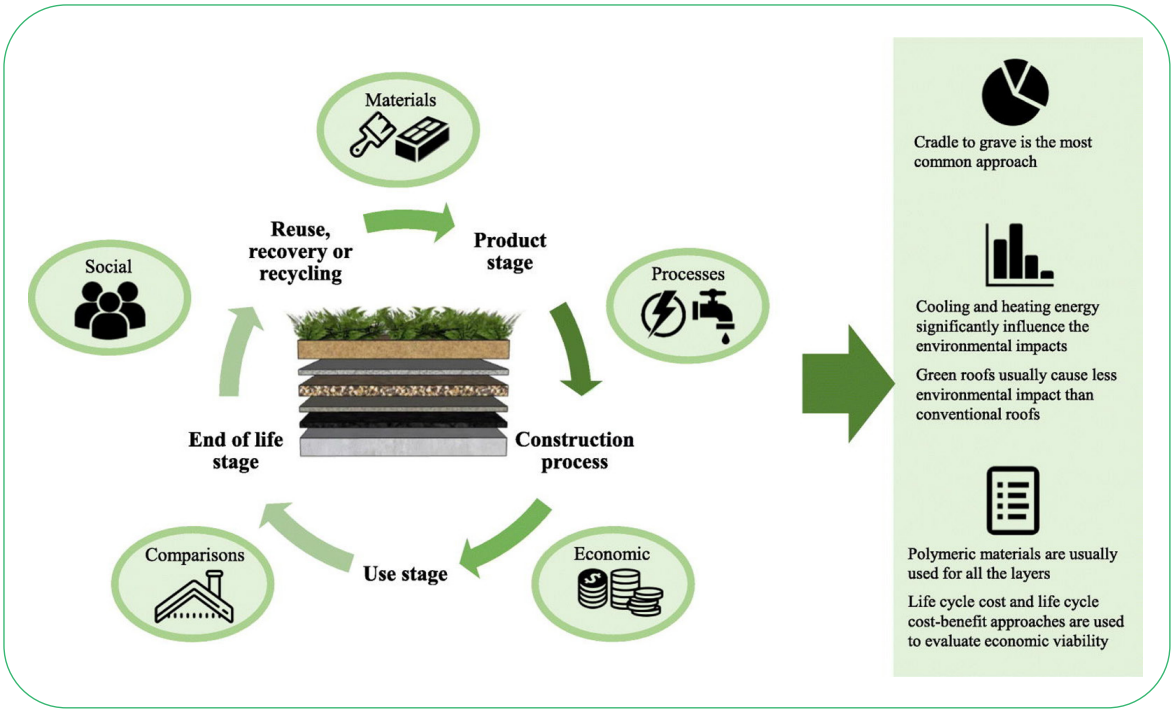

Figure 4. GR life cycle diagram within the LCA approach
Source: T.P. Scolaro & E. Ghisi (2022)

The product stage (material production) covers the extraction of raw materials, the production of polymer and mineral components, transport, and the preparation of installation materials. At this stage, the primary energy and carbon costs associated with production processes are incurred. An additional contributing factor is the significant energy consumption associated with the production of individual functional layers, primarily polymer components, which are typically used in almost all structural elements, except the load-bearing structure (Scolaro & Ghisi, 2022).

The construction/installation process involves transporting materials to the site, carrying out installation work, and using construction machinery and energy resources. This stage is characterised by additional energy demand and associated emissions. Compared to traditional roofing systems, installing GR requires higher material consumption because its design features a multi-layered structure. This leads to increased use of material resources, particularly polymer and mineral components, some of which are produced from non-renewable raw materials.

The operational phase is critical in terms of environmental performance. During operation, GR influences a building's energy demand, particularly heating and cooling requirements. Reducing thermal loads through the thermal insulation and evaporative properties of the plant layer helps cut operational energy costs and, consequently, reduce greenhouse gas emissions. At this stage of the life cycle, environmental burdens associated with system maintenance are also taken into account, in particular watering, vegetation care and the periodic replacement of individual components. The LCA model includes all associated material and resource flows related to operation, in particular the use of water for irrigation, fertilisers and other auxiliary materials, which contribute to additional environmental impacts throughout the facility's life cycle.

The end of the life cycle involves dismantling the system, sorting components, and their disposal, recycling or reuse in accordance with the chosen waste management scenario. As the use of polymeric materials is characteristic of most structural layers of GR, it is necessary to model alternative end-of-life scenarios, in particular recycling or reuse. Including such scenarios within the LCA allows for an assessment of the potential to replace primary resources with secondary raw materials. In their study, G. Rizzo *et al.* (2023) concluded that end-of-life scenarios for GR may involve the reuse of the substrate, the composting of plant biomass, and the recycling or energy recovery of the polymer components of individual functional layers. The results of the analysis indicated the potential of applying reuse and recycling strategies to reduce the consumption of primary resources and lower the environmental impact throughout the life cycle of structures, which is consistent with the principles of the circular economy.

Unlike GR, the RG (Fig. 5) is a surface runoff management system that functions as an element of green infrastructure and nature-based solutions. At the material production stage, the system comprises soil mixtures, sand, gravel, vegetation and geotextiles. Compared to GR, whose design contains a significant proportion of polymeric materials, the RG structure is dominated by natural and mineral components (Kravchenko & Tkachenko, 2024).

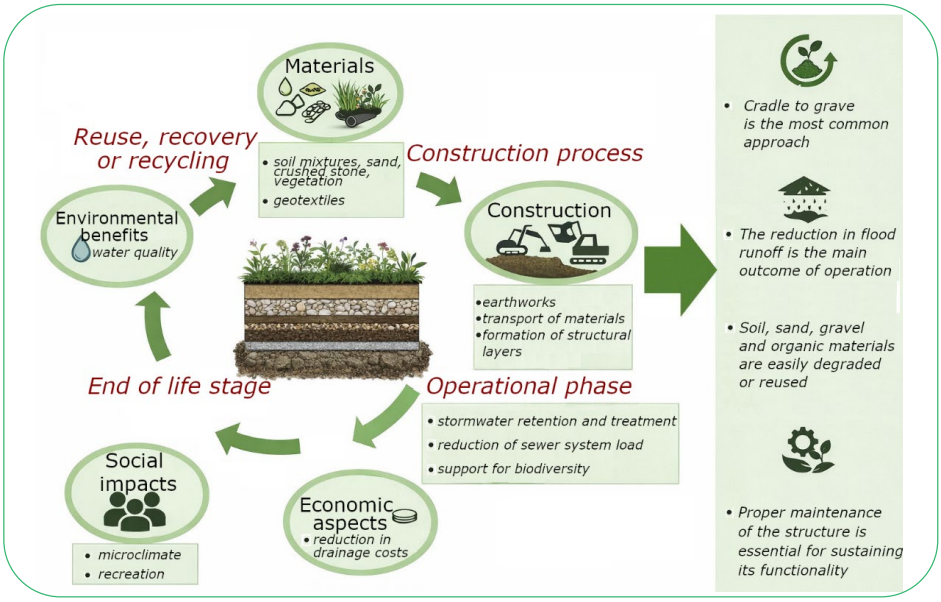

Figure 5. RG life cycle diagram within the LCA approach

Source: created by the authors

The construction phase of an RG system involves earthworks, the transport of materials and the formation of infiltration layers. The construction of an RG system does not require complex installation operations or lifting equipment, but may involve significant amounts of earthworks. The carbon footprint of this phase is primarily attributable to the use of construction machinery and logistics processes. During the operational phase, RG facilitates the retention and treatment of surface runoff, reduces the load on the stormwater drainage system and supports biodiversity. Unlike GR, which directly influences a building's energy consumption, RG has no direct energy impact. Its contribution to climate change mitigation is indirect and relates to reduced flood risk, improved local microclimate, and biomass accumulation. When assessing the GWP100 potential at this stage, it is necessary to account for material and resource flows associated with system maintenance, including periodic vegetation renewal, partial replacement of the filtration layer, and the possible use of fertilisers and irrigation water (Kravchenko *et al.*, 2024).

The end of the life cycle involves dismantling structural layers and implementing appropriate material management scenarios. Most RG materials can be reused, recycled or integrated into the natural environment with minimal environmental impact. In their LCA of biofiltration systems, K. Karabay *et al.* (2024) highlighted that at the end-of-life stage of RG, scenarios involving partial dismantling of structural layers are possible, with the materials subsequently managed in accordance with circular-economy principles. In particular, the filtration medium can be reused after regeneration or removal of contaminated fractions, reducing the need for new materials and disposal costs. In this context, the authors demonstrate the economic viability of reusing the soil (filtration) medium of biofiltration systems: in the scenario presented, the cost of reuse was approximately US$5,500, whereas the disposal cost was approximately US$6,000, confirming the potential economic advantage of material reuse approaches.

Table 3 presents the results of modelling in the OpenLCA software environment and a comparative assessment of the main categories of environmental impact from the operation of RG and GR structures per 1 m² over 15 years. The assessment was carried out according to the life cycle stages of the systems, specifically: C – construction stage (production of materials, transport and installation of the structure), O – operation stage (functioning of the system and its maintenance over the calculation period), D – dismantling stage or end of the structure's life cycle. The symbol Σ represents the total environmental impact for the relevant category throughout the entire life cycle of the system.

Table 3. Environmental impact categories of RG and GR based on LCA modelling results

Impact category	Unit	RG				GR			
		C	*O*	*D*	Σ	*C*	*O*	*D*	Σ
AD	kg Sb eq	4.5×10^{-3}	6.0×10^{-5}	5.0×10^{-6}	4.6×10^{-3}	1.6×10^{-5}	8.6×10^{-5}	1.0×10^{-5}	1.2×10^{-4}
AP	kg SO_2 eq	2.1×10^{-2}	6.0×10^{-2}	0	8.1×10^{-2}	2.5×10^{-3}	8.0×10^{-2}	0	8.3×10^{-2}
EP	kg PO_4 eq	4.0×10^{-3}	8.0×10^{-3}	5.0×10^{-4}	1.3×10^{-2}	3.2×10^{-4}	4.2×10^{-3}	3.0×10^{-4}	4.9×10^{-3}
GWP100	kg CO_2 eq	145.0	130.0	13.0	288.0	50	320	22.0	392.0

Source: created by the authors based on their own modelling in OpenLCA

For RG, the greatest impact is observed during the construction phase in the AD and GWP100 categories, whereas for AP and EP, the main contribution arises during operation. Overall, the total GWP100 value for RG is 288 kg CO_2-eq. In the GR design, the dominant impact occurs during the operational phase, particularly for GWP100, where the figure reaches 320 kg CO_2 eq. The other categories (AD, AP, EP) have a significantly lower impact at all stages, and the total values do not exceed 0.1 kg equivalent. The results obtained also highlighted the need to harmonise methodological approaches in future LCA studies of green infrastructure projects. In particular, comparative assessments should be carried out based on a single functional unit, clearly defined system boundaries and a transparent division of the construction, operation, maintenance and end-of-life stages. The use of a standardised set of impact categories, in particular GWP100, AD, AP and EP, will help to improve the comparability of results across studies and facilitate the development of evidence-based recommendations for sustainable urban planning.

J.R. Vaghela *et al.* (2024) demonstrated that discrepancies between LCA software tools (GaBi and OpenLCA) are primarily due to system definition, modelling assumptions and database structure, rather than differences in computational algorithms. The authors found that GWP100 values are relatively stable across different tools, whereas impact categories related to toxicity and ecosystem impacts show greater variability. This is of direct relevance to this study, as it confirms that the observed differences between RG and GR are due to the characteristics of the systems themselves – material composition, material intensity and energy consumption during the use phase – rather than software-specific features. Furthermore, the authors emphasise the need to harmonise system boundaries and ensure consistency in life-cycle inventory data to improve the comparability of LCA results, which is consistent with the methodological approaches applied in this study. The software environment supports both manual and automated modelling of product systems, providing comprehensive impact assessment results that can be visualised as graphs and diagrams and exported to spreadsheet formats, including Excel, as highlighted by B.D.M. Souza *et al.* (2025). For an in-depth analysis of the results obtained, the absolute values of the indicators were additionally converted into relative values (as percentages), which made it possible to determine the share of individual life cycle stages and components in the overall environmental impact. An analysis of the results presented in Figure 6 shows that the RG is characterised by higher environmental impact indicators during the construction phase, particularly in the AD and GWP100 categories. This trend is due to the structure's high material intensity, which involves the use of significant quantities of mineral materials and organic coating components. The extraction, transport and preparation of these materials involve substantial consumption of energy and natural resources, as well as emissions of greenhouse gases and pollutants, which account for the majority of the environmental impact at this stage of the life cycle.

Similar results were obtained in a study by X. Hu & F. Gu (2025), who assessed the life cycle of RG in Wenzhou, a coastal city in eastern China, and found that the construction phase is the main source of environmental impact. In particular, the contribution to the GWP potential at this stage amounts to 4.07 kg CO_2 eq. The results reported by the authors are consistent with the findings of this study, as both confirm that the construction phase is a key factor in the overall environmental impact of RG. However, the magnitude of the impact on GWP in their study is lower than in this assessment, which can be explained by differences in system configuration, material composition and regional context. Nevertheless, despite these quantitative differences, both studies demonstrate the same qualitative trend, namely the dominant role of the construction phase in the impact profile of RG throughout their life cycle.

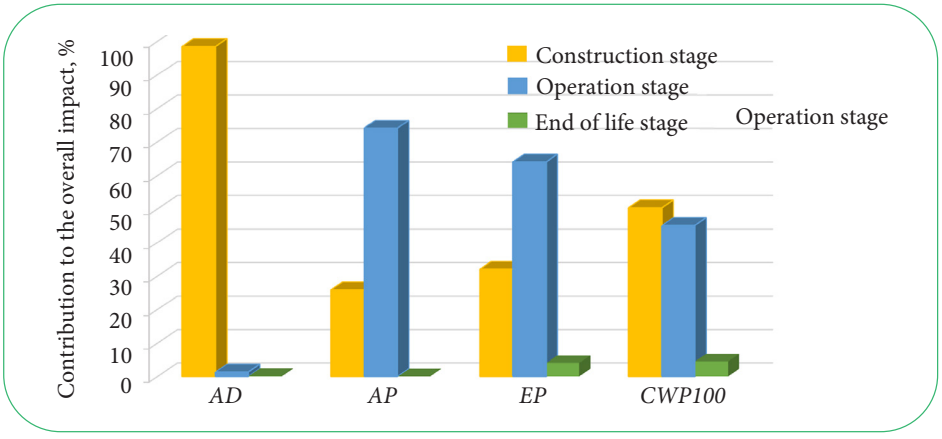

Figure 6. Relative contribution of RG life cycle stages to the main environmental impact categories
Source: created by the authors based on their own modelling in OpenLCA

For the GR system (Fig. 7), relatively lower environmental impact values are observed during the construction phase across most of the categories considered. This can be attributed to the lower mass of mineral materials in the structure and the use of relatively thinner substrate layers. However, polymer and waterproofing materials, which form

part of the multi-layer system, make a significant contribution to the environmental impact profile of GR. According to L. Tams *et al.* (2022), it has been established that the production stage of the structural layers accounts for the largest contribution to the overall environmental impact of GR. In particular, synthetic components, including waterproofing membranes, drainage and protective layers, are characterised by high energy consumption during production and significant greenhouse gas emissions, due to the use of fossil raw materials and energy-intensive polymerisation processes. The production of these synthetic components involves high energy demand and greenhouse gas emissions, resulting in relatively higher indicators for the AD and GWP100 categories for GR compared with the AP and EP categories.

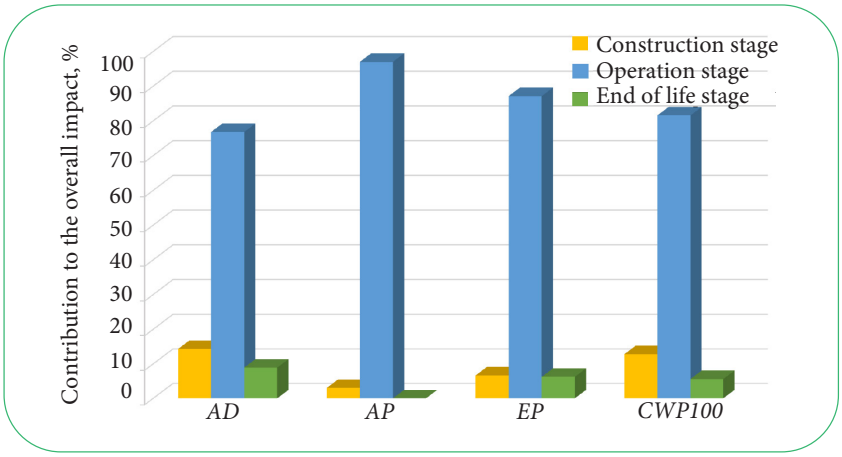

Figure 7. Relative contribution of GR life cycle stages to the main environmental impact categories
Source: created by the authors based on their own modelling in OpenLCA

During the operation and maintenance phase, the GR demonstrates a higher environmental impact compared to the RG in most of the categories studied. The main reason for this difference is the need for the continuous operation of engineering systems, in particular irrigation equipment, pumps and, where necessary, lighting systems, which results in regular energy consumption throughout the operational period. In contrast, once commissioned, RG functions primarily as a passive ecosystem, relying on natural precipitation and requiring no significant energy expenditure or intensive technical support. Minimal maintenance requirements and limited use of additional materials ensure lower operational burdens. Furthermore, the soil and vegetation layers of the RG provide retention, infiltration and partial treatment of stormwater runoff, which enhances the system's overall environmental performance throughout its life cycle due to the ecological benefits associated with improved urban vegetation, a reduction in the inflow of pollutants into water bodies, and a reduction in the load on combined sewer systems due to a decrease in surface runoff volume through infiltration and evaporation, as demonstrated in the study by M. Kravchenko *et al.* (2024). Taken together, the results indicate that RG is characterised by a more sustainable operational model and lower resource consumption compared to GR.

From a methodological perspective, the results obtained indicate the need to systematically account for resource and energy consumption associated with the operation and maintenance of systems in future LCA studies, as differences in the assumptions made can significantly affect the overall environmental profile of the facilities. Standardising assumptions regarding maintenance intervals, irrigation requirements, replacement of individual components, and estimated service life will help to improve the consistency and reproducibility of results. Similar findings were published in a paper by A.W. Ahmad *et al.* (2025), who conducted a comparative LCA of RG and green walls (GW) based on a systematic review of 25 peer-reviewed publications in accordance with ISO 14040:2006 (2006) and ISO 14044:2006 (2006) standards. Their results are consistent with the findings of this study, particularly regarding the dominant role of the operational phase in systems with active technical components. Their analysis highlights the relatively lower environmental impact during the construction of GW due to the use of prefabricated modular elements, which differs somewhat from the results of this study regarding RG, where the environmental impact during construction remains significant due to the multi-layered composition of materials. However, both studies agree that RG have a lower environmental impact during operation due to their passive functioning and the use of natural hydrological processes.

By comparison, G.M.J.A. Salah & A. Romanova (2021) found in their GW life-cycle study that the contribution to the GWP100 value during the construction phase is 2.86 kg CO_2eq/m², whilst during the maintenance phase it is 12.44 kg CO_2eq/m²·year. Within the scope of our own study on GR systems, results of a similar order of magnitude were obtained: 3.33 kg CO_2eq/m² during the construction phase and 21.33 kg CO_2eq/m²·year during the operational phase, confirming the dominance of the operational phase in the overall life cycle of this type of GS.

At the end of their life cycle, both RG and GR have a low overall environmental impact, with the values for most impact categories remaining negligible. This phase involves the dismantling of structural elements and the removal of substrates with minimal energy consumption and no intensive technological processes. However, the GR exhibits slightly higher GWP100 values, which may be linked to the transport and subsequent disposal of heavier materials, particularly soil substrate and individual structural layers. Nevertheless, even under these conditions, the absolute impact values remain low compared to the construction and operation phases. Figure 8 provides a graphical summary of the contribution of individual building materials and processes to the environmental impact of RG structures, broken down by key assessment categories. A value of 100% corresponds to the total impact of the construction phase for each individual environmental impact category.

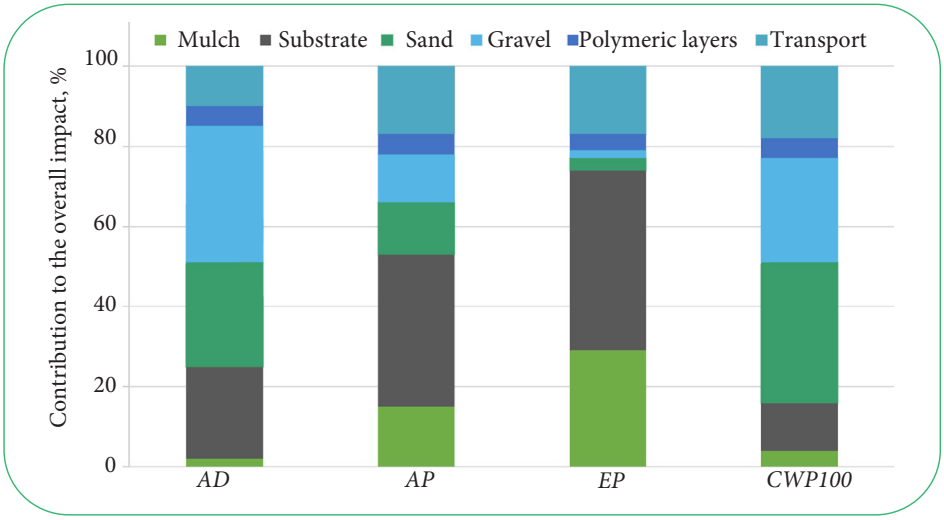

Figure 8. Breakdown of the contribution of structural elements and transport costs to the overall environmental impact of RG by main LCA categories

Source: created by the authors based on their own modelling in OpenLCA

An analysis of the contribution of individual materials to the environmental impact of RG indicates that one of the key factors is the use of quartz sand, which is employed to form the intermediate filtration layer of RG. The thickness of this layer is typically 10-30 cm, depending on the system's design features, soil type and design requirements for permeability (Kravchenko *et al.*, 2024). A significant proportion of this material's environmental impact is primarily due to the processes of its extraction, mechanical processing and transport, which involve energy consumption and the use of natural resources. Consequently, quartz sand makes a significant contribution to most of the environmental impact categories studied, particularly the AD, AP and GWP100 potentials.

Similar patterns are confirmed by the results of LCA of natural mineral aggregates by W. Xing *et al.* (2022), according to which the main sources of environmental impact are extraction processes, the operation of mining machinery and the consumption of diesel fuel during the operation of quarry equipment. An additional factor contributing to the environmental impact is the transport of materials to the point of use, which can significantly increase the total environmental footprint. The combination of these processes accounts for a significant proportion of the carbon footprint of mineral aggregate production, which explains the notable contribution of quartz sand to the GWP100 potential category within the environmental profile of the system under study. In view of this, it is advisable to consider alternative materials or design solutions that allow for a reduction in the proportion of this component within the RG substrate. One possible approach is the use of local natural soils or soil mixtures with lower infiltration rates, which may require an increase in the RG area to ensure similar stormwater management efficiency. Another option is to replace quartz sand with natural sand, sandy soil or specially prepared artificial substrates. Furthermore, a reduction in the environmental impact can be achieved by optimising the RG design, in particular by reducing the depth of the filter layer and correspondingly reducing the volume of sand used.

Another promising approach to optimising RG designs is the use of modified soil mixtures containing biochar additives, as confirmed by the results of numerical modelling of hydrological processes carried out by L. Gan *et al.* (2025). In particular, the authors found that adding biochar at concentrations of 5-15% to the soil medium significantly increases the substrate's water-holding capacity and the efficiency of rainwater runoff regulation. Substrates with a combined layered structure demonstrate a reduction in peak surface runoff of up to 19.52% and an increase in runoff retention time of up to 24 minutes, depending on the configuration of the layers, which indicates the potential

to improve hydrological efficiency without a significant increase in the material intensity of the system.

The top layer of the substrate makes the greatest contribution to the formation of AP and EP potential. This is due to the presence of organic components (compost, peat, organic additives), the production and transport of which are accompanied by emissions of nitrogen and phosphorus compounds. Furthermore, during the system's operation, organic matter undergoes mineralisation, which can lead to the release of nutrients and increase the risk of eutrophication and acidification of natural ecosystems (Silva *et al.*, 2024). An additional source of environmental impact is bark mulch, which is used to form a surface cover, suppress unwanted vegetation and support the growth of target plant species. Its contribution is most noticeable in the AP and EP potential categories, which is explained by the biochemical decomposition of organic matter and the possible release of nutrients (Fér *et al.*, 2022). In addition, the stages of harvesting, preparation and transport of mulch are accompanied by additional greenhouse gas emissions, which account for its contribution to the GWP100 potential. Although mulching is an effective and economically viable method for protecting soil cover and stabilising RG vegetation, it is advisable to consider alternative materials with a smaller environmental footprint. In particular, the use of mulch produced on-site from shredded wood residues or other organic waste generated during the maintenance of green spaces is promising. In some cases, the use of recycled materials is also possible, such as rubber mulch from recycled tyres, as demonstrated by A. Mohajerani *et al.* (2020).

When using bark mulch, it is advisable to limit its application to the initial stage of RG vegetation establishment, when it is necessary to stabilise the soil and promote plant rooting. Further regular renewal of the mulch layer throughout the entire operational period of the system should only be carried out if there is an actual need to maintain the proper condition of the vegetation cover. Polymer elements in the RG are present in limited quantities (in particular, geotextiles or auxiliary protective layers), so their contribution to the overall environmental impact is relatively insignificant compared to the mineral and organic components of the system. Transport processes also make a significant contribution to all the environmental impact categories under investigation. This is due to the use of fossil fuels during the transport of construction materials to the project site. These emissions directly influence the GWP100 potential and also contribute to the AP and, to a lesser extent, the AD categories.

The distribution of the contribution of structural elements and transport costs to the overall environmental impact of GR across the main LCA categories (Fig. 9) demonstrates a different impact structure, determined by the specific design features of the system. The largest contribution to the EP potential is provided by the mulch or organic surface layer, which is associated with the presence of organic matter and the potential release of nutrients.

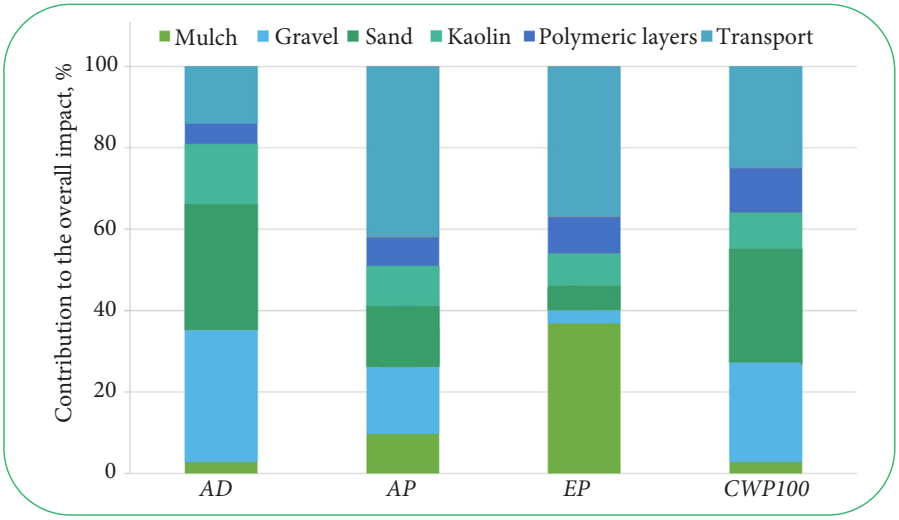

Figure 9. Breakdown of the contribution of structural elements and transport costs to the overall environmental impact of GR by main LCA categories

Source: created by the authors based on their own modelling in OpenLCA

The gravel used in the drainage layer makes the largest contribution to the AD, AP and GWP100 categories, which is explained by the energy-intensive processes of extraction, crushing and transport of mineral materials. Similar findings are reported in life cycle studies of natural aggregates conducted by J. Los Santos-Ortega *et al.* (2025), who show that the production of 1 tonne of coarse gravel aggregate is associated with emissions of approximately 4.3 kg CO_2-eq, along with significant fossil energy consumption (over 100 MJ) and resource use. These results are generally consistent with the present study, although differences in emission magnitude can be attributed to variations in processing technologies, system boundaries, and inventory assumptions. Nevertheless, both studies confirm that

gravel production is a key hotspot in terms of environmental impact, driven by high energy demand and associated CO_2 emissions, which contribute substantially to AD, AP, and GWP100 impact categories.

Quartz sand in the GR also makes a significant contribution to the AD and GWP100 potential, due to similar processes involved in its extraction and preparation. Kaolin, used as a mineral additive to the substrate, is characterised by a relatively uniform contribution to all the impact categories considered. Unlike RG, in the environmental impact profile of GR, the polymer and waterproofing layers, which are necessary to ensure the watertightness of the roof structure, play a more prominent role. These observations are consistent with the findings of A. Al Rashid *et al.* (2024), who reported high energy demand and greenhouse gas emissions associated with the use of polymer and waterproofing materials in green roof systems. However, the results obtained suggest that the relative contribution of these components may vary depending on the system configuration and layer thickness. Furthermore, E. Sierka *et al.* (2026), in their study of the impact of extensive GR based on an LCA of a 4 m² test sample carried out using OpenLCA software and the PEF (Product Environmental Footprint) database, demonstrated that the production of structural components, particularly synthetic materials (polyvinyl chloride and polypropylene), is a key factor in the deterioration of the system's environmental performance. The authors found that removing the vapour and thermal insulation layers from the GR model reduces CO_2-eq emissions by 28.36 kg compared to the baseline scenario, highlighting the significant potential for optimising the material structure of GR to reduce their environmental impact.

Transport processes, as in the case of RG, make an additional contribution to all categories of environmental impact, since the transportation of materials involves fuel consumption and associated emissions of pollutants. J.L. Osorio-Tejada *et al.* (2022) reported that, within LCA-based road freight transport modelling, emissions from a diesel van with a payload of up to 1.3 tonnes are approximately 0.142 kg CO_2eq/km, demonstrating the significant contribution of the transport phase to the overall carbon footprint. Their study applied a diesel-fuel transport scenario, ensuring consistency with standard LCA modelling practices. These results are methodologically consistent with the present study, as both confirm that transport activities represent a measurable and non-negligible contributor to the total environmental impact within LCA models. This supports the inclusion of transport-related emissions across all impact categories considered, particularly GWP100, AP, and AD.

Based on the results obtained, it is advisable to recommend that the further standardisation of LCA studies of GR and RG should involve the use of standardised transport scenarios, harmonised baseline datasets, uniform impact assessment methods, and standardised formats for presenting results. Such an approach will reduce methodological uncertainty and improve the comparability of environmental assessments of different types of green infrastructure across varying geographical and climatic conditions. The need for harmonisation is strongly supported by Y. Zhu *et al.* (2023), who identify the lack of methodological consistency as a key limitation in comparative LCA studies across different systems and regions. The authors emphasise that differences in system boundaries, life-cycle inventory data, impact assessment methods and reporting structures significantly reduce the reliability of comparisons between studies. Their conclusions, therefore, align with the findings of this study, highlighting the importance of establishing a standardised methodological framework specifically designed for the assessment of GR and RG.

The LCA results obtained demonstrate differing environmental performance between RG and GR systems, which correlates directly with the European Union's strategic priorities regarding climate neutrality and the development of nature-based solutions. In particular, it has been established that RG systems have a lower impact during the operational phase due to their passive mode of operation, lack of energy consumption, and the use of natural processes of infiltration and surface runoff retention. This is consistent with EU provisions prioritising solutions that minimise energy consumption and enhance the ecosystem functions of the urban environment. In contrast, GR demonstrate higher operational environmental impacts, as confirmed by LCA results, primarily due to the continuous energy consumption of technical systems. This partly contradicts EU requirements regarding the reduction of energy consumption throughout the life cycle, but at the same time aligns with other policy objectives, in particular improving the energy efficiency of buildings and reducing thermal loads. The patterns identified are consistent with the European Green Deal (European Commission, 2019), which aims to reduce carbon emissions and improve resource efficiency, as well as with the EU Strategy on adaptation to climate change (European Commission, 2021), which supports the implementation of nature-based solutions to mitigate climate risks. In addition, Committee of the Regions (2013) explicitly highlights the effectiveness of systems that regulate the water balance and reduce anthropogenic pressure. Thus, the LCA results confirm that RG are more aligned with EU priorities regarding low-energy nature-based solutions, whilst GR, despite higher operational impacts, provide other ecosystem and energy benefits at the building level. This highlights the value of using LCA as a tool for quantitatively comparing the environmental performance of different types of green infrastructure within the context of EU policies.

Conclusions

The study carried out a comparative assessment of the environmental impact of two types of green urban infrastructure systems, RG and GR, using the LCA method within the OpenLCA software environment. The modelling covered the main stages of the systems' life cycle – construction, operation and end-of-life – using the ELCD 3.2 reference

database and a design life of 15 years. The results indicate that the RG system is characterised by a higher environmental impact during the construction phase, due to the significant mass of mineral materials, particularly quartz sand and gravel, required to form the filtration and drainage layers. In the AD and GWP100 categories, the main contribution comes from the processes of extraction, transport and preparation of these materials. During the operational phase, the RG demonstrates relatively low impact indicators due to the predominantly passive nature of its operation, which does not require significant energy resources.

The GR system, by contrast, is characterised by lower environmental impact values during the construction phase, which is explained by the structure's lower material intensity and the use of thinner substrate layers. However, during operation, the GR generates higher impact values, which are linked to the need for regular maintenance and the operation of auxiliary engineering systems. As a result, the total global warming potential for GR is 392 kg CO_2-eq per 1 m^2 over 15 years, whereas for RG it is 288 kg CO_2-eq. An analysis of the structure of environmental impact showed that for RG, the largest contribution to the AD, AP, and GWP100 indicators comes from the mineral components of the structure, primarily quartz sand, as well as transport processes. In the GR, polymer and waterproofing materials play a significant role, the production of which is accompanied by increased energy consumption and corresponding greenhouse gas emissions.

From a practical point of view, the study's results confirm the advisability of the integrated use of various types of green structures in the urban environment, depending on the functional requirements of the area. RG systems are more effective for passive surface runoff management and reducing operational environmental impacts, whilst GR systems provide additional benefits related to improved thermal insulation performance of buildings and microclimate regulation. Furthermore, the study's results confirm the importance of applying standardised approaches to defining system boundaries, selecting databases and impact assessment methods in LCA studies of green structures. Standardising such approaches will help improve the comparability of results, justify design decisions and shape effective policies for the sustainable development of urban green infrastructure.

Acknowledgements
None.

Funding
None.

Conflict of Interest
None.

References

[1] Ahmadi, A.W., Balkaya, N., & Vrielink, S. (2025). Evaluating the life cycle assessment of rain gardens and green walls for a sustainable environment. *Research Square*. doi: 10.21203/rs.3.rs-7779844/v1.

[2] Al Rashid, A., Khan, S.A., & Koç, M. (2024). Life cycle assessment on fabrication and characterization techniques for additively manufactured polymers and polymer composites. *Cleaner Environmental Systems*, 12, article number 100159. doi: 10.1016/j.cesys.2023.100159.

[3] Bagheri, K., & Davani, H. (2024). An integrated framework for stormwater management and life cycle assessment of rainwater harvesting: A comparative study of two underserved communities. *Science of The Total Environment*, 956, article number 177220. doi: 10.1016/j.scitotenv.2024.177220.

[4] Committee of the Regions. (2013). *Opinion of the committee of the regions: Green infrastructure – enhancing Europe's natural capital*. Retrieved from https://edz.bib.uni-mannheim.de/edz/doku/adr/2013/cdr-2013-4577-en.pdf.

[5] European Commission. (2019). *The European green deal. (COM(2019) 640 final)*. Retrieved from https://surl.li/iftqgh.

[6] European Commission. (2021). *Forging a climate-resilient Europe – the new EU strategy on adaptation to climate change (COM(2021) 82 final)*. Retrieved from https://eur-lex.europa.eu/legal-content/EN/TXT/PDF/?uri=CELEX:52021DC0082.

[7] Fér, M., Nikodem, A., Trejbalová, S., Klement, A., Pavlů, L., & Kodešová, R. (2022). How various mulch materials can affect the soil hydro-physical properties. *Journal of Hydrology and Hydromechanics*, 70(3), 269-275. doi: 10.2478/johh-2022-0016.

[8] Gan, L., Garg, A., Huang, S., Wang, J., Mei, G., & Zhang, K. (2025). Experimental and numerical investigation on rainwater management of dual substrate layer green roofs using biochar-amended soil. *Biomass Conversion and Biorefinery*, 15(20), 27387-27396. doi: 10.1007/s13399-022-02754-0.

[9] Hu, X., & Gu, F. (2025). Urban rainwater resource utilization: A sustainable environmental impact assessment using life cycle assessment (LCA) and water balance model. *Desalination and Water Treatment*, 322, article number 101094. doi: 10.1016/j.dwt.2025.101094.

[10] ISO 14040:2006. (2006). *Environmental management – life cycle assessment – principles and framework*. Retrieved from https://www.iso.org/obp/ui/en/#iso:std:iso:14040:ed-2:v1:en.

[11] ISO 14044:2006. (2006). *Environmental management – life cycle assessment – requirements and guidelines*. Retrieved from https://www.iso.org/obp/ui#iso:std:iso:14044:ed-1:v1:en.

[12] Karabay, K., Öztürk, H., Ceylan, E., & Ayral Çınar, D. (2024). Assessment of urban rain gardens within climate change adaptation and circularity challenge. In *Nature-based solutions for circular management of urban water* (pp. 51-72). Cham: Springer. doi: 10.1007/978-3-031-50725-0_4.

[13] Kravchenko, M., Trach, Y., Trach, R., Tkachenko, T., & Mileikovskyi, V. (2024). Behaviour and peculiarities of oil hydrocarbon removal from rain garden structures. *Water*, 16(13), article number 1802. doi: 10.3390/w16131802.
[14] Kravchenko, M.V., & Tkachenko, T.M. (2024). Development of methods for quantifying the effectiveness of rain garden design in the context of rainwater management. *Environmental Safety and Natural Resources*, 50(2), 19-35. doi: 10.32347/2411-4049.2024.2.19-35.
[15] Los Santos-Ortega, J., Fraile-García, E., & Ferreiro-Cabello, J. (2025). Environmental assessment of natural coarse aggregate production in gravel pits – assessing CO_2 offsets through vine cultivation. *Applied Sciences*, 15(4), article number 1868. doi: 10.3390/app15041868.
[16] Mohajerani, A., *et al.* (2020). Recycling waste rubber tyres in construction materials and associated environmental considerations: A review. *Resources, Conservation and Recycling*, 155, article number 104679. doi: 10.1016/j.resconrec.2020.104679.
[17] Osorio-Tejada, J.L., Llera-Sastresa, E., & Scarpellini, S. (2022). Environmental assessment of road freight transport services beyond the tank-to-wheels analysis based on LCA. *Environment, Development and Sustainability*, 26(1), 421-451. doi: 10.1007/s10668-022-02715-7.
[18] Ostovar, A., Hajj, E., Mehdizadeh, G., & Hand, A. (2026). Environmental analysis of emulsified asphalt products in the United States: A comparative cradle-to-gate life cycle assessment. *Sustainability*, 18(4), article number 1821. doi: 10.3390/su18041821.
[19] Pamu, Y., Kumar, V.S.S., Shakir, M.A., & Ubbana, H. (2022). Life cycle assessment of a building using Open-LCA software. *Materials Today: Proceedings*, 52, 1968-1978. doi: 10.1016/j.matpr.2021.11.621.
[20] Peng, Y., Wang, Y., Chen, H., Wang, L., Luo, B., Tong, H., Zou, Y., Lei, Z., & Chen, S. (2024). Carbon reduction potential of a rain garden: A cradle-to-grave life cycle carbon footprint assessment. *Journal of Cleaner Production*, 434, article number 139806. doi: 10.1016/j.jclepro.2023.139806.
[21] Perivoliotis, D., Arvanitis, I., Tzavali, A., Papakostas, V., Kappou, S., Andreakos, G., Fotiadi, A., Paravantis, J.A., Souliotis, M., & Mihalakakou, G. (2023). Sustainable urban environment through green roofs: A literature review with case studies. *Sustainability*, 15(22), article number 15976. doi: 10.3390/su152215976.
[22] Pique, L., Blanchet, P., & Breton, C. (2023). Global warming potential comparison between green and conventional roofs in a cold climate using life cycle assessment. *Journal of Cleaner Production*, 420, article number 138314. doi: 10.1016/j.jclepro.2023.138314.
[23] Pons Fiorentin, D., Martín-Gamboa, M., Rafael, S., & Quinteiro, P. (2024). Life cycle assessment of green roofs: A comprehensive review of methodological approaches and climate change impacts. *Sustainable Production and Consumption*, 45, 598-611. doi: 10.1016/j.spc.2024.02.004.
[24] Popowicz, M., Katzer, N.J., Kettele, M., Schöggl, J.-P., & Baumgartner, R.J. (2025). Digital technologies for life cycle assessment: A review and integrated combination framework. *The International Journal of Life Cycle Assessment*, 30(3), 405-428. doi: 10.1007/s11367-024-02409-4.
[25] Rizzo, G., Cirrincione, L., La Gennusa, M., Peri, G., & Scaccianoce, G. (2023). Green roofs' end of life: A literature review. *Energies*, 16(2), article number 596. doi: 10.3390/en16020596.
[26] Salah, G.M.J.A., & Romanova, A. (2021). Life cycle assessment of felt system living green wall: Cradle to grave case study. *Environmental Challenges*, 3, article number 100046. doi: 10.1016/j.envc.2021.100046.
[27] Scolaro, T.P., & Ghisi, E. (2022). Life cycle assessment of green roofs: A literature review of layers, materials and purposes. *Science of The Total Environment*, 829, article number 154650. doi: 10.1016/j.scitotenv.2022.154650.
[28] Sečkár, M., Schwarz, M., Golej, J., & Veverková, D. (2025). Life cycle assessment and software tools comparison. *International Journal of Environment and Sustainable Development*, 24(2), 145-162. doi: 10.1504/IJESD.2025.145333.
[29] Sierka, E., Bedlińska, Z., Biela, M., Chen, H.-Y., Larysz, K., & Stolarczyk, M. (2026). Life cycle assessment of an experimental extensive green roof – a case study. *Archives of Environmental Protection*, 52(1), 136-146. doi: 10.24425/aep.2026.158389.
[30] Silva, M.E.F., Saetta, R., Raimondo, R., Costa, J.M., Ferreira, J.V., & Brás, I. (2024). Forest waste composting – operational management, environmental impacts, and application. *Environmental Science and Pollution Research*, 32(48), 27608-27624. doi: 10.1007/s11356-024-32279-0.
[31] Souza, B.D.M., Oliveira, R.D., Nascimento, R.S.D., & Medeiros, K.T.D.B. (2025). Comparative life cycle assessment in wastewater treatment plants: Scenario analysis with OpenLCA. *Revista Brasileira de Ciências Ambientais*, 60, article number e2330. doi: 10.5327/Z2176-94782330.
[32] Tams, L., Nehls, T., & Calheiros, C.S.C. (2022). Rethinking green roofs- natural and recycled materials improve their carbon footprint. *Building and Environment*, 219, article number 109122. doi: 10.1016/j.buildenv.2022.109122.
[33] Vaghela, J.R., Valaki, J.B., Joshi, H.I., Thanki, S.J., & Pandey, A.B. (2024). Comparative analysis on sustainability parameters of traditional tool manufacturing processes using life cycle. *Journal of Engineering Science and Technology Review*, 17(2), 23-34. doi: 10.25103/jestr.172.04.

[34] Xing, W., Tam, V.W., Le, K.N., Hao, J.L., & Wang, J. (2022). Life cycle assessment of recycled aggregate concrete on its environmental impacts: A critical review. *Construction and Building Materials*, 317, article number 125950. doi: 10.1016/j.conbuildmat.2021.125950.
[35] Zhu, Y., Ma, H., Sha, C., Yang, Y., Sun, H., & Ming, F. (2023). Which strategy among avoid, shift, or improve is the best to reduce CO2 emissions from sand and gravel aggregate transportation? *Journal of Cleaner Production*, 391, article number 136089. doi: 10.1016/j.jclepro.2023.136089.

Порівняльна оцінка життєвого циклу конструкції дощового саду та зеленого покриття із застосуванням програмного середовища OpenLCA

Марина Кравченко
Доктор технічних наук, професор
Київський національний університет будівництва і архітектури
03037, просп. Повітряних Сил, 31, м. Київ, Україна
https://orcid.org/0000-0003-0428-6440
Тетяна Ткаченко
Доктор технічних наук, професор
Київський національний університет будівництва і архітектури
03037, просп. Повітряних Сил, 31, м. Київ, Україна
https://orcid.org/0000-0003-2105-5951
Леся Василенко
Кандидат технічних наук, доцент
Київський національний університет будівництва і архітектури
03037, просп. Повітряних Сил, 31, м. Київ, Україна
https://orcid.org/0000-0003-4201-5481

Анотація. Глобальні кліматичні зміни та посилення урбанізації посилюють тиск на міську інфраструктуру та природні ресурси, підкреслюючи важливість впровадження зеленої інфраструктури для підвищення стійкості міст та зменшення впливу на довкілля. Метою дослідження було проведення порівняльної оцінки життєвого циклу дощового саду та зеленого даху за допомогою програмного забезпечення OpenLCA (версія 2.6, 2025) шляхом моделювання їхніх екологічних показників, що дозволило визначити ключові кліматичні та ресурсні параметри їхньої ефективності. Для моделювання було зібрано дані на всіх етапах життєвого циклу споруд та нормалізовано їх на квадратний метр за 15-річний період експлуатації. Основними категоріями екологічного впливу було обрано потенціал глобального потепління, потенціал евтрофікації, потенціал підкислення та вичерпання абіотичних ресурсів. Результати продемонстрували різний баланс екологічних наслідків на різних етапах життєвого циклу. Зелений дах характеризувався меншим впливом на етапі будівництва (наприклад, потенціал глобального потепління становить 50 кг CO2-екв./м^2) завдяки використанню збірних модульних блоків. Натомість дощові сади продемонстрували менший вплив на етапі експлуатації (130 проти 320 кг CO2-екв./м^2 для зелених дахів за 15 років) завдяки пасивній фільтрації дощового стоку та мінімальним вимогам до технічного обслуговування. Значна частина впливу на етапі будівництва пов'язана з використанням кварцового піску як ґрунтової добавки для дощових садів та мульчі з деревної кори для покриття ґрунту, що пригнічує небажану рослинність та сприяє закріпленню цільової рослинності. На етапі закінчення терміну експлуатації обидві системи продемонстрували мінімальний загальний вплив на довкілля, причому більшість показників залишалися незначними. Результати підтвердили, що жодна з досліджених зелених інфраструктурних систем не є універсально оптимальною; їхня ефективність залежить від конкретного етапу життєвого циклу та місцевих умов, що підкреслює необхідність враховувати місцеві цілі та пріоритети під час вибору системи

Ключові слова: зелені споруди; аналіз впливу протягом життєвого циклу; моделювання на основі сценаріїв; потенціал глобального потепління; потенціал евтрофікації; потенціал підкислення; вичерпання абіотичних ресурсів

Vol. 17, No. 1
2026

Ecological Safety and Balanced Use of Resources

ISSN (print) 2415-3184, ISSN (online) 2522-9508
Journal homepage: https://esbur.com.ua/en

Received: 12.11.2025. Revised: 06.05.2026. Accepted: 12.06.2026. Published: 30.06.2026.

UDC 502.3:556

DOI: 10.63341/esbur/1.2026.144

Disposal of polluted bentonite clays as a means of minimising environmental risk

Halyna Sakalova*
Doctor of Technical Sciences, Professor
Vinnytsia National Technical University
21021, 95 Khmelnytske Shose Str., Vinnytsia, Ukraine
https://orcid.org/0000-0002-9610-0967

Roman Boiko
Postgraduate Student
Vinnytsia National Technical University
21021, 95 Khmelnytske Shose Str., Vinnytsia, Ukraine
https://orcid.org/0009-0007-3206-0533

Olena Mokrousova
Doctor of Technical Sciences, Professor, Head of the Department
Kyiv National University of Technologies and Design
01011, 2, Mala Shyianovska Str., Kyiv, Ukraine
State University of Trade and Economics
02156, 19, Kyoto Str., Kyiv, Ukraine
https://orcid.org/0000-0003-1943-8048

Tetiana Sydoruk
Associate Professor
Vinnytsia National Technical University
21021, 95 Khmelnytske Shose Str., Vinnytsia, Ukraine
https://orcid.org/0000-0002-5489-6397

Abstract. The effective disposal of spent clay sorbents reduce the anthropogenic impact on the environment and to improve recycling technologies for highly dispersed clays. Study aimed to investigate the sorption of organic dye molecules by spent bentonite, previously saturated with chromium (III) ions, with possible subsequent utilisation of the bentonite in pigment compositions. The study was based on a comparative analysis of natural, modified and spent montmorillonite using thermogravimetric analysis, the determination of the colloidal-chemical characteristics of the dispersions, the construction of adsorption isotherms and spectrophotometric monitoring of dye concentrations. Changes in the structure, surface charge, interplanar distance, specific surface area and sorption activity of the samples were analysed. The study established that the saturation of montmorillonite with chromium (III) ions does not lead to a significant deterioration in its properties. This study demonstrated that spent bentonite retains its porous structure, active sorption sites and the ability to effectively adsorb anionic dyes over a wide range of concentrations. The study established that chromium-containing sites can enhance the fixation of dye molecules through complex formation and interaction with the functional groups of the adsorbates. The characteristics of the adsorption of anionic green, blue and black dyes have been analysed, in particular the influence of molecular structure, molecular size and spatial hindrance on adsorption. The study developed an approach for the utilisation of spent bentonite as a secondary mineral base to produce organo-mineral pigment compositions without additional chemical modification. The practical value of these

Suggested Citation: Sakalova, H., Boiko, R., Mokrousova, O., & Sydoruk, T. (2026). Disposal of polluted bentonite clays as a means of minimising environmental risk. *Ecological Safety and Balanced Use of Resources*, 17(1), 144-151. doi: 10.63341/esbur/1.2026.144.

*Corresponding author (*sakalovag@gmail.com*)

results is determined by their potential application by specialists in environmental safety, wastewater treatment, materials science and pigment coating technologies

Keywords: sorption; spent sorbents; montmorillonite; dyes; chromium (III) ions

Introduction

Cobalt-based technologies are the most promising method for treating surface water and wastewater and are widely used in many countries. The main advantages of highly dispersed clays as sorbents are their high efficiency, availability and relatively low cost. Given this last point, the regeneration and reuse of such sorbents is often impractical; consequently, these materials are usually landfilled or incorporated into soil mixtures or building materials, provided that the spent sorbents do not contain toxic pollutants.

Review of studies shows that highly dispersed clays are widely used in various industries (building materials, nanocomposites, fillers, etc.) (Shamsuddin *et al.*, 2025). Their ease of processing, environmental friendliness and cost-effectiveness are constantly fuelling growing interest in the use of clay for the development of a wide range of products. Considerable experience has been gained in the use of natural highly dispersed clays and their modified forms for the sorption-based treatment of wastewater to remove ammonium ions, heavy metals (Ranskiy *et al.*, 2025) and organic pollutants (Alhalafi, 2026), in particular oil and petroleum products (Dong *et al.*, 2024). The main mineral in highly dispersed clays – montmorillonite – has found widespread use in fillers and multifunctional materials due to its specific colloidal-chemical properties and crystalline structure. A. Zaiets & O. Andreyeva (2024) presented the potential for using clay minerals with sorption properties in the preparation of fat and filler compositions for the treatment of semi-finished leather products. An overview of all areas of application for clay-based sorbent minerals in the leather industry is provided by A. Thomasset & S. Benayoun (2024), in which the authors examined in detail the balance between the technological advantages of traditional methods and modern environmental requirements.

The chemical composition and characteristics of the crystal structure of montmorillonite (bentonite), as determined by the ratio of aluminium- to silicon-oxygen layers, give rise to a complex set of sorption, exchange and coagulation phenomena, as well as a capacity for dispersion, which is effective when filling polar polymers, in particular R. Kryklyvyi *et al.* (2022) proposed a formulation for filling polystyrene-butadiene rubbers and noted an improvement in the physicochemical properties of the polymeric materials due to the use of bentonite. Use of montmorillonite for filling polyester premixes is also promising, as it can increase the content of the dispersed filler and improve its aggregation stability. S. Paszkiewicz *et al.* (2024) synthesised block copolymers and used both carbon-based and mineral sorbent materials as fillers.

A.A. Rahimi & F. Alihosseini (2022) proposed using a dye-saturated clay adsorbent, obtained following the treatment of dyeing effluent, as a pigment for textile printing. It is worth noting that the methods described relate to the use of native clays that were further treated with complex compounds containing heavy metals, as outlined in the review by M. Chokri *et al.* (2025), which describes the industrial application of native and modified bentonite clays in nanocomposites, water treatment, the oil and gas sector, and catalysis; whilst the question of the analogous use of spent clay-based sorbents, which contain pollutants – heavy metal ions – within their structure, remains a matter of debate. M. Malovanyy *et al.* (2021) noted that economic factors are decisive in determining the feasibility of disposing of or reusing sorbents.

Although highly dispersed clays are widely used in many sectors of the economy, the limited scope of scientific research results in a low level of utilisation of spent clay-based sorbents in the production and processing of natural and synthetic polymers, fillers and pigment sorbent bases, although many experts consider this field to be highly promising. In view of this, the industrial application of spent clay-based sorbents and the development of composite and multifunctional materials are topical and promising areas of research. The study aimed to evaluate the effectiveness of sorption-based wastewater treatment for the removal of organic dyes using spent bentonite activated with chromium (III) ions, followed by a reduction in environmental risk through its utilisation in pigment compositions.

Materials and Methods

This paper presents a comparative study of the ability of montmorillonite, modified with chromium (III) complex compounds, and spent montmorillonite that has sorbed chromium (III) ions from waste water, to subsequently adsorb anionic dyes. It also analyses possible changes in the clay structure following the sorption process. The analysis of the studies was conducted by comparing the properties of three samples.

Sample 1 (control): Natural bentonite clay with a montmorillonite content of 85%; Sample 2: Modified montmorillonite following treatment with a solution of chromium (III) sulphate complex (dosage 10.0% by mass of dry mineral, calculated as Cr_2O_3); Sample 3: Spent montmorillonite with a residual chromium (III) content of 7-8 % by mass of the dry mineral, calculated as Cr_2O_3. The sorption capacity of modified montmorillonite and the mechanism of adsorption of synthetic anionic dyes on the surface of the mineral sorbent were investigated for dispersions prepared based on samples 2 (modified montmorillonite) and 3 (spent montmorillonite).

The modification of the second sample involved the sequential treatment of bentonite from the Cherkasy deposit (85% montmorillonite content) with sodium carbonate (6.0 per cent by mass of the dry mineral) (Na^+ – MMT) and a solution of hydroxochrome complexes in the form of basic chromium sulphate $Cr_2(SO_4)\ n(OH)_{6-2n}$ (Cr_2O_3 content – 25.6%, basicity – 33%). The chromium cation content in the sample was a maximum of 10% on a Cr_2O_3 basis. As a result of the modification, montmorillonite modified with hydroxochromium complexes – Cr^{3+}-montmorillonite (Cr^{3+}-MMT) was obtained. Spent montmorillonite (sample 3) was treated with a sodium carbonate solution (6.0 % by mass of the dry mineral) to convert it into a dispersed form. The chromium cation content in the sample was a maximum of 8% on a Cr_2O_3 basis. The colloidal and rheological properties of the bentonite-based dispersions were evaluated using standard methods (Bondaryeva *et al.*, 2022). The adsorption of dyes and, before that, chromium ions for sample 3 with a stationary sorbent bed was conducted using a glass column with model solutions and a bentonite bed weighing 15-20 g (Fig. 1).

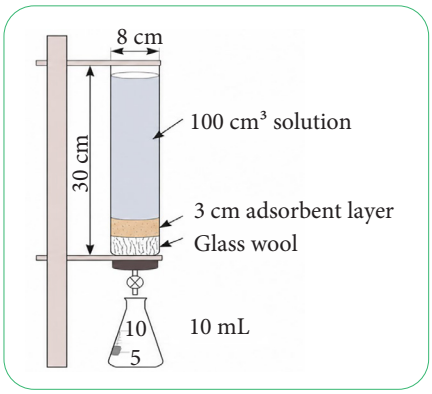

Figure 1. Schematic diagram of a fixed-bed montmorillonite adsorption system

Source: I. Andriulaityte *et al.* (2024)

Sorption of anionic dyes from the dispersions of samples 2 and 3 onto the surface of montmorillonite was investigated as follows. A 20% paste dispersion of the test sample was used, containing 0.1 g of the mineral component. To this dispersion, 100 ml each of anionic dye solutions with concentrations ranging from 2.5×10^{-5} to 1.0×10^{-3} mol/l were added. The resulting mixture was shaken periodically. The shaking duration was 24 hours. The precipitates were then separated from the liquid phase by centrifugation (8,000 rpm). The concentration of anionic dyes on the surface of montmorillonites was determined by measuring the intensity of the optical absorption spectra of the initial and equilibrium solutions in the wavelength range 570-580 nm (Ismail *et al.*, 2022). A Specord UV-V is spectrophotometer (Germany) was used. A calibration curve was employed to determine the concentration. The equilibrium concentration of the dyes was determined in the resulting solution. Anionic black, anionic dark green and anionic blue were used as dyes.

A comparative assessment of the surface structure of modified and spent bentonite samples against native clay was conducted in previous studies, described in greater detail in the paper by H. Sakalova *et al.* (2025). To determine the surface structure of the samples, a comprehensive thermal analysis was first conducted using a Q-1500 derivatograph from the "Paulik-Erdei" system, connected to a personal computer. The sample was heated in an air atmosphere to a temperature of 1,000°C. The heating rate of the sample was 5°C per minute. The mass of the enriched clay sample was 500 mg. Aluminium oxide served as the reference substance.

Results and Discussion

Preliminary thermogravimetric studies of montmorillonites were used to assess their surface structure and predict their properties in a dispersed form. The results of the comprehensive thermal analysis of samples 1, 2 and 3 are summarised in Table 1.

Table 1. Results of a comprehensive thermal analysis of montmorillonite samples

Sample	Stage	Temperature range, °C	Mass loss, %	Interpretation
Sample 1 (pure montmorillonite)	I	20-194	9.59	Release of physically bound water
	II	194-280	1.26	Removal of interlayer water
	III	280-800	3.82	Dehydroxylation
Sample 2. Mixture of montmorillonite with chromium (III) sulfate crystal hydrate	I	20-202	7.57	Physically bound water release
	II	202-306	2.01	Loss of crystallisation water
	III	306-800	7.64	Clay structure destruction
Sample 3. Spent montmorillonite with Cr^{3+} ions content (Cr_2O_3 7-8%)	I	20-190	7.50	Bound water release
	II	190-280	1.78	Interlayer water removal
	III	280-800	5.03	Chromium compound decomposition

Source: developed by the authors

Loss of the first layer of water, which is coordinatively bound to the exchange cations Ca^{2+} and Mg^{2+}, occurs in the range 20-194°C (the first stage of thermolysis). The next layer of water is lost in the range 194-280°C (the second stage of thermolysis) (Kochubei *et al.*, 2022). The intense mass loss (9.59%) observed for the pure montmorillonite sample (sample 1) in the temperature range 20-280°C corresponds to the release of residual physically bound water. In this range, the loss of interlayer water, which is coordinatively bound to the exchangeable cations of montmorillonite, is also possible. The mass loss (3.82%) of the bentonite sample in the 280-800°C range (the third stage of thermolysis) corresponds to dehydroxylation (loss of constitutional water) associated with the destruction of the structure of the clay mineral present in the sample.

Rapid loss of mass (7.57%) of sample 2 in the range 20-202°C (the first stage of thermolysis) corresponds to the release of physically bound water and part of the interlayer water. The mass loss (2.01%) of sample 2 in the 202-306°C range (the second stage of thermolysis) is associated with the release of residual interlayer water from montmorillonite and the loss of crystallisation water from $Cr_2(SO_4)_3 \cdot 6H_2O$. The mass loss (7.64%) of sample 2 in the 280-800 °C range (the third stage of thermolysis) corresponds to the destruction of the clay mineral's structure with the release of constitutional water. In this temperature range, the decomposition of chromium sulphate also occurs, resulting in the formation of volatile decomposition products (Singh *et al.*, 2021).

Similar destructive processes occurred during the heating of sample 3. The significant mass loss (7.5%) of sample 3 in the 20-190°C range (the first stage of thermolysis) corresponds to the release of physically bound water and some of the interlayer water from the bentonite. The mass loss (1.78%) of sample 3 in the 190-280°C range (the second stage of thermolysis) was primarily associated with the release of residual interlayer water from montmorillonite. The mass loss (5.03%) of sample 3 in the 280-800°C range (the third stage of thermolysis) corresponded to the destruction of the clay mineral's structure with the release of constitutional water. In this temperature range, the decomposition of chromium-containing compounds also took place, resulting in the formation of volatile decomposition products. The more significant mass loss of the spent sample 3 during the third stage of thermolysis (5.03%) compared with the natural montmorillonite sample (3.82%) indicates the presence of a certain amount of sorbed chromium (III) compounds, possibly including sulphates. The results of the thermal analysis suggest the possibility of sulphate sorption on the surface of bentonite particles, which decompose during heating, releasing gaseous products. Covering decomposition mechanism of $Cr_2(SO_4)_3$ (reaction 1) and the difference in mass loss between samples 1 and 2 during the third stage of thermolysis, a control calculation of the chromium (III) oxide content for sample number 3 (spent clay mineral) can be performed:

$$Cr_2(SO_4)_3 \cdot 6H_2O \rightarrow Cr_2O_3 + 3SO_3\uparrow + 6H_2O\uparrow. \quad (1)$$

According to stoichiometric calculations, chromium ion content, expressed as Cr_2O_3, in the spent clay sample is 7.25% (Sakalova *et al.*, 2025).

Comparison of the results of thermal analysis of the three samples leads to the following conclusion:

- for samples 2 and 3, similar rheological characteristics are to be expected at low temperatures (20-190°C);
- interlayer water content, which affects the degree of clay swelling, is approximately the same for all samples;
- experiments indicate that chromium ions are more strongly bound in spent bentonite; therefore, the chromium ions in sample 3 may also act as complexing agents;
- comparative analysis of samples 2 and 3 across all the temperature ranges studied indicates that they have a similar porous structure.

Characteristics of the sorbents in dispersed form are given in Table 2. The table presents the characteristics of samples 2 (modified bentonite) and 3 (spent bentonite), which were used for the subsequent adsorption of dyes.

Table 2. Colloidal and chemical characteristics of montmorillonite dispersions

Sample number	Base, OH/Cr	Surface charge, μC/cm²	Inter-plane distance (d_{001}), Å	Specific area (S), m²/r	pH	Specific electrical conductivity (K), 10^{-4} S/cm	Zeta potential (ζ), mW
2	1.5	1.07	16.8	280	4.9	3.70	+32.3
3	1.3	1.1	17.4	260	4.5	3.43	+30.7

Source: developed by the authors

Obtained sorbent dispersions are characterised by a high specific surface area and a positive charge on the sorption surface. The basicity values are consistent with the results of thermal analysis, which indicate similar amounts of absorbed OH groups and chromium ions on the montmorillonite surface; furthermore, the dispersions based on samples 2 and 3 have approximately the same pH and specific electrical conductivity values. Similar values for surface charge, ζ-potential, interlayer distance and specific surface area indicate that the preliminary adsorption of chromium (III) ions does not lead to a significant deterioration in the colloidal-chemical properties of the clay sorbent. The adsorption isotherms for anionic dyes on the surface of modified montmorillonite (sample 2) and spent montmorillonite (sample 3), shown in Figure 2, generally indicate a similar adsorption behaviour for the test samples.

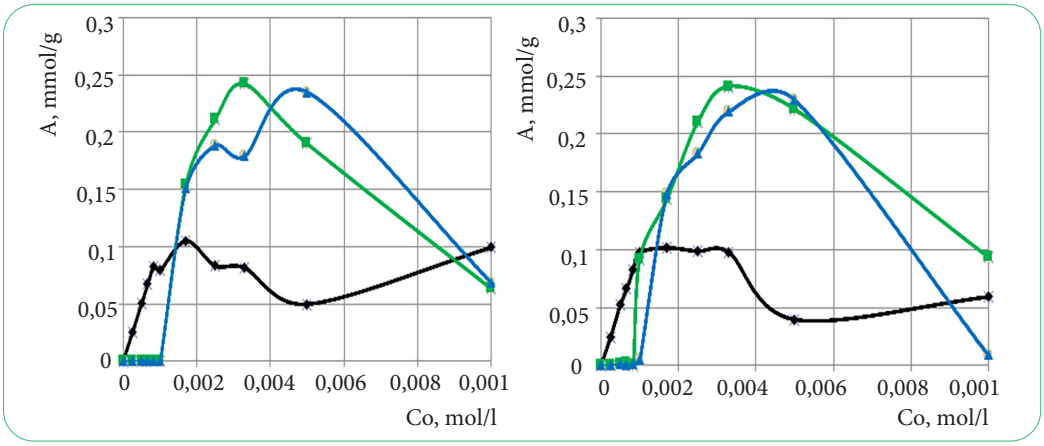

Figure 2. Adsorption isotherms for anionic dyes on the surface of modified montmorillonite (A) and spent montmorillonite (B)
Note: –■– anionic green dye; –▲– anionic blue dye; –×– anionic black dye
Source: developed by the authors

The results obtained can also be compared with those of A.F. Nabhani *et al.* (2024), who investigated the effectiveness of natural bentonite in removing dyes from real textile effluent. The authors found that the maximum dye removal efficiency was 91.25% at an initial wastewater concentration of 10%, a sorbent mass of 20 g and a contact time of 60 minutes. It was also shown that increasing the amount of bentonite helps to reduce the concentration of dyes in the aqueous phase; however, it may reduce the specific adsorption capacity due to particle aggregation and a reduction in the available sorbent surface area. In this case, maintaining a high specific surface area and the positive charge of the spent montmorillonite dispersions is also a substantial condition for the effective fixation of anionic dyes.

A comparison of the adsorption of different dyes (Fig. 2) indicates that maximum adsorption occurs when the anionic green dye with the highest molecular weight is used in both cases. The greatest increase in adsorption is observed for the high-molecular-weight anionic green and the low-molecular-weight blue dye, whilst the smallest increase is observed for the higher-molecular-weight anionic black. The reduction in the adsorption capacity of the anionic black solutions is most likely due to the premature aggregation of their molecules into micelles. Consequently, the spatial (steric) factor becomes critical during the penetration of such associates into the slit-like microporous structure of Cr^{3+}-montmorillonite, which leads to minimal adsorption values. Similar steric hindrances in micellar systems, as compared to molecular ones, are described by A.H. Jawad *et al.* (2022). The results of these studies on the sorption of methylene blue are very similar to the adsorption curves shown in Figure 2.

According to the results of thermogravimetric analysis (Table 1), the spent montmorillonite exhibits mass losses in the first and second stages of thermolysis that are similar to those of the modified sample, indicating a comparable content of physically bound and interlayer water. This is consistent with the similar values of the d001 interplanar spacing and confirms the preservation of swelling properties and the accessibility of the interlayer space to dye molecules. Furthermore, the slightly larger interplanar spacing in sample 3 (17.4 Å) may facilitate the penetration of dye molecules into the inner layers of the structure and their additional fixation. The results of the analysis of the colloid-chemical properties of the dispersions are consistent with the data reported by A. Bondaryeva *et al.* (2021) for dispersions based on pure bentonite modified with heavy metal sulphates. A. Bondaryeva *et al.* (2021) proposed a method for preparing pigments used for coating natural and synthetic polymers. Study noted that the use of montmorillonite, the surface of which is modified with ions of various metals (chromium, copper, cadmium, etc.), reduces pigment consumption when used in coating compositions.

The relationship between the structural composition of dye molecules and their adsorption capacity on montmorillonite is evident from the adsorption isotherms of the anionic dark green and anionic black dyes. Although they have similar molecular weights and structures, these compounds differ in their auxochromic substituents (-OH versus $-NH_2$). The phenolic moieties of anionic dark green confer weakly acidic (more electronegative) characteristics, whilst the amino groups of the benzene ring in anionic black give rise to weakly basic (electronegative) properties. This factor alone explains the greater affinity of the mineral montmorillonite for the anionic dark green compound (Fig. 2). In contrast, the role of sulphate groups in the adsorption process is practically identical across the entire series of compounds due to their equal abundance. At the same time, an increase in the number of sulphate groups in the adsorbate structure usually significantly inhibits sorption, as lateral electrostatic repulsion is enhanced in the adsorption zone. N. Palic *et al.* (2025), in their study of the sorption of pharmaceuticals and pesticides, also note that the influence of the natural

aqueous matrix reduces sorption efficiency by no more than 10%; the authors consider it appropriate to agree with this statement in the present case as well. Therefore, the influence of the aqueous component of the dispersion on sorption was not considered separately.

Addressing results of similar studies, in particular by M. Debnath *et al.* (2025), devoted to the optimisation of Congo red azo dye removal using Bent/Fe nanoparticles, it is possible to note that electrostatic and specific surface interactions between the adsorbed particles are decisive in the fixation of anionic dyes on clay sorbents. Accordingly, in addition to aggregation and spatial hindrance, the intermolecular repulsive forces – which increase as the surface becomes coated – can cause a non-linear profile of adsorption isotherms with extrema (maxima and minima). The appearance of these regions depends on the balance between repulsion and specific retention. At the same time, the presence of aromatic rings may provide such a strong bond with the mineral matrix that sorption remains positive even when the ionogenic groups and the surface carry the same charge. In addition to classical van der Waals forces, there is a high probability of specific interactions occurring between the π-electron clouds of the aromatic dye nuclei and the positively charged chromium polycations on the surface of Cr^{3+}-montmorillonite.

Following the adsorption mechanism, it should also be noted that the presence on the surface of Cr^{3+}-montmorillonite of chromium oligocations with strong complex-forming ability allows the formation of complex compounds between them and the functional groups of dyes (for example, $-SO_3H^+$), which act as ligands. The latter may enter the inner coordination sphere of hydroxychrome cations, penetrating quite deeply into the interlayer space of montmorillonite. Since thermal analysis indicated a higher probability of chromium complex formation in the deeper layers of the clay for sample 3, this may well explain the wider range of maximum adsorption values for spent montmorillonite. A similar relationship between maximum adsorption values and the presence of heavy metal complexes not only on the clay surface has been identified in studies by A.A. Rahimi & F. Alihosseini (2022).

The adsorption isotherms (Fig. 2) demonstrate that spent montmorillonite is practically on a par with the modified sorbent in terms of its ability to adsorb anionic dyes. This confirms the conclusion of the thermal analysis regarding the preservation of the porous structure and active sorption sites following prior saturation with chromium (III) ions. Furthermore, the slightly higher d001 values and the presence of strongly bound chromium complexes in sample 3, as shown in Table 1, may account for the broadening of the concentration range for effective adsorption and the enhanced interaction between the functional groups of the dyes and the sorbent surface. Thus, the results in Table 1 and Table 2 consistently correspond to the nature of the isotherms shown in Figure 2 and confirm the feasibility of using spent bentonite as a fully-fledged base to produce pigment compositions.

The study established that the preliminary saturation of montmorillonite with chromium (III) ions not only does not reduce its sorption capacity for anionic dyes, but may also contribute to the additional fixation of dyes through complex formation with chromium-containing centres. This paves the way to produce stable organo-mineral pigments based on spent sorbents without the need for additional chemical modification. R. Kryklyvyi *et al.* (2022) investigated the use of spent bentonite in the filling of polymer materials and noted the influence of such a filler on the formation of the functional properties of elastomeric blends. In this context, the results obtained indicate that spent montmorillonite, following the sorption of chromium (III) ions and anionic dyes, can be regarded not only as a sorbent but also as a functional mineral component for the subsequent formation of polymer-mineral or pigment composites. The study confirmed that the interaction between the organic dye and the inorganic clay matrix improves the characteristics of the final material. Such pigments will exhibit enhanced thermal stability, resistance to ultraviolet radiation and chemical influences.

Conclusions

Use of spent montmorillonite in multifunctional materials as a base for the sorption of anionic dyes and for pigment production contributes to significant resource savings and enhances the environmental sustainability of industrial processes. The similar mass loss observed for montmorillonite samples in the temperature range 20-190°C (corresponding to the release of physically bound and partial interlayer water) indicates that spent montmorillonite (sample 3) and modified montmorillonite (sample 2) may exhibit similar rheological properties, swelling capacity and porosity under appropriate processing conditions. It is reasonable to predict that the stronger fixation of chromium ions observed in spent bentonite may enhance the dye adsorption effect, as this would involve more than just surface processes. The high efficiency of sorption and precipitation of anionic dyes (dark green, black and blue) on the surface of montmorillonite, resulting in the formation of an excess monolayer, has been demonstrated; this serves as the basis for the subsequent synthesis of pigment concentrates for polymer-mineral coatings.

Dispersions based on spent montmorillonite ensure high dye adsorption across a wide range of concentrations and better fixation of dye molecules, as chromium complexes are formed in the deeper layers of the clay. Despite prior saturation with the pollutant, namely the chromium (III) ion, spent bentonite retains high adsorption activity towards anionic dyes, as confirmed by the nature of the adsorption isotherms. This allows the spent sorbent to be regarded not as waste, but as a secondary raw material to produce pigment compositions, thereby implementing the principles of the circular economy and minimising the environmental risks associated with its disposal. Due to similar colloidal and chemical properties of dispersions

based on modified and spent bentonites, alongside maximum adsorption values, spent bentonite can be used in to produce pigment concentrates without significant changes to the production procedures for pigments and colouring compositions. Prospects for further research include an in-depth study of the potential for using spent clay-based sorbents in various technological processes and in assessing their long-term environmental and practical potential.

Acknowledgements

None.

Funding

None.

Conflict of Interest

None.

References

[1] Alhalafi, Z.H. (2026). Photocatalytic efficiency of bentonite-TQD via recycling and photodegradation of organic pollutants and industrial wastewater. *Arabian Journal of Chemistry*, 19, article number 11252025. doi: 10.25259/AJC_1125_2025.

[2] Andriulaityte, I., Valentukeviciene, M., & Zurauskiene, R. (2024). Research on the reusability of bentonite waste materials for residual chlorine removal. *Materials*, 17(22), article number 5647. doi: 10.3390/ma17225647.

[3] Bondaryeva, A., Zhaldak, M., Mokrousova, O., & Okhmat, O. (2022). Nanopigments for leather finishing coating. In *ICAMS 2022 – 9th international conference on advanced materials and systems* (pp. 37-42). Bucharest: National Research and Development Institute for Textiles and Leather. doi: 10.24264/icams-2022.I.4.

[4] Bondaryeva, A., Mokrousova, O., & Okhmat, O. (2021). Hybrid pigments based on montmorillonite and anionic dyes for leather finishing. *Solid State Phenomena*, 320, 198-203. doi: 10.4028/www.scientific.net/SSP.320.198.

[5] Chokri, M., *et al.* (2025). Progress in bentonite clay modification and enhancing properties to industrial applications: A review. *Materials Chemistry and Physics*, 337, article number 130486. doi: 10.1016/j.matchemphys.2025.130486.

[6] Debnath, M., Barman, M.P., Basak, D., Borah, D., & Saikia, H. (2025). Optimizing Congo red dye removal using sodium borohydride-reduced Bent/Fe NPs and bentonite in aqueous solutions. *Current Indian Science*, 3(1). doi: 10.2174/012210299X370390250429053029.

[7] Dong, Y., Abbasi, A., Mohammadnejad, S., Nasrollahzadeh, M., Sheibani, R., & Otadi, M. (2024). Recent progresses in bentonite/lignin or polysaccharide composites for sustainable water treatment. *International Journal of Biological Macromolecules*, 278(3), article number 134747. doi: 10.1016/j.ijbiomac.2024.134747.

[8] Ismail, M., Khan, M.A., & Khan, S.A. (2022). Effective removal of reactive and direct dyes from colored wastewater using modified bentonite nanocomposites. *Water*, 14(22), article number 3604. doi: 10.3390/w14223604.

[9] Jawad, A.H., Saber, S.E.M., Abdulhameed, A.S., Farhan, A., ALOthman, Z.A., & Wilson, L.D. (2022). Characterization and applicability of the natural Iraqi bentonite clay for toxic cationic dye removal: Adsorption kinetic and isotherm study. *Journal of King Saud University – Science*, 35(5), article number 102630. doi: 10.1016/j.jksus.2023.102630.

[10] Kochubei, V., Yaremchuk, Y., Malovanyy, M., Yaholnyk, S., & Lutek, W. (2022). Studies of adsorption capacity of montmorillonite-enriched clay from the Khmelnytskyi Region. *Key Engineering Materials*, 925, 143-149. doi: 10.4028/p-i713sy.

[11] Kryklyvyi, R., Sakalova, H., Petrushka, K., & Luchyt, L. (2022). Use of clay sorptive materials in the synthesis of polymer materials. *Environmental Problems*, 7(1), 18-22. doi: 10.23939/ep2022.01.018.

[12] Malovanyy, M., Blazhko, O., Sakalova, H., & Vasylinych, T. (2021). Ecological aspects of clay sorption materials usage in leather and fur production technologies. *Materials Science Forum*, 1038, 276-281. doi: 10.4028/www.scientific.net/MSF.1038.276.

[13] Nabhani, A.F., Zahidah, Z., Herawati, H., & Zulti, F. (2024). Assessment of natural bentonite efficacy for dye removal in textile wastewater treatment: Implication for mitigating River Citarum pollution. *Journal of Limnology and Water Resources*, 31(1), 4-15. doi: 10.55981/limnotek.2024.4848.

[14] Palic, N., Vukcevic, M., Maletic, M., Mirkovic, M., Ristic, M., Peric-Grujic, A., & Trivunac, K. (2025). Amino-starch derivates for adsorption of specific pharmaceuticals and pesticides in contaminated water: Examination in both spiked and real water samples. *Journal of the Serbian Chemical Society*, 90(5), 693-707. doi: 10.2298/JSC240919007P.

[15] Paszkiewicz, S., Walkowiak, K., & Barczewski, M. (2024). Biobased polymer nanocomposites prepared by in situ polymerization: Comparison between carbon and mineral nanofillers. *Journal of Materials Science*, 59(30), 13805-13823. doi: 10.1007/s10853-024-10025-8.

[16] Rahimi, A.A., & Alihosseini, F. (2022). Application of dye saturated clay adsorbent from dyeing wastewater treatment as an industrial pigment for textile printing. *Journal of Chemical Technology & Biotechnology*, 97(11), 3120-3129. doi: 10.1002/jctb.7183.

[17] Ranskiy, A.P., Gordienko, O.A., Didenko, N.O., Titov, T.S., & Sydoruk, T.I. (2025). Synthesis of thioamide complex compounds of copper (II) and study of their mutual transformations. *Journal of Chemistry and Technologies*, 33(2), 352-362. doi: 10.15421/jchemtech.v33i2.321442.

[18] Sakalova, H., Malovanyy, M., Kochubei, V., Boiko, R., & Vasylinych, T. (2025). Determination of utilization directions for spent bentonite sorbents. *Pollack Periodica*. doi: 10.1556/606.2025.01396.

[19] Shamsuddin, R., Almohamadi, H., Siyal, A.A., & Ghumman, A.S.M. (2025). Charge properties, characteristics and applications of bentonite: A concise review. *Semarak Engineering Journal*, 11(1), 68-83. doi: 10.37934/sej.11.1.6883.
[20] Singh, R., Patanjali, P., Chopra, I., & Mandal, A. (2021). Organobentonite as an efficient and reusable adsorbent for cationic dyes removal from aqueous solution. *Journal of Scientific & Industrial Research*, 80(1), 80-86.
[21] Thomasset, A., & Benayoun, S. (2024). Review: Leather sustainability, an industrial ecology in process. *Journal of Industrial Ecology*, 28(6), 1842-1856. doi: 10.1111/jiec.13547.
[22] Zaiets, A., & Andreyeva, O. (2024). Evaluation of the efficiency of liquid leather finishing using polymers and modified fats. In *The 10th international conference on advanced materials and systems (ICAMS 2024)* (pp. 289-296). Bucharest: National Research and Development Institute for Textiles and Leather. doi: 10.2478/9788367405805.

Утилізація насичених полютантами бентонітових глин як спосіб мінімізації екологічного ризику

Галина Сакалова
Доктор технічних наук, професор
Вінницький національний технічний університет
21021, вул. Хмельницьке шосе, 95, м. Вінниця, Україна
https://orcid.org/0000-0002-9610-0967
Роман Бойко
Аспірант
Вінницький національний технічний університет
21021, вул. Хмельницьке шосе, 95, м. Вінниця, Україна
https://orcid.org/0009-0007-3206-0533
Олена Мокроусова
Доктор технічних наук, професор, завідувач кафедри
Київський національний університет технологій та дизайну
01011, вул. Мала Шияновська, 2, м. Київ, Україна
Державний торговельно-економічний університет
02156, вул. Кіото, 19, м. Київ, Україна
https://orcid.org/0000-0003-1943-8048
Тетяна Сидорук
Доцент
Вінницький національний технічний університет
21021, вул. Хмельницьке шосе, 95, м. Вінниця, Україна
https://orcid.org/0000-0002-5489-6397

Анотація. Ефективна утилізація відпрацьованих глинистих сорбентів допомагає зменшити техногенне навантаження на довкілля і вдосконалити технології повторного використання (Recycling) високодисперсних глин. Мета роботи полягала у дослідженні сорбційного поглинання молекул органічних барвників відпрацьованим бентонітом, попередньо насиченим іонами хрому (III), з можливістю подальшої утилізації бентоніту у складі пігментних композицій. Дослідження ґрунтувалося на порівняльному аналізі природного, модифікованого та відпрацьованого монтморилоніту із застосуванням термогравіметричного аналізу, визначення колоїдно-хімічних характеристик дисперсій, побудови ізотерм адсорбції та спектрофотометричного контролю концентрації барвників. Проаналізовано зміни структури, поверхневого заряду, міжплощинної відстані, питомої площі поверхні та сорбційної активності зразків. Встановлено, що насичення монтморилоніту іонами хрому (III) не призводить до суттєвого погіршення його властивостей. Доведено, що відпрацьований бентоніт зберігає пористу структуру, активні центри сорбції та здатність ефективно поглинати аніонні барвники у широкому інтервалі концентрацій. Встановлено, що хромовмісні центри можуть посилювати фіксацію молекул барвників за рахунок комплексоутворення та взаємодії з функціональними групами адсорбатів. Проаналізовано особливості адсорбції аніонного зеленого, синього та чорного барвників, зокрема вплив молекулярної будови, розміру молекул і просторових перешкод на поглинання. Розроблено підхід до утилізації відпрацьованого бентоніту як вторинної мінеральної основи для одержання органо-мінеральних пігментних композицій без додаткової хімічної модифікації. Практична цінність результатів полягає у можливості їх використання фахівцями з екологічної безпеки, очищення стічних вод, матеріалознавства та технологій пігментних покриттів

Ключові слова: сорбція; відпрацьовані сорбенти; монтморилоніт; барвники; іони хрому (III)

Vol. 17, No. 1
2026

Ecological Safety and Balanced Use of Resources

ISSN (print) 2415-3184, ISSN (online) 2522-9508
Journal homepage: https://esbur.com.ua/en

Received: 26.11.2025. Revised: 28.04.2026. Accepted: 12.06.2026. Published: 30.06.2026.

UDC 662.612.3:338.45:502.3

DOI: 10.63341/esbur/1.2026.152

Global ammonium perchlorate market: Environmental challenges and imperatives of sustainable resource use

Oleksandr Kryvokon
Doctor of Historical Sciences, Professor
Ivano-Frankivsk National Technical University of Oil and Gas
76019, 15 Karpatska Str., Ivano-Frankivsk, Ukraine
https://orcid.org/0000-0002-2495-7371

Maryna Kryvokon*
PhD in Economic Sciences
Independent Researcher
https://orcid.org/0000-0002-0228-6538

Abstract. The relevance of this study is driven by the expanding use of ammonium perchlorate in the aerospace and defence industries, which is accompanied by increasing anthropogenic pressure on the environment and the need to implement the principles of sustainable resource use. The aim of the study was to analyse the dynamics, structure, and development factors of the global ammonium perchlorate market, taking environmental risks into account. The research employed methods of generalisation, comparative and economic analysis, as well as market trend analysis based on analytical reports and scientific publications. The results showed that the global ammonium perchlorate market is characterised by steady growth with an average annual rate of approximately 5.37%, driven by the development of the aerospace and defence sectors. It was established that the market exhibits a pronounced inertial development pattern and depends on state funding of strategic programmes. Key growth drivers were identified, including technological innovation, geopolitical tensions, and an increasing number of space launches. It was demonstrated that environmental risks associated with water contamination and the toxic effects of perchlorates create additional constraints on market functioning and contribute to stronger regulatory frameworks. Structural analysis revealed that the largest share by volume is held by the extractive industry and construction sector (43.65%), while the aerospace and defence sector provides the most stable strategic demand. It was substantiated that the environmental factor is transforming into an innovation driver, stimulating the development of safer production and utilisation technologies. The practical significance of the findings lies in their potential use for developing market strategies that account for environmental requirements and improving the efficiency of production processes

Keywords: solid rocket propellant; aerospace industry; environmental safety; water contamination; perchlorates; market dynamics; environmental regulation

Introduction

The global development of high-technology industries, particularly the aerospace and defence sectors, sustains steady growth in demand for specialised chemical components, among which ammonium perchlorate occupies a key position. This compound is widely used as an oxidiser in solid rocket propellants, which determines its strategic importance for ensuring the functioning of modern space launch systems and defence technologies. In the context of intensifying space programmes, a growing number of launches, and the modernisation of military-technological capabilities of leading nations, the ammonium perchlorate market demonstrates stable positive growth dynamics. At

Suggested Citation: Kryvokon, O., & Kryvokon, M. (2026). Global ammonium perchlorate market: Environmental challenges and imperatives of sustainable resource use. *Ecological Safety and Balanced Use of Resources*, 17(1), 152-159. doi: 10.63341/esbur/1.2026.152.

*Corresponding author (*maryna.a.kr@gmail.com*)

the same time, the expanding scale of production and use of this substance is accompanied by a range of environmental risks associated with its toxic properties, its ability to accumulate in natural environments, and its potential impact on water resources and human health. In the context of tightening environmental regulation and growing requirements for the safety of chemical production, the issue of minimising the negative impact of perchlorates on the environment is becoming highly relevant. This necessitates a rethinking of traditional approaches to organising production processes and the introduction of more environmentally oriented technological solutions.

According to B. Zhang *et al.* (2022), perchlorates are widely distributed water contaminants that are regularly detected in groundwater and surface waters in various regions of the world, including drinking water supply systems. The researchers emphasised that their presence in the aquatic environment has a global character and is associated with the high migratory capacity of these compounds, which determines their long-term persistence and dispersal even beyond the immediate sources of contamination. E.N. Pearce (2024), analysing the biomedical aspects of perchlorate exposure, noted that these compounds act as competitive inhibitors of the sodium-iodide symporter in the thyroid gland, leading to reduced iodine uptake and potential disruption of thyroid hormone synthesis. The author stressed that the greatest risk is observed in vulnerable population groups, particularly pregnant women and young children, for whom even low levels of chronic exposure may have significant consequences for endocrine development. B. Predieri *et al.* (2022), in their study, examined perchlorates as persistent inorganic pollutants of anthropogenic origin and emphasised that their environmental hazard is determined by the combination of toxicity and stability in natural environments. The authors concluded that effective risk management requires a comprehensive approach encompassing monitoring, regulatory control, and the implementation of remediation technologies.

C. Fang & R. Naidu (2023) conducted a systematic review of perchlorate contamination and concluded that the high mobility of these compounds in natural environments significantly complicates the processes of their localisation and remediation. K.S. Kumar *et al.* (2022) analysed the environmental occurrence, toxicity, and remediation methods for perchlorates across various natural environments, emphasising the need for comprehensive approaches. R. Acevedo-Barrios *et al.* (2025) examined the global extent of perchlorate distribution, including their detection in Antarctica, demonstrating the transboundary nature of the contamination. R. Acevedo-Barrios & J. Olivero-Verbel (2021) systematised the sources of perchlorate contamination and the available remediation technologies, pointing to significant gaps in the regulatory framework. C.-Y. Lai *et al.* (2021) investigated mechanisms of biological perchlorate reduction and established that microbial remediation is a promising approach for the treatment of contaminated groundwater. O.A. Pivovarov & M.M. Cheltonov (2020) examined technological approaches to extracting ammonium perchlorate from solid rocket fuel disposal products. M.E. Gilbert *et al.* (2024) demonstrated that ammonium perchlorate exerts neurotoxic effects on thyroid development in neonatal rats. C. Serrano-Nascimento & M.T. Nunes (2022) investigated the effects of perchlorate and other NIS inhibitors on thyroid function and human health, concluding that there is a significant risk for pregnant women and children.

Alongside environmental aspects, significant importance attaches to the effective use of resources in the production of ammonium perchlorate. In this context, the concept of sustainable resource use entails optimising production cycles, reducing resource expenditure, and introducing innovative technologies. Thus, the available scientific base primarily covers the environmental and toxicological dimensions of the perchlorate issue. Market processes remain insufficiently studied: a comprehensive analysis of the structural factors driving the development of the ammonium perchlorate market – accounting for the interaction of environmental, technological, and institutional factors – is absent, and this gap provided the rationale for the present study. The aim of the study was to analyse contemporary trends in the development of the global ammonium perchlorate market, taking into account environmental risks and the operational features of the relevant production processes. To achieve this aim, the following objectives were defined: to analyse the dynamics and structure of the global ammonium perchlorate market; to identify the key factors that influenced its development; to investigate the environmental consequences of perchlorate production and use.

Materials and Methods

The study employed a comprehensive analytical approach combining methods of economic, comparative, and environmental analysis. The object of the study was the global ammonium perchlorate market; the subject was the trends in its development and the environmental aspects of its functioning. The information base of the study was formed from two categories of sources. The first category comprises scientific publications indexed in the international databases Scopus and Web of Science, dedicated to the environmental impact of perchlorates, their toxicity, and their technological applications (Motzer, 2001; Urbansky, 2002; Kucharzyk *et al.*, 2009; Lai *et al.*, 2021; Kumar *et al.*, 2022; Serrano-Nascimento & Nunes, 2022; Zhang *et al.*, 2022; Fang & Naidu, 2023; Gilbert *et al.*, 2024; Pearce, 2024; Acevedo-Barrios & Puentes, 2025). The second category consists of analytical reports from leading research agencies on the development of the ammonium perchlorate market (MarketsandMarkets, 2024; Research and Markets, 2025), which are compiled using an approach that integrates information from open sources, corporate reporting, industry surveys, and expert assessments. This approach ensures a sufficient level of reliability and representativeness of the results for further scientific generalisation. To analyse

market dynamics, the compound annual growth rate (CAGR) calculation method was applied according to the formula:

$$CAGR = \frac{V_n^{\frac{1}{n}}}{V_0} - 1, \quad (1)$$

where V_0 is the market volume in the base year; V_n is the market volume in the final year; n is the number of years in the period under analysis. Based on available market data for 2018-2024 and projected values through to 2030, a compound annual growth rate of 5.37% was calculated. The projections presented in the analytical reports of Research and Markets (2025) and MarketsandMarkets (2024) are based on methods of trend extrapolation, regression analysis, and scenario modelling, taking into account the dynamics of government defence expenditure, the number of space launches, and the state of the regulatory environment.

Comparative analysis was conducted across three dimensions. The first stage involved a comparison of regional markets (Asia-Pacific, North America, Europe) by share and relative growth dynamics in order to identify differences in development rates. This was followed by a comparison of industry segments by consumption volume – specifically, the aerospace and defence sector, the extractive industry and construction, and pyrotechnic production. Finally, an analysis was conducted of the overall impact of environmental constraints and regulatory pressure on market development. The method of generalisation was applied to form a holistic picture of the interaction between economic, environmental, and technological factors of market development. For a visual representation of this interaction, the method of systematisation was employed, followed by the development of an environmental factor impact matrix. In addition, the analysis of biomedical and toxicological data (in particular, relating to the effects of perchlorates on the endocrine system) was used in the study not as an independent research object, but as a qualitative indicator for assessing the regulatory environment. The depth of the negative health impact of chemicals was considered a key criterion explaining the formation of market constraints and stimulating innovation in treatment technologies. A limitation of the study was the absence of a unified system of indicators of environmental loading from ammonium perchlorate production in the public domain, which precludes quantitative assessment of the energy intensity and material consumption parameters of production cycles. This determined the predominantly qualitative character of the analysis of the resource aspect of market functioning.

Results and Discussion

The functioning of the global ammonium perchlorate market is determined by its critical role in supplying the aerospace and defence industries, where this substance is used as the primary oxidiser in composite solid rocket propellants. Ammonium perchlorate is an inorganic compound characterised by high oxidising capacity and efficient combustion, which accounts for its widespread application in the production of rocket engines. This functional specificity generates a highly specialised demand for the product (Sutton & Biblarz, 2016). Analysis of the dynamics of the global ammonium perchlorate market reveals an overall growth trend in the medium term (Fig. 1). In particular, the market volume in 2023 was estimated at approximately USD 812.21 million, and in 2024 at USD 854.77 million, while by 2030 it is projected to reach USD 1,171.80 million. The CAGR amounts to approximately 5.37% (Research and Markets, 2025). These data are consistent with the estimates for the solid rocket motor market contained in the MarketsandMarkets (2024) report, which confirms the representativeness of the database used.

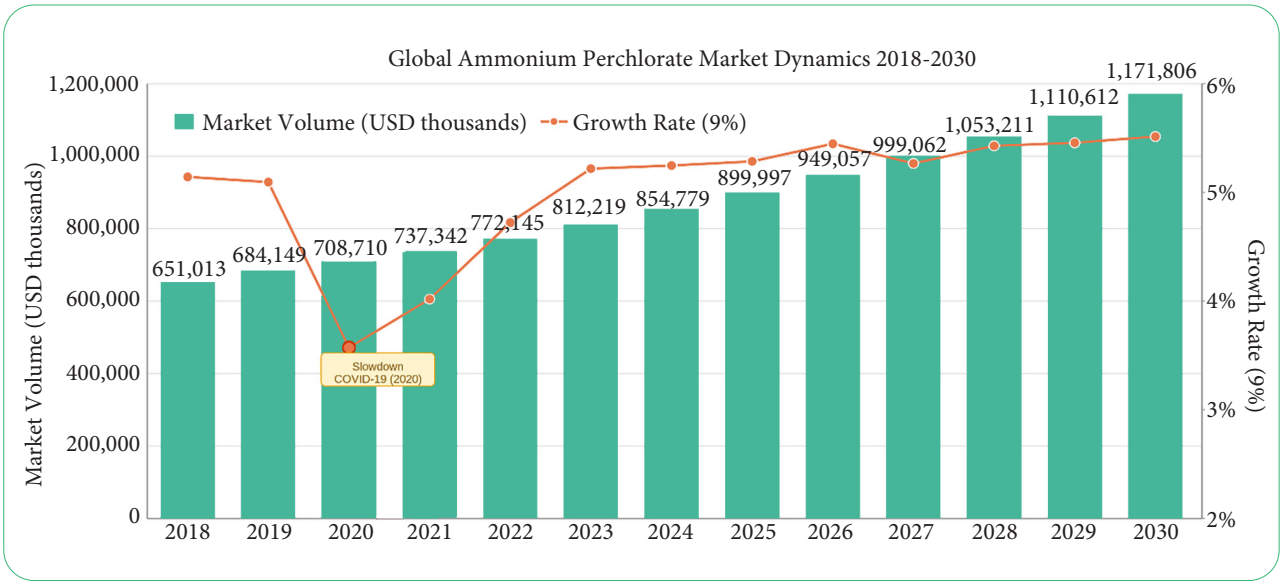

Figure 1. Dynamics of the global ammonium perchlorate market, 2018-2030

Source: compiled by the authors based on Research and Markets (2025)

It should be noted that the overall growth trend is not entirely uniform. An analysis of data for 2018-2022 reveals a noticeable short-term decline associated with a reduction in government orders and disruption to supply chains during the COVID-19 pandemic. This is consistent with general trends in the aerospace and defence industries in 2020-2021. After 2022, the market demonstrates recovery and accelerated growth, linked to geopolitical escalation and increased defence spending. This aspect is important for understanding the inertial character of market development, which is determined primarily by government funding cycles.

Analysis of the presented dynamics allows several structural characteristics of market development to be identified. The rate of market expansion remains moderate, due to the limited scope of application of the product and the high degree of specialisation of production. A dependence of market development on long-term programmes in the field of defence and space exploration is also observed, forming an inertial type of growth characteristic of sectors dominated by government funding. The growth of the ammonium perchlorate market is driven by a combination of technological and geopolitical factors. The key driver is the development of the aerospace industry, accompanied by an increase in the number of launches and an expansion of the range of space programmes. Simultaneously, defence budgets are growing in many countries, stimulating demand for rocket systems and, accordingly, for solid rocket propellants. Technological innovations aimed at improving the efficiency of rocket engines also sustain demand for ammonium perchlorate as a key component of such systems (Fig. 2).

Structural analysis of the ammonium perchlorate market reveals its sectoral diversification (Fig. 2). According to the data presented, the largest segment in 2023 is mining and construction (43.65%), where ammonium perchlorate is used primarily as a component of explosives. The aerospace and defence sector occupies the second position, yet generates the most stable and strategically predictable demand. Thus, the ammonium perchlorate market is commercially diversified: while the aerospace and defence industries determine the strategic significance of the product, the predominant consumption volume in 2023 falls on the extractive and construction sectors. Growing demand for high-purity ammonium perchlorate (concentration above 99%) is driven by the needs of the aerospace industry, where the stability of characteristics and predictability of material behaviour are of critical importance. This stimulates the development of more complex and energy-intensive production technologies, in particular electrochemical synthesis (Fig. 3).

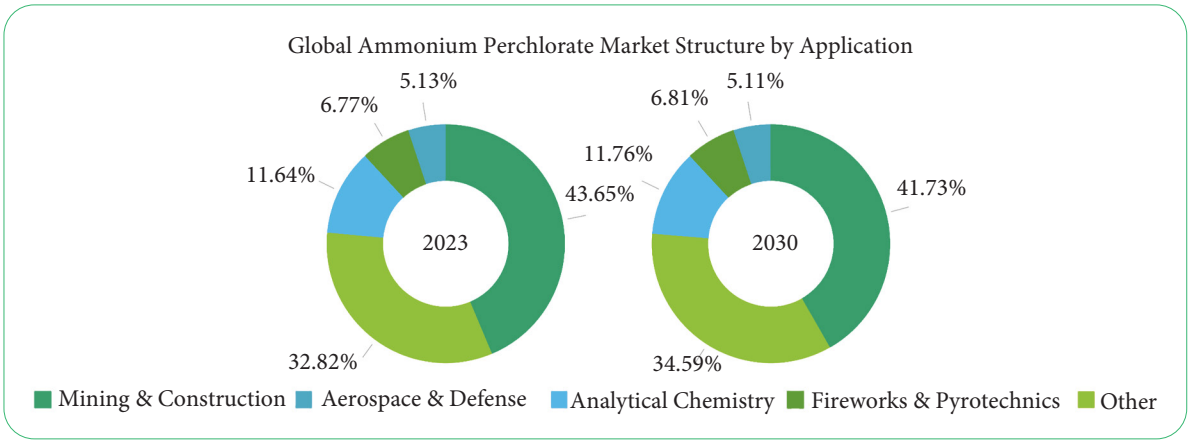

Figure 2. Structure of the global ammonium perchlorate market by application segment
Source: compiled by the authors based on MarketsandMarkets (2024), Research and Markets (2025)

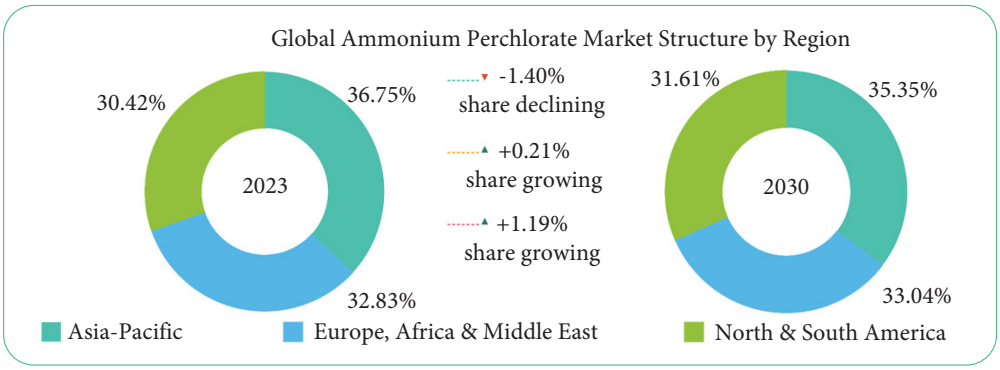

Figure 3. Geographic structure of the global ammonium perchlorate market by region
Source: compiled by the authors based on Research and Markets (2025)

The geographic structure of the market reveals important spatial differences in growth dynamics (Fig. 3). In terms of absolute volumes, the Asia-Pacific region leads; however, an analysis of market shares over time reveals a gradual decline in its relative share – from 36.75% in 2023 to 35.35% in 2030. Meanwhile, the shares of North America (from 30.42% to 31.61%) and Europe (from 32.83% to 33.04%) show an upward trend. This means that the markets of North America and Europe are growing in relative terms more rapidly than the Asia-Pacific market. Such dynamics may be associated with increased investment in rocket programmes in the United States and Europe after 2022, against the backdrop of geopolitical escalation.

The intensification of demand for ammonium perchlorate brings environmental safety issues to the fore. The entry of perchlorates into groundwater and surface waters can lead to their accumulation and subsequent inclusion in trophic chains, creating risks for ecosystems and human health. The impact of perchlorates on thyroid function is confirmed by contemporary toxicological research. C.-Y. Lai *et al.* (2021) emphasise that microbial remediation is one of the most promising approaches for reducing the environmental load of perchlorates in groundwater. The strengthening of environmental risks directly affects the regulatory environment. In a number of countries, strict requirements have been introduced with respect to the production, transportation, and disposal of perchlorates, which complicates the activities of manufacturers (Kucharzyk *et al.*, 2009). At the same time, the environmental factor is gradually transforming into an additional driver of innovative development: safety requirements stimulate the introduction of new treatment technologies and the development of alternative oxidisers with a lesser environmental impact. A systematic representation of environmental factors and their market impacts is provided in Table 1.

Table 1. Impact of environmental factors on the functioning of the ammonium perchlorate market

Environmental Factor	Manifestation	Market Impact
Water resource contamination by perchlorates	Accumulation in groundwater and surface waters	Tightening of environmental controls and restrictions on use
Emissions from rocket propellant combustion products	Release of toxic compounds into the atmosphere	Growing requirements for environmental standards
Environmental risks of production	Generation of waste and wastewater	Increased expenditure on purification and production modernisation
Strengthened regulatory frameworks	Introduction of environmental norms and standards	Creation of market entry barriers and stimulation of innovation

Source: developed by the authors

The findings indicate stable growth of the ammonium perchlorate market at a CAGR of approximately 5.37%, characterised by pronounced inertia and critical dependence on government funding for strategic programmes. The identified growth trend is fully consistent with the general trends in the development of the aerospace and defence industries (in particular, the increase in the number of space launches and geopolitical tensions) documented in the analytical reports of Research and Markets (2025) and MarketsandMarkets (2024). From a technological perspective, these market indicators are explained by the fundamental work of G.P. Sutton & O. Biblarz (2016), which confirms the central role of ammonium perchlorate as the primary oxidiser in solid rocket propellants, and provides a detailed analysis of its unique physicochemical properties that currently make it practically irreplaceable in this field.

At the same time, the study demonstrates that the expanding use of ammonium perchlorate is accompanied by increased anthropogenic pressure on the environment. The identified environmental constraints of the market (in particular, water resource contamination) are reliably confirmed by the conclusions of K.S. Kumar *et al.* (2022) and C. Fang & R. Naidu (2023) regarding the high mobility and persistence of perchlorates in natural environments. The problem of accumulation of these persistent anthropogenic contaminants in aquatic systems was conceptualised in the studies of W.E. Motzer (2001) and E.T. Urbansky (2002), where the lack of unified standards for risk assessment and sources of the chemical's entry into the environment was highlighted. In the contemporary context, the scale of the problem is illustrated by the study of B. Zhang *et al.* (2022), which identified high-risk zones in drinking water sources near industrial agglomerations in China.

An important aspect that creates additional pressure on producers and stimulates stricter regulatory frameworks is the impact of perchlorates on human health. The conclusions of the present work regarding toxic risks resonate with substantive biomedical research. C.M. Steinmaus (2016) detailed the pathways of perchlorate exposure via water supply systems and health consequences, while R.C. Pleus & L.M. Corey (2018) provided a comprehensive toxicological assessment of the effects of these compounds on the human body. A key mechanism of this impact – disruption of thyroid function – is described by R.E. Tarone *et al.* (2010) in an epidemiological review. These risks are particularly critical for vulnerable population groups: B. Predieri *et al.* (2022) classified perchlorates as serious endocrine disruptors that are among the key factors causing hormonal imbalance in children. Awareness of these threats earlier prompted K.H. Kucharzyk *et al.* (2009) to substantiate the need to establish strict drinking water quality standards in the United States.

The most significant conclusion of the analysis conducted is that environmental risks not only create constraints but are also transforming into a powerful driver of innovation, stimulating the development of safer production technologies and treatment systems. The development of water treatment technologies for perchlorates has progressed from the basic methods reviewed in detail by L. Ye *et al.* (2012) to modern high-technology solutions. M.R. Sijimol & M. Mohan (2014) examined pyrotechnics – in particular the production and use of fireworks – as a significant source of perchlorate environmental contamination. It was established that following fireworks launches, perchlorate concentrations in water rise sharply within a few hours and can exceed background levels tens or even thousands of times, before gradually declining over several weeks. The authors stress that the health and environmental consequences of this contamination source remain insufficiently studied, necessitating further research. In contrast to most existing works, which are narrowly specialised and focus either on economic and technical aspects and ballistics, or exclusively on epidemiology and ecology, the present study examines the ammonium perchlorate market as a unified ecological-economic system. This approach makes it possible to identify the dual role of the environmental factor: simultaneously as a rigid regulatory constraint on an inertial market and as the primary catalyst for structural and technological change within the paradigm of sustainable resource use.

Conclusions

The results of the analysis indicate that the ammonium perchlorate market is shaped by a complex set of economic, technological, and environmental factors whose interaction is acquiring an increasingly systemic character. Whereas in the early stages of industry development the dominant factors were exclusively the functional and technical parameters of the substance as a rocket propellant component, there is a gradual shift of emphasis towards the integration of environmental constraints into the decision-making processes at all levels of market functioning. The global ammonium perchlorate market demonstrated an overall growth trend at a CAGR of 5.37% with a projected volume of USD 1,171.80 million in 2030, although this dynamic is not uniform and experienced a temporary decline under the impact of the COVID-19 pandemic. Structural analysis revealed that the largest segment by volume is mining and construction (43.65% in 2023), while the aerospace and defence sector generates the most stable strategic demand. Geographic analysis showed that the markets of North America and Europe demonstrate higher relative growth rates compared to the Asia-Pacific region. The environmental factor acquires a dual role: it simultaneously constrains the market through regulatory pressure and stimulates innovation in the field of safer production technologies.

At the same time, the study indicates that the environmental component is not yet fully institutionalised as an autonomous regulator of market development, and is manifested primarily through fragmented constraints and local monitoring practices. Ensuring the balanced development of the ammonium perchlorate market requires the integration of environmental criteria into the strategic management system of the industry, in particular through the improvement of production technologies, the strengthening of regulatory frameworks, and the stimulation of innovative solutions in the field of alternative materials. A promising direction for further research is the study of the relationship between the development of alternative oxidisers, the tightening of environmental requirements, and the transformation of the market structure, as well as the analysis of mechanisms for harmonising environmental standards across different jurisdictions and their impact on global ammonium perchlorate supply chains.

Acknowledgements

None.

Funding

None.

Conflict of Interest

None.

References

[1] Acevedo-Barrios, R., & Olivero-Verbel, J. (2021). Perchlorate contamination: Sources, effects, and technologies for remediation. In P. de Voogt (Ed.), *Reviews of environmental contamination and toxicology* (pp. 103-120). Cham: Springer. doi: 10.1007/398_2021_66.

[2] Acevedo-Barrios, R., Puentes Martínez, D.A., Hernández Rocha, I.O., Rubiano-Labrador, C., De la Parra-Guerra, A.C., Carranza-López, L., Monroy-Licht, A., Leal, M.A., & Tovar, D. (2025). Perchlorate in antarctica, origin, effects, treatments, environmental fate, and astrobiological perspectives: A review. *International Journal of Environmental Science and Technology*, 21(13), 3855-3872. doi: 10.1007/s13762-024-06004-w.

[3] Fang, C., & Naidu, R. (2023). A review of perchlorate contamination: Analysis and remediation strategies. *Chemosphere*, 332, article number 139562. doi: 10.1016/j.chemosphere.2023.139562.

[4] Gilbert, M.E., Hassan, I., O'Shaughnessy, K.L., Wood, C., Stoker, T.E., Riutta, C., & Ford, J.L. (2024). Ammonium perchlorate: Serum dosimetry, neurotoxicity, and resilience of the neonatal rat thyroid system. *Toxicological Sciences*, 198(1), 113-127. doi: 10.1093/toxsci/kfad133.

[5] Kucharzyk, K.H., Crawford, R L., Cosens, B., & Hess, T.F. (2009). Development of drinking water standards for perchlorate in the United States. *Journal of Environmental Management*, 91(2), 303-310. doi: 10.1016/j.jenvman.2009.09.023.

[6] Kumar, K.S., Kavitha, S., Parameswari, K., Sakunthala, A., & Sathishkumar, P. (2022). Environmental occurrence, toxicity and remediation of perchlorate – a review. *Environmental Chemosphere*, 311, article number 137017. doi: 10.1016/j.chemosphere.2022.137017.
[7] Lai, C.-Y., Wu, M., Lu, X., Wang, Y., Yuan, Z., & Guo, J. (2021). Microbial perchlorate reduction driven by ethane and propane. *Environmental Science & Technology*, 55(3), 2006-2015. doi: 10.1021/acs.est.0c04103.
[8] MarketsandMarkets. (2024). *Solid rocket motors market report*. Retrieved from https://www.marketsandmarkets.com/Market-Reports/solid-rocket-motors-market-161743301.html.
[9] Motzer, W.E. (2001). Perchlorate: Problems, detection, and solutions. *Environmental Forensics*, 2(4), 301-311. doi: 10.1006/enfo.2001.0059.
[10] Pearce, E.N. (2024). Endocrine disruptors and thyroid health. *Endocrine Practice*, 30(2), 172-176. doi: 10.1016/j.eprac.2023.11.002.
[11] Pivovarov, O.A., & Cheltonov, M.M. (2020). Features of the technology for extracting ammonium perchlorate from solid rocket fuel disposal products. *Science, Technologies, Innovations*, 1, 58-63. doi: 10.35668/2520-6524-2020-1-08.
[12] Pleus, R.C., & Corey, L.M. (2018). Environmental exposure to perchlorate: A review of toxicology and human health. *Toxicology and Applied Pharmacology*, 358, 102-109. doi: 10.1016/j.taap.2018.09.001.
[13] Predieri, B., Iughetti, L., Bernasconi, S., & Street, M.E. (2022). Endocrine disrupting chemicals' effects in children: What we know and what we need to learn? *International Journal of Molecular Sciences*, 23(19), article number 11899. doi: 10.3390/ijms231911899.
[14] Research and Markets. (2025). *Ammonium perchlorate market size and share outlook – forecast trends and growth analysis report (2025-2034)*. Retrieved from https://www.researchandmarkets.com/reports/5921581/ammonium-perchlorate-market-size-share-outlook.
[15] Serrano-Nascimento, C., & Nunes, M.T. (2022). Perchlorate, nitrate, and thiocyanate: Environmental relevant NIS-inhibitors pollutants and their impact on thyroid function and human health. *Frontiers in Endocrinology*, 13, 995503. doi: 10.3389/fendo.2022.995503.
[16] Sijimol, M.R., & Mohan, M. (2014). Environmental impacts of perchlorate with special reference to fireworks – a review. *Environmental Monitoring and Assessment*, 186(11), 7203-7210. doi: 10.1007/s10661-014-3921-4.
[17] Steinmaus, C.M. (2016). Perchlorate in water supplies: Sources, exposures, and health effects. *Current Environmental Health Reports*, 3(2), 136-143. doi: 10.1007/s40572-016-0087-y.
[18] Sutton, G.P., & Biblarz, O. (2016). *Rocket propulsion elements* (7th ed.). Hoboken: John Wiley & Sons.
[19] Tarone, R.E., Lipworth, L., & McLaughlin, J.K. (2010). The epidemiology of environmental perchlorate exposure and thyroid function: A comprehensive review. *Journal of Occupational and Environmental Medicine*, 52(6), 653-660. doi: 10.1097/JOM.0b013e3181e31955.
[20] Urbansky, E. T. (2002). Perchlorate as an environmental contaminant. *Environmental Science and Pollution Research*, 9(3), 187-192. doi: 10.1007/BF02987487.
[21] Ye, L., You, H., Yao, J., & Su, H. (2012). Water treatment technologies for perchlorate: A review. *Desalination*, 298, 1-12. doi: 10.1016/j.desal.2012.05.006.
[22] Zhang, B., An, W., Shi, Y., & Yang, M. (2022). Perchlorate occurrence, sub-basin contribution and risk hotspots for drinking water sources in China based on industrial agglomeration method. *Environment International*, 158, article number 106995. doi: 10.1016/j.envint.2021.106995.

Глобальний ринок перхлорату амонію: екологічні виклики та імперативи збалансованого ресурсокористування

Олександр Кривоконь
Доктор історичних наук, професор
Івано-Франківський національний технічний університет нафти і газу
76019, вул. Карпатська, 15, м. Івано-Франківськ, Україна
https://orcid.org/0000-0002-2495-7371
Марина Кривоконь
Кандидат економічних наук
Незалежний дослідник
https://orcid.org/0000-0002-0228-6538

Анотація. Актуальність дослідження зумовлена розширенням використання перхлорату амонію у ракетно-космічній та оборонній галузях, що супроводжується підвищенням техногенного навантаження на довкілля та необхідністю впровадження принципів збалансованого ресурсокористування. Метою дослідження став аналіз динаміки, структури та факторів розвитку глобального ринку перхлорату амонію з урахуванням екологічних ризиків. У роботі були використані методи узагальнення, порівняльного та економічного аналізу, а також аналіз динаміки ринку на основі аналітичних звітів і наукових публікацій. У результаті було встановлено, що глобальний ринок перхлорату амонію характеризується стабільним зростанням із середньорічним темпом близько 5,37 %, що обумовлено розвитком аерокосмічного та оборонного секторів. Було визначено, що ринок має виражений інерційний характер розвитку та залежить від державного фінансування стратегічних програм. Були виявлені ключові фактори зростання, серед яких технологічні інновації, геополітична напруженість та збільшення обсягів космічних запусків. Було доведено, що екологічні ризики, пов'язані із забрудненням водних ресурсів і токсичним впливом перхлоратів, формують додаткові обмеження для функціонування ринку та сприяють посиленню нормативного регулювання. Структурний аналіз показав, що найбільшу частку за обсягом займають видобувна промисловість і будівництво (43,65 %), тоді як аерокосмічний та оборонний сектор забезпечує найстабільніший стратегічний попит. Було обґрунтовано, що екологічний фактор трансформується у драйвер інновацій, стимулюючи розвиток безпечніших технологій виробництва та використання. Практичне значення отриманих результатів полягає у можливості їх використання для формування стратегій розвитку ринку з урахуванням екологічних вимог та підвищення ефективності виробничих процесів

Ключові слова: тверде ракетне паливо; аерокосмічна промисловість; екологічна безпека; забруднення водних ресурсів; перхлорати; ринкова динаміка; екологічне регулювання

Vol. 17, No. 1
2026

Ecological Safety and Balanced Use of Resources

ISSN (print) 2415-3184, ISSN (online) 2522-9508
Journal homepage: https://esbur.com.ua/en

Received: 02.02.2026. Revised: 22.04.2026. Accepted: 12.06.2026. Published: 30.06.2026.

UDC 351.862:004:338.43

DOI: 10.63341/esbur/1.2026.160

Harnessing digital technologies for food security in developing countries: A focus on conflict-affected regions (literature review)

Szilvia Veress Juhaszne*
Postgraduate Student
Óbuda University Doctoral School on Safety and Security Sciences
1081, 8 Népszínház Str., Budapest, Hungary
https://orcid.org/0000-0003-0421-6119

Zoltan Rajnai
Deputy Rector
Óbuda University
1034, 96/B Bécsi Str., Budapest, Hungary
https://orcid.org/0000-0002-9139-736X

Abstract. Food insecurity has become an increasingly urgent global challenge, particularly in conflict-affected developing countries where armed violence, climate-related shocks, institutional fragility, and market disruptions undermine the resilience of food systems and threaten sustainable development. The aim of this study was to examine how digital technologies can contribute to strengthening food security governance in conflict-affected regions, with particular emphasis on Sub-Saharan Africa, and to develop an integrated framework supporting monitoring and decision-making processes. The research adopted a qualitative approach based on an integrative literature review, comparative case analysis, and conceptual framework development. The findings demonstrated that digital technologies can significantly enhance the monitoring and management of food security by improving information availability, supply chain transparency, risk assessment, and early warning capabilities. Mobile-based advisory systems facilitate communication with vulnerable populations and support agricultural decision-making. Remote sensing and GIS technologies enable the continuous observation of environmental and agricultural conditions, while blockchain-based solutions can improve transparency and accountability within food supply chains. Furthermore, predictive analytics and artificial intelligence offer new opportunities for anticipating food security risks and supporting evidence-based humanitarian interventions. Based on these findings, the study proposed an integrated digital food security monitoring framework that combines household-level monitoring, environmental observation, supply chain transparency, and predictive decision-support functions within a unified socio-technical system. An illustrative pilot implementation scenario was also presented to demonstrate the practical applicability of the proposed framework. The results may support policymakers, humanitarian organisations, development agencies, and food security practitioners in designing more effective, data-driven, and resilience-oriented monitoring systems for conflict-affected environments

Keywords: remote sensing; predictive analytics; humanitarian logistics; blockchain applications; resilience governance; early warning systems

Introduction

Food security has become one of the most pressing challenges of the twenty-first century. In many developing countries, particularly those affected by armed conflict, food systems are simultaneously exposed to violence,

Suggested Citation: Juhaszne, S.V., & Rajnai, Z. (2026). Harnessing digital technologies for food security in developing countries: A focus on conflict-affected regions (literature review). *Ecological Safety and Balanced Use of Resources*, 17(1), 160-171. doi: 10.63341/esbur/1.2026.160.

*Corresponding author (*juhaszne.szilvia@uni-obuda.hu*)

climate-related shocks, institutional fragility, market disruptions, and demographic pressures. These interconnected challenges weaken agricultural production, disrupt supply chains, and limit access to food. At the same time, rapid advances in digital technologies create new opportunities for monitoring risks, supporting decision-making, and strengthening food security governance. Understanding how these technologies can contribute to food security management in fragile environments has therefore become an increasingly important scientific and practical challenge.

Studies have increasingly examined the relationship between food security, humanitarian governance, and digital transformation. B. Faith *et al.* (2022) investigated the opportunities and risks associated with digital technologies in humanitarian operations. Their findings indicated that digital tools can improve accountability and information management, but may also create challenges related to privacy and data governance. The authors concluded that technological innovation requires appropriate institutional safeguards. FAO (2023) analysed global food security and nutrition trends and found that food insecurity remains particularly severe in conflict-affected and economically vulnerable regions. The report identified conflict, economic shocks, climate extremes, and structural vulnerabilities as major drivers of food insecurity and emphasised the need for integrated, data-driven approaches, strengthened food system resilience, and targeted investments to address both immediate needs and long-term challenges. The GNAFC (2023) examined the principal drivers of contemporary food crises. The analysis identified armed conflict as one of the most significant contributors to acute food insecurity and highlighted the importance of effective monitoring and early-warning systems. P.G. Juhász & C. Szeremley (2024) examined the role of local organisations in conflict-affected communities in the Democratic Republic of Congo. Their findings demonstrated that community participation and local ownership are essential factors in successful development and humanitarian interventions. From a technological perspective, P. Paillé *et al.* (2024) investigated the use of artificial intelligence, remote sensing, digital platforms, and advanced analytics in humanitarian contexts. The authors concluded that these technologies can significantly improve decision support but require interoperability and appropriate governance arrangements.

P. Devidal (2024) focused on the ethical implications of digital transformation in humanitarian operations. The study highlighted concerns regarding data ownership, surveillance, and accountability, concluding that technological innovation must be accompanied by strong ethical oversight. J. Besenyő & A.H. Sólyomfi (2024) analysed governance instability and security challenges in the Sahel region. Their findings demonstrated that prolonged conflict weakens institutional capacity and undermines food system resilience, emphasising the importance of improved coordination and information systems.

Although these studies provided valuable insights into digital technologies, humanitarian governance, and food security, important research gaps remain. Existing research has primarily focused on individual technologies or specific operational challenges. Comparatively limited attention has been devoted to integrated frameworks that combine technological, institutional, governance, and community-level dimensions within a unified food security monitoring architecture. Furthermore, relatively few studies have examined how such solutions can be operationalised in conflict-affected environments characterised by institutional fragility and limited resources. Therefore, the aim of this study was to examine the role of digital technologies in strengthening food security governance in conflict-affected developing countries and to develop an integrated Digital Food Security Monitoring Framework tailored to fragile environments.

The study addressed three interrelated research questions. The first question examined which digital technologies can be effectively applied in conflict-affected food systems. The second question explored the technological, institutional, governance-related, and ethical challenges influencing their implementation. The third question investigated how these technologies can be integrated into a coherent monitoring framework that supports food security governance, resilience-building, and evidence-based decision-making in conflict-affected regions.

To address these questions, the study adopted a qualitative research design based on an integrative literature review, comparative case analysis, and conceptual framework development, combining perspectives from food security research, humanitarian logistics, digital transformation, information systems, and development studies. The literature review was conducted between January and May 2025. The search combined keywords related to food security, digital technologies, conflict-affected regions, humanitarian logistics, remote sensing, blockchain, predictive analytics, artificial intelligence, and Sub-Saharan Africa, focusing primarily on publications from 2015 to 2025 while incorporating earlier foundational works where necessary. The retained publications were systematically examined through thematic analysis and organised into five overarching domains: mobile-based agricultural advisory systems, remote sensing and GIS-based monitoring, blockchain-enabled supply chain transparency, predictive analytics and artificial intelligence, and institutional governance and community participation. Building on this categorisation, the analysis further explored cross-cutting success factors and implementation constraints – including infrastructure availability, digital literacy, institutional capacity, data governance, and long-term sustainability – which together serve as the basis for the development of the proposed Digital Food Security Monitoring Framework.

Conceptual and regional prerequisites for food vulnerability in conflict conditions

Food security is increasingly understood as a complex socio-ecological system rather than solely an agricultural or economic issue. According to the widely accepted

definition, food security exists when all people, at all times, have physical and economic access to sufficient, safe, and nutritious food. This concept encompasses four interrelated dimensions: availability, access, utilisation, and stability (Serraj & Pingali, 2018).

Contemporary food systems are embedded within global production, trade, and logistics networks. Consequently, local disruptions may generate cascading effects across wider regional and international food systems. Geopolitical instability, market disruptions, climatic shocks, and armed conflicts can simultaneously affect agricultural production, food distribution, and household access to food. In developing countries, particularly in conflict-affected environments, these vulnerabilities often reinforce one another, creating systemic risks for food security (Kovács & Spens, 2007). Existing scholarship emphasises that food security should be analysed through a systems perspective integrating environmental, technological, institutional, and social dimensions. R. Serraj & P. Pingali (2018) argued that food security outcomes are increasingly shaped by interactions between ecological conditions, agricultural production systems, and governance mechanisms. Similarly, FAO (d23) highlighted that conflict, economic shocks, climate extremes, and structural vulnerabilities continue to undermine food system resilience across many regions, including Sub-Saharan Africa. Within this perspective, food security is not merely determined by food production levels but by the capacity of interconnected socio-ecological systems to absorb shocks and maintain essential functions.

Digital transformation has emerged as an increasingly important component of food security governance. Data-driven decision-making, remote monitoring, predictive modelling, and digital communication technologies create new opportunities for improving agricultural management, humanitarian response, and risk assessment. Remote sensing technologies, geographic information systems (GIS), artificial intelligence, and mobile-based information platforms enable the continuous observation of environmental and socio-economic conditions and support the development of early warning systems (Serraj & Pingali, 2018). At the same time, resilience has become a central concept in understanding food security in fragile environments. Resilience refers to the capacity of systems to adapt to external shocks while maintaining their core functions. In conflict-affected food systems, resilience depends not only on agricultural production but also on the quality of information flows, institutional coordination, and adaptive governance mechanisms (Kovács & Spens, 2007).

Several studies emphasised that technological innovation alone cannot ensure sustainable improvements in food security. FAO (2023) demonstrated that digital solutions are most effective when accompanied by investments in institutional and human capacities. Likewise, P.G. Juhász & C. Szeremley (2024), analysing conflict-affected communities in the Democratic Republic of Congo, conclude that local ownership and community participation are essential preconditions for successful development and humanitarian interventions. P. Paillé *et al*. (2024) similarly argued that digital technologies generate the greatest benefits when integrated into broader governance frameworks characterised by interoperability, institutional support, and stakeholder cooperation. The literature therefore suggests that digital technologies should not be regarded as stand-alone solutions. Their contribution to food security depends on their integration into institutionally supported and socially embedded systems capable of strengthening resilience and supporting evidence-based governance.

Sub-Saharan Africa remains one of the regions most exposed to food insecurity due to the combined effects of ecological vulnerability, demographic pressure, infrastructural limitations, and political instability. Existing assessments continue to identify the region as a global hotspot of hunger and food insecurity, with several conflict-affected countries experiencing particularly severe levels of food-system stress (von Grebmer *et al*., 2023). Population growth continues to increase demand for food, while agricultural productivity often remains constrained by environmental degradation, limited technological access, and insufficient investment in rural infrastructure (Serraj & Pingali, 2018).

The agricultural sector is dominated by smallholder farming systems that frequently operate under conditions of limited access to credit, agricultural inputs, market information, and irrigation infrastructure (FAO, 2023; von Grebmer *et al*., 2023). These structural constraints increase vulnerability to environmental stressors, including droughts, rainfall variability, soil degradation, and land-use change. Climate anomalies may significantly reduce agricultural productivity and intensify existing food security challenges, particularly in regions already affected by conflict. Infrastructure deficiencies further increase vulnerability. Damage to transportation networks, storage facilities, irrigation systems, and communication infrastructure can reduce market access, increase transaction costs, and limit the effectiveness of food distribution systems (Justino, 2012). Although mobile phone penetration has increased significantly throughout the region, substantial disparities in internet access and digital connectivity persist, particularly in rural and conflict-affected areas (von Grebmer *et al*., 2023). These ecological and infrastructural vulnerabilities create conditions in which relatively small environmental or political shocks may trigger disproportionately severe food security consequences. Consequently, effective monitoring systems must simultaneously address environmental dynamics, agricultural performance, and infrastructural constraints.

Armed conflicts affect food systems through multiple interconnected pathways, including disruptions to agricultural production, market fragmentation, population displacement, and reduced humanitarian access (Martin-Shields & Stojetz, 2019; Brück *et al*., 2019; GNAFC, 2023). Beyond conventional military violence, deliberate attacks targeting food production systems, storage facilities, transportation networks, or food supply chains

may further intensify food insecurity and increase the need for robust monitoring and early-warning mechanisms (Juhaszné, 2024). Furthermore, conflicts often generate long-term environmental and economic consequences that undermine food system resilience.

Conflict conditions frequently restrict access to agricultural land, reduce labour availability, interrupt planting and harvesting activities, and damage critical infrastructure. In addition, insecurity may disrupt local and regional markets, increase food price volatility, and weaken supply chain reliability. Food price volatility may itself become a source of social instability, reinforcing existing conflict dynamics and further limiting household food access (Bellemare, 2015). Humanitarian assistance systems also face significant challenges related to coordination, information asymmetries, and logistical constraints (Faith *et al*., 2022; Sundarakani & Ghouse, 2024).

The literature further highlights the importance of digital infrastructure in conflict-affected environments. While mobile communication technologies create new opportunities for information sharing and monitoring, unstable connectivity and limited digital capacity remain significant barriers to implementation (Rajnai & Fregan, 2016). Consequently, digital interventions frequently require adaptive solutions such as offline-first architectures, SMS-based communication systems, and decentralised data management approaches. Overall, conflict-related food insecurity emerges from the interaction of environmental vulnerability, infrastructural fragility, governance constraints, and disrupted socio-economic systems. This complexity underscores the need for integrated monitoring approaches capable of capturing both ecological and human dimensions of food security and provides the rationale for examining the role of digital technologies in food security governance.

Digital technologies for monitoring and forecasting the state of agroecological and food systems

Mobile-based agricultural advisory systems reduce information asymmetries among smallholder farmers and support production-related decision-making in fragile environments. In conflict-affected regions, where physical extension services may be disrupted, SMS-, USSD-, and low-data mobile applications can provide farmers with information on weather conditions, market prices, pest risks, input use, and food security conditions. Their main advantage lies in their relatively low infrastructure requirements and their ability to reach dispersed rural populations. Such systems typically operate through three interconnected layers: data collection, data processing, and advisory output. The data collection layer may include farmer-reported information through SMS or USSD channels, while the processing layer connects these inputs with meteorological, market, and agronomic databases. The output layer then delivers simplified recommendations in text- or voice-based formats (Paillé *et al*., 2024). Machine learning models can further support yield forecasting, pest detection, and input optimisation, particularly when local calibration data are available (Jain *et al*., 2016; Wolfert *et al*., 2017; Kamilaris & Prenafeta-Boldú, 2018).

The reviewed literature agrees that mobile-based systems can improve access to agricultural information and strengthen community-level monitoring. FAO (2023) emphasised their value in reducing information gaps among smallholder farmers, while B. Faith *et al*. (2022) underlined the importance of participatory design and local ownership. However, these tools remain constrained by digital illiteracy, unstable network coverage, limited electricity access, and weak institutional support. Therefore, mobile advisory platforms are most effective when embedded within wider governance and capacity-building systems rather than introduced as isolated technological solutions.

Remote sensing and GIS-based monitoring systems are among the most relevant digital technologies for food security governance in conflict-affected regions. Their importance derives from the fact that they enable continuous observation of agricultural and environmental processes without requiring regular physical access to insecure areas. This makes them particularly suitable for monitoring vegetation stress, drought dynamics, land degradation, land-use change, soil moisture variability, and crop production risks in fragile environments. Beyond agricultural monitoring, satellite imagery combined with machine-learning techniques has also demonstrated significant potential for estimating socio-economic conditions and poverty levels in data-scarce environments, creating additional opportunities for food-security vulnerability assessment (Burke *et al*., 2016).

Satellite-derived vegetation indices, especially the Normalised Difference Vegetation Index (NDVI), remain central tools for assessing vegetation health and biomass dynamics. NDVI time series can reveal seasonal vegetation patterns and anomalies associated with drought, conflict-related abandonment of agricultural land, input shortages, or market disruption. In addition, GIS platforms allow the integration of remote sensing data with precipitation records, soil moisture indicators, conflict-event datasets such as ACLED, market price information, and population movement data (Raleigh *et al*., 2010). This creates a multivariate analytical framework for identifying spatial patterns of agroecological vulnerability.

Existing studies confirm the increasing value of remote sensing for environmental and agricultural monitoring in African contexts. N. Heiss *et al*. (2025) reviewed the potential of Earth observation for mapping small-scale agriculture and cropping systems in West Africa. Their study highlighted the usefulness of Sentinel-1 and Sentinel-2 data for identifying cropland patterns, crop types, and smallholder production systems. The authors concluded that Earth observation can significantly improve food security monitoring, but they also noted that fragmented field data, heterogeneous smallholder plots, and cloud contamination remain major methodological limitations.

A.W. Moomen *et al*. (2024) examined remote sensing applications for sustainable agriculture in the Northern

Savannah regions of Ghana. Their review showed that satellite-based indicators can support land-use monitoring, crop condition assessment, and detection of environmental degradation. The study emphasised that Sentinel-2-derived NDVI patterns are particularly useful for tracking vegetation changes in rainfed agricultural systems. However, the authors also stressed that remote sensing outputs need to be combined with local agronomic knowledge to avoid misinterpretation of spectral signals.

N. Mubonderi *et al*. (2025) focused specifically on optical remote sensing for monitoring soil erosion in Sub-Saharan grassland biomes. Their systematic review found that multispectral Landsat and Sentinel-2 data, combined with indices such as modified NDVI, Normalised Difference Soil Index, and tasseled cap transformation, are increasingly applied to estimate erosion risk and land degradation. The study is particularly relevant for food security because soil erosion directly reduces long-term agricultural productivity. Its limitation is that optical remote sensing may be less effective under persistent cloud cover or dense vegetation, and erosion processes often require complementary field validation. M.B. Moisa *et al*. (2025) analysed the impact of land-use and land-cover change on soil moisture variability in southwestern Ethiopia using GIS and remote sensing techniques. Their research demonstrated that agricultural expansion, vegetation loss, and land-cover transformation influence soil moisture availability, with direct implications for drought vulnerability and crop productivity. The study strengthens the argument that food security monitoring should not rely only on crop indicators but should also incorporate land-use dynamics and hydrological variables.

M. Mustapha & M. Zineddine (2024) developed an evaluative technique for analysing drought impacts on agricultural land-use and land-cover variation using remote sensing and machine learning. Their work shows that combining satellite data, soil information, NDVI, and machine learning methods can improve the identification of drought-affected agricultural areas. This approach is especially useful for early-warning systems, although its reliability depends on data quality, model calibration, and the availability of validation datasets. M.G. Alemu & F.A. Zimale (2025) integrated remote sensing and machine learning for agricultural drought early warning in the Genale Dawa river basin in Ethiopia. Their study tracked drought severity between 2003 and 2023 and demonstrated that combined geospatial and machine-learning approaches can strengthen early warning capacity. The value of this approach lies in its ability to transform environmental indicators into operational risk information. However, as with other predictive models, its practical use requires regular recalibration and institutional capacity for interpretation.

Comparing these studies reveals several common conclusions. First, remote sensing is most effective when used as a continuous monitoring tool rather than as a one-time assessment method. Second, vegetation indices such as NDVI are useful but insufficient on their own; stronger results emerge when NDVI is combined with soil moisture, precipitation, land-use, and socio-economic indicators. Third, Sentinel-based systems offer high spatial resolution and are particularly promising for smallholder agriculture, while MODIS-based systems remain useful for long-term regional drought monitoring. Fourth, remote sensing cannot fully replace local knowledge or field validation, especially in complex agroecological systems where spectral changes may result from multiple interacting causes.

From the perspective of conflict-affected food systems, the most promising approach is therefore an integrated GIS-based monitoring model that combines satellite-derived vegetation indices, land degradation indicators, soil moisture data, precipitation anomalies, conflict-event data, and market indicators. Such a model can identify not only where agricultural stress is occurring, but also whether it is primarily driven by climatic, environmental, infrastructural, or conflict-related factors. This distinction is essential for designing appropriate humanitarian and development interventions. Predictive analytics and artificial intelligence enable food security monitoring systems to move beyond descriptive assessment toward anticipatory decision support. In conflict-affected regions, where risks evolve rapidly and nonlinearly, predictive models can integrate meteorological data, vegetation indices, market prices, conflict events, and population movement patterns to estimate the probability of food shortages or humanitarian crises (Funk *et al*., 2019).

Machine learning approaches, including random forests, gradient boosting models, and time-series neural networks, can identify nonlinear relationships between climate stress, agricultural productivity, market volatility, and conflict intensity. These models may support early warning, vulnerability mapping, and intervention prioritisation. However, their effectiveness depends heavily on data completeness, contextual calibration, and institutional capacity for interpretation.

The reviewed literature consistently emphasises that predictive analytics should complement rather than replace expert judgement. C. Funk *et al*. (2019) demonstrated the value of integrated predictive models for famine forecasting, while P. Paillé *et al*. (2024) highlighted the increasing role of AI-supported decision tools in humanitarian operations. At the same time, concerns remain regarding data gaps, algorithmic bias, explainability, and accountability. Existing advances in explainable artificial intelligence, including SHAP-based interpretation techniques, may improve the transparency of predictive food-security models and facilitate their adoption by humanitarian decision-makers (Lundberg & Lee, 2017). In conflict settings, where data may be incomplete, manipulated, or politically sensitive, predictive models must be transparent, regularly validated, and interpreted through local contextual knowledge.

Blockchain technology can contribute to food security governance by improving transparency, traceability, and accountability in food supply chains and humanitarian logistics. Similar blockchain-based architectures have recently

been proposed for refugee management and humanitarian resource allocation, demonstrating their potential to improve transparency and accountability in fragile governance environments (Abraha, 2025). Its decentralised and immutable structure can reduce opportunities for data manipulation, fraud, and resource diversion, particularly in environments where institutional trust is weak (Sundarakani & Ghouse, 2024). In conflict-affected regions, permissioned blockchain systems are more appropriate than open public blockchain architectures because they allow controlled access, stakeholder-specific permissions, and more energy-efficient operation. Blockchain can be strengthened through geo-tagging, digital signatures, and IoT-based monitoring of storage or transport conditions. However, the technology does not solve the problem of unreliable source data. If incorrect or manipulated data are entered into the system, blockchain merely preserves inaccurate information.

The literature therefore suggests that blockchain should not be treated as a universal solution. B. Sundarakani & A. Ghouse (2024) emphasised its potential for improving transaction visibility and traceability, while B. Faith *et al.* (2022) cautioned that technological transparency cannot replace institutional accountability. Blockchain-based systems are most useful when combined with independent audits, community oversight, clear governance rules, and reliable data validation mechanisms. The reviewed technologies differ in their primary functions, strengths, and limitations. Mobile advisory systems are relatively accessible and useful for household-level communication but depend on mobile coverage and digital literacy. Remote sensing and GIS provide the strongest environmental monitoring capacity, especially in inaccessible areas, but require technical expertise and analytical infrastructure. Predictive analytics can strengthen early warning and resource allocation, but its reliability depends on data quality and model transparency. Blockchain can improve supply chain accountability, but only when supported by institutional oversight and valid source data, as summarised in Tables 1 and 2.

Table 1. Comparative assessment matrix of digital technologies for food security monitoring in conflict-affected regions

Technology	Primary function	Main advantages	Key limitations	Relevance for conflict-affected regions
Mobile-based advisory systems	Dissemination of agricultural, market, and weather information	Low implementation cost; direct communication with vulnerable populations; supports local participation	Dependence on mobile coverage, electricity access, and digital literacy	High
Remote sensing and GIS	Environmental and agricultural monitoring; detection of droughts, land degradation, and crop stress	Large spatial coverage; continuous monitoring; suitable for inaccessible and insecure areas	Requires technical expertise, satellite data processing capacity, and field validation	Very High
Predictive analytics and artificial intelligence	Risk forecasting and decision support	Early warning capability; identification of complex risk patterns; supports resource prioritisation	Dependence on data quality; model uncertainty; explainability challenges	High
Blockchain-based systems	Supply chain transparency and traceability	Improved accountability; tamper-resistant records; enhanced transparency	Governance requirements; interoperability issues; does not guarantee data accuracy at input stage	Medium

Source: compiled by authors

Table 2. Comparative assessment of digital technologies supporting food security monitoring

Technology	Main data sources	Spatial scale	Temporal scale	Typical outputs
Mobile-based advisory systems	Farmer reports, SMS surveys, local extension data, market information	Household and community level	Daily to weekly	Advisory messages, vulnerability profiles, market alerts
Remote sensing and GIS	Satellite imagery (Sentinel, Landsat, MODIS), weather data, soil moisture indicators	Local, regional, national	Near real-time to seasonal	Vegetation maps, drought indicators, land-use change analysis, risk maps
Predictive analytics and AI	Multi-source databases, conflict-event datasets, climate data, market data	Community to national level	Short- and medium-term forecasting	Early warning alerts, food security forecasts, intervention prioritisation

Table 2. Continued

Technology	Main data sources	Spatial scale	Temporal scale	Typical outputs
Blockchain-based systems	Supply chain records, logistics data, digital transactions, IoT sensors	Local to international supply chains	Continuous	Traceability records, audit trails, transparency dashboards

Source: compiled by authors

Overall, the literature indicates that no single technology can address the multidimensional nature of food insecurity in conflict-affected regions. The highest strategic value emerges when these tools are integrated into an interoperable digital ecosystem. In such a system, mobile platforms provide local data, remote sensing captures regional environmental dynamics, predictive analytics generates risk forecasts, and blockchain strengthens transparency in supply chains. This integrated approach provides the strongest basis for proactive, evidence-based food security governance.

Building on the comparative assessment of digital technologies, an integrated Digital Food Security Monitoring Framework is proposed. The framework combines household-level monitoring, environmental observation, supply-chain information, and contextual conflict-related data within a unified governance-oriented architecture. Figure 1 presents food security monitoring as a multi-layered socio-technical system operating under conditions of conflict, climatic uncertainty, market volatility, and population displacement.

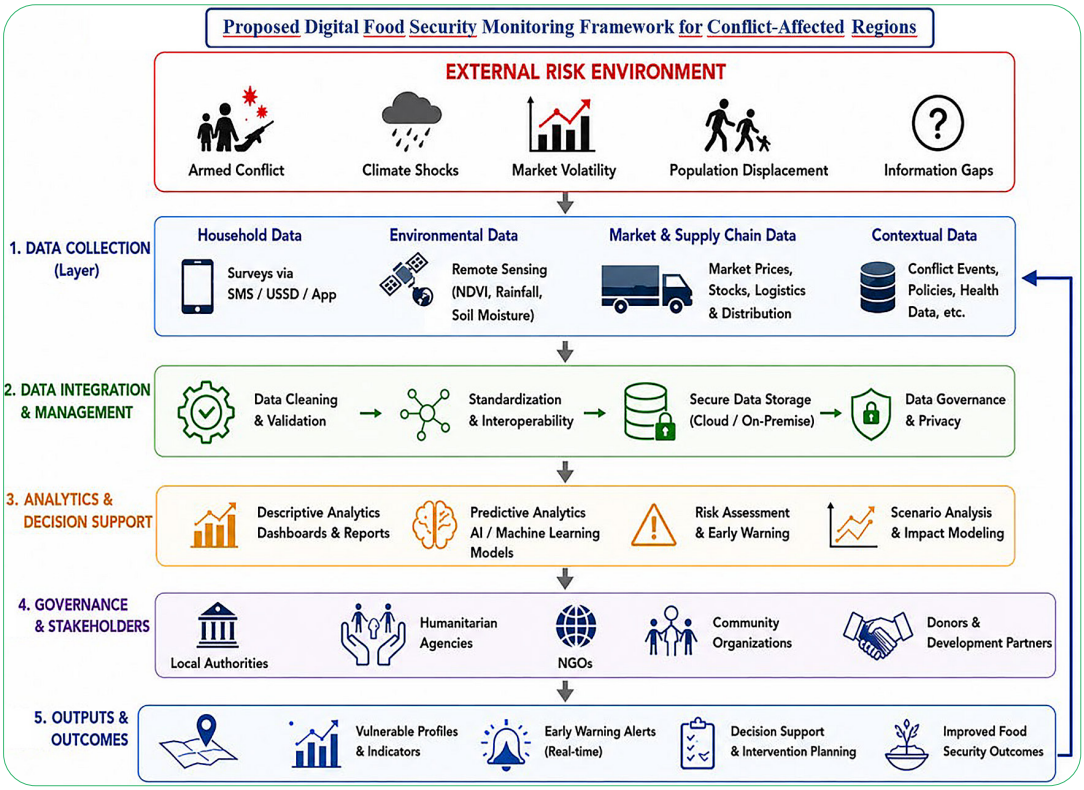

Figure 1. Proposed digital food security monitoring framework for conflict-affected regions

Source: compiled by authors

The framework consists of five interconnected layers. The first layer focuses on data collection from household, environmental, market, and contextual sources. The second layer ensures data integration, validation, storage, and governance. The third layer transforms raw information into decision-support outputs through descriptive and predictive analytics. The fourth layer highlights the role of institutional stakeholders, while the fifth layer translates analytical results into operational outputs such as vulnerability assessments, early-warning alerts, and intervention planning. While Figure 1 presents the conceptual logic of the proposed monitoring system, Figure 2 illustrates its operational data architecture. The architecture specifies how data flows from multiple sources through processing and analytical layers before reaching decision-makers and humanitarian actors. The architecture emphasises interoperability, continuous feedback, and adaptive learning. By integrating household surveys, Earth observation data, market information, and contextual conflict indicators, the system can generate near real-time assessments of food security conditions and support evidence-based interventions in fragile environments.

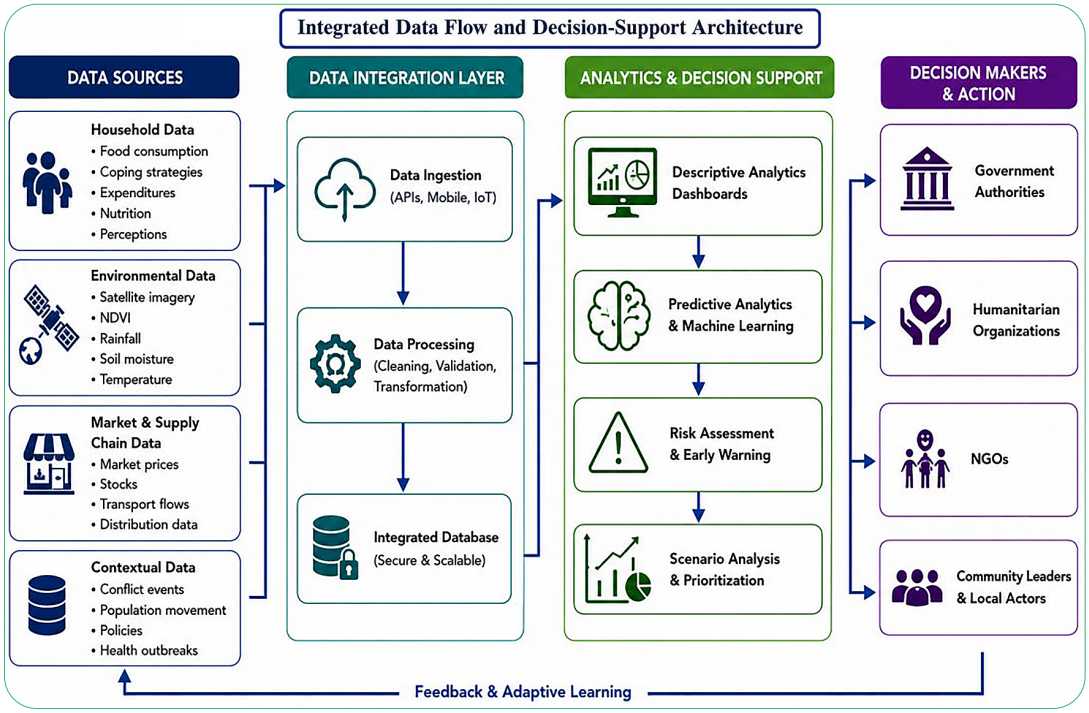

Figure 2. Integrated data flow and decision-support architecture

Source: compiled by authors

Table 3. Key risks and mitigation strategies for digital food security monitoring systems in conflict-affected regions

Risk Category	Example of Risk	Potential Consequences	Affected Technology Domains	Recommended Mitigation Measures
Technical Risks	Network outages, power interruptions, hardware failures	Data loss, delayed reporting, interrupted monitoring activities	Mobile systems, GIS platforms, AI systems, blockchain networks	Offline functionality, cloud backup, redundant communication channels, decentralised data storage
Data Quality Risks	Missing observations, inaccurate reporting, inconsistent datasets	Reduced reliability of forecasts, incorrect risk assessments, poor decision-making	Remote sensing, AI models, mobile reporting systems	Data validation procedures, triangulation of multiple data sources, periodic audits, field verification
Institutional Risks	Weak governance structures, insufficient technical expertise, fragmented responsibilities	Low sustainability, poor system adoption, ineffective coordination among stakeholders	All technology domains	Capacity-building programmes, stakeholder coordination mechanisms, institutional ownership, long-term funding strategies
Ethical Risks	Privacy violations, unauthorised access to personal information, surveillance concerns	Loss of trust, reduced participation, reputational and legal risks	Mobile systems, AI systems, blockchain databases	Data protection policies, encryption, informed consent procedures, ethical oversight mechanisms
Social Risks	Digital divide, exclusion of vulnerable populations, limited digital literacy	Unequal access to information and services, biased monitoring outcomes	Mobile systems, digital platforms, AI-supported tools	Community engagement, inclusive system design, multilingual interfaces, hybrid data collection methods
Security Risks	Cyberattacks, manipulation of datasets, conflict-related destruction of infrastructure	Operational disruption, compromised data integrity, reduced system reliability	GIS platforms, AI systems, blockchain networks	Cybersecurity protocols, access control systems, secure authentication, contingency planning
Operational Risks	Lack of interoperability between platforms and databases	Duplication of effort, information silos, delayed responses	All technology domains	Adoption of common data standards, interoperable architectures, integrated information management frameworks
Financial Risks	Insufficient long-term funding and maintenance resources	System degradation, project discontinuation, technology obsolescence	All technology domains	Multi-year financing mechanisms, public-private partnerships, phased implementation strategies

Source: compiled by authors

Ethical and privacy-related concerns represent a critical challenge for digital food security monitoring systems. Similar concerns have been identified in the application of big-data analytics within fragile and conflict-affected states, where weak governance structures may amplify risks related to data misuse and exclusion (Idris, 2019). Existing studies highlight risks associated with personal data processing, group privacy, algorithmic accountability, and the outsourcing of data governance responsibilities in humanitarian contexts (Masinde *et al*., 2023; Diepeveen *et al*., 2025; Kreutzer *et al*., 2025). These challenges underline the importance of transparent governance arrangements, clear accountability mechanisms, and robust data protection measures when implementing digital monitoring systems in conflict-affected environments.

Illustrative pilot implementation scenario

To demonstrate the practical applicability of the proposed Digital Food Security Monitoring Framework, an illustrative pilot implementation scenario is presented. The scenario is not intended as empirical validation but as a conceptual operationalisation of the framework within a realistic conflict-affected environment. Nyangezi, located in South Kivu Province of the Democratic Republic of Congo (DRC), represents a suitable illustrative context due to its combination of chronic food insecurity, recurring security challenges, agricultural dependence, and infrastructural limitations. Similar conditions are observed in numerous conflict-affected regions across Sub-Saharan Africa, making the area an appropriate reference point for demonstrating the potential functionality of the proposed monitoring system.

The local economy is predominantly based on smallholder agriculture, while households remain highly vulnerable to market disruptions, population displacement, climatic shocks, and fluctuations in security conditions. These characteristics create a complex environment in which continuous food security monitoring could provide substantial decision-support value for both local stakeholders and humanitarian actors. The illustrative monitoring system would track a set of indicators representing all four dimensions of food security. The availability dimension would be assessed through indicators related to crop production conditions, vegetation health, and the availability of agricultural inputs. Food access would be monitored using measures such as market prices, the share of household expenditure devoted to food, and transportation accessibility. The utilisation dimension would be evaluated through indicators reflecting dietary diversity, meal frequency, and nutritional status. Stability would be assessed by monitoring conflict intensity, population displacement, climatic anomalies, and market volatility.

Based on the continuous collection and analysis of these indicators, the system would generate a range of operational outputs. These would include household vulnerability profiles, community-level food security dashboards, risk maps, early-warning alerts, and intervention prioritisation reports. Such outputs could support local authorities, humanitarian organisations, and development agencies in making evidence-based decisions and allocating resources more effectively under rapidly changing and uncertain conditions.

Conclusions

This study examined the potential of digital technologies to strengthen food security governance in conflict-affected developing countries, with particular emphasis on Sub-Saharan Africa. The review demonstrated that mobile-based advisory systems, remote sensing and GIS technologies, predictive analytics, artificial intelligence, and blockchain-based solutions can significantly enhance food security monitoring, risk assessment, and decision-making processes. The analysis further revealed that technological effectiveness depends not only on technical performance but also on institutional capacity, governance quality, stakeholder cooperation, and community participation. Consequently, integrated digital ecosystems offer greater potential for strengthening resilience and supporting evidence-based interventions than isolated technological solutions.

Based on the reviewed literature, the study proposed an integrated Digital Food Security Monitoring Framework that combines household-level monitoring, environmental observation, supply-chain information, and predictive decision-support functions within a unified socio-technical architecture. The framework may support governments, humanitarian organisations, and development agencies in designing more adaptive and data-driven food security monitoring systems for fragile environments. Future research should focus on the empirical validation of the proposed framework through pilot implementation projects in conflict-affected regions and on assessing the long-term effectiveness of integrated digital monitoring systems under real-world operational conditions.

Acknowledgements

None.

Funding

None.

Conflict of Interest

None.

References

[1] Abraha, D.T. (2025). Blockchain-based solution for addressing refugee management in the Global South: Transparent and accessible resource sharing in humanitarian organizations. *Frontiers in Human Dynamics*, 7, article number 1391163. doi: 10.3389/fhumd.2024.1391163.

[2] Alemu, M.G., & Zimale, F.A. (2025). Integration of remote sensing and machine learning algorithm for agricultural drought early warning over Genale Dawa river basin, Ethiopia. *Environmental Monitoring and Assessment*, 197, article number 243. doi: 10.1007/s10661-025-13708-0.
[3] Bellemare, M.F. (2015). Rising food prices, food price volatility, and social unrest. *American Journal of Agricultural Economics*, 97(1), 1-21. doi: 10.1093/ajae/aau038.
[4] Besenyő, J., & Sólyomfi, A.H. (2024). Mali: Safe heaven to terrorist? In J. Besenyő, L. Issaev & A. Korotayev (Eds.), *Terrorism and political contention. Perspectives on development in the Middle East and North Africa (MENA) Region* (pp. 153-167). Cham: Springer. doi: 10.1007/978-3-031-53429-4_8.
[5] Brück, T., d'Errico, M., & Pietrelli, R. (2019). The effects of violent conflict on household resilience and food security. *World Development*, 119, 203-223. doi: 10.1016/j.worlddev.2018.01.002.
[6] Burke, M., Driscoll, A., Lobell, D.B., & Ermon, S. (2016). Using satellite imagery and machine learning to predict poverty. *Science*, 353(6301), 790-794. doi: 10.1126/science.aaf7894.
[7] Devidal, P. (2024). Lost in digital translation? The humanitarian principles in the digital age. *International Review of the Red Cross*, 106(925), 120-154. doi: 10.1017/S181638312400008.
[8] Diepeveen, S., Bryant, J., & Wasuge, M. (2025). Outsourcing accountability: Extractive data practice and inequities of power in humanitarian third-party monitoring. *Big Data & Society*, 12(1). doi: 10.1177/20539517251328250.
[9] Faith, B., Roberts, T., & Hernandez, K. (2022). *Risks, accountability and technology: Thematic working paper*. Brighton: Institute of Development Studies. doi: 10.19088/BASIC.2022.003.
[10] FAO. (2023). *The state of food security and nutrition in the world 2023*. Retrieved from https://doi.org/10.4060/cc3017en.
[11] Funk, C., *et al.* (2019). Recognizing the famine early warning systems network: Over 30 years of early warning science advances and partnerships promoting global food security. *Bulletin of the American Meteorological Society*, 100(6), 1011-1027. doi: 10.1175/BAMS-D-17-0233.1.
[12] GNAFC. (2023). *Global report on food crises 2023*. Retrieved from https://www.fsinplatform.org/report/global-report-food-crises-2023.
[13] Heiss, N., Meier, J., Gessner, U., & Kuenzer, C. (2025). A review: Potential of Earth observation (EO) for mapping small-scale agriculture and cropping systems in West Africa. *Land*, 14(1), article number 171. doi: 10.3390/land14010171.
[14] Idris, I. (2019). *Benefits and risks of big data analytics in fragile and conflict affected states*. Brighton: Institute of Development Studies.
[15] Jain, M., Mondal, P., DeFries, R.S., Small, C., & Galford, G.L. (2016). Mapping cropping intensity of smallholder farms: A comparison of methods using multiple sensors. *Remote Sensing of Environment*, 134, 210-223. doi: 10.1016/j.rse.2013.02.029.
[16] Juhász, P.G., & Szeremley, C. (2024). Work of a local NGO VETO, in contrast with the international organisations in the Eastern Congo. *Journal of Central and Eastern European African Studies*, 3(3), 18-39. doi: 10.59569/jceeas.2023.3.3.221.
[17] Juhaszné, S.V. (2024). Food terrorism as a real threat. In T.A. Kovács & I. Fürstner (Eds.), *Critical infrastructure protection: Advanced technologies for crisis prevention and response* (pp. 177-188). Dordrecht: Springer. doi: 10.1007/978-94-024-2308-2_12.
[18] Justino, P. (2012). War and poverty. *IDS Working Papers*, 2012, 21-29. doi: 10.1111/j.2040-0209.2012.00391.x.
[19] Kamilaris, A., & Prenafeta-Boldú, F.X. (2018). Deep learning in agriculture: A survey. *Computers and Electronics in Agriculture*, 147, 70-90. doi: 10.1016/j.compag.2018.02.016.
[20] Kovács, G., & Spens, K.M. (2007). Humanitarian logistics in disaster relief operations. *International Journal of Physical Distribution & Logistics Management*, 37(2), 99-114. doi: 10.1108/09600030710734820.
[21] Kreutzer, T., Orbinski, J., Appel, L., An, A., Marston, J., Boone, E., & Vinck, P. (2025). Ethical implications related to processing of personal data and artificial intelligence in humanitarian crises: A scoping review. *BMC Medical Ethics*, 26, article number 49. doi: 10.1186/s12910-025-01189-2.
[22] Lundberg, S.M., & Lee, S.-I. (2017). A unified approach to interpreting model predictions. In *NIPS'17: Proceedings of the 31st international conference on neural information processing systems* (pp. 4768-4777). Long Beach: Neural Information Processing Systems Foundation.
[23] Martin-Shields, C.P., & Stojetz, W. (2019). Food security and conflict: Empirical challenges and future opportunities. *World Development*, 119, 150-164. doi: 10.1016/j.worlddev.2018.07.011.
[24] Masinde, B.K., Gevaert, C.M., Nagenborg, M.H., & Zevenbergen, J.A. (2023). Group-privacy threats for geodata in the humanitarian context. *ISPRS International Journal of Geo-Information*, 12(10), article number 393. doi: 10.3390/ijgi12100393.
[25] Moisa, M.B., Roba, Z.R., Purohit, S., Deribew, K.T., & Gemeda., D.O. (2025). Evaluating the impact of land use and land cover change on soil moisture variability using GIS and remote sensing technology in southwestern Ethiopia. *Environmental Monitoring and Assessment*, 197, article number 824. doi: 10.1007/s10661-025-14301-1.

[26] Moomen, A.W., Yevugah, L.L., Boakye, L., Osei, J.D., & Muthoni, F. (2024). Review of applications of remote sensing towards sustainable agriculture in the Northern Savannah Regions of Ghana. *Agriculture*, 14(4), article number 546. doi: 10.3390/agriculture14040546.
[27] Mubonderi, N., Manyevere, A., & Mashamaite, C.V. (2025). Optical remote sensing for monitoring soil erosion in sub-Saharan grassland biomes: A systematic review. *Environmental Monitoring and Assessment*, 197, article number 976. doi: 10.1007/s10661-025-14426-3.
[28] Mustapha, M., & Zineddine, M. (2024). An evaluative technique for drought impact on variation in agricultural LULC using remote sensing and machine learning. *Environmental Monitoring and Assessment*, 196, article number 515. doi: 10.1007/s10661-024-12677-0.
[29] Paillé, P., Besse, J., Toole, H., Politi, C., Viswanathan, S., Namirembe, E., & Ohrvik-Stott, J. (2024). *Emerging technologies in the humanitarian sector*. Retrieved from https://www.rand.org.
[30] Rajnai, Z., & Fregan, B. (2016). Critical infrastructures protection (legislation). *Technical Scientific Publications*, 5, 349-352. doi: 10.33895/mtk-2016.05.78.
[31] Raleigh, C., Linke, A., Hegre, H., & Karlsen, J. (2010). Introducing ACLED: Armed conflict location and event dataset. *Journal of Peace Research*, 47(5), 651-660. doi: 10.1177/0022343310378914.
[32] Serraj, R., & Pingali, P. (2018). *Agriculture and food systems to 2050: Global trends, challenges and opportunities*. Singapore: World Scientific. doi: 10.1142/11212.
[33] Sundarakani, B., & Ghouse, A. (2024). A systematic literature review and bibliometric analysis of blockchain technology for food security. *Foods*, 13(22), article number 3607. doi: 10.3390/foods13223607.
[34] von Grebmer, K., *et al*. (2023). *2023 Global Hunger Index: The power of youth in shaping food systems*. Retrieved from https://www.globalhungerindex.org/pdf/en/2023.pdf.
[35] Wolfert, S., Ge, L., Verdouw, C., & Bogaardt, M.-J. (2017). Big data in smart farming – a review. *Agricultural Systems*, 153, 69-80. doi: 10.1016/j.agsy.2017.01.023.

Використання цифрових технологій для продовольчої безпеки в країнах, що розвиваються: акцент на регіонах, які постраждали від конфлікту (огляд літератури)

Сільвія Вереш Юхашне
Аспірант
Докторська школа наук з безпеки Обудського університету
1081, вул. Népszínház, 8, м. Будапешт, Угорщина
https://orcid.org/0000-0003-0421-6119
Золтан Раджнаї
Проректор
Обудський університет
1034, вул. Bécsi, 96/B, м. Будапешт, Угорщина
https://orcid.org/0000-0002-9139-736X

Анотація. Продовольча незабезпеченість стала дедалі гострішою глобальною проблемою, особливо в країнах, що розвиваються та потерпають від конфліктів, де збройне насильство, кліматичні потрясіння, інституційна нестабільність і порушення ринкових механізмів підривають стійкість продовольчих систем і загрожують сталому розвитку. Метою цієї статті було дослідити, як цифрові технології можуть сприяти зміцненню управління продовольчою безпекою в регіонах, уражених конфліктами, з особливим акцентом на країнах Африки на південь від Сахари, а також розроблення інтегрованої системи підтримки моніторингу та процесів прийняття рішень. У дослідженні застосовано якісний підхід, що базувався на інтегративному огляді літератури, порівняльному аналізі кейсів і розробленні концептуальної моделі. Результати дослідження засвідчили, що цифрові технології можуть суттєво підвищити ефективність моніторингу та управління продовольчою безпекою завдяки покращенню доступності інформації, прозорості ланцюгів постачання, оцінювання ризиків і можливостей систем раннього попередження. Мобільні консультаційні сервіси сприяють комунікації з уразливими групами населення та підтримують прийняття рішень у сільському господарстві. Технології дистанційного зондування Землі та геоінформаційні системи забезпечують безперервне спостереження за станом довкілля й аграрного сектору, тоді як рішення на основі блокчейну можуть підвищити прозорість і підзвітність у продовольчих ланцюгах постачання. Крім того, предиктивна аналітика та штучний інтелект відкривають нові можливості для прогнозування ризиків продовольчої безпеки та підтримки гуманітарних заходів, що ґрунтуються на доказових даних. На основі отриманих результатів запропоновано інтегровану цифрову систему моніторингу продовольчої безпеки, яка поєднує моніторинг на рівні домогосподарств, екологічне спостереження, забезпечення прозорості ланцюгів постачання та функції прогнозно-аналітичної підтримки прийняття рішень у межах єдиної соціотехнічної системи. Також представлено ілюстративний сценарій пілотного впровадження для демонстрації практичної придатності запропонованої моделі. Отримані результати можуть бути корисними для політиків, гуманітарних організацій, агенцій розвитку та фахівців у сфері продовольчої безпеки під час розроблення більш ефективних, орієнтованих на дані та стійкість систем моніторингу в умовах конфліктів

Ключові слова: дистанційне зондування Землі; предиктивна аналітика; гуманітарна логістика; застосування блокчейну; управління стійкістю; системи раннього попередження

ЕКОЛОГІЧНА БЕЗПЕКА ТА ЗБАЛАНСОВАНЕ РЕСУРСОКОРИСТУВАННЯ

Науково-технічний журнал

Том 17, № 1, 2026

Відповідальний редактор:
Я. Адаменко

Підписано до друку 12.06.2026 р.
Формат 60*84/8
Умовн. друк. арк. 20,2
Тираж 100 прим.

Адреса видавництва:
Івано-Франківський національний технічний університет нафти і газу
76019, вул. Карпатська, 15, м. Івано-Франківськ, Україна
Тел.: +380 (342) 54-72-66
Факс: +380 (342) 54-71-39
E-mail: mail@esbur.com.ua
https://esbur.com.ua/uk

ECOLOGICAL SAFETY AND BALANCED USE OF RESOURCES

Scientific and Technical Journal

Vol. 17, No. 1, 2026

Managing Editor:
Ya. Adamenko

Signed for print 12.06.2026.
Format 60*84/8
Conventional printed pages 20.2
Circulation 100 copies

Publishing Address:
Ivano-Frankivsk National Technical University of Oil and Gas
76019, 15 Karpatska Str., Ivano-Frankivsk, Ukraine
Tel.: +380 (342) 54-72-66
Fax: +380 (342) 54-71-39
E-mail: mail@esbur.com.ua
https://esbur.com.ua/en